From: Sydney B. Griffin <sydney.griffin@pressmail.ch>
Sent: 9/27/2023 5:00:11 PM
To: Public Comment <PublicComment@trpa.gov>
Subject: Governing Board Documents September 27, 2023-Hybrid Meeting — Housing Amendments — Public Commentary
Attachments: d9b7d042.jpeg , 6df0c693.jpeg , b640401a.jpeg , 00fb1acc.jpeg , e83b7fb5.jpeg , 4ba47355.jpeg , 9ec87d83.jpeg , 247e2208.jpeg , 2f24aa8d.jpeg , 9e3f0dbc.jpeg , ae745f50.jpeg , 447d2d88.jpeg , Sugar Pine Village.pdf , 032-291-028-100_ELDCO Recorder.pdf , 032-291-028-100_HPI.pdf , 032-291-031-100_ELDCO Recorder.pdf , 032-291-031-100_HPI.pdf , Up in smoke—California's greenhouse gas reductions could be wiped out by 2020 wildfires.pdf , NATURE—Rate of tree carbon accumulation increases continuously with tree size.pdf , Exceeding 1.5°C Global Warming Could Trigger Multiple Climate Tipping Points.pdf , Tipping elements in the Earth's climate system.pdf , CTC_TCAP_Amendment_Public_Comments.pdf , 06-LTS_1.PDF , Low-elevation conifers in California's Sierra Nevada are out of equilibrium with climate.pdf

---

Dear City Council,

Don't destroy our conserved land parcels! This will release thousands of tons of sequestered carbon dioxide into the atmosphere, and **set a horrible precedent on developing conserved lands**. The highly divisive Tahoe "Prosperity" Center, all its real estate investment capitalist board members, Chase Janvrin, and Heidi Hill-Drum have rigged the housing debate such that we can have housing or save the environment, but not both. It is a completely bogus argument. **Do not develop Tahoe Conservancy lands**. This will have a significant effect on the environment. It is a carbon sink which is needed more than ever to mitigate climate change. Most of our carbon offset credits are created by planting trees and promising not to cut them down. Your development planning approvals are proving what a scam this really is. Conserved lands are ineligible for streamlined development into housing projects (PRC §§ 9951-9953, & 21159.21(i)&(j)). This conserved land was supposed to be retired in a natural state without impervious coverage in accordance with the TRPA threshold standards and the regional plan.

Moreover, the federal TRPA Compact expressly states that "urbanization is threatening the ecological values of the region and threatening the public opportunities for use of the public lands" (PUBLIC LAW 96-551 – DEC. 19, 1980, ARTICLE I(a)(5)). Urbanization of public lands is precisely what is occurring when we inappropriately place high density multi-story apartments on public conservancy land. The Regional Plan and Code of Ordinances may not violate the Compact (*Decker v. Northwest Environmental Defense Center*, 568 U.S. 597, 609 (2013) (Regulations, in order to be valid, must be consistent with the statute under which they are promulgated); *U.S. v. Larionoff*, 431 U.S. 864, 873 (1977) (In order to be valid, regulations must be consistent with the statute under which they are promulgated); *Credit One Bank, N.A. v. Hestrin*, 60 F.4th 1220, 1231 (9th Cir. 2023) (An agency's regulation cannot trump the Supreme Court or Congress)). Agencies must abide by their own rules and regulations (*Accardi v. Shaughnessy*, 347 U.S. 260, 268 (1954) (objecting to administrative body's "failure to exercise its own discretion, contrary to existing valid regulations"); *Service v. Dulles*, 354 U.S. 363, 388 (1957) ("Secretary…could not, so long as the Regulations remained unchanged, proceed without regard to them"); *Vitarelli v. Seaton*, 359 U.S. 535, 539-40 (1959) ("Secretary…was bound by the regulations which he himself had promulgated"); *United States v. Nixon*, 418 U.S. 683, 695 (1974) (So long as regulation was extant, it had force of law, Executive Branch was bound by it, and United States as sovereign composed of three branches was bound to respect and enforce it); *Bennett v. Spear*, 520 U.S. 154, 172 (1997) ("It is rudimentary administrative law that discretion as to the substance of the ultimate decision does not confer discretion to ignore the required procedures of decisionmaking"); s*ee also*, *Nat'l Cable & Telecomms. Ass'n v. Brand X Internet Servs.*, 545 U.S. 967, 981 (2005) (an agency action that departs from a prior policy without acknowledging the change, or that creates an "unexplained inconsistency" with prior policy is generally viewed as arbitrary and capricious)). If the regulation's text is unambiguous, there is no deference to an agency's interpretation (*Kisor v. Wilkie*, 88 U. S. ____, 139 S. Ct. 2400, 2415 (2019) ("The regulation then just means what it means"); *Attias v. Crandall*, 968 F.3d 931, 937 (9th Cir. 2020); *Larson v. Saul*, 967 F.3d 914, 922 (9th Cir. 2020)). TRPA ordinances are federal law and may not be preempted by City or State conservancy (*Lake Tahoe Watercraft Recreation Ass'n v. TRPA*, 24 F.Supp.2d 1062, 1069 (1998) (TRPA ordinance was federal law rather than state law, and compact under which ordinance was adopted did not reserve rights of states which had any bearing on substance of ordinance)). The TRPA Regional Plan itself is being violated (*e.g.*, CD-2.1(A)(v), SR-1, & OS-1) (Planning shall "where feasible, establish park or open space corridors connecting undisturbed sensitive areas within Centers to undisturbed areas outside of Centers"; "Maintain and restore the scenic qualities of the natural appearing landscape"; "Manage areas of open space to promote conservation of vegetation and Protection of watersheds").

SUGAR PINE VILLAGE WILL DESTROY 11 ACRES OF CONSERVED LANDS

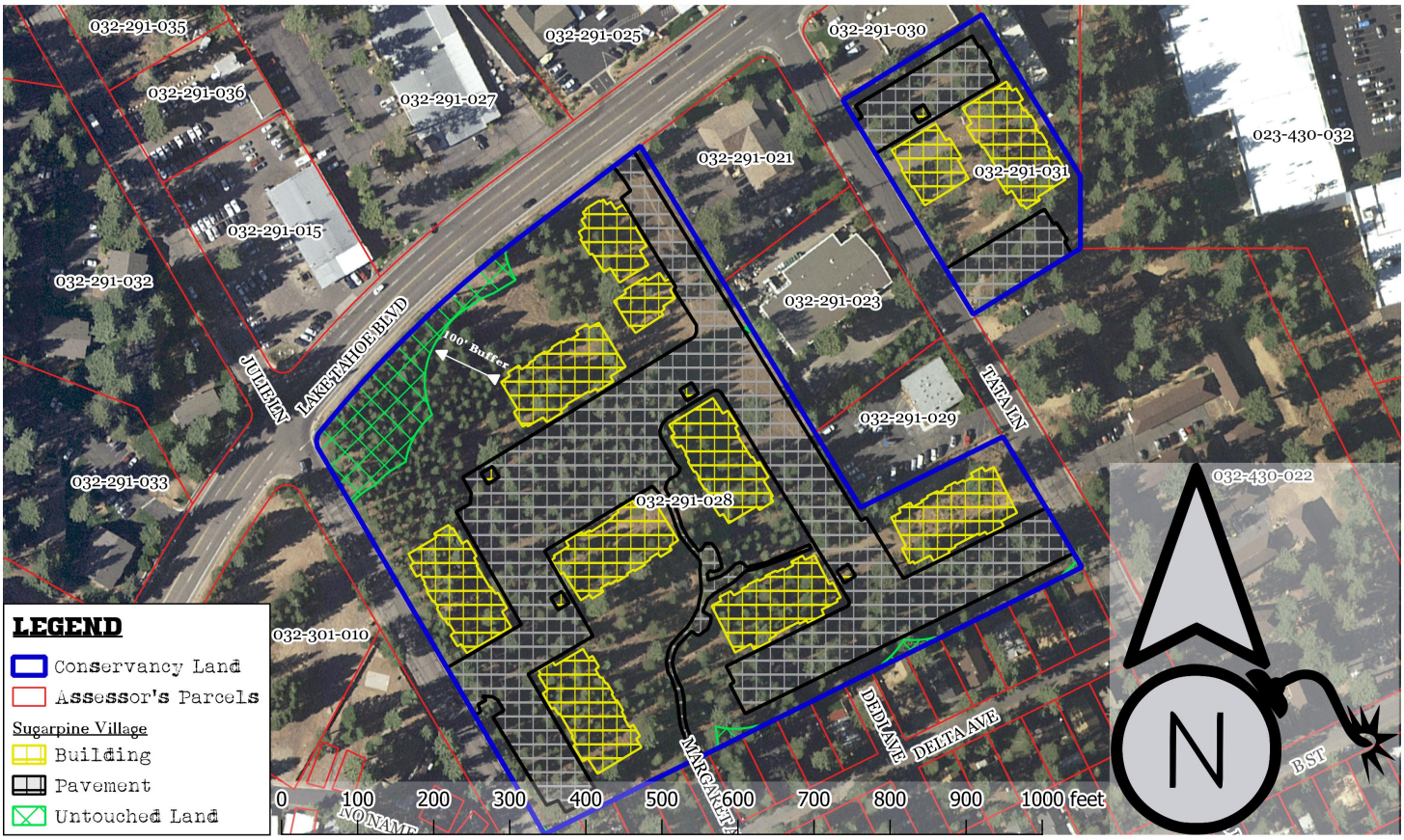

The California Tahoe Conservancy was established in 1985 to lead efforts to restore and enhance the extraordinary natural and recreational resources of the Lake Tahoe Basin. Parcels 28 and 31 were purchased just a few years later in the spring of 1989 towards this goal. In the decades since, development interests have hijacked the Conservancy, with plans to destroy and pave over a healthy stand of forest habitat releasing thousands of tons of climate-warming CO2 from this "carbon sink." The construction footprint will be 6.5 acres of the combined 11.6 acre lot. A statutory (PRC § 4291) 100' buffer from structures for "defensible space" will result in the clearcutting of 95% of the conserved lands with only 0.56 acres of habitat remaining.

Cutting down our last remaining carbons sinks while simultaneously thinking we can somehow offset climate change is a **SCAM**.

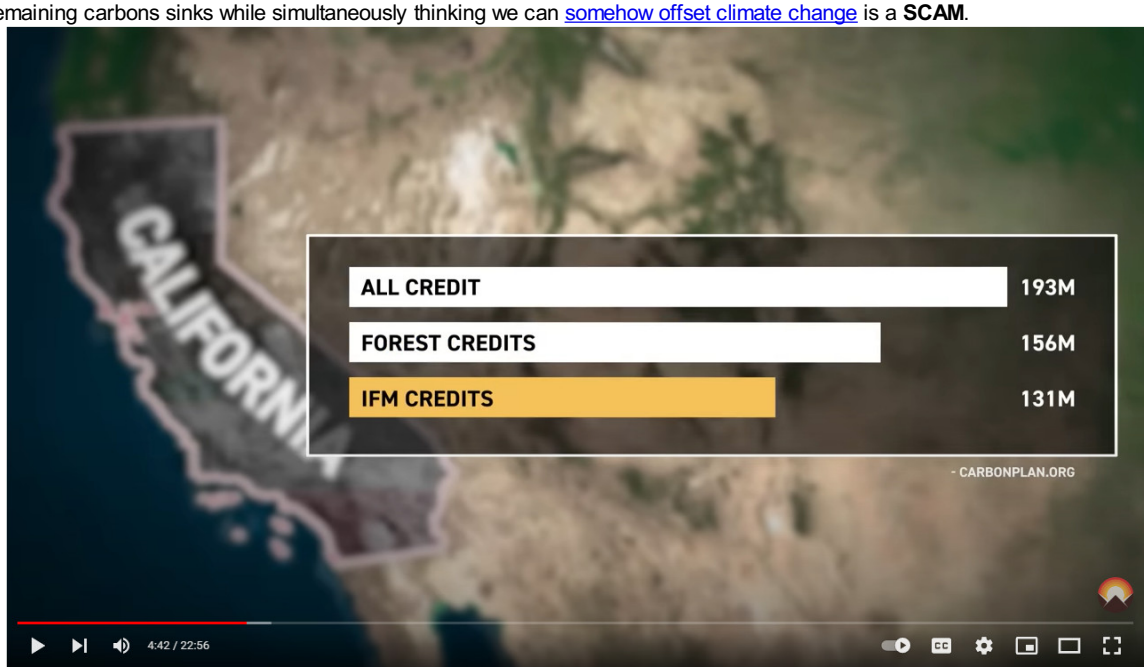

It is a scam so obvious, even a comedian can blow it to pieces:

Moreover, we pretend to plant new trees to offset carbon emissions, but then they all burn down in a single fire season:

Environmental Pollution 310 (2022) 119888

Contents lists available at ScienceDirect

Environmental Pollution

journal homepage: www.elsevier.com/locate/envpol

Up in smoke: California's greenhouse gas reductions could be wiped out by 2020 wildfires☆

Michael Jerrett [a,*], Amir S. Jina [b], Miriam E. Marlier [a]

[a] Department of Environmental Health Sciences, Fielding School of Public Health, University of California, Los Angeles, 650 Charles E. Young Dr. S., 56-070 CHS Box 951772, Los Angeles, CA, 90095, USA
[b] Harris School of Public Policy, University of Chicago, 1307 East 60th Street, Chicago, IL, 60637, USA

ARTICLE INFO

Keywords:
Climate change
Wildfires
Greenhouse gas emissions
Economic impacts

ABSTRACT

In this short communication, we estimate that California's wildfire carbon dioxide equivalent (CO_2e) emissions from 2020 are approximately two times higher than California's total greenhouse gas (GHG) emission reductions since 2003. Without considering future vegetation regrowth, CO_2e emissions from the 2020 wildfires could be the second most important source in the state above either industry or electrical power generation. Regrowth may partly of fully occur over a long period, but due to exigencies of the climate crisis most of the regrowth will not occur quickly enough to avert greater than 1.5 degrees of warming. Global monetized damages caused by CO_2e from in 2020 wildfire emissions amount to some $7.1 billion USD. Our analysis suggests that significant societal benefits could accrue from larger investments in improved forest management and stricter controls on new development in fire-prone areas at the wildland-urban interface.

1. Introduction

Recent evidence suggests that climate change contributes to increased wildfire activity in the western United States (Abatzoglou and Williams, 2016). California's summer wildfire burned area increased eightfold from 1972 to 2018 (Williams et al., 2019), and statewide climate change projections predict an amplification of wildfire risk due to higher temperatures and drier conditions (Westerling, 2018). Climate change exacerbates fire risks already stoked by increasing development near the wildland-urban interface (WUI) that have made humans the main ignition source in California (Keeley and Syphard, 2018), as well as decades of fire suppression and underinvestment in preventive measures such as mechanical clearing or prescribed burns (Keeley and Syphard, 2021; Kolden, 2019; Radeloff et al., 2018). Wildfires, in turn, release GHG emissions that can contribute to climate change.

California experienced its most disastrous wildfire year on record in 2020. CalFire, the state agency responsible for leading California's wildfire prevention and suppression, reports that 1.7 million hectares burned in 2020 (CalFire, 2022). Many of the worst fire years in California's history have occurred in the past 20 years, with eighteen of the top 20 most destructive fires in terms of loss of life and property since 2000 and five in 2020 alone (CalFire, 2021). The 2020 fires have been followed by another extreme fire season with 1.0 million hectares burned in 2021.

In addition to the immediate loss of life and property, hospital admissions and premature deaths have likely happened because of the smoke exposure (Cascio, 2018; Fann et al., 2018; Reid et al., 2016; Wang et al., 2020), which blanketed large parts of the state with tens of millions of people with unhealthy air quality that persisted for months in some locations. Recent estimates put the economic costs of direct health costs at $32 billion for 2018 (Wang et al., 2020). Future climate projections suggest that wildfires will become an increasingly important source of air pollution in the western U.S. (Ford et al., 2018; Liu et al., 2016).

When forests burn and are not balanced by vegetation regrowth, they shift from a natural sink to a source of carbon (van der Werf et al., 2017). This can represent a positive climate feedback loop in which increased GHG emissions contribute to climate change and further increase wildfire risk. Although wildfires are a natural feature of many ecosystems in California, the increase in severe and frequent wildfire events has raised the possibility of transformed post-fire ecosystems as new plant communities regrow following fire events that alter carbon

☆ This paper has been recommended for acceptance by Pavlos Kassomenos.
* Corresponding author.
E-mail addresses: mjerrett@ucla.edu (M. Jerrett), mmarlier@ucla.edu (M.E. Marlier).

https://doi.org/10.1016/j.envpol.2022.119888
Received 10 April 2022; Received in revised form 1 July 2022; Accepted 31 July 2022
Available online 5 August 2022
0269-7491/© 2022 The Authors. Published by Elsevier Ltd. This is an open access article under the CC BY license (http://creativecommons.org/licenses/by/4.0/).

Moreover, mature trees such as this protected Tahoe Conservancy grove—*which is also protected by the city from wildfire*—obviously store way more carbon dioxide than new carbon offset tree plantings:

LETTER

doi:10.1038/nature12914

Rate of tree carbon accumulation increases continuously with tree size

N. L. Stephenson[1], A. J. Das[1], R. Condit[2], S. E. Russo[3], P. J. Baker[4], N. G. Beckman[3]†, D. A. Coomes[5], E. R. Lines[6], W. K. Morris[7], N. Rüger[2,8]†, E. Álvarez[9], C. Blundo[10], S. Bunyavejchewin[11], G. Chuyong[12], S. J. Davies[13], Á. Duque[14], C. N. Ewango[15], O. Flores[16], J. F. Franklin[17], H. R. Grau[10], Z. Hao[18], M. E. Harmon[19], S. P. Hubbell[2,20], D. Kenfack[13], Y. Lin[21], J.-R. Makana[15], A. Malizia[10], L. R. Malizia[22], R. J. Pabst[19], N. Pongpattananurak[23], S.-H. Su[24], I-F. Sun[25], S. Tan[26], D. Thomas[27], P. J. van Mantgem[28], X. Wang[18], S. K. Wiser[29] & M. A. Zavala[30]

Forests are major components of the global carbon cycle, providing substantial feedback to atmospheric greenhouse gas concentrations[1]. Our ability to understand and predict changes in the forest carbon cycle—particularly net primary productivity and carbon storage—increasingly relies on models that represent biological processes across several scales of biological organization, from tree leaves to forest stands[2,3]. Yet, despite advances in our understanding of productivity at the scales of leaves and stands, no consensus exists about the nature of productivity at the scale of the individual tree[4–7], in part because we lack a broad empirical assessment of whether rates of absolute tree mass growth (and thus carbon accumulation) decrease, remain constant, or increase as trees increase in size and age. Here we present a global analysis of 403 tropical and temperate tree species, showing that for most species mass growth rate increases continuously with tree size. Thus, large, old trees do not act simply as senescent carbon reservoirs but actively fix large amounts of carbon compared to smaller trees; at the extreme, a single big tree can add the same amount of carbon to the forest within a year as is contained in an entire mid-sized tree. The apparent paradoxes of individual tree growth increasing with tree size despite declining leaf-level[8–10] and stand-level[10] productivity can be explained, respectively, by increases in a tree's total leaf area that outpace declines in productivity per unit of leaf area and, among other factors, age-related reductions in population density. Our results resolve conflicting assumptions about the nature of tree growth, inform efforts to understand and model forest carbon dynamics, and have additional implications for theories of resource allocation[11] and plant senescence[12].

A widely held assumption is that after an initial period of increasing growth, the mass growth rate of individual trees declines with increasing tree size[4,5,13–16]. Although the results of a few single-species studies have been consistent with this assumption[15], the bulk of evidence cited in support of declining growth is not based on measurements of individual tree mass growth. Instead, much of the cited evidence documents either the well-known age-related decline in net primary productivity (hereafter 'productivity') of even-aged forest stands[10] (in which the trees are all of a similar age) or size-related declines in the rate of mass gain per unit leaf area (or unit leaf mass)[8–10], with the implicit assumption that declines at these scales must also apply at the scale of the individual tree. Declining tree growth is also sometimes inferred from life-history theory to be a necessary corollary of increasing resource allocation to reproduction[11,16]. On the other hand, metabolic scaling theory predicts that mass growth rate should increase continuously with tree size[6], and this prediction has also received empirical support from a few site-specific studies[6,7]. Thus, we are confronted with two conflicting generalizations about the fundamental nature of tree growth, but lack a global assessment that would allow us to distinguish clearly between them.

To fill this gap, we conducted a global analysis in which we directly estimated mass growth rates from repeated measurements of 673,046 trees belonging to 403 tropical, subtropical and temperate tree species, spanning every forested continent. Tree growth rate was modelled as a function of log(tree mass) using piecewise regression, where the independent variable was divided into one to four bins. Conjoined line segments were fitted across the bins (Fig. 1).

For all continents, aboveground tree mass growth rates (and, hence, rates of carbon gain) for most species increased continuously with tree mass (size) (Fig. 2). The rate of mass gain increased with tree mass in each model bin for 87% of species, and increased in the bin that included the largest trees for 97% of species; the majority of increases were statistically significant (Table 1, Extended Data Fig. 1 and Supplementary Table 1). Even when we restricted our analysis to species achieving the largest sizes (maximum trunk diameter >100 cm; 33% of species), 94% had increasing mass growth rates in the bin that included the largest trees. We found no clear taxonomic or geographic patterns among the 3% of species with declining growth rates in their largest trees, although the small number of these species (thirteen) hampers inference. Declining species included both angiosperms and gymnosperms in seven of the 76 families in our study; most of the seven families had only one or two declining species and no family was dominated by declining species (Supplementary Table 1).

When we log-transformed mass growth rate in addition to tree mass, the resulting model fits were generally linear, as predicted by metabolic scaling theory[6] (Extended Data Fig. 2). Similar to the results of our main

[1]US Geological Survey, Western Ecological Research Center, Three Rivers, California 93271, USA. [2]Smithsonian Tropical Research Institute, Apartado 0843-03092, Balboa, Republic of Panama. [3]School of Biological Sciences, University of Nebraska, Lincoln, Nebraska 68588, USA. [4]Department of Forest and Ecosystem Science, University of Melbourne, Victoria 3121, Australia. [5]Department of Plant Sciences, University of Cambridge, Cambridge CB2 3EA, UK. [6]Department of Geography, University College London, London WC1E 6BT, UK. [7]School of Botany, University of Melbourne, Victoria 3010, Australia. [8]Spezielle Botanik und Funktionelle Biodiversität, Universität Leipzig, 04103 Leipzig, Germany. [9]Jardín Botánico de Medellín, Calle 73, No. 51D-14, Medellín, Colombia. [10]Instituto de Ecología Regional, Universidad Nacional de Tucumán, 4107 Yerba Buena, Tucumán, Argentina. [11]Research Office, Department of National Parks, Wildlife and Plant Conservation, Bangkok 10900, Thailand. [12]Department of Botany and Plant Physiology, Buea, Southwest Province, Cameroon. [13]Smithsonian Institution Global Earth Observatory—Center for Tropical Forest Science, Smithsonian Institution, PO Box 37012, Washington, DC 20013, USA. [14]Universidad Nacional de Colombia, Departamento de Ciencias Forestales, Medellín, Colombia. [15]Wildlife Conservation Society, Kinshasa/Gombe, Democratic Republic of the Congo. [16]Unité Mixte de Recherche—Peuplements Végétaux et Bioagresseurs en Milieu Tropical, Université de la Réunion/CIRAD, 97410 Saint Pierre, France. [17]School of Environmental and Forest Sciences, University of Washington, Seattle, Washington 98195, USA. [18]State Key Laboratory of Forest and Soil Ecology, Institute of Applied Ecology, Chinese Academy of Sciences, Shenyang 110164, China. [19]Department of Forest Ecosystems and Society, Oregon State University, Corvallis, Oregon 97331, USA. [20]Department of Ecology and Evolutionary Biology, University of California, Los Angeles, California 90095, USA. [21]Department of Life Science, Tunghai University, Taichung City 40704, Taiwan. [22]Facultad de Ciencias Agrarias, Universidad Nacional de Jujuy, 4600 San Salvador de Jujuy, Argentina. [23]Faculty of Forestry, Kasetsart University, ChatuChak Bangkok 10900, Thailand. [24]Taiwan Forestry Research Institute, Taipei 10066, Taiwan. [25]Department of Natural Resources and Environmental Studies, National Dong Hwa University, Hualien 97401, Taiwan. [26]Sarawak Forestry Department, Kuching, Sarawak 93660, Malaysia. [27]Department of Botany and Plant Pathology, Oregon State University, Corvallis, Oregon 97331, USA. [28]US Geological Survey, Western Ecological Research Center, Arcata, California 95521, USA. [29]Landcare Research, PO Box 40, Lincoln 7640, New Zealand. [30]Forest Ecology and Restoration Group, Department of Life Sciences, University of Alcalá, Alcalá de Henares, 28805 Madrid, Spain. †Present addresses: Mathematical Biosciences Institute, Ohio State University, Columbus, Ohio 43210, USA (N.G.B.); German Centre for Integrative Biodiversity Research (iDiv), Halle-Jena-Leipzig, 04103 Leipzig, Germany (N.R.).

©2014 Macmillan Publishers Limited. All rights reserved

and

PNAS Nexus, 2023, 2, 1–9
https://doi.org/10.1093/pnasnexus/pgad004
Advance access publication 28 February 2023
Research Report

Low-elevation conifers in California's Sierra Nevada are out of equilibrium with climate

Avery P. Hill[a,*], Connor J. Nolan[b], Kyle S. Hemes[b], Trevor W. Cambron[c] and Christopher B. Field[a,b,c]

[a]Department of Biology, Stanford University, Stanford, CA, USA
[b]Woods Institute for the Environment, Stanford University, Stanford, CA, USA
[c]Department of Earth System Science, Stanford University, Stanford, CA, USA
*To whom correspondence should be addressed: Email: aph82@stanford.edu
Edited By: Adelia Bovell-Benjamin

Abstract

Since the 1930s, California's Sierra Nevada has warmed by an average of 1.2°C. Warming directly primes forests for easier wildfire ignition, but the change in climate also affects vegetation species composition. Different types of vegetation support unique fire regimes with distinct probabilities of catastrophic wildfire, and anticipating vegetation transitions is an important but undervalued component of long-term wildfire management and adaptation. Vegetation transitions are more likely where the climate has become unsuitable but the species composition remains static. This vegetation climate mismatch (VCM) can result in vegetation conversions, particularly after a disturbance like wildfire. Here we produce estimates of VCM within conifer-dominated forests in the Sierra Nevada. Observations from the 1930s Wieslander Survey provide a foundation for characterizing the historical relationship between Sierra Nevada vegetation and climate before the onset of recent, rapid climate change. Based on comparing the historical climatic niche to the modern distribution of conifers and climate, ~19.5% of modern Sierra Nevada coniferous forests are experiencing VCM, 95% of which is below an elevation of 2356 m. We found that these VCM estimates carry empirical consequences: likelihood of type-conversion increased by 9.2% for every 10% decrease in habitat suitability. Maps of Sierra Nevada VCM can help guide long-term land management decisions by distinguishing areas likely to transition from those expected to remain stable in the near future. This can help direct limited resources to their most effective uses—whether it be protecting land or managing vegetation transitions—in the effort to maintain biodiversity, ecosystem services, and public health in the Sierra Nevada.

Keywords: ecology, habitat suitability modeling, vegetation transitions, vegetation climate mismatch, climate change, California

Significance Statement

Warming climatic conditions over the last century have led to observable shifts in the spatial organization of dominant tree species in California's Sierra Nevada. Little is known, however, about the extent to which these shifts have tracked the magnitude of climate change. This study maps Vegetation Climate Mismatch in the Sierra Nevada—areas where climate change has left trees in climatic conditions where they have not historically occurred. Different vegetation types support different wildfire regimes, ecosystems, and ecosystem services. Our maps will be useful for anticipating vegetation transitions and informing long-term wildfire and ecosystem management across the Sierra Nevada mountains of California.

Introduction

Warmer and drier conditions prime forests for ignition (1), but climate change also directly affects the species composition of future vegetation. Climate-driven vegetation conversion is an understudied phenomenon in general and a potentially significant determinant of catastrophic wildfire risk that could require changes in management strategies (2–4).

Broadly, climate change has caused vegetation to shift poleward and up-slope (5–7). In long-lived ecosystems like forests, climate change is occurring faster than the ability of many plants to shift their distributions or adapt, resulting in vegetation disequilibrium (8) or vegetation climate mismatch (VCM). Forests experiencing VCM are at risk of converting to alternative species assemblages, particularly after stand-replacing disturbances such as severe wildfire (4). In some cases, VCM can even make forests more susceptible to wildfires (9).

VCM is likely to be found in California's transition zone between low-elevation conifer-dominated forest and angiosperm-dominated vegetation (including mixed chaparral, oak woodland, and mixed broadleaf forest) (Fig. 1; elevation ~1000–1400 m)—where the foothills of the Sierra Nevada end and the mountains of the western flank begin. These forests lie on the warm end of mixed conifer distributions, where canopy dominants include ponderosa pine, sugar pine, and Douglas-fir (10), and understories

Competing Interest: The authors declare that they have no competing interests.
Received: July 16, 2022. **Revised:** December 19, 2022. **Accepted:** January 4, 2023
© The Author(s) 2023. Published by Oxford University Press on behalf of National Academy of Sciences. This is an Open Access article distributed under the terms of the Creative Commons Attribution License (https://creativecommons.org/licenses/by/4.0/), which permits unrestricted reuse, distribution, and reproduction in any medium, provided the original work is properly cited.

Downloaded from https://academic.oup.com/pnasnexus/article/2/2/pgad004/7059010 by guest on 23 March 2023

No Joke, Tahoe Forest are going towards extinct:

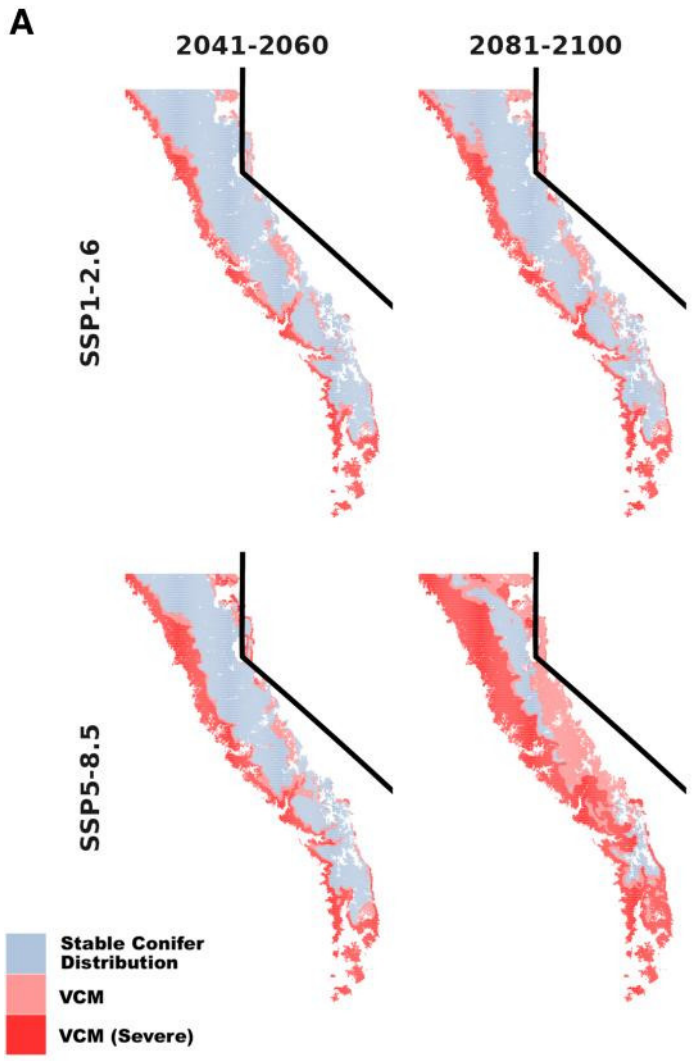

The black angled line is the California-Nevada Border which changes direction in the middle of Lake Tahoe. The colored areas are conifer forests along the 400 mile-long Sierra Nevada mountain range. The red areas are where current forests will become zombie forests in the near future meaning they will not naturally regrow once they are cut or burnt down. The columns depict the forests at the future years 2041 and 2081, the rows bracket the forest degradation between the expected future CO2 emissions range. The image below shows the forest's current status:

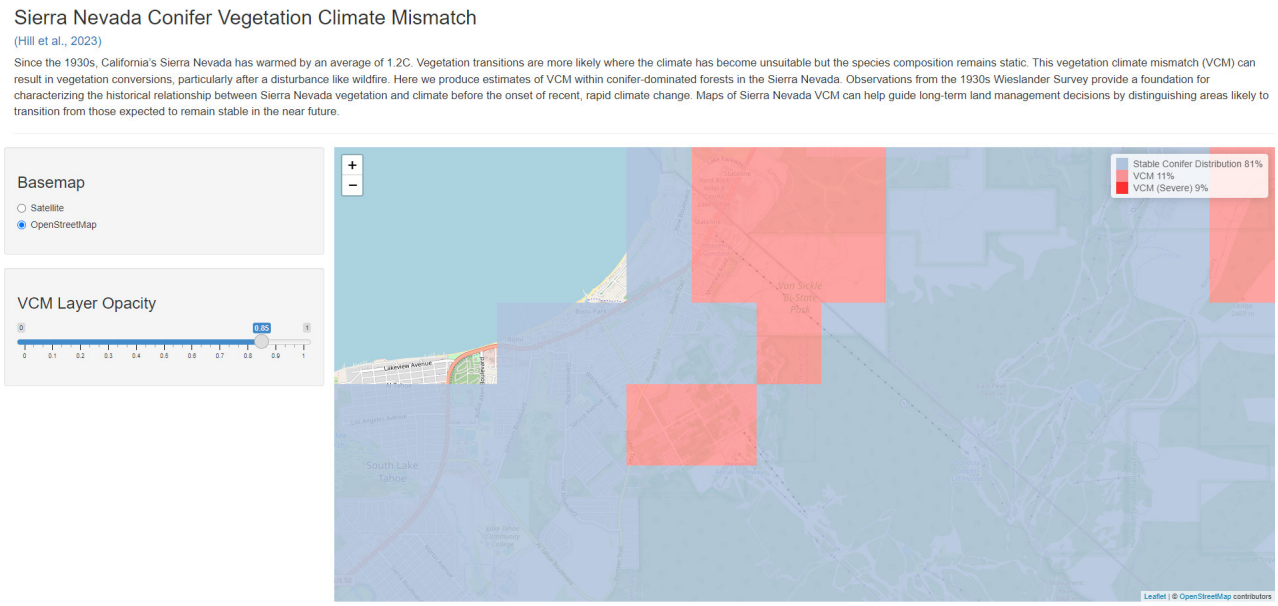

Current "zombie forest" areas include the upper Ski Run neighborhood being diseased by a macro cell tower and the trees immediately south of Montreal Road which are to be clear cut for high-end condos. The TRPA has failed to protect current and anticipated Zombie's forests with much needed threshold standards.

The corrupt Tamara Wallace and Stuart Roll (Julie Roll's spouse) are undermining the environmental mission of the Tahoe Conservancy through Wallace's board membership. Despite her bragging how well she understood city planning laws and plans, she already illegally tried to stop the restoration of the "Motel 6" stream environmental zone, despite such being mandated by the regional plan:

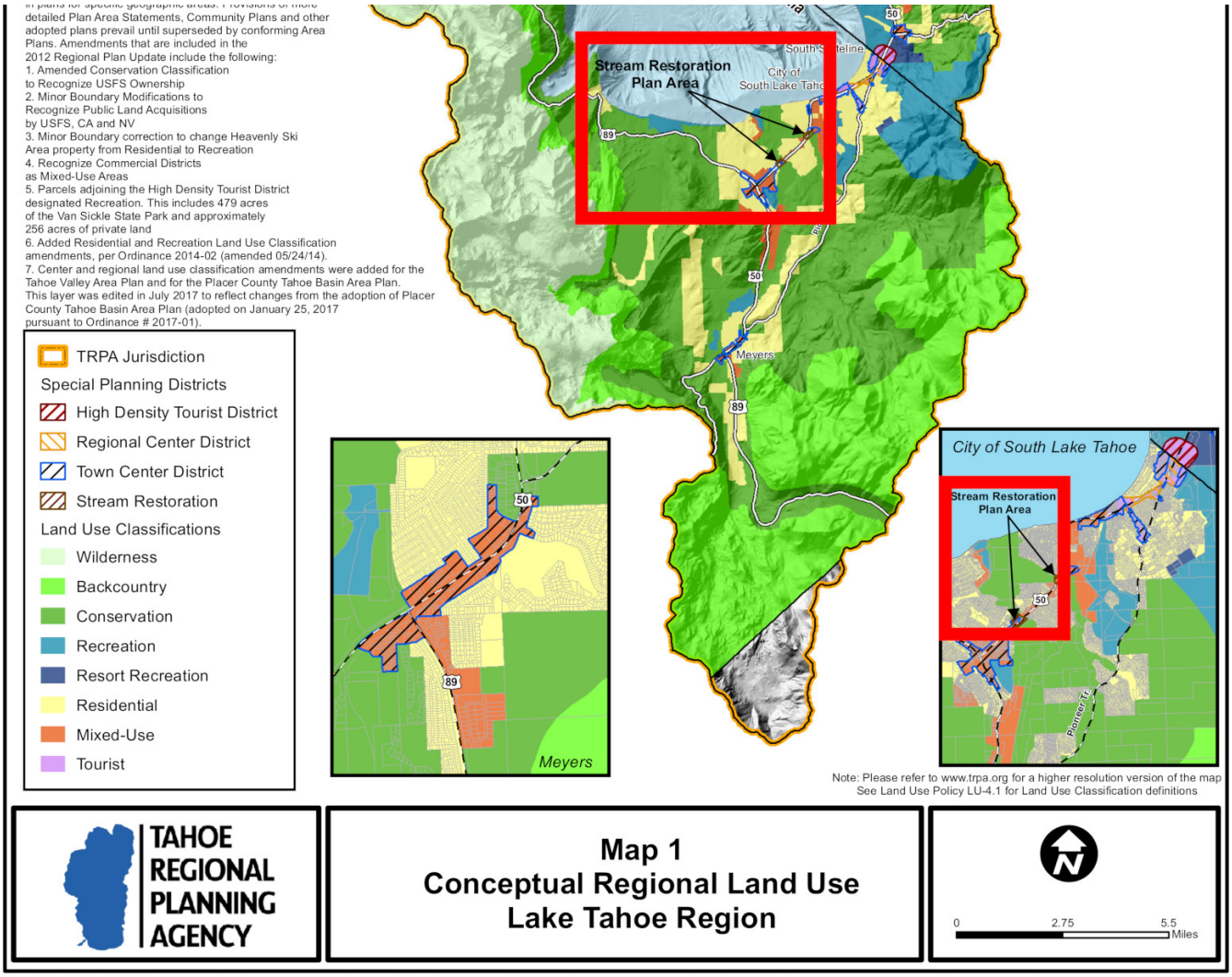

TRPA MAP DISCLAIMER: This map was developed and produced by the TRPA GIS department. It is provided for reference only and is not intended to show map scale accuracy or all inclusive map features. The material on this map was compiled using the most current data available, but the data is dynamic and accuracy cannot be guaranteed. Document Path: F:\GIS\MXDS\Regional Plan Update\Jan2014Recreated\Map1_ConceptualRegLandUse_2017amendment.mxd

We already have enough vacant housing stock (BAE Urban Economics. "*Analysis of Local Funding Source(s) for Housing Initiatives*," p.18 (01/13/2023)):

To estimate the possible order of magnitude of the revenue that may be generated under a likely residential vacancy tax scenario, BAE assumed a tax of $3,000 per vacant unit, which is generally consistent with the tax being charged in Oakland. Assuming that all housing units held vacant for seasonal or occasional use would be subject to the tax, BAE estimates that a vacancy tax could theoretically generate up to around $16.8 million per year.

Table 6: Housing Units by Vacancy Status and Tenure, 2020

		Occupied		
Units in Structure	**Vacant**	Renter	Owner	**Total**
1, detached	4,507	1,751	3,314	9,609
1, attached	175	396	73	636
2	292	526	162	971
3 or 4	566	729	17	1,315
5 to 9	397	750	3	1,144
10 to 19	161	575	13	738
20 to 49	197	319	21	536
50 or more	296	89	34	428
Mobile home	103	254	240	585
Boat, RV, van, etc.	0	0	0	0
Total, All Units	**6,695**	**5,390**	**3,876**	**15,961**
Percent	*42%*	*34%*	*24%*	*100%*

Source: U.S. Census Bureau, 2020 Decennial Census, Table H1; U.S. Census Bureau, 2020 American Community Survey 5-Year, Tables B25024 and B25032; BAE, 2022.

This report also considered applying the residential vacancy tax only to single-family properties held for seasonal or occasional use. While the Census Bureau does not specifically report the required statistic, the available data does indicate that there were around 4,500 single-family homes that were vacant for any reason as of the 2020 Decennial Census (i.e., roughly 47 percent of the single-family housing stock).[32] Assuming that the vacancy tax applies to single-family properties only, that are vacant for any reason, the tax could yield roughly $13.5 million per year in revenue.

Applying the citywide seasonal vacancy rate of 84 percent (i.e., the percent of vacant units held for seasonal or occasional use) to the 2020 vacant single-family inventory produces a conservative estimate of around 3,800 single-family units held for seasonal or occasional use. If the vacancy tax is applied only to single-family units held vacant for seasonal or occasional use, the tax may generate approximately nearly $11.4 million per year in revenue.

And there is a high enough housing turnover rate to buy them (2,610 units in six years—we can't even build that fast!) (*supra* at p.8):

Table 2: Residential Sales Activity, 2017 to 2022 YTD

All Residential Units	**2017**	**2018**	**2019**	**2020**	**2021**	**2022 YTD** (a)	**All Sales**
Number of Sales	348	341	389	625	513	394	2,610
Median Sale Price	$385,000	$420,000	$435,000	$500,000	$602,000	$642,500	$500,000
Ave. Sale price	$462,097	$514,954	$557,259	$624,223	$765,300	$791,868	$631,386
Ave. Size (sq. ft.)	1,494	1,495	1,552	1,626	1,561	1,548	1,556
Ave. Sale Price per sq.ft.	$311	$345	$365	$384	$493	$521	$408
Maximum Sale Price	$2,337,500	$2,450,000	$5,300,000	$5,200,000	$5,550,000	$5,300,000	$5,550,000
Minimum Sale Price	$71,000	$100,500	$46,000	$3,500	$50,000	$75,000	$3,500

Single Family Homes	**2017**	**2018**	**2019**	**2020**	**2021**	**2022 YTD** (a)	**All Sales**
Number of Sales	333	322	368	585	483	367	2,458
Median Sale Price	$389,000	$425,000	$440,000	$505,000	$613,000	$650,000	$505,000
Ave. Sale price	$462,217	$525,288	$563,064	$632,835	$783,050	$809,834	$641,131
Ave. Size (sq. ft.)	1,505	1,512	1,577	1,659	1,585	1,579	1,580
Ave. Sale Price per sq.ft.	$310	$349	$362	$381	$496	$522	$408
Maximum Sale Price	$2,200,000	$2,450,000	$5,300,000	$5,200,000	$5,550,000	$5,300,000	$5,550,000
Minimum Sale Price	$71,000	$100,500	$46,000	$3,500	$75,000	$75,000	$3,500

Condominiums	**2017**	**2018**	**2019**	**2020**	**2021**	**2022 YTD** (a)	**All Sales**
Number of Sales	15	19	21	40	30	27	152
Median Sale Price	$295,000	$265,000	$346,500	$354,250	$417,500	$480,000	$363,750
Ave. Sale price	$459,433	$339,816	$455,524	$498,275	$479,533	$547,667	$473,803
Ave. Size (sq. ft.)	1,236	1,203	1,106	1,144	1,171	1,118	1,156
Ave. Sale Price per sq.ft.	$328	$289	$421	$417	$445	$505	$414
Maximum Sale Price	$2,337,500	$799,000	$1,250,000	$2,700,000	$1,180,000	$1,349,000	$2,700,000
Minimum Sale Price	$180,000	$168,000	$97,500	$165,000	$50,000	$232,500	$50,000

Note:
(a) As of December 15, 2022.

Sources: ListSource; BAE, 2022.

Here is the housing stock—as you can see it is cheaper per room than Sugarpine's **$800,000** dollar per unit (Each unit...will cost about $808,823):

City of South Lake Tahoe — VHR Housing Stock

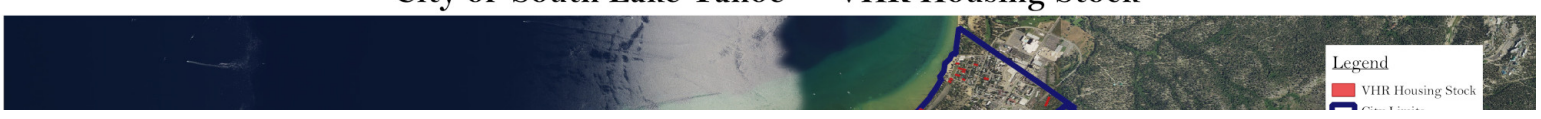

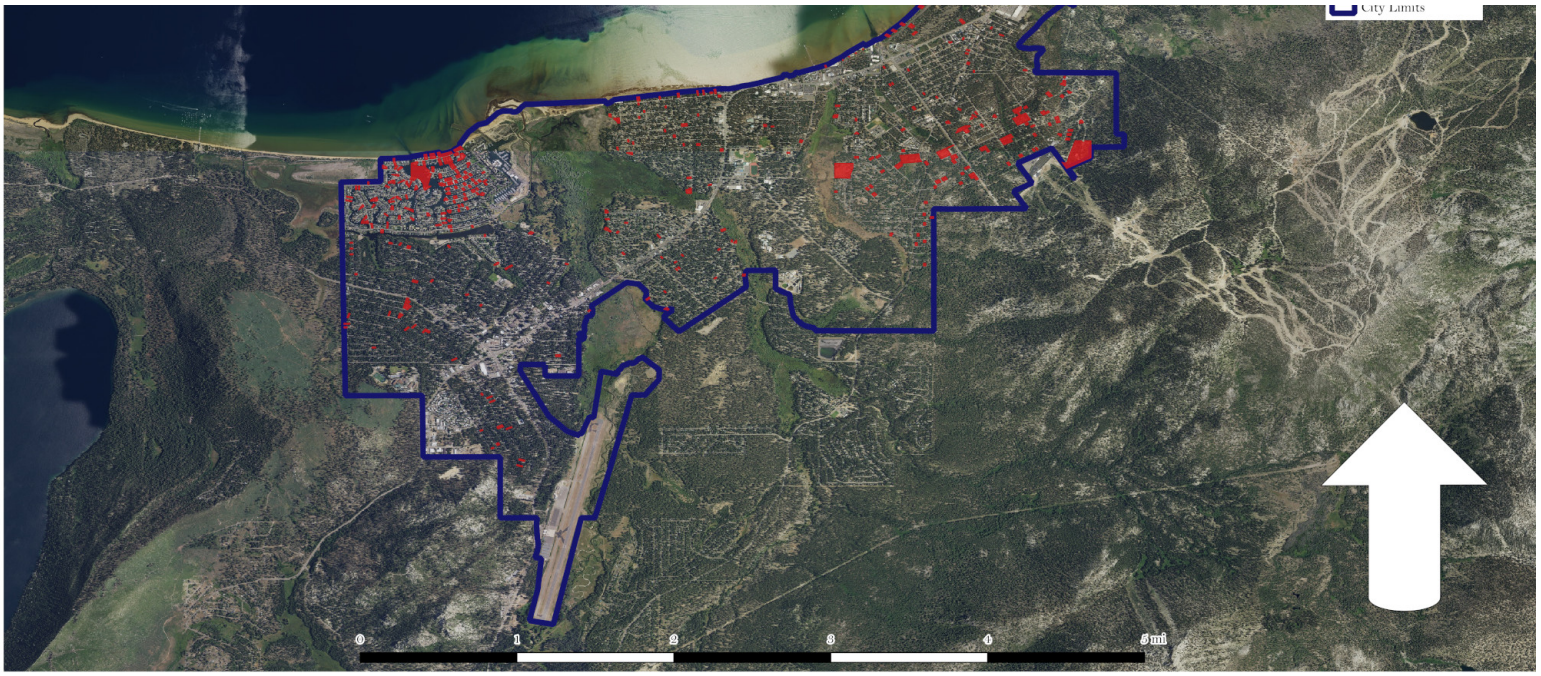

Within the City of South Lake Tahoe's municipal boundary limits, there are nearly 800 residences with five or more bedrooms. Depicted in this map are just the 360 "VHR mansion" style residences with five or more bedrooms, with 88 of them having six or more bedrooms. The City is currently spending over $800,000 per unit on the wasteful Sugarpine Village debacle which destroyed, urbanized, and privatized public conservancy land. The price per bedroom of these mansions is well below the cost the City is currently spending on low income housing. The City should acquire these mansions and deed restrict them into a workforce housing cooperative. One primary purpose of "Measure T" was to free up VHR residences for local residents.

ASSESSOR's #	PROPERTY ADDRESS	OWNER NAME	C/O DBA	OWNER ADDRESS	CITY	STATE	ZIP	BEDROOMS	VALUE	Value/Bedroom
022-031-067	2137 VENICE DR	2137 VENICE A DELAWARE LLC		529 GREENWICH ST	SAN FRANCISCO	CA	94133	9	$3,111,274	$345,697
030-380-070	3739 SADDLE RD	MORAN NEIL		3219 E CAMELBACK ROAD #120	PHOENIX	AZ	85018	9	$3,650,000	$405,556
022-261-005	287 BEACH DR	CAREN BARRY L TR & B LIV TRUST 10/9/98		PO BOX 5365	CARSON	CA	90749	8	$1,899,699	$237,462
025-510-072	1466 FRONTIER CT	SNYDER DARIN & CLAIRE		15 MAOLI DRIVE	SAN RAFAEL	CA	94903	8	$3,253,800	$406,725
026-061-012	3135 BELLEVUE AVE	SUTTLE JOHN C & JARIRI VIJEH MOJDEH & MCBRIDE SEAN		162 TOYON ROAD	ATHERTON	CA	94027	8	$2,741,760	$342,720
026-061-015	3123 BELLEVUE AVE	MOONHAVEN LODGE LLC		251 OAKHURST PL	MENLO PARK	CA	94025	8	$4,029,000	$503,625
031-121-010	1068 RENO AVE	CASALINO FAMILY TRUST 5/23/2006		1636 POMONA AVE	SAN JOSE	CA	95110	8	$126,000	$15,750
022-081-001	327 BEACH DR	ROSENDIN RAYMOND J TR & NANCY BURKE TR		443 WHISKEY HILL RD	WOODSIDE	CA	94062	7	$991,846	$141,692
022-231-031	1975 MARCONI WAY	ELLENOFF ERIC MATTHEW & BISHOP OLIVIA HSU	DBA RECOVERY RANCH	1975 MARCONI WAY	SOUTH LAKE TAHOE	CA	96150	7	$2,050,000	$292,857
022-262-004	296 BEACH DR	XATIVA NV LLC	DBA ORDAZ VACATION RENTAL	13 THORNHURST	SAN ANTONIO	TX	78218	7	$2,257,890	$322,556
025-021-038	3425 PIONEER TRL	WIRJO MAX & STECIA ANGELINE		11303 WINTER COTTAGE	LAS VEGAS	NV	89135	7	$1,147,500	$163,929
025-032-003	1460 SKI RUN BLVD	BEECH CRAIG		KINGSWOOD GORSE AVE	LITTLE HAMPTON BN 16 1SG			7	$1,716,222	$245,175
025-032-016	3639 SADDLE RD	PAUL JASON MATTHEW & JANINE PANIAGUA		3639 SADDLE ROAD	SOUTH LAKE TAHOE	CA	96150	7	$2,648,000	$378,286
026-084-004	3121 PASADENA AVE APT 1	LEE SUNG WOOK		12045 LLAGAS AVE	SAN MARTIN	CA	95046	7	$950,000	$135,714
026-154-009	2861 OAKLAND AVE	KALI KONA REAL ESTATE INVESTMENTS LLC CA LLC		9515 SOQUEL DR #211	APTOS	CA	95003	7	$1,917,600	$273,943
028-062-013	3908 BRIDLE RD	POONJA MOHAMED TR & ZAITUN TR		630 MILVERTON RD	LOS ALTOS	CA	94022	7	$1,465,683	$209,383
028-070-018	1387 NEBELHORN CT	DINEEN STEPHANIE A TR & FAMILY TRUST OF 2/13/80		31620 CITRUS AVE	REDLANDS	CA	92374	7	$1,197,590	$171,084
028-090-045	1399 WILDWOOD AVE	ODLAND DERRICK & KIMBERLEY		1780 CALLE PACIFICO	ARROYO GRANDE	CA	93420	7	$1,740,592	$248,656
028-090-070	1393 WILDWOOD AVE	CHANG HARRISON K TR		4354 SILVA CT	PALO ALTO	CA	94306	7	$1,118,500	$159,786
028-123-009	3752 OVERLOOK CT	NASH DANIEL TR & BETH TR		83 TUM SUDEN WAY	WOODSIDE	CA	94062	7	$1,698,787	$242,684
029-041-038	4081 MANZANITA AVE	MORENO EDDIE J & PATRICIA		PO BOX 16367	SOUTH LAKE TAHOE	CA	96151	7	$313,765	$44,824
029-403-033	3778 PIONEER TRL	NYE WILLIAM THOMAS TR & HULL NYE THERESA LORRAINE		16083 GRAMERCY DR	SAN LEANDRO	CA	94578	7	$251,659	$35,951
030-352-023	3717 REGINA RD	GALIATA JEFFREY J & SUSAN J		973 PALMER CIRCLE	FOLSOM	CA	95630	7	$1,494,320	$213,474
030-402-001	1707 SHERMAN WAY	MCGLYNN DANIEL J		861 DELGADO DRIVE	BATON ROUGE	LA	70808	7	$1,488,000	$212,571
032-251-016	1231 TATA LN	NISHIHIRA GAVIN & ARNETT SAVANNA		1231 TATA LANE	SOUTH LAKE TAHOE	CA	96150	7	$540,000	$77,143
022-051-008	2168 MONTEREY DR	CURRY DERRICK D TR & MAXINE A TR		17 FAIRWAY PL	HALF MOON BAY	CA	94019	6	$828,518	$138,086
022-051-060	2144 INVERNESS DR	MCNEAL MICHAEL & CHALLENOR ANGELA		PO BOX 66832	SCOTTS VALLEY	CA	95067	6	$1,550,000	$258,333
022-051-065	2131 INVERNESS DR	KUNHART JOHN & PAMELA		6015 ALTA LOMA PL	GRANITE BAY	CA	95746	6	$1,415,000	$235,833
022-061-024	2175 CATALINA DR	PHILIP BRIDGET M & BARRETT DIANA MARCHETTI		1440 VANCOUVER AVE	BURLINGAME	CA	94010	6	$629,552	$104,925
022-061-056	2158 BALBOA DR	NIKKAR ARASH & EDIE NICOLE TR		13 WOODHILL DRIVE	REDWOOD CITY	CA	94061	6	$2,698,776	$449,796
022-061-068	2229 BALBOA DR	MCCARTHY ROBERT J TR & SUZANNE B TR		354 SANTA CLARA AVE	SAN FRANCISCO	CA	94127	6	$486,958	$81,160
022-081-003	343 BEACH DR	MENG JIANHAO & JI JIANHUA		849 MELVILLE AVE	PALO ALTO	CA	94301	6	$3,171,079	$528,513
022-134-010	2197 TEXAS AVE	JIA JI 2015 FAM TR 11/12/2015		241 CLARA COURT	FREMONT	CA	94539	6	$1,326,000	$221,000
022-161-026	741 COLORADO CT	DEL NORTE LLC CA LLC		PO BOX 18533	SOUTH LAKE TAHOE	CA	96151	6	$552,110	$92,018
022-222-025	1997 GARMISH CT	SOTOODEH JOHN K TR & DELAINA C TR		133 15TH ST	MANHATTAN BEACH	CA	90266	6	$1,106,814	$184,469
022-251-071	2016 KOKANEE WAY	GUERRA FRANK VINCENT		45 SUNRISE DR	HOLLISTER	CA	95023	6	$691,991	$115,332
022-261-004	295 BEACH DR	PAVICICH ANDREW P TR & HELEN K TR		2435 FOREST AVE #200	SAN JOSE	CA	95128	6	$2,256,281	$376,047
022-262-003	300 BEACH DR	CASTANON PAULINA TR & DOZAR SEP PROP TR OF 11-12-8		13 THORNHURST	SAN ANTONIO	TX	78218	6	$1,077,502	$179,584
022-301-011	2051 ALOHA DR	VICARIO ANDRE & KIMBERLY		8814 E ANN WAY	SCOTTSDALE	AZ	85260	6	$2,503,591	$417,265
022-332-055	618 ALPINE DR	YUAN XINGCHAO CHUCK TR & YU JACKIE JIE TR		818 MELVILLE AVE	PALO ALTO	CA	94301	6	$796,812	$132,802
022-332-062	576 ALPINE DR	BAILON JOEL & RAYCHEL		730 VISTA GRANDE AVE	LOS ALTOS	CA	94024	6	$2,091,000	$348,500
023-152-007	703 ROGER AVE	LE LEON HUULAN & NGUYEN MINH CHAU LE CO TR		3913 CADWALLADER AVE	SAN JOSE	CA	95121	6	$2,575,000	$429,167
025-031-020	3583 MACKEDIE WAY	TAHO LTD CA LLC		6918 HIGLAND SPRING LANE	HIGHLAND	CA	92346	6	$2,193,000	$365,500
025-261-004	1291 HEATHER LAKE RD	SALOMON WAYNE		3863 ARBUTUS CT	HAYWARD	CA	94542	6	$95,649	$15,942
025-510-067	3478 SADDLE RD	KATANA GROUP LLC CA LLC		912 DIABLO DOWNS DRIVE	CLAYTON	CA	94517	6	$1,453,500	$242,250
025-552-001	3574 APRIL DR	HERMAN BRADLEY & TIMKINA ALENA		3574 APRIL DRIVE	SOUTH LAKE TAHOE	CA	96150	6	$1,798,000	$299,667
025-552-008	3482 EDNA ST	KELBUS KRISTY SUCC TR		3482 EDNA ST	SOUTH LAKE TAHOE	CA	96150	6	$99,236	$16,539
025-580-002	3353 NEEDLE PEAK RD	COLTON BENJAMIN ROWLAND TR & AUBREE NICOLE TR		8925 PLAZA PARK DR	ELK GROVE	CA	95624	6	$559,380	$93,230
025-580-006	3605 NEEDLE PEAK RD	DWELLEY MARK S & JEANETTE M TR		P O BOX 1081	BRENTWOOD	CA	94513	6	$1,800,000	$300,000
025-670-018	3511 PONY EXPRESS WAY	LE TOAN & DAO TRUONG AN THI		3511 PONY EXPRESS RD	SOUTH LAKE TAHOE	CA	96150	6	$862,068	$143,678
026-032-012	833 LAKEVIEW AVE	BETSCHART BARRETT E TR & B E LIV TR 10/11/07		827 LAKEVIEW AVE	SOUTH LAKE TAHOE	CA	96150	6	$306,756	$51,126
026-061-030	688 LILY AVE	SAVAS NIKKOS M C/O ANTHONY SAVAS & TERRY SAVAS	C/O ANTHONY SAVAS & TERRY		SOUTH LAKE TAHOE	CA	96150	6	$3,029,400	$504,900
026-102-027	830 SAN FRANCISCO AVE UNIT A	HUCK PROPERTIES CA LLC		57 GREEN HILLS COURT	HENDERSON	NV	89012	6	$512,190	$85,365
027-075-013	3669 FOREST AVE	EYMANN DARRELL R & THERESA C		3669 SOUTH FOREST AVE	SOUTH LAKE TAHOE	CA	96150	6	$205,887	$34,315
027-083-007	1033 PINE GROVE AVE	STATE OF CALIFORNIA & CALIFORNIA TAHOE CONSERVANCY		1061 3RD ST	SOUTH LAKE TAHOE	CA	96150	6	$1,040	$173
027-155-012	3689 SPRUCE AVE	D COSTA FAMILY TRUST 8/25/2005		21095 GARY DR #306	HAYWARD	CA	94546	6	$683,400	$113,900
027-344-039	1144 FAIRWAY AVE	MILLER TERRY E TR & T E REV TRUST 6/29/12		1120 SPRING ST #1604	SEATTLE	WA	98104	6	$409,415	$68,236
028-061-034	1475 BONITA RD	HEAVENLY HIDEAWAY CA LLC	DBA HEAVENLY HIDEAWAY VAC	4394 PEBBLE BEACH RD	ROCKLIN	CA	95765	6	$2,024,700	$337,450
028-082-002	3673 DAVID LN	KEMP CHRISTINA & GANJEI JAY		44815 INDUSTRIAL DR	FREMONT	CA	94538	6	$727,739	$121,290
028-082-003	3677 DAVID LN	GUPTA SARJU & UMESH		3520 LAKE TAHOE BLVD	SOUTH LAKE TAHOE	CA	96150	6	$795,600	$132,600
028-123-004	3774 OVERLOOK CT	RABISHAW ELISABETH & GARY		3829 ENCINO HILLS PLACE	ENCINO	CA	91436	6	$1,152,600	$192,100
028-320-004	3861 NEEDLE PEAK RD	SHEARER JOHN LYLE & SHANNON M TR		3861 NEEDLE PEAK RD	SOUTH LAKE TAHOE	CA	96150	6	$1,892,076	$315,346
029-101-023	3779 BEACH RD	SPELLMAN PATRICK M & WENDY A TR		38539 MISSION BLVD	FREMONT	CA	94536	6	$2,754,000	$459,000

029-103-001	3820 MEADOW RD	MCKEE REBECCA I TR		425 61ST ST	OAKLAND	CA	94609	6	$1,125,000	$187,500
029-106-001	3809 AZURE AVE	ROZANCE PAUL JOSEPH & BIRCHLER BRENDA MICHELE		130 SOUTH IVY STREET	DENVER	CO	80224	6	$1,223,490	$203,915
029-161-010	3835 PENTAGON RD	HILDEBRANDT ELZBIETA & DANIEL		1096 DAPHNE CT	MINDEN	NV	89423	6	$559,080	$93,180
029-181-020	3821 PIONEER TRL	JWD VENTURES CA LLC		PO BOX 1690	DIAMOND SPRINGS	CA	95619	6	$657,900	$109,650
029-422-031	3540 ROCKY POINT RD	LAWTON BRADLEY G & ROSEMARY N		PO BOX 1725	ZEPHYR COVE	NV	89448	6	$207,861	$34,644
029-604-004	4069 GREENWOOD RD	JEUNG PATRICIA Y TR & FONG JANICE	C/O JANICE FONG	156 CSM DR	SAN MATEO	CA	94402	6	$193,248	$32,208
029-710-007	UNASSIGNED	GONDOLA VISTA DEVE COMPANY LLC		PO BOX 121	ZEPHYR COVE	NV	89448	6	$1,619,446	$269,908
029-710-009	UNASSIGNED	GONDOLA VISTA DEVE COMPANY LLC		PO BOX 121	ZEPHYR COVE	NV	89448	6	$1,619,446	$269,908
029-710-011	UNASSIGNED	GONDOLA VISTA DEVE COMPANY LLC		PO BOX 121	ZEPHYR COVE	NV	89448	6	$1,619,446	$269,908
029-710-013	UNASSIGNED	GONDOLA VISTA DEVE COMPANY LLC		PO BOX 121	ZEPHYR COVE	NV	89448	6	$1,619,446	$269,908
029-710-015	UNASSIGNED	GONDOLA VISTA DEVE COMPANY LLC		PO BOX 121	ZEPHYR COVE	NV	89448	6	$1,619,446	$269,908
030-352-009	3708 VERDON LN	SAFDIE JUSTIN & GRETCHEN		971 PLEASANT HILL RD	LAFAYETTE	CA	94549	6	$1,351,500	$225,250
030-352-010	3714 VERDON LN	WILSON GERALD & TIFFANY		PO BOX 9050	SOUTH LAKE TAHOE	CA	96150	6	$700,000	$116,667
030-581-004	1468 JUNE WAY	NATSUM INVESTMENTS LLC CA LLC		1046 AL TAHOE BLVD BOX #13151	SOUTH LAKE TAHOE	CA	96150	6	$1,339,737	$223,290
031-174-008	1169 O MALLEY DR	BERMAN HAVA A TR & IRWIN IRREV TR 2/18/03		636 NORTH KIEL ST	HENDERSON	NV	89015	6	$113,777	$18,963
031-322-003	957 SILVERWOOD CIR	PITCHER EDWARD J & KATHY D		957 SILVERWOOD CIR	SOUTH LAKE TAHOE	CA	96150	6	$253,209	$42,202
031-331-015	2853 SPRINGWOOD DR	SZYPULA MICHAEL EDWARD & ERMINERO ELISA TR		222 8TH AVE	SAN MATEO	CA	94401	6	$601,503	$100,251
032-252-031	1220 TATA LN	HENDRIX B & C REV TRUST 8/14/2019		8855 ROCKY CANYON ROAD	ATASCADERO	CA	93422	6	$1,150,000	$191,667
032-282-060	1271 MARGARET AVE	DOHERTY FRANCES E & FAULKNOR GRAHAM DBA SHARED HOME RENTAL	DBA SHARED HOME RENTAL		SOUTH LAKE TAHOE	CA	96150	6	$566,100	$94,350
022-031-044	2156 MORRO DR	SCHONES HAUS CA LLC		2156 MORRO DR	SOUTH LAKE TAHOE	CA	96150	5	$1,576,869	$315,374
022-032-013	2196 VENICE DR	GAVRILOV ARTEM & GAVRILOVA HELEN		40353 LESLIE ST	FREMONT	CA	94538	5	$715,961	$143,192
022-032-025	2140 VENICE DR	PAKES FLOYD KIRK & BONNIE JEAN		2140 VENICE DR	SOUTH LAKE TAHOE	CA	96150	5	$287,135	$57,427
022-041-008	445 CAPRI DR	YING DANIEL & LIU HONGYING TR		10496 SOUTH STELLING RD	CUPERTINO	CA	95014	5	$699,318	$139,864
022-042-003	2249 INVERNESS DR	KULKA PETER & MARIA CO TR		5587 FORBES DR	NEWARK	CA	94560	5	$896,557	$179,311
022-051-013	2146 MONTEREY DR	CHEN LIANG L & LU QIAOLING		16799 POTTER CT	LOS GATOS	CA	95032	5	$867,108	$173,422
022-051-017	2126 MONTEREY DR	FRY MICHAEL FRANCIS CO TR & DEBORAH FAY CO TR		2733 WELLINGTON SOUTH	CARSON CITY	NV	89703	5	$984,928	$196,986
022-051-023	2151 MONTEREY DR	TAHOE HOUSE LLC		2400 MAIN ST #201	IRVINE	CA	92614	5	$351,529	$70,306
022-051-025	2161 MONTEREY DR	GOLDENBERG THOMAS A TR & GOLDENBERG T A REV TRUST		2161 MONTEREY DR	SOUTH LAKE TAHOE	CA	96150	5	$629,998	$126,000
022-051-046	2210 INVERNESS DR	HERSHEY STEVEN & LISA		1369 CORVIDAE ST	CARLSBAD	CA	92011	5	$734,524	$146,905
022-051-069	2149 INVERNESS DR	TRITSCHLER CHARLES G & DALE O TR		486 PACO DRIVE	LOS ALTOS	CA	94024	5	$1,224,312	$244,862
022-051-070	2155 INVERNESS DR	IWATA TOMOKO & TASHIRO MASAYUKI		2155 INVERNESS DR	SOUTH LAKE TAHOE	CA	96150	5	$1,440,240	$288,048
022-051-075	2179 INVERNESS DR	LEWALLEN LARRY DAVID & DEBRA DIANE CO TR		1040 E HERNDON #205	FRESNO	CA	93720	5	$1,098,480	$219,696
022-051-080	2205 INVERNESS DR	MCDEVITT ANDREW & KRISTEN		27 CORTE MORADA	KENTFIELD	CA	94904	5	$3,250,000	$650,000
022-051-081	2211 INVERNESS DR	WERCHICK GARY SR		2211 INVERNESS DR	SOUTH LAKE TAHOE	CA	96150	5	$366,339	$73,268
022-051-083	2221 INVERNESS DR	OGNESS MARTHA TR & MARTHA REV TR 7/14/10		22649 E JUDE LN	GILBERT	AZ	85298	5	$851,449	$170,290
022-051-087	534 TAHOE KEYS BLVD	FAETH JAMES J PATRICK & CAROL ANNE TR		6181 COBBLESTONE ROAD	PLACERVILLE	CA	95667	5	$1,257,291	$251,458
022-051-088	2170 INVERNESS DR	JOHNSON ROBERT B		2170 INVERNESS SR	SOUTH LAKE TAHOE	CA	96150	5	$1,655,457	$331,091
022-061-001	470 CAPRI DR	KUNDU NIRVANA		470 CAPRI DR	SOUTH LAKE TAHOE	CA	96150	5	$888,141	$177,628
022-061-005	2240 CATALINA DR	KNISLEY MARK E & DEBORAH E TR		2240 CATALINA DR	SOUTH LAKE TAHOE	CA	96150	5	$604,921	$120,984
022-061-007	2228 CATALINA DR	PEKOWSKY KEVIN & JANET TR		3031 MELBOURNE CT	PLEASANTON	CA	94588	5	$1,000,000	$200,000
022-061-010	2210 CATALINA DR	ORDEMANN WALT & CAROL		108 KINGS COURT	SAN CARLOS	CA	94070	5	$3,366,000	$673,200
022-061-013	2190 CATALINA DR	HAGENS PETER A JR TR & CATHERINE R TR		930 SOMERSBY WAY	SACRAMENTO	CA	95864	5	$644,391	$128,878
022-061-019	2154 CATALINA DR	MCCOSKER BRIAN & JACQUELINE TR		3165 SANTA MARIA DR	CONCORD	CA	94518	5	$2,019,426	$403,885
022-061-021	2155 CATALINA DR	SFC LEASING CA LP		11390 WHITE ROCK RD STE 200	RANCHO CORDOVA	CA	95742	5	$2,399,000	$479,800
022-061-028	2201 CATALINA DR	SFC LEASING LP		11390 WHITE ROCK RD STE 200	RANCHO CORDOVA	CA	95742	5	$1,160,446	$232,089
022-061-032	2227 CATALINA DR	SHORTRIDGE CHAD & LAURA		2227 CATALINA DR	SOUTH LAKE TAHOE	CA	96150	5	$864,275	$172,855
022-061-043	2236 BALBOA DR	MCLOUGHLIN PATRICK R & KATHERINE M		44410 S EL MACERO DR	EL MACERO	CA	95618	5	$1,092,399	$218,480
022-061-045	2220 BALBOA DR	CONNELLY DOUGLAS RICHARD & BONETTI PAULETTE		2220 BALBOA DRIVE	SOUTH LAKE TAHOE	CA	96150	5	$1,453,500	$290,700
022-061-046	2216 BALBOA DR	LAGORIO BRETT & LORA		20001 E FLOOD RD	LINDEN	CA	95236	5	$1,453,500	$290,700
022-061-050	2190 BALBOA DR	DIGIORNO A & S REV TRUST 3/14/2006		2190 BALBOA DRIVE	SOUTH LAKE TAHOE	CA	96150	5	$494,869	$98,974
022-061-052	2176 BALBOA DR	BARSEMA DENNIS TR & STACEY TR		128 BRINKER RD	BARRINGTON	IL	60010	5	$763,172	$152,634
022-061-053	2172 BALBOA DR	LAWSON BALBOA PROPERTIES LLC C/O LAWSON RODNEY K	C/O LAWSON RODNEY K		RANCHO MURIETA	CA	95683	5	$1,500,000	$300,000
022-061-055	2160 BALBOA DR	MUNCE A CURRIE JR TR & CLAUDIA FAN TR		2322 MAR EAST STREET	TIBURON	CA	94920	5	$1,711,584	$342,317
022-061-059	2165 BALBOA DR	DILLIE JOHN & MAUREEN C		365 ELVIES LANE	FOLSOM	CA	95630	5	$1,094,827	$218,965
022-061-060	2175 BALBOA DR	BARBA JORGE L TR & MARCY TR		1675 DAVIS LN	RENO	NV	89511	5	$659,843	$131,969
022-061-061	2181 BALBOA DR	GANN JEFFERY F & MALIA A TR		9373 SOUTH PRIEST	FRENCH CAMP	CA	95231	5	$1,918,399	$383,680
022-061-064	2201 BALBOA DR	2201 BALBOA DRIVE LLC		39 REGINA WAY	SAN RAFAEL	CA	94903	5	$3,003,900	$600,780
022-061-065	2209 BALBOA DR	MAIER FRED TR & KATHARINE E TR		PO BOX 7675	SOUTH LAKE TAHOE	CA	96158	5	$559,080	$111,816
022-081-002	335 BEACH DR	GILL STEPHEN E TR & LINDA L TR		731 HILLCREST AVE	LA CANADA	CA	91011	5	$3,684,266	$736,853
022-082-014	346 BEACH DR	CRAWFORD WILLIAM H TR & LINDA C TR		3429 CIMMERON CT	ROCKLIN	CA	95677	5	$1,024,842	$204,968
022-082-015	359 BEACH LN	WEBER RALF		840 S RANCHO DR STE 4-257	LAS VEGAS	NV	89106	5	$1,116,458	$223,292
022-084-002	2252 WHITE SANDS DR	KNIESEL ROBERT L & KELLI A TR		9713 CHELEN CT	GRANITE BAY	CA	95746	5	$788,865	$157,773
022-111-003	602 LUCERNE WAY	HELFERT GARY G TR & VU HELFERT LIV REV TR 11/20/01		925 PEREGRINE CT	SANTA CLARA	CA	95051	5	$213,335	$42,667
022-111-017	565 LUCERNE WAY	ROKITTA FAM TR		15759 OAK KNOLL COURT	LOS GATOS	CA	95030	5	$3,091,700	$618,340
022-111-020	581 LUCERNE WAY	FOEY SHIRLEY J TR & S J LIV REV TRUST 8/14/07		32151 NARROW LN	SCAPPOOSE	OR	97056	5	$268,844	$53,769
022-111-023	597 LUCERNE WAY	ELSTOP MARK & ELSTOB ERIN CO TR		415 CROCKER AVE	PACIFIC GROVE	CA	93950	5	$1,891,089	$378,218
022-123-013	802 LASSEN DR	KNUTSON HARRY LOUIS III		802 LASSEN DR	SOUTH LAKE TAHOE	CA	96150	5	$833,634	$166,727
022-171-020	394 WEDELN CT	RENALDI MARCIA TR		49524 REDFORD WAY	INDIO	CA	92201	5	$191,485	$38,297
022-171-021	392 WEDELN CT	GLEIN RANDALL S & SHARON J TR		364 BLANCA AVE	TAMPA	FL	33606	5	$2,293,011	$458,602
022-182-040	2078 SLALOM CT	GREEN WILLIAM M & MARY M		PO BOX 800	SHINGLE SPRINGS	CA	95682	5	$684,569	$136,914
022-221-009	2028 GARMISH CT	LAM KWOK H TR & LAURA R TR		2161 GOLDORADO TRAIL	EL DORADO	CA	95623	5	$641,924	$128,385
022-231-032	453 LIDO DR	PANAYOTOU NICKITAS & NARIMANE H		2200 REDINGTON ROAD	HILLSBOROUGH	CA	94010	5	$2,805,000	$561,000
022-232-014	2016 MARCONI WAY	SCHUBERT ROBERT C & PATRICIA L		202 GLORIETTA BLVD	ORINDA	CA	94563	5	$657,371	$131,474
022-241-011	1950 MARCONI WAY	QVISTGAARD FAM TRUST 1/29/2002		4216 BOXELDER PLACE	DAVIS	CA	95618	5	$2,195,000	$439,000
022-251-003	426 EMERALD DR	MORRIS JIMMIE C TR & MELINDA L TR		827 ROJO WAY	GARDNERVILLE	NV	89460	5	$289,665	$57,933
022-251-006	412 EMERALD DR	CALLAHAN HAROLD P SURV TR & FAM TR 10/19/01 (LE)		1604 SIR FRANCIS DRAKE BLVD	SAN ANSELMO	CA	94960	5	$237,188	$47,438
022-251-043	382 CRYSTAL CT	SOKOLOFF IGOR & GALINA		150 SAN MARCOS AVE	SAN FRANCISCO	CA	94116	5	$814,460	$162,892
022-251-087	1990 KOKANEE WAY	TOUCHE STEVEN DAVID TR & PERRI SUNDT TR		6256 PASEO TIERRA ALTA	TUCSON	AZ	85715	5	$2,338,344	$467,669
022-261-002	315 BEACH DR	GREEN BANKER CA LLC		398 PRIMROSE RD FL 1	BURLINGAME	CA	94010	5	$2,066,755	$413,351
022-261-003	305 BEACH DR	GARNETT LINDA H TR & HARRISON EXEMPT TRUST FBO		1710 GRANGER AVE	LOS ALTOS	CA	94024	5	$1,692,803	$338,561
022-262-005	288 BEACH DR	LAURSEN STEFAN		2236 PARK PL STE D	MINDEN	NV	89423	5	$1,501,291	$300,258
022-301-009	2045 ALOHA DR	LARRY J RITCHIE FAMILY LIMITED PARTNERSHIP CA LP		11878 AVE 328	VISALIA	CA	93291	5	$5,150,000	$1,030,000
022-301-010	2049 ALOHA DR	TAHOE BELLA VISTA CA LLC		1430 SAN RAYMUNDO RD	HILLSBOROUGH	CA	94010	5	$1,457,500	$291,500
022-301-018	2064 ALOHA DR	SPURRELL SANDRA A SURV TR & REV TR OF 02/08/2000		2064 ALOHA DR	SOUTH LAKE TAHOE	CA	96150	5	$1,500,000	$300,000
022-301-023	2046 ALOHA DR	NELSEN KAREN TR		1575 STERLING OAKS CT	MORGAN HILL	CA	95037	5	$978,810	$195,762
022-301-026	477 CARSON CT	KHATOONIAN KATHERINE ANN TR & KA REV TR 6/16/17		44444 EL MACERO DR	EL MACERO	CA	95618	5	$898,000	$179,600
022-301-027	481 CARSON CT	CARSON COURT A CA LLC		9812 CARLTON COURT	GRANITE BAY	CA	95746	5	$905,000	$181,000
022-301-037	2030 ALOHA DR	WAGNER NICHOLAS J & BECKHAM RHONDA		2030 ALOHA DR	SOUTH LAKE TAHOE	CA	96150	5	$901,634	$180,327
022-301-044	1966 DAGGETT CT	BARSTOW KAREN TR & K 2005 REV TRUST		1966 DAGGETT CT	SOUTH LAKE TAHOE	CA	96150	5	$376,537	$75,307
022-301-045	1962 DAGGETT CT	HOSKING JOANN H TR & LIV RESID TRUST		PO BOX 689	GOLD HILL	OR	97525	5	$1,141,906	$228,381
022-311-031	2008 ALOHA DR	ANDERSON DOUGLAS R TR & NORIS A TR		921 ACORN WAY	WATSONVILLE	CA	95076	5	$983,293	$196,659
022-312-009	1983 ALOHA DR	CAVINESS DEWAYNE E TR & DOROTHY M TR		PO BOX 1496	CHICO	CA	95927	5	$838,158	$167,632
022-312-011	1991 ALOHA DR	FREITAS RENTALS 4 A CA LP		983 E LEVIN AVE	TULARE	CA	93274	5	$2,492,868	$498,574
022-312-017	3 LIGHTHOUSE SHORES DR	D & F VENTURES CA LLC		3712 RANCHO ESTATES	WALNUT CREEK	CA	94598	5	$3,345,013	$669,003
022-321-030	1648 VENICE DR	HARKINS MALCOLM W TR & KIMBERLY D TR		1276 LORDEN CT	FOLSOM	CA	95630	5	$841,280	$168,256
022-322-032	1759 VENICE DR	COLLIER BARBARA		4647 JENKINSON CIR	POLLOCK PINES	CA	95726	5	$1,474,276	$294,855
022-322-035	1747 VENICE DR	GALATOLO RONALD D		1330 UNIVERSITY DR #67	MENLO PARK	CA	94025	5	$836,000	$167,200
022-322-049	1681 VENICE DR	MERIMAA JUHA OSKARI & PONDER ELIZABETH LENZ		616 42ND AVE	SAN MATEO	CA	94403	5	$1,850,000	$370,000
022-322-051	1673 VENICE DR	SMITH WESLEY P & OTTO LOUISE M TR		13 GREENS LN	PLEASANTON	CA	94566	5	$455,107	$91,021
022-331-016	1921 CATHEDRAL CT	RUTHERFORD JASON S & MIRANDA JON CO TR & VOTA PAUL		2201 FRANCISCO DR STE 140-278	EL DORADO HILLS	CA	95762	5	$1,402,500	$280,500
022-332-039	636 ALPINE DR	MC 2019 TRUST 11/04/2019 & SC 2019 TRUST 11/04/201		4465 S JONES BOULEVARD	LAS VEGAS	NV	89103	5	$2,600,000	$520,000
022-341-002	1963 VENICE DR	POLITO MARY JOANNE TR & ARMSTRONG JUDITH DOMENICA		3255 BEAUDRY TER	GLENDALE	CA	91208	5	$372,782	$74,556
022-341-012	651 ALPINE DR	SANTO ANTHONY F & MICHELLE A		1243 JESSIE RD	HENDERSON	NV	89002	5	$1,024,897	$204,979
022-343-027	1954 VENICE DR	MOHLER MARLEYNA SUCC TR		275 ELEANOR DR	WOODSIDE	CA	94062	5	$1,260,511	$252,102

022-381-002	276 BEACH DR	DONAHUE DEISELL & JAMES FRANCIS TR		PO BOX 2247	STATELINE	NV	89449	5	$2,496,347	$499,269
022-381-008	234 BEACH DR	MCNAUGHTON FOY SCOTT TR & BARBARA G TR		2908 CORONA DR	DAVIS	CA	95616	5	$1,339,984	$267,997
022-381-011	218 BEACH DR	VINCIQUERRA WAYNE D & SUSAN R TR	C/O COLO STEVEN	5002 CORONADO DR	EL DORADO HILLS	CA	95762	5	$3,876,000	$775,200
022-381-016	241 BEACH DR	KEYS 241 RENTAL CA LLC		3585 WOODSIDE RD	WOODSIDE	CA	94062	5	$4,101,927	$820,385
022-381-021	281 BEACH DR	TERSIGNI TAHOE PROPERTIES LLC		1830 HAMILTON AVE	SAN JOSE	CA	95125	5	$2,019,633	$403,927
022-381-022	259 BEACH DR	BEACH TANGO LLC DE LLC		259 BEACH DRIVE	SOUTH LAKE TAHOE	CA	96150	5	$9,174,900	$1,834,980
022-391-004	2144 WHITE SANDS DR	MARIETTI GARY L & BENITO VALERIE A TR		126 ESTATES DR	SANTA CRUZ	CA	95060	5	$3,076,241	$615,248
022-391-005	2140 WHITE SANDS DR	FAUPS DE LLC		548 MARKET STREET #55801	SAN FRANCISCO	CA	94104	5	$5,750,000	$1,150,000
022-391-006	2141 WHITE SANDS DR	SOUZA WILLIAM D & MCCLELLAND GREGORY D & MERILYN H		23731 EL TORO RD STE A	LAKE FOREST	CA	92630	5	$2,645,146	$529,029
022-391-008	2151 WHITE SANDS DR	GEISLER ERIC GERARD TR & JENNIFER ANN TR		6060 ROCK CREEK CT	RENO	NV	89511	5	$2,208,427	$441,685
022-401-006	2214 WHITE SANDS DR	GIUSTI MARCIA CUSTODIAN & THOMPSON YOLANDA CUSTODI		121 GOLD RUSH CT	CLAYTON	CA	94517	5	$613,876	$122,775
022-401-013	2168 WHITE SANDS DR	GOEJENOLA PAUL A & GOJENOLA LINDA A TR		13941 CAMINO BARCO	SARATOGA	CA	95070	5	$2,316,340	$463,268
022-402-007	2209 WHITE SANDS DR	MALMED LEON TR & PATRICIA TR		2209 WHITE SANDS DR	SOUTH LAKE TAHOE	CA	96150	5	$1,478,702	$295,740
022-402-008	2219 WHITE SANDS DR	TSANG AUDREY KON LO & THEODORE HING JOE		16115 GREENWOOD LN	MONTE SERENO	CA	95030	5	$902,130	$180,426
022-431-006	16 LIGHTHOUSE SHORES DR	MENDEZ MARCO A TR & M A QLFD PERS RES TRUST		747 ARROYO RD	LOS ALTOS	CA	94024	5	$5,662,645	$1,132,529
023-102-041	2107 LUKINS WAY	JUNQUEIRO STEVEN A TR & THERESA F TR		3321 VANCOUVER DR	MODESTO	CA	95355	5	$753,518	$150,704
023-102-046	2127 LUKINS WAY	MAREK JOHN T JR TR & JT JR & MK REV TR2/10/05		1960 CAZADERO HWY	CAZADERO	CA	95421	5	$245,233	$49,047
023-102-051	2147 LUKINS WAY	TESSIER G ANTHONY JR TR & ELLEENE K TR		4432 THOR WAY	SACRAMENTO	CA	95864	5	$145,332	$29,066
023-111-052	2038 LUKINS WAY	SHORT DAVID E TR & JULIE A TR		1505 EUREKA RD	ROSEVILLE	CA	95661	5	$120,805	$24,161
023-152-005	735 GLORENE AVE	MCCARTHY KEITH D & DENISE M CO TR		735 GLORENE AVE	SOUTH LAKE TAHOE	CA	96150	5	$921,217	$184,243
023-271-020	2056 12TH ST	BRAYTON SARAH JANE & ERICSON BRADLEY LOGAN		2056 12TH STREET	SOUTH LAKE TAHOE	CA	96150	5	$1,475,000	$295,000
023-341-021	0	LAMBERT ANDREW JON		11 PARK CIRCLE	SAUSALITO	CA	94965	5	$510,000	$102,000
023-451-006	719 TATA LN	CLINTON ROSE MARY & LUCKIE TAMI RENE		719 TATA LN	SOUTH LAKE TAHOE	CA	96150	5	$1,504,500	$300,900
023-461-001	745 TATA LN	BENNETT EDWARD & CYNTHIA		21025 PASEO MONTANA	MURRIETA	CA	92562	5	$1,770,493	$354,099
023-461-013	795 TATA LN	ABBOTT SUSAN		PO BOX 10526	SOUTH LAKE TAHOE	CA	96158	5	$163,178	$32,636
023-462-009	786 TATA LN	BLADES JANELLE A TR		3846 MADERA ST	PINOLE	CA	94564	5	$265,631	$53,126
023-471-023	1934 10TH ST	SITES MADISON MARIE & HOFFMAN SHAWN PATRICK		1934 10TH STREET	SOUTH LAKE TAHOE	CA	96150	5	$510,000	$102,000
023-482-009	956 TATA LN	GOLDAMMER ERIK		956 TATA LANE	SOUTH LAKE TAHOE	CA	96150	5	$469,171	$93,834
023-491-003	629 CLEMENT ST	XIAO KEVIN & MA YEFEI		310 SCHROEDER STREET	SUNNYVALE	CA	94085	5	$1,110,000	$222,000
023-541-002	625 TAHOE ISLAND DR	BAILEY DAVID H TR & LINDA J TR		35 TODD CT	ALAMO	CA	94507	5	$987,014	$197,403
023-542-014	600 TAHOE ISLAND DR	MASELLI DOUGLAS L & SINGLER DUSTIN R		600 TAHOE ISLAND DR	SOUTH LAKE TAHOE	CA	96150	5	$298,670	$59,734
023-551-015	653 TAHOE ISLAND DR	WHITTEN ANDREW C TR & CARLA W TR		8232 THORNTREE DR	SCOTTSDALE	AZ	85266	5	$1,065,000	$213,000
023-551-016	649 TAHOE ISLAND DR	CELENTANO PAUL JOSEPH & MARIA BEATRICE TR		16 ACACIA LANE	REDWOOD CITY	CA	94062	5	$1,280,100	$256,020
023-561-011	739 PATRICIA LN	ST MICHEL MICHAEL TR & MICHEL LUCINDA TR		739 PATRICIA LN	SOUTH LAKE TAHOE	CA	96150	5	$224,308	$44,862
023-591-005	544 GARDNER ST	NGUYEN ANDREW K TR & VU MINHDIEU T TR		21150 HAZELBROOK DR	CUPERTINO	CA	95014	5	$720,440	$144,088
023-591-008	556 GARDNER ST	PENCE RICHARD DON TR & COLLEEN C PENCE TR		556 GARDNER ST	SOUTH LAKE TAHOE	CA	96150	5	$68,311	$13,662
023-623-010	1804 13TH ST	WALKER SETH JONATHAN & APRIL ANN		1804 13TH STREET	SOUTH LAKE TAHOE	CA	96150	5	$569,160	$113,832
023-731-003	2360 CALIFORNIA AVE	LEDESMA MICHAEL & CAROL L		PO BOX 16312	SOUTH LAKE TAHOE	CA	96151	5	$264,078	$52,816
023-781-006	809 SOUTH SHORE DR	JONES DAVID M & ALICE H		809 SOUTH SHORE DR	SOUTH LAKE TAHOE	CA	96150	5	$885,277	$177,055
023-782-007	895 LAPHAM DR	BRAUN ANTHONY WAYSON & KUNIBE BRAUN CHARLENE TR		895 LAPHAM DR	SOUTH LAKE TAHOE	CA	96150	5	$250,615	$50,123
023-891-011	2215 TAHOE VISTA DR	FONG DENNIS E & MARTIN TR		37 KILLYBEGS RD	ALAMEDA	CA	94502	5	$206,576	$41,315
023-902-005	2281 CALIFORNIA AVE	DOAK JEFFERY M TR & NANCY L TR		10916 MISSION LAKES AVE	LAS VEGAS	NV	89134	5	$395,053	$79,011
023-911-013	786 JEFFERY ST	SIMPKINS MCGEE BRENDA LYNN		786 JEFFERY ST	SOUTH LAKE TAHOE	CA	96150	5	$1,270,688	$254,138
023-912-008	783 JEFFERY ST	PUSZKA JOANNA		PO BOX 16860	SOUTH LAKE TAHOE	CA	96151	5	$375,956	$75,191
025-031-013	3633 MACKEDIE WAY	JLSC FAMILY PARTNERSHIP CA LP		412 VILLA TER	SAN MATEO	CA	94401	5	$977,749	$195,550
025-032-018	3606 MACKEDIE WAY	HAMMOND PAUL TR		236 CLIPPER STREET	SAN FRANCISCO	CA	94114	5	$1,366,800	$273,360
025-201-019	1407 WALKUP RD	STRAIN R ANDREW TR & KATHERINE L TR		PO BOX 822	ZEPHYR COVE	NV	89448	5	$481,862	$96,372
025-214-001	1381 WALKUP RD	OBERHAUSER CHRISTIAN & ANDERSON MARK R		1381 WALKUP RD	SOUTH LAKE TAHOE	CA	96150	5	$750,000	$150,000
025-214-003	3350 WOODLAND RD	LEW MICHAEL & TSAI LYNETTE		55 S KUKUI ST APT 1403	HONOLULU	HI	96813	5	$501,125	$100,225
025-223-007	1363 SUSIE LAKE RD	LITTLEFIELD ANDREW W		PO BOX 1414	ZEPHYR COVE	NV	89448	5	$919,850	$183,970
025-231-008	1316 HERBERT AVE	WEBSTER DONALD L JR & BAIK MARY ANN		614 HARBOR COLONY CT	REDWOOD CITY	CA	94065	5	$633,077	$126,615
025-231-010	1308 ANGORA LAKE RD	ELIAS JOEL & IRMA		120 GREENBANK DR	LAFAYETTE	CA	94549	5	$821,077	$164,215
025-282-016	3738 ROCKWOOD RD	WILLIAMS ROGER S CO TR & MICHELLE C CO TR		3738 ROCKWOOD DR	SOUTH LAKE TAHOE	CA	96150	5	$477,372	$95,474
025-291-003	1278 GILMORE LAKE RD	ZHAI HUILING & CAI JIAN		50 ROXBURY LANE	SAN MATEO	CA	94402	5	$1,734,000	$346,800
025-371-003	1191 JOBS PEAK DR	SIN HON CHAY CO TR & TRAN MAI NGOC CO TR		PO BOX 13486	SOUTH LAKE TAHOE	CA	96151	5	$487,208	$97,442
025-371-004	1193 JOBS PEAK DR	CASTILLO GONZALEZ KAREM & ABIGAIL GONZALEZ		P O BOX 19985	SOUTH LAKE TAHOE	CA	96151	5	$450,356	$90,071
025-376-008	1229 MONUMENT DR	VIAU ELSIE DORIS TR & LIV TRUST DATED 4/24/12		5452 SANDPIPER LN	LAS VEGAS	NV	89146	5	$99,272	$19,854
025-483-009	1624 GLENWOOD WAY	ALONZO JOHN L TR		1624 GLENWOOD WAY	SOUTH LAKE TAHOE	CA	96150	5	$276,954	$55,391
025-541-010	3511 BODE DR	WINKELMAN KARL B & KATHERINE R CO TR		16395 ROSELEAF CT	LOS GATOS	CA	95032	5	$613,532	$122,706
025-542-008	3482 BODE DR	RAMIREZ PETER & SELINA		1215 LOMOND DR	EL DORADO HILLS	CA	95762	5	$1,224,000	$244,800
025-543-005	3548 BODE DR	KLEBIG MICHAEL J & JANIS L		5047 AMETHYST CT	SAN JOSE	CA	95136	5	$803,077	$160,615
025-544-010	3470 APRIL DR	BREWER DANIEL		PO BOX 17922	SOUTH LAKE TAHOE	CA	96151	5	$1,096,500	$219,300
025-554-005	3552 RALPH DR	HAASE CAROL S TR & C LIV REV TR 4/08/1993		3560 RALPH DR	SOUTH LAKE TAHOE	CA	96150	5	$395,211	$79,042
025-580-009	3624 NEEDLE PEAK RD	NEL GUILLIAM		PO BOX 19531	SOUTH LAKE TAHOE	CA	96151	5	$300,632	$60,126
025-580-015	1400 SKI RUN BLVD	REINHARD TRACY L		PO BOX 14464	SOUTH LAKE TAHOE	CA	96151	5	$184,138	$36,828
025-633-013	3477 RANCHO CIR	HETHERTON JONATHAN P & WENCK HETHERTON KELARY		3477 RANCHO CIR	SOUTH LAKE TAHOE	CA	96150	5	$795,000	$159,000
025-770-002	1460 FRONTIER CT	RAUT DEVENDRA & GOTMARE SONALI		21150 MARIA LN	SARATOGA	CA	95070	5	$1,124,418	$224,884
025-770-004	1440 FRONTIER CT	DELANEY KATHERINE ELIZABETH TR		764 CRANE AVE	FOSTER CITY	CA	94404	5	$1,336,380	$267,276
026-022-014	771 LAKEVIEW AVE	TETZ LAURIE TR		PO BOX 100	DEER PARK	CA	94576	5	$1,278,942	$255,788
026-025-003	768 LAKEVIEW AVE	FERNANDEZ P & A M 2022 REV TRUST 8/2/2022		1579 26TH AVENUE	SAN FRANCISCO	CA	94122	5	$433,175	$86,635
026-026-026	3149 FRESNO AVE	SRIRO ANDREW I TR & FAM TRUST 8/14/09 C/O TAHOE PROPERTY MGMT	C/O TAHOE PROPERTY MGMT		SOUTH LAKE TAHOE	CA	96150	5	$729,809	$145,962
026-033-015	881 LAKEVIEW AVE	MALIK ROMAN TR & NORMA JEAN TR		2298 HERITAGE DR	SAN JOSE	CA	95124	5	$1,706,465	$341,293
026-038-003	842 MERCED AVE	FARNWORTH DON & JEONG SARAH TR		1436 HIDDEN BRIDGE RD	EL DORADO HILLS	CA	95762	5	$447,465	$89,493
026-042-002	3192 PASADENA AVE	TEIXEIRA DEAN M TR & NANCY M TR		1975 PRELL RD	SANTA MARIA	CA	93454	5	$1,706,086	$341,217
026-042-008	949 LAKEVIEW AVE	COCKRUM DANIEL J TR & SUZANNE M TR		PO BOX 2348	TRUCKEE	CA	96160	5	$905,182	$181,036
026-043-017	981 LAKEVIEW AVE	CERESKE WILLIAM H JR CO TR & JEANETTE A CO TR		1193 S KINGFISHER WAY	BOISE	ID	83709	5	$1,340,490	$268,098
026-046-014	988 LAKEVIEW AVE	PHILLIPS DAVID & MARIA ISABEL		4146 MARSTON LANE	SANTA CLARA	CA	95054	5	$1,173,000	$234,600
026-046-018	992 LAKEVIEW AVE	AMIRI SERIO TR		11040 BOLLINGER CANYON RD E510	SAN RAMON	CA	94582	5	$566,132	$113,226
026-061-013	3131 BELLEVUE AVE	PLATCHECK TERRY SCOTT		1618 ALABAMA ST	SAN FRANCISCO	CA	94110	5	$3,250,000	$650,000
026-061-014	3127 BELLEVUE AVE	GONZALO MARCOS G & BETTY S CO TR		6517 CRYSTAL SPRINGS DRIVE	SAN JOSE	CA	95120	5	$2,397,000	$479,400
026-063-013	765 ALAMEDA AVE	GOGUELY HERVE TR		2911 OAKLAND AVE	SOUTH LAKE TAHOE	CA	96150	5	$1,224,000	$244,800
026-079-002	885 SAN FRANCISCO AVE	CHRISTIANSEN ROBERT A & TERRI J TR & BUCK ROBERT W		25605 WILLOW POND LANE	LOS ALTOS HILLS	CA	94022	5	$214,732	$42,946
026-094-026	724 MODESTO AVE	HONOROF ANETA		P O BOX 18109	SOUTH LAKE TAHOE	CA	96151	5	$793,820	$158,764
026-094-042	737 LOS ANGELES AVE	WANG WEIJIA TR & LIU JING TR		1214 RUPPELL PL	CUPERTINO	CA	95014	5	$486,670	$97,334
026-096-003	688 LOS ANGELES AVE	MCCORMACK BRUCE TR & B TRUST		1581 BRENTWOOD CT	WALNUT CREEK	CA	94595	5	$379,996	$75,999
026-105-022	3067 SACRAMENTO AVE UNIT 7	SCHLAEFER JOHN B & LIN JOAN Y		17510 MANZANITA DR	MORGAN HILL	CA	95037	5	$669,867	$133,973
026-109-018	873 STANFORD AVE	BEZEMER JASON R & PEREZ JANELLE M TR		5541 MONTE CLAIRE LN	LOOMIS	CA	95650	5	$661,980	$132,396
026-123-011	730 STANFORD AVE	KASPAR MICHAEL F & CHRISTOPHER C		107 CLARK AVE	SANTA CRUZ	CA	95060	5	$591,076	$118,215
026-146-018	2907 OAKLAND AVE	CASTEJON BRUNO TR & VALERIE TR		2907 OAKLAND AVE	SOUTH LAKE TAHOE	CA	96150	5	$604,235	$120,847
026-154-014	2873 OAKLAND AVE	DEVRIES RICHARD L TR & R L FAM REV TRUST		PO BOX 17815	SOUTH LAKE TAHOE	CA	96151	5	$338,271	$67,654
026-221-024	880 EDGEWOOD CIR	NARVARTE TERESITA LOPEZ & RANY R		PO BOX 18646	SOUTH LAKE TAHOE	CA	96151	5	$280,503	$56,101
026-243-009	991 GOLD TIP AVE	LOPEZ GEORGENE K TR & G K REV TR 05/14/1999		1633 BERNA ST	SANTA CLARA	CA	95050	5	$139,694	$27,939
026-244-003	3007 FREEL PEAK AVE	DEDASCALOU STEPHEN A TR & MARGARET TR		460 AVENUE DEL ORA	REDWOOD CITY	CA	94062	5	$76,154	$15,231
026-310-001	969 LAKEVIEW DR BLDG A	MGJ DEVELOPMENT CA CORP		80 LARK PLACE	ALAMO	CA	94507	5	$5,061,750	$1,012,350
026-310-002	969 LAKEVIEW DR BLDG B	SOGT LLC		80 LARK PLACE	ALAMO	CA	94507	5	$4,949,550	$989,910
027-053-012	3615 OSGOOD AVE	MOSBACHER LISA		160 BELLE AVE	PLEASANT HILL	CA	94523	5	$429,470	$85,894
027-123-020	3607 ALDER AVE	STANAWAY DONALD F TR & FAMILY TRUST		1200 MILLBRAE AVE	MILLBRAE	CA	94030	5	$214,589	$42,918
027-123-022	1081 BOWERS AVE	ROUBANIS ALEXANDER A & KATHRYN		7387 WEST LN	GRANITE BAY	CA	95746	5	$525,376	$105,075
027-153-004	3664 BIRCH AVE	CHRISSAN DOUGLAS A & KIM E		16865 KENNEDY RD	LOS GATOS	CA	95032	5	$366,176	$73,235
027-231-005	1132 CRAIG AVE	BLACK JAN P TR & DIANE L TR		10500 LAKEVIEW RD	YUCAIPA	CA	92399	5	$233,658	$46,732
027-232-020	1138 JUNIPER AVE	CUELLAR SERVANDO & HENDERSON NICHOLE		1702 GROVE ST #2	SAN FRANCISCO	CA	94117	5	$513,650	$102,730
027-321-017	3617 SPRUCE AVE	NOBRIGA LOUIS & GLADYS TR		3617 SPRUCE AVE	SOUTH LAKE TAHOE	CA	96150	5	$79,616	$15,923
027-343-001	1160 GLENWOOD WAY	TRUJILLO SANDOVAL FRANCISCO J & MEDRANO SANCHEZ JA		1160 GLENWOOD WAY	SOUTH LAKE TAHOE	CA	96150	5	$407,072	$81,414
027-344-038	1150 FAIRWAY AVE	HOLLEY JILL DENISE		1150 FAIRWAY AVE	SOUTH LAKE TAHOE	CA	96150	5	$470,967	$94,193
027-344-045	1112 FAIRWAY AVE	REYNOLDS DAVID M & YASMINE N TR		3677 BARRY AVE	LOS ANGELES	CA	90066	5	$900,000	$180,000

027-344-050	1209 GLENWOOD WAY	MORGAN BRIAN MICHAEL TR		16755 VISTA DEL VALLE COURT	MORGAN HILL	CA	95037	5	$723,180	$144,636
027-371-013	940 BAL BIJOU RD	FREDERICKSON ROBERT B TR & KATHLEEN M TR C/O SMITH STEVEN	C/O SMITH STEVEN		PARK CITY	UT	84098	5	$494,893	$98,979
027-451-007	3535 LAKE TAHOE BLVD UNIT 607	TWENTY TWENTY NINETY LLC CA LLC DBA 20 20 90 VACATION RENTAL	DBA 20 20 90 VACATION RENTA		SAN DIEGO	CA	92169	5	$655,785	$131,157
027-491-007	3535 LAKE TAHOE BLVD UNIT 619	TAYLOR GREG STERLING & TAYLOR GREG STERLING		2654 DEL SUR CT	MINDEN	NV	89423	5	$2,506,189	$501,238
027-521-007	3535 LAKE TAHOE BLVD UNIT 642	AZIMI SHAHRAM TR & REV TRUST OF 11/1/91		26770 DURHAM WAY	HAYWARD	CA	94542	5	$345,208	$69,042
027-551-008	3535 LAKE TAHOE BLVD UNIT 632	FOSTER KIMBERLY M TR & BLAKE SEAN H & JENNIFER M C		11303 LAKE RIM ROAD	SAN DIEGO	CA	92131	5	$1,239,382	$247,876
028-051-010	3737 TERRACE DR	PAC 1 CA 2020 LLC CA LLC		18 EAST 4TH ST SUITE 902	CINCINNATI	OH	45202	5	$1,728,900	$345,780
028-052-012	3692 TERRACE DR	BARRAGAN RAYMOND JR		3125 E ROBERTSON BLVD STE A	CHOWCHILLA	CA	93610	5	$1,850,652	$370,130
028-061-027	3932 BRIDLE RD	LIBOV KSENIA & ANDREY		1956 SAN CARLOS AVE	SAN CARLOS	CA	94070	5	$649,546	$129,909
028-070-010	3933 BRIDLE RD	BUKOV KONSTANTIN DAMIANOV		9 BELL WAVER WAY	OAKLAND	CA	94619	5	$1,120,000	$224,000
028-070-026	1392 BONITA RD	BAMA TWO FL LLC C/O STEPHENS JOHN	C/O STEPHENS JOHN		TREASURE ISLAND	FL	33706	5	$1,044,000	$208,800
028-070-027	1323 KELLER RD	ANGELL JOHN B & SIDHU JAISIMARAN		2574 WEST MEMORY LANE	PORTERVILLE	CA	93257	5	$1,213,800	$242,760
028-090-093	1325 WILDWOOD AVE	BURGESS STUART & HRDLICKA ZUZANA K		1717 SE 7 STREET	FORT LAUDERDALE	FL	33316	5	$4,300,000	$860,000
028-100-030	1318 KNOLL LN	AVERY TIMOTHY K & SANDRA F		2644 TORREY PINES DR	BRENTWOOD	CA	94513	5	$745,518	$149,104
028-100-046	1321 SKI RUN BLVD	BROWN MARK J & MELISSA M TR		1600 LOS ALTOS COURT	EL DORADO HILLS	CA	95762	5	$2,888,000	$577,600
028-122-009	3730 RUBY WAY UNIT A	SMITH JONATHAN		3730 RUBY WAY UNIT A	SOUTH LAKE TAHOE	CA	96150	5	$382,265	$76,453
028-123-007	3758 OVERLOOK CT	BOREN PHILIP JAMES III		3758 OVERLOOK COURT	SOUTH LAKE TAHOE	CA	96150	5	$1,224,000	$244,800
028-131-002	1396 KELLER RD	SAIDIN ZAIN K TR & SPETZ JOANNE TR		545 EDINBURGH ST	SAN MATEO	CA	94402	5	$778,685	$155,737
028-131-006	1381 TIMBER LAKE PL	MILLIKEN ENTERPRISES CA LP		111 NEWTON DR	BURLINGAME	CA	94010	5	$727,500	$145,500
028-153-012	4210 SADDLE RD	YOKOTA RONALD TR & BONITA A T TR		96 SAN BENANCIO RD	SALINAS	CA	93908	5	$865,578	$173,116
028-154-003	4027 CREST RD	FRIDLAND ALEXANDER TR & PETROSOVA NATALIA TR		640 RIVERA ST	SAN FRANCISCO	CA	94116	5	$1,255,063	$251,013
028-162-034	4228 SADDLE RD	FANUCCHI SHEILA R SURV TR		1415 LOVALL VALLEY RD	SONOMA	CA	95476	5	$289,945	$57,989
028-163-003	3961 CREST RD	DICKERSON JUNE D TR & REV TR OF 08/02/01		3961 CREST RD	SOUTH LAKE TAHOE	CA	96150	5	$397,176	$79,435
028-171-010	1322 KELLER RD	STEIN ANATOLI & SIMA		7 COWELL LN	ATHERTON	CA	94027	5	$630,500	$126,100
028-190-031	3854 REGINA RD	TAHOE PALACE ONE CA LLC		25521 ALTAMONT RD	LOS ALTOS HILLS	CA	94022	5	$1,491,489	$298,298
028-301-060	4042 CREST RD	FURGERSON SCOTT P & PAULA L TR		1570 RIVERVIEW CIR E	RIPON	CA	95366	5	$1,400,000	$280,000
028-301-062	4041 CREST RD	REVZINA L & REVZINE L FAMILY TR		1631 HOLT AVENUE	LOS ALTOS	CA	94024	5	$802,825	$160,565
028-320-012	3852 PRIVATE RD	MARGERUM TERRY R TR & CHRISTINE TR		990 EUCLID AVE	BERKELEY	CA	94708	5	$282,802	$56,560
029-072-001	840 PARK AVE	GIANNOTTI FRANCES JOANNE & DOMINIKUS JAIMIE		PO BOX 16070	SOUTH LAKE TAHOE	CA	96151	5	$216,290	$43,258
029-072-004	4020 LAKESHORE BLVD	VANACHT FILIP MJMC TR & LISA SHARPLEY TR		633 HOLLINGSWORTH DR	LOS ALTOS	CA	94022	5	$968,307	$193,661
029-096-023	3912 CEDAR DR	HUGHES TIMOTHY H TR & STACI D TR		3912 CEDAR AVE	SOUTH LAKE TAHOE	CA	96150	5	$734,000	$146,800
029-101-001	3811 BEACH RD	JAMIESON TOM TR & TERRI TR		PO BOX 82515	BAKERSFIELD	CA	93380	5	$1,323,326	$264,665
029-101-013	3889 BEACH RD	3889 BEACH ROAD CA LLC		PO BOX 354	ORINDA	CA	94563	5	$1,796,182	$359,236
029-101-020	3755 BEACH RD	KALETA PAUL FREDERICK TR & VICKY ELIZABETH B TR		PO BOX 2508	STATELINE	NV	89449	5	$1,247,013	$249,403
029-181-031	3809 PIONEER TRL	WADE TERENCE C & DARLENE KAREN		1188 BISHOP ST #3205	HONOLULU	HI	96813	5	$309,445	$61,889
029-352-013	1026 MOSS RD	MEKRAKSEREE CHIRAWAT		904 PATRICIA LANE	SOUTH LAKE TAHOE	CA	96150	5	$452,005	$90,401
029-374-006	3704 ROCKY POINT RD	KOPANOS SANDRA LEE		PO BOX 32504	SAN JOSE	CA	95152	5	$339,502	$67,900
029-404-003	1129 KELLER RD	BARAJAS JOEL MEDINA & LOPEZ ITZAYARY ACOSTA		PO BOX 13098	SOUTH LAKE TAHOE	CA	96151	5	$453,448	$90,690
029-603-001	4087 SUNRISE LN	QUEIROLO SILVIO J TR & QUEIROLO SILVIO J TR & LIND		PO BOX 802	HOPLAND	CA	95449	5	$966,003	$193,201
029-604-002	4081 GREENWOOD RD	DE LA FUENTE VALENTIN SHAUN		855 FOLSOM ST #541	SAN FRANCISCO	CA	94107	5	$2,050,000	$410,000
029-604-020	4046 SUNRISE LN	HOOZ JASON L TR & JULIE G TR		325 MUIR DR	SOQUEL	CA	95073	5	$320,071	$64,014
029-604-024	4070 SUNRISE LN	TURNER JULIE ANN & KENNETH M TR		1348 MILBRAE AVE	MILLBRAE	CA	94030	5	$1,041,619	$208,324
029-605-007	4043 AZURE AVE	HASMAN NORMAN & SHIH ESTHER		35 28TH AVENUE 101	SAN MATEO	CA	94403	5	$2,150,000	$430,000
029-610-010	4104 AZURE AVE	WILLIAMS KIRK W TR & K W REV TRUST		32504 RIVER RD	SOLEDAD	CA	93960	5	$1,339,713	$267,943
029-710-008	UNASSIGNED	GONDOLA VISTA DEVE COMPANY LLC		PO BOX 121	ZEPHYR COVE	NV	89448	5	$1,598,835	$319,767
029-710-010	UNASSIGNED	GONDOLA VISTA DEVE COMPANY LLC		PO BOX 121	ZEPHYR COVE	NV	89448	5	$1,598,835	$319,767
029-710-012	UNASSIGNED	GONDOLA VISTA DEVE COMPANY LLC		PO BOX 121	ZEPHYR COVE	NV	89448	5	$1,598,835	$319,767
029-710-014	UNASSIGNED	GONDOLA VISTA DEVE COMPANY LLC		PO BOX 121	ZEPHYR COVE	NV	89448	5	$1,598,835	$319,767
029-710-016	UNASSIGNED	GONDOLA VISTA DEVE COMPANY LLC		PO BOX 121	ZEPHYR COVE	NV	89448	5	$1,598,835	$319,767
030-352-008	3702 VERDON LN	BOOKER RACHEL DEANN		PO BOX 14149	SOUTH LAKE TAHOE	CA	96151	5	$972,500	$194,500
030-363-012	3832 WOODS AVE	BUROLA GLORIA DEMAY TR & G D REV TRUST 12/13/17		3832 WOODS AVE	SOUTH LAKE TAHOE	CA	96150	5	$286,654	$57,331
030-363-014	3822 WOODS AVE	SERRANO MAURILLO & OFELIA		P O BOX 2382	SALINAS	CA	93902	5	$995,000	$199,000
030-401-001	3914 SADDLE RD	PAC 23 CA 2021 LLC CA LLC		18 E 4TH ST	CINCINNATI	OH	45202	5	$2,856,000	$571,200
030-401-003	3930 SADDLE RD	HOLDEN BRENT C CO TR & KATHRYN G CO TR		5251 PEARCE DR	HUNTINGTON BEACH	CA	92649	5	$400,354	$80,071
030-401-005	3946 SADDLE RD	HOFFMAN ROBERT B & ROBERT B & LINDA J		5758 RIVER BIRCH DR	RENO	NV	89511	5	$195,835	$39,167
030-581-003	1474 JUNE WAY	INDIANOS CATHERINE R TR		PO BOX 17173	SOUTH LAKE TAHOE	CA	96151	5	$248,372	$49,674
031-044-002	1045 TRUCKEE DR	KUDEY EDMUND A & KRISTINE M		20 NORTHVIEW CT	DANVILLE	CA	94506	5	$319,561	$63,912
031-076-012	2569 CHRIS AVE	BOONE SCOTT C		2055 CENTER ST APT 218	BERKELEY	CA	94704	5	$612,000	$122,400
031-095-005	1079 BLUE LAKE AVE	JOHNSON KENT		PO BOX 17691	SOUTH LAKE TAHOE	CA	96151	5	$198,668	$39,734
031-122-006	2616 WILLIAM AVE	PALFY KURT N TR & FAM TRUST U/T/A 3/01/13		14932 BLAKELY WAY	ALEDO	TX	76008	5	$212,996	$42,599
031-123-012	2581 ARMSTRONG AVE	HAM LIVING TRUST		2129 OSPREY DRIVE	FOLSOM	CA	95630	5	$601,800	$120,360
031-123-014	2573 ARMSTRONG AVE	JOICE TERRI L & STEADMAN TIMOTHY L		3313 ARISTIDES CT	MODESTO	CA	95355	5	$289,167	$57,833
031-143-014	2493 BERTHA AVE	LOGE ALAIN & SANTANE SANDRA		911 HAN ST	SOUTH LAKE TAHOE	CA	96150	5	$343,072	$68,614
031-162-020	2707 KNOX AVE	BUECKER ANDREW WILLIAM & AMIE JO TR		1170 IDYLBERRY ROAD	SAN RAFAEL	CA	94903	5	$589,000	$117,800
031-174-006	1163 O MALLEY DR	SCARDINA ROBERT A CO TR & KATHRYN L CO TR		200 IRIS CANYON RD APT D5	MONTEREY	CA	93940	5	$99,183	$19,837
031-203-009	1183 CARSON AVE	BUTZ GARTH A & KRISTAL L		1183 CARSON AVE	SOUTH LAKE TAHOE	CA	96150	5	$279,588	$55,918
031-236-015	1301 O MALLEY DR	KELLY JAMES & ANNA TR		2 SAN BENITO WAY	NOVATO	CA	94945	5	$1,597,403	$319,481
031-256-006	2609 SUSSEX AVE	BARRY CHARLES		23451 E CLIFF DRIVE	SANTA CRUZ	CA	95062	5	$451,860	$90,372
031-261-057	1186 LINDBERG AVE	BURBA DAVID TR & MARY D TR		1186 LINDBERG AVE	SOUTH LAKE TAHOE	CA	96150	5	$373,729	$74,746
031-261-064	1120 LINDBERG AVE	RAU LESLIE & UTTER RITA		1120 LINDBERG AVE	SOUTH LAKE TAHOE	CA	96150	5	$253,211	$50,642
031-284-017	2499 PONDEROSA ST	HERNANDEZ LAZARO & MARIA		2499 PONDEROSA ST	SOUTH LAKE TAHOE	CA	96150	5	$447,154	$89,431
031-321-032	952 SILVERWOOD CIR	GLENN NORMAN F & MATUS GLENN VIRGINIA TR		952 SILVERWOOD CIRCLE	SOUTH LAKE TAHOE	CA	96150	5	$767,771	$153,554
031-322-017	957 SPRINGWOOD CT	LABRADO JOHN & KILEIGH		957 SPRINGWOOD CT	SOUTH LAKE TAHOE	CA	96150	5	$498,722	$99,744
031-331-010	2875 SPRINGWOOD DR	ARCHIBALD DONALD F TR & VICTORIA J TR		PO BOX 14194	SOUTH LAKE TAHOE	CA	96151	5	$696,596	$139,319
031-333-006	926 CREEKWOOD DR	ODEN ROBERT O & SVEA J		926 CREEKWOOD DR	SOUTH LAKE TAHOE	CA	96150	5	$251,339	$50,268
032-241-013	1129 TATA LN	FIGEROA D D TRUST 5/17/2022		PO BOX 7178	SOUTH LAKE TAHOE	CA	96158	5	$148,247	$29,649
032-241-017	1117 TATA LN	GUARDINO RICHARD V TR & LORI ANNE TR		30 ANALISA LN	WALNUT CREEK	CA	94596	5	$825,000	$165,000
032-242-027	1098 TATA LN	PHAM KEVIN QUANG ANH & BILLER DANIEL EDWARD		129 N 13TH ST	SAN JOSE	CA	95112	5	$384,662	$76,932
032-261-001	1931 G ST	WENDELL TED C TR & TC LV RV TRUST 1/19/11		1931 G ST	SOUTH LAKE TAHOE	CA	96150	5	$212,790	$42,558
032-262-009	1365 TATA LN	MUONIO FRANCIS & VALERIE		PO BOX 8380	SOUTH LAKE TAHOE	CA	95158	5	$840,941	$168,188
032-281-006	1197 JULIE LN	WALLACE JON K II		PO BOX 14483	SOUTH LAKE TAHOE	CA	96151	5	$601,800	$120,360
032-281-023	1265 JULIE LN	SHIELDS GORDON S TR & JANE M TR		1265 JULIE LN	SOUTH LAKE TAHOE	CA	96150	5	$217,300	$43,460
023-392-015	1134 3RD ST	CLEAR WATER CADRE INVEST LLC CA LLC		P O BOX 304	CAMINO	CA	95709	14	$1,133,622	$80,973
030-421-002	1639 SHERMAN WAY	LA BANDERA RANCH TX LP		PO BOX 2135	LAKE DALLAS	TX	75065	14	$12,469,862	$890,704
025-021-080	1379 HERBERT AVE	CLARK T J & P T FAM TRUST 2/14/2000		PO BOX 88	LODI	CA	95241	13	$5,000,000	$384,615
025-360-018	1340 GLENWOOD WAY	OKLAHOMA STEEL & WIRE CO OK LLC		PO BOX 220	MADILL	OK	73446	12	$8,030,000	$669,167
025-032-002	1468 SKI RUN BLVD	CLARK TERRENCE J & PAULETTE T TR		PO BOX 88	LODI	CA	95241	10	$3,927,000	$392,700
030-380-055	3773 REGINA RD	A P A S FAM TRUST		8915 LOS LAGOS CIR	GRANITE BAY	CA	95746	10	$2,850,000	$285,000

QED

Stop this nonsense.

Sydney B. Griffin

SUGAR PINE VILLAGE WILL DESTROY 11 ACRES OF CONSERVED LANDS

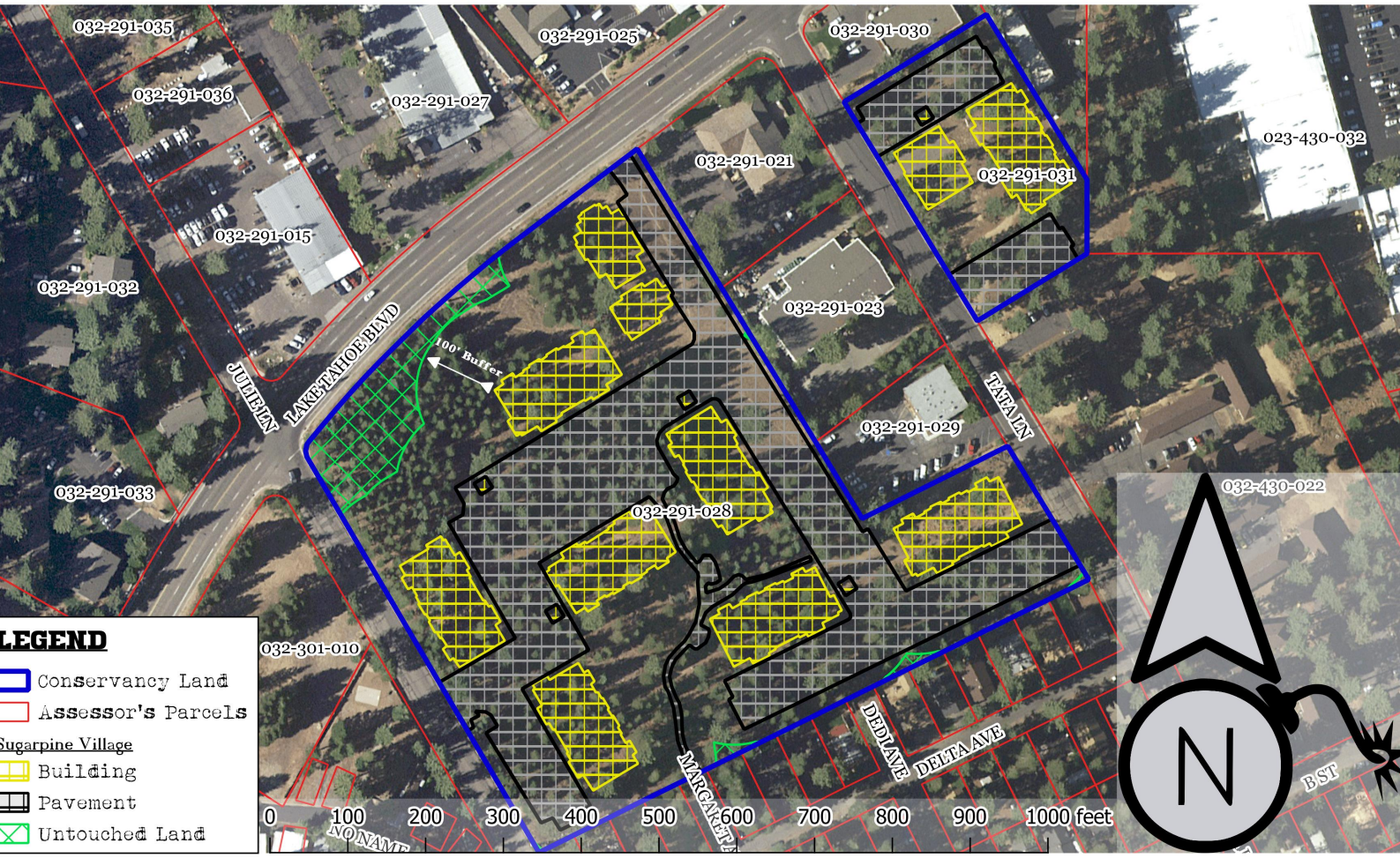

he California Tahoe Conservancy was established in 1985 to lead efforts to restore and enhance the extraordinary natural and recreational resources of the Lake Tahoe Basin. Parcels 2
nd 31 were purchased just a few years later in the spring of 1989 towards this goal. In the decades since, development interests have hijacked the Conservancy, with plans to destroy ar
ave over a healthy stand of forest habitat releasing thousands of tons of climate-warming CO2 from this "carbon sink." The construction footprint will be 6.5 acres of the combined 11.6 ac
t. A statutory (PRC § 4291) 100' buffer from structures for "defensible space" will result in the clearcutting of 95% of the conserved lands with only 0.56 acres of habitat remaining.

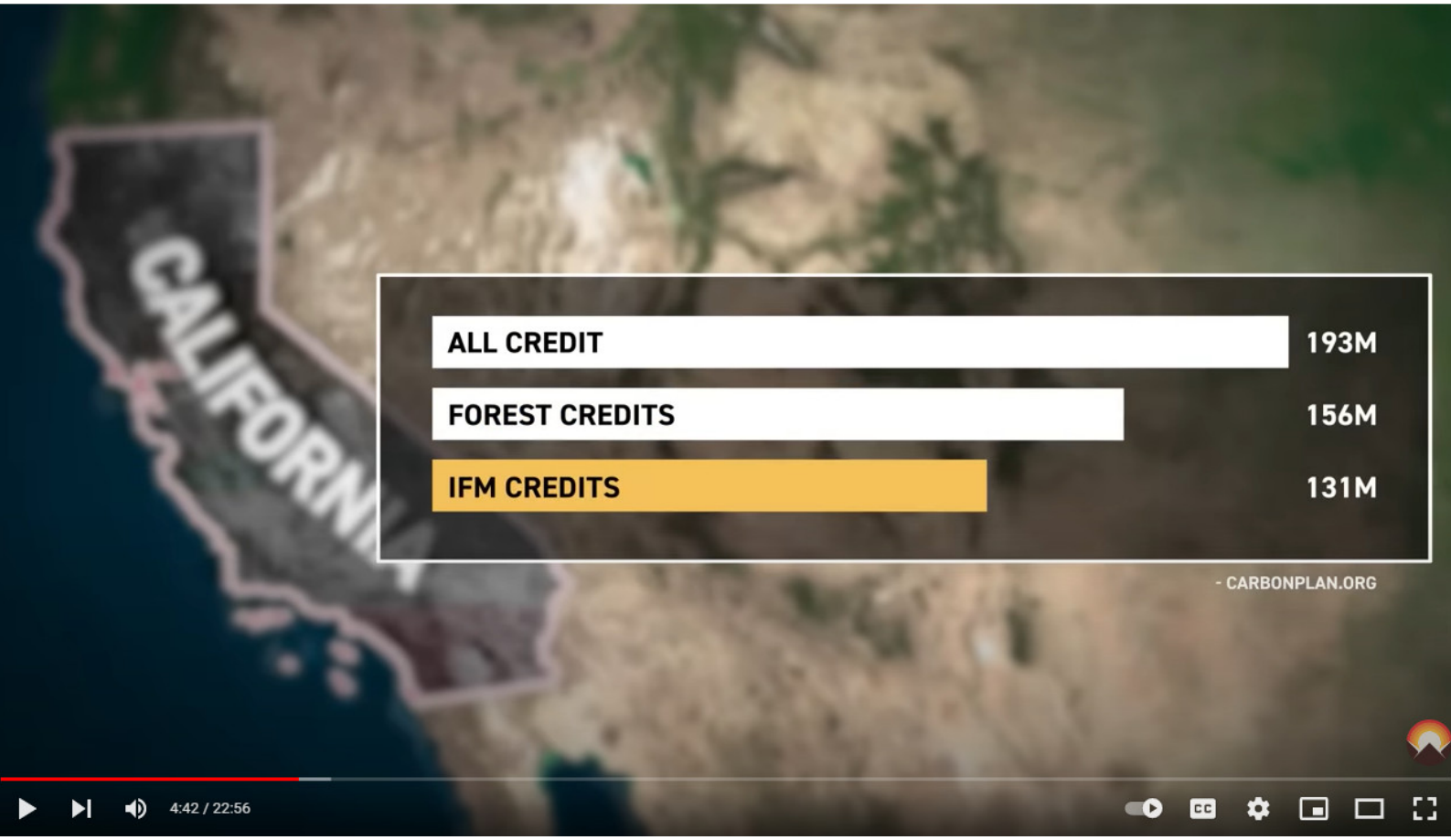
CALIFORNI
ALL CREDIT
193M
FOREST CREDITS
156M
IFM CREDITS
131M
- CARBONPLAN.ORG
4:42 / 22:56

CARBON
OFFSETS
2:00 / 23:37

Environmental Pollution 310 (2022) 119888

Contents lists available at ScienceDirect

Environmental Pollution

journal homepage: www.elsevier.com/locate/envpol

Up in smoke: California's greenhouse gas reductions could be wiped out by 2020 wildfires☆

Michael Jerrett [a,*], Amir S. Jina [b], Miriam E. Marlier [a]

[a] Department of Environmental Health Sciences, Fielding School of Public Health, University of California, Los Angeles, 650 Charles E. Young Dr. S., 56-070 CHS Box 951772, Los Angeles, CA, 90095, USA

[b] Harris School of Public Policy, University of Chicago, 1307 East 60th Street, Chicago, IL, 60637, USA

ARTICLE INFO

Keywords:
Climate change
Wildfires
Greenhouse gas emissions
Economic impacts

ABSTRACT

In this short communication, we estimate that California's wildfire carbon dioxide equivalent (CO_2e) emissions from 2020 are approximately two times higher than California's total greenhouse gas (GHG) emission reductions since 2003. Without considering future vegetation regrowth, CO_2e emissions from the 2020 wildfires could be the second most important source in the state above either industry or electrical power generation. Regrowth may partly of fully occur over a long period, but due to exigencies of the climate crisis most of the regrowth will not occur quickly enough to avert greater than 1.5 degrees of warming. Global monetized damages caused by CO_2e from in 2020 wildfire emissions amount to some $7.1 billion USD. Our analysis suggests that significant societal benefits could accrue from larger investments in improved forest management and stricter controls on new development in fire-prone areas at the wildland-urban interface.

1. Introduction

Recent evidence suggests that climate change contributes to increased wildfire activity in the western United States (Abatzoglou and Williams, 2016). California's summer wildfire burned area increased eightfold from 1972 to 2018 (Williams et al., 2019), and statewide climate change projections predict an amplification of wildfire risk due to higher temperatures and drier conditions (Westerling, 2018). Climate change exacerbates fire risks already stoked by increasing development near the wildland-urban interface (WUI) that have made humans the main ignition source in California (Keeley and Syphard, 2018), as well as decades of fire suppression and underinvestment in preventive measures such as mechanical clearing or prescribed burns (Keeley and Syphard, 2021; Kolden, 2019; Radeloff et al., 2018). Wildfires, in turn, release GHG emissions that can contribute to climate change.

California experienced its most disastrous wildfire year on record in 2020. CalFire, the state agency responsible for leading California's wildfire prevention and suppression, reports that 1.7 million hectares burned in 2020 (CalFire, 2022). Many of the worst fire years in California's history have occurred in the past 20 years, with eighteen of the top 20 most destructive fires in terms of loss of life and property since 2000 and five in 2020 alone (CalFire, 2021). The 2020 fires have been followed by another extreme fire season with 1.0 million hectares burned in 2021.

In addition to the immediate loss of life and property, hospital admissions and premature deaths have likely happened because of the smoke exposure (Cascio, 2018; Fann et al., 2018; Reid et al., 2016; Wang et al., 2020), which blanketed large parts of the state with tens of millions of people with unhealthy air quality that persisted for months in some locations. Recent estimates put the economic costs of direct health costs at $32 billion for 2018 (Wang et al., 2020). Future climate projections suggest that wildfires will become an increasingly important source of air pollution in the western U.S. (Ford et al., 2018; Liu et al., 2016).

When forests burn and are not balanced by vegetation regrowth, they shift from a natural sink to a source of carbon (van der Werf et al., 2017). This can represent a positive climate feedback loop in which increased GHG emissions contribute to climate change and further increase wildfire risk. Although wildfires are a natural feature of many ecosystems in California, the increase in severe and frequent wildfire events has raised the possibility of transformed post-fire ecosystems as new plant communities regrow following fire events that alter carbon

☆ This paper has been recommended for acceptance by Pavlos Kassomenos.

* Corresponding author.
E-mail addresses: mjerrett@ucla.edu (M. Jerrett), mmarlier@ucla.edu (M.E. Marlier).

https://doi.org/10.1016/j.envpol.2022.119888
Received 10 April 2022; Received in revised form 1 July 2022; Accepted 31 July 2022
Available online 5 August 2022
0269-7491/© 2022 The Authors. Published by Elsevier Ltd. This is an open access article under the CC BY license (http://creativecommons.org/licenses/by/4.0/).

LETTER

doi:10.1038/nature12914

Rate of tree carbon accumulation increases continuously with tree size

N. L. Stephenson[1], A. J. Das[1], R. Condit[2], S. E. Russo[3], P. J. Baker[4], N. G. Beckman[3]†, D. A. Coomes[5], E. R. Lines[6], W. K. Morris[7], N. Rüger[2,8]†, E. Álvarez[9], C. Blundo[10], S. Bunyavejchewin[11], G. Chuyong[12], S. J. Davies[13], Á. Duque[14], C. N. Ewango[15], O. Flores[16], J. F. Franklin[17], H. R. Grau[10], Z. Hao[18], M. E. Harmon[19], S. P. Hubbell[2,20], D. Kenfack[13], Y. Lin[21], J.-R. Makana[15], A. Malizia[10], L. R. Malizia[22], R. J. Pabst[19], N. Pongpattananurak[23], S.-H. Su[24], I-F. Sun[25], S. Tan[26], D. Thomas[27], P. J. van Mantgem[28], X. Wang[18], S. K. Wiser[29] & M. A. Zavala[30]

Forests are major components of the global carbon cycle, providing substantial feedback to atmospheric greenhouse gas concentrations[1]. Our ability to understand and predict changes in the forest carbon cycle—particularly net primary productivity and carbon storage—increasingly relies on models that represent biological processes across several scales of biological organization, from tree leaves to forest stands[2,3]. Yet, despite advances in our understanding of productivity at the scales of leaves and stands, no consensus exists about the nature of productivity at the scale of the individual tree[4–7], in part because we lack a broad empirical assessment of whether rates of absolute tree mass growth (and thus carbon accumulation) decrease, remain constant, or increase as trees increase in size and age. Here we present a global analysis of 403 tropical and temperate tree species, showing that for most species mass growth rate increases continuously with tree size. Thus, large, old trees do not act simply as senescent carbon reservoirs but actively fix large amounts of carbon compared to smaller trees; at the extreme, a single big tree can add the same amount of carbon to the forest within a year as is contained in an entire mid-sized tree. The apparent paradoxes of individual tree growth increasing with tree size despite declining leaf-level[8–10] and stand-level[10] productivity can be explained, respectively, by increases in a tree's total leaf area that outpace declines in productivity per unit of leaf area and, among other factors, age-related reductions in population density. Our results resolve conflicting assumptions about the nature of tree growth, inform efforts to understand and model forest carbon dynamics, and have additional implications for theories of resource allocation[11] and plant senescence[12].

A widely held assumption is that after an initial period of increasing growth, the mass growth rate of individual trees declines with increasing tree size[4,5,13–16]. Although the results of a few single-species studies have been consistent with this assumption[15], the bulk of evidence cited in support of declining growth is not based on measurements of individual tree mass growth. Instead, much of the cited evidence documents either the well-known age-related decline in net primary productivity (hereafter 'productivity') of even-aged forest stands[10] (in which the trees are all of a similar age) or size-related declines in the rate of mass gain per unit leaf area (or unit leaf mass)[8–10], with the implicit assumption that declines at these scales must also apply at the scale of the individual tree. Declining tree growth is also sometimes inferred from life-history theory to be a necessary corollary of increasing resource allocation to reproduction[11,16]. On the other hand, metabolic scaling theory predicts that mass growth rate should increase continuously with tree size[6], and this prediction has also received empirical support from a few site-specific studies[6,7]. Thus, we are confronted with two conflicting generalizations about the fundamental nature of tree growth, but lack a global assessment that would allow us to distinguish clearly between them.

To fill this gap, we conducted a global analysis in which we directly estimated mass growth rates from repeated measurements of 673,046 trees belonging to 403 tropical, subtropical and temperate tree species, spanning every forested continent. Tree growth rate was modelled as a function of log(tree mass) using piecewise regression, where the independent variable was divided into one to four bins. Conjoined line segments were fitted across the bins (Fig. 1).

For all continents, aboveground tree mass growth rates (and, hence, rates of carbon gain) for most species increased continuously with tree mass (size) (Fig. 2). The rate of mass gain increased with tree mass in each model bin for 87% of species, and increased in the bin that included the largest trees for 97% of species; the majority of increases were statistically significant (Table 1, Extended Data Fig. 1 and Supplementary Table 1). Even when we restricted our analysis to species achieving the largest sizes (maximum trunk diameter >100 cm; 33% of species), 94% had increasing mass growth rates in the bin that included the largest trees. We found no clear taxonomic or geographic patterns among the 3% of species with declining growth rates in their largest trees, although the small number of these species (thirteen) hampers inference. Declining species included both angiosperms and gymnosperms in seven of the 76 families in our study; most of the seven families had only one or two declining species and no family was dominated by declining species (Supplementary Table 1).

When we log-transformed mass growth rate in addition to tree mass, the resulting model fits were generally linear, as predicted by metabolic scaling theory[6] (Extended Data Fig. 2). Similar to the results of our main

[1]US Geological Survey, Western Ecological Research Center, Three Rivers, California 93271, USA. [2]Smithsonian Tropical Research Institute, Apartado 0843-03092, Balboa, Republic of Panama. [3]School of Biological Sciences, University of Nebraska, Lincoln, Nebraska 68588, USA. [4]Department of Forest and Ecosystem Science, University of Melbourne, Victoria 3121, Australia. [5]Department of Plant Sciences, University of Cambridge, Cambridge CB2 3EA, UK. [6]Department of Geography, University College London, London WC1E 6BT, UK. [7]School of Botany, University of Melbourne, Victoria 3010, Australia. [8]Spezielle Botanik und Funktionelle Biodiversität, Universität Leipzig, 04103 Leipzig, Germany. [9]Jardín Botánico de Medellín, Calle 73, No. 51D-14, Medellín, Colombia. [10]Instituto de Ecología Regional, Universidad Nacional de Tucumán, 4107 Yerba Buena, Tucumán, Argentina. [11]Research Office, Department of National Parks, Wildlife and Plant Conservation, Bangkok 10900, Thailand. [12]Department of Botany and Plant Physiology, Buea, Southwest Province, Cameroon. [13]Smithsonian Institution Global Earth Observatory—Center for Tropical Forest Science, Smithsonian Institution, PO Box 37012, Washington, DC 20013, USA. [14]Universidad Nacional de Colombia, Departamento de Ciencias Forestales, Medellín, Colombia. [15]Wildlife Conservation Society, Kinshasa/Gombe, Democratic Republic of the Congo. [16]Unité Mixte de Recherche—Peuplements Végétaux et Bioagresseurs en Milieu Tropical, Université de la Réunion/CIRAD, 97410 Saint Pierre, France. [17]School of Environmental and Forest Sciences, University of Washington, Seattle, Washington 98195, USA. [18]State Key Laboratory of Forest and Soil Ecology, Institute of Applied Ecology, Chinese Academy of Sciences, Shenyang 110164, China. [19]Department of Forest Ecosystems and Society, Oregon State University, Corvallis, Oregon 97331, USA. [20]Department of Ecology and Evolutionary Biology, University of California, Los Angeles, California 90095, USA. [21]Department of Life Science, Tunghai University, Taichung City 40704, Taiwan. [22]Facultad de Ciencias Agrarias, Universidad Nacional de Jujuy, 4600 San Salvador de Jujuy, Argentina. [23]Faculty of Forestry, Kasetsart University, ChatuChak Bangkok 10900, Thailand. [24]Taiwan Forestry Research Institute, Taipei 10066, Taiwan. [25]Department of Natural Resources and Environmental Studies, National Dong Hwa University, Hualien 97401, Taiwan. [26]Sarawak Forestry Department, Kuching, Sarawak 93660, Malaysia. [27]Department of Botany and Plant Pathology, Oregon

PNAS Nexus, 2023, 2, 1–9
https://doi.org/10.1093/pnasnexus/pgad004
Advance access publication 28 February 2023
Research Report

Low-elevation conifers in California's Sierra Nevada are out of equilibrium with climate

Avery P. Hill[a,*], Connor J. Nolan[b], Kyle S. Hemes[b], Trevor W. Cambron[c] and Christopher B. Field[a,b,c]

[a]Department of Biology, Stanford University, Stanford, CA, USA
[b]Woods Institute for the Environment, Stanford University, Stanford, CA, USA
[c]Department of Earth System Science, Stanford University, Stanford, CA, USA
*To whom correspondence should be addressed: Email: aph82@stanford.edu
Edited By: Adelia Bovell-Benjamin

Abstract

Since the 1930s, California's Sierra Nevada has warmed by an average of 1.2°C. Warming directly primes forests for easier wildfire ignition, but the change in climate also affects vegetation species composition. Different types of vegetation support unique fire regimes with distinct probabilities of catastrophic wildfire, and anticipating vegetation transitions is an important but undervalued component of long-term wildfire management and adaptation. Vegetation transitions are more likely where the climate has become unsuitable but the species composition remains static. This vegetation climate mismatch (VCM) can result in vegetation conversions, particularly after a disturbance like wildfire. Here we produce estimates of VCM within conifer-dominated forests in the Sierra Nevada. Observations from the 1930s Wieslander Survey provide a foundation for characterizing the historical relationship between Sierra Nevada vegetation and climate before the onset of recent, rapid climate change. Based on comparing the historical climatic niche to the modern distribution of conifers and climate, ~19.5% of modern Sierra Nevada coniferous forests are experiencing VCM, 95% of which is below an elevation of 2356 m. We found that these VCM estimates carry empirical consequences: likelihood of type-conversion increased by 9.2% for every 10% decrease in habitat suitability. Maps of Sierra Nevada VCM can help guide long-term land management decisions by distinguishing areas likely to transition from those expected to remain stable in the near future. This can help direct limited resources to their most effective uses—whether it be protecting land or managing vegetation transitions—in the effort to maintain biodiversity, ecosystem services, and public health in the Sierra Nevada.

Keywords: ecology, habitat suitability modeling, vegetation transitions, vegetation climate mismatch, climate change, California

Significance Statement

Warming climatic conditions over the last century have led to observable shifts in the spatial organization of dominant tree species in California's Sierra Nevada. Little is known, however, about the extent to which these shifts have tracked the magnitude of climate change. This study maps Vegetation Climate Mismatch in the Sierra Nevada—areas where climate change has left trees in climatic conditions where they have not historically occurred. Different vegetation types support different wildfire regimes, ecosystems, and ecosystem services. Our maps will be useful for anticipating vegetation transitions and informing long-term wildfire and ecosystem management across the Sierra Nevada mountains of California.

Introduction

Warmer and drier conditions prime forests for ignition (1), but climate change also directly affects the species composition of future vegetation. Climate-driven vegetation conversion is an understudied phenomenon in general and a potentially significant determinant of catastrophic wildfire risk that could require changes in management strategies (2–4).

Broadly, climate change has caused vegetation to shift poleward and up-slope (5–7). In long-lived ecosystems like forests, climate change is occurring faster than the ability of many plants to shift their distributions or adapt, resulting in vegetation disequilibrium (8) or vegetation climate mismatch (VCM). Forests experiencing VCM are at risk of converting to alternative species assemblages, particularly after stand-replacing disturbances such as severe wildfire (4). In some cases, VCM can even make forests more susceptible to wildfires (9).

VCM is likely to be found in California's transition zone between low-elevation conifer-dominated forest and angiosperm-dominated vegetation (including mixed chaparral, oak woodland, and mixed broadleaf forest) (Fig. 1; elevation ~1000–1400 m)—where the foothills of the Sierra Nevada end and the mountains of the western flank begin. These forests lie on the warm end of mixed conifer distributions, where canopy dominants include ponderosa pine, sugar pine, and Douglas-fir (10), and understories

Competing Interest: The authors declare that they have no competing interests.
Received: July 16, 2022. **Revised:** December 19, 2022. **Accepted:** January 4, 2023
© The Author(s) 2023. Published by Oxford University Press on behalf of National Academy of Sciences. This is an Open Access article

Downloaded from https://academic.oup.com/pnasnexus/article/2/2/pgad004/7059010 by guest on 23 March 2023

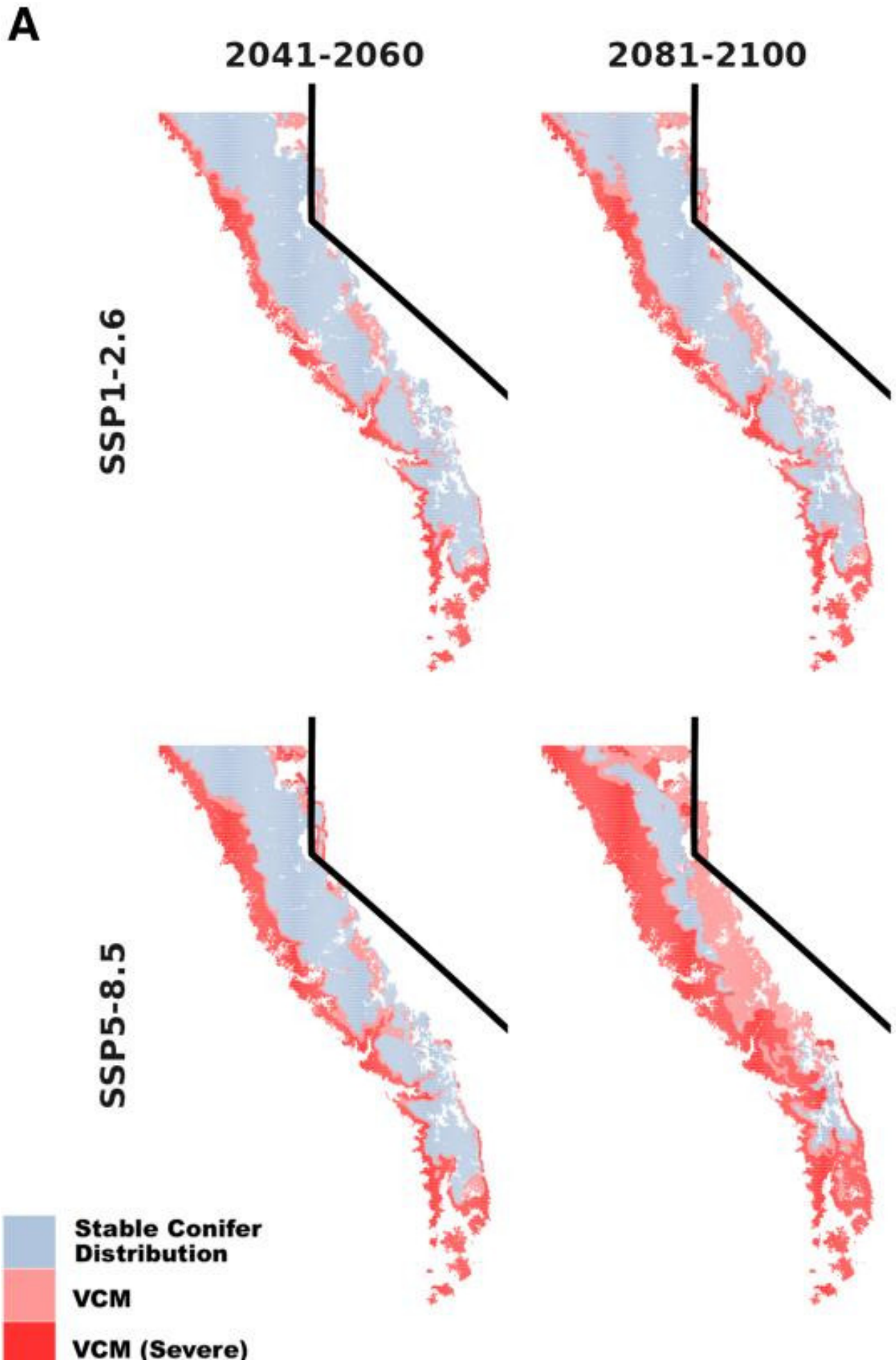
A
2041-2060
2081-2100
SSP1-2.6
SSP5-8.5
Stable Conifer Distribution
VCM
VCM (Severe)

Sierra Nevada Conifer Vegetation Climate Mismatch

(Hill et al., 2023)

Since the 1930s, California's Sierra Nevada has warmed by an average of 1.2C. Vegetation transitions are more likely where the climate has become unsuitable but the species composition remains static. This vegetation climate mismatch (VCM) can result in vegetation conversions, particularly after a disturbance like wildfire. Here we produce estimates of VCM within conifer-dominated forests in the Sierra Nevada. Observations from the 1930s Wieslander Survey provide a foundation for characterizing the historical relationship between Sierra Nevada vegetation and climate before the onset of recent, rapid climate change. Maps of Sierra Nevada VCM can help guide long-term land management decisions by distinguishing areas likely to transition from those expected to remain stable in the near future.

Basemap

- Satellite
- OpenStreetMap

VCM Layer Opacity

0 0.85 1

0 0.1 0.2 0.3 0.4 0.5 0.6 0.7 0.8 0.9 1

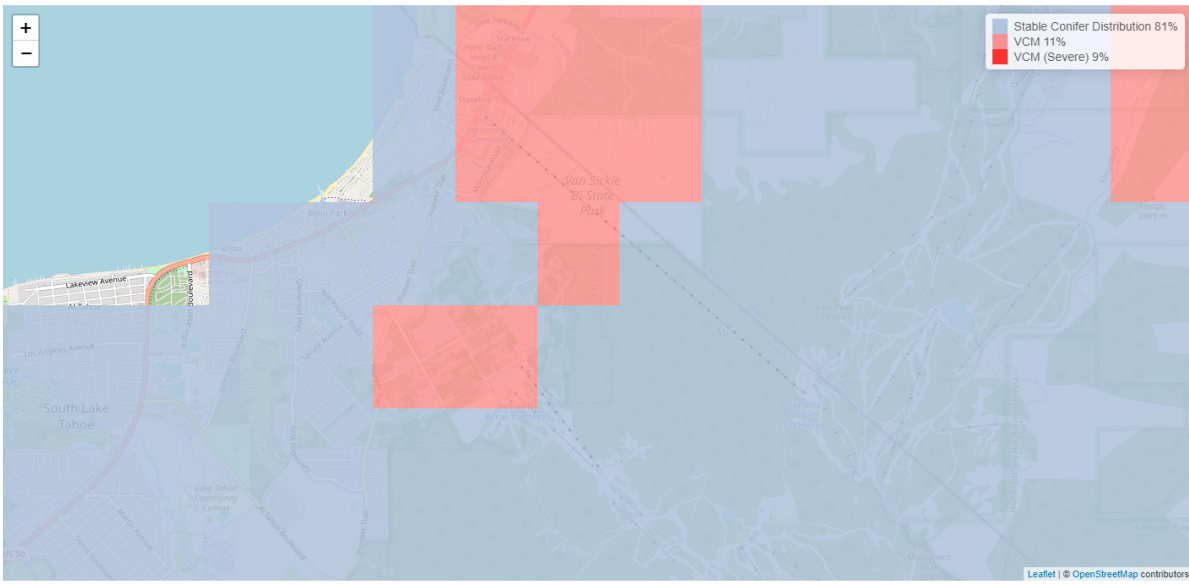

in plans for specific geographic areas. Provisions of more detailed Plan Area Statements, Community Plans and other adopted plans prevail until superseded by conforming Area Plans. Amendments that are included in the 2012 Regional Plan Update include the following:

1. Amended Conservation Classification to Recognize USFS Ownership
2. Minor Boundary Modifications to Recognize Public Land Acquisitions by USFS, CA and NV
3. Minor Boundary correction to change Heavenly Ski Area property from Residential to Recreation
4. Recognize Commercial Districts as Mixed-Use Areas
5. Parcels adjoining the High Density Tourist District designated Recreation. This includes 479 acres of the Van Sickle State Park and approximately 256 acres of private land
6. Added Residential and Recreation Land Use Classification amendments, per Ordinance 2014-02 (amended 05/24/14).
7. Center and regional land use classification amendments were added for the Tahoe Valley Area Plan and for the Placer County Tahoe Basin Area Plan. This layer was edited in July 2017 to reflect changes from the adoption of Placer County Tahoe Basin Area Plan (adopted on January 25, 2017 pursuant to Ordinance # 2017-01).

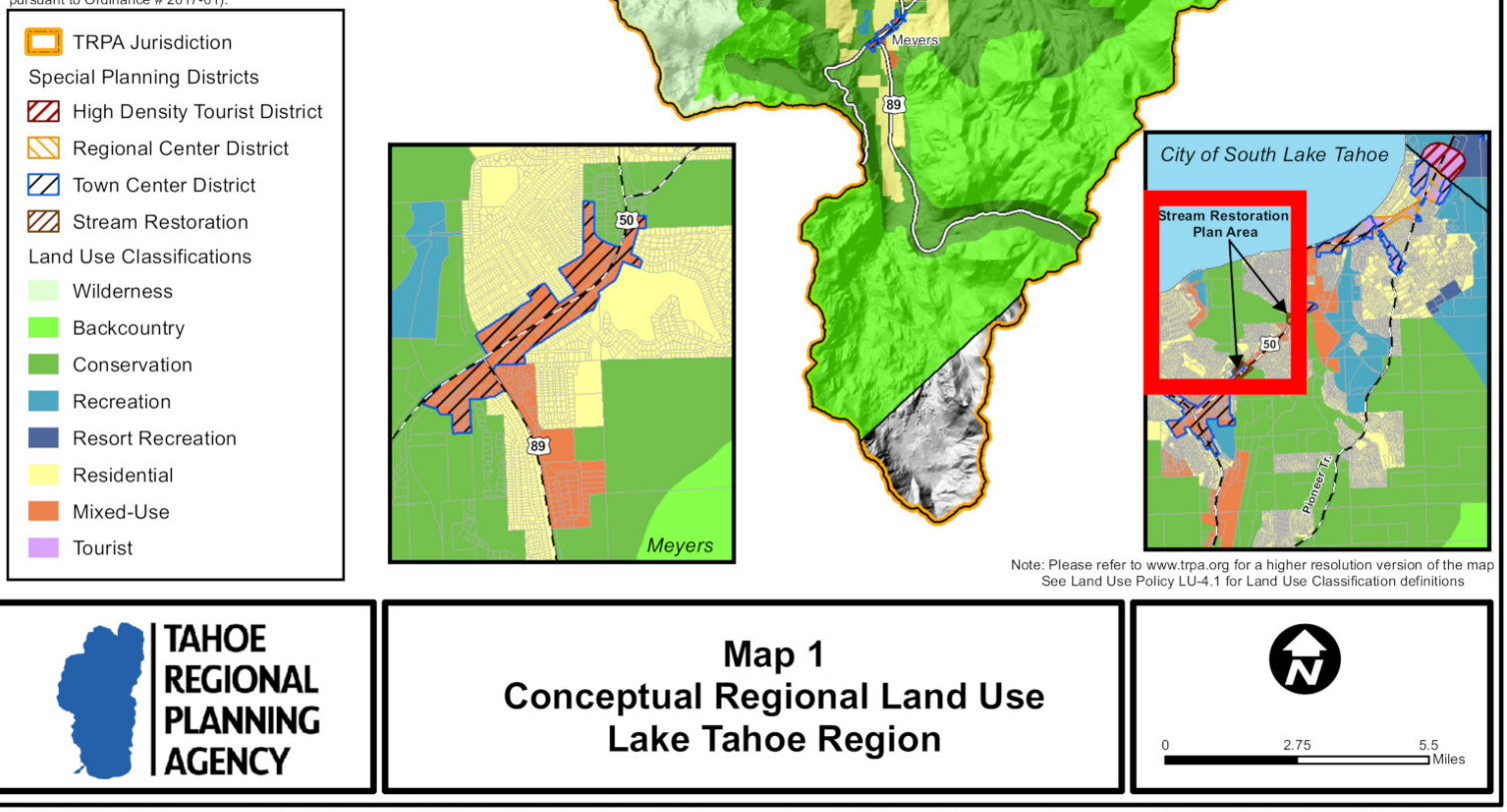

Note: Please refer to www.trpa.org for a higher resolution version of the map
See Land Use Policy LU-4.1 for Land Use Classification definitions

TAHOE REGIONAL PLANNING AGENCY

Map 1
Conceptual Regional Land Use
Lake Tahoe Region

0 2.75 5.5 Miles

TRPA MAP DISCLAIMER: This map was developed and produced by the TRPA GIS department. It is provided for reference only and is not intended to show map scale accuracy or all inclusive map features. The material on this map was compiled using the most current data available, but the data is dynamic and accuracy cannot be guaranteed. Document Path: F:\GIS\MXDS\Regional Plan Update\Jan2014Recreated\Map1_ConceptualRegLandUse_2017amendment.mxd

To estimate the possible order of magnitude of the revenue that may be generated under a likely residential vacancy tax scenario, BAE assumed a tax of $3,000 per vacant unit, which is generally consistent with the tax being charged in Oakland. Assuming that all housing units held vacant for seasonal or occasional use would be subject to the tax, BAE estimates that a vacancy tax could theoretically generate up to around $16.8 million per year.

Table 6: Housing Units by Vacancy Status and Tenure, 2020

		Occupied		
Units in Structure	**Vacant**	Renter	Owner	**Total**
1, detached	4,507	1,751	3,314	9,609
1, attached	175	396	73	636
2	292	526	162	971
3 or 4	566	729	17	1,315
5 to 9	397	750	3	1,144
10 to 19	161	575	13	738
20 to 49	197	319	21	536
50 or more	296	89	34	428
Mobile home	103	254	240	585
Boat, RV, van, etc.	0	0	0	0
Total, All Units	**6,695**	**5,390**	**3,876**	**15,961**
Percent	*42%*	*34%*	*24%*	*100%*

Source: U.S. Census Bureau, 2020 Decennial Census, Table H1; U.S. Census Bureau, 2020 American Community Survey 5-Year, Tables B25024 and B25032; BAE, 2022.

This report also considered applying the residential vacancy tax only to single-family properties held for seasonal or occasional use. While the Census Bureau does not specifically report the required statistic, the available data does indicate that there were around 4,500 single-family homes that were vacant for any reason as of the 2020 Decennial Census (i.e., roughly 47 percent of the single-family housing stock).[32] Assuming that the vacancy tax applies to single-family properties only, that are vacant for any reason, the tax could yield roughly $13.5 million per year in revenue.

Applying the citywide seasonal vacancy rate of 84 percent (i.e., the percent of vacant units held for seasonal or occasional use) to the 2020 vacant single-family inventory produces a conservative estimate of around 3,800 single-family units held for seasonal or occasional use. If the vacancy tax is applied only to single-family units held vacant for seasonal or occasional use, the tax may generate approximately nearly $11.4 million per year in revenue.

Table 2: Residential Sales Activity, 2017 to 2022 YTD

All Residential Units	2017	2018	2019	2020	2021	2022 YTD (a)	All Sales
Number of Sales	348	341	389	625	513	394	2,610
Median Sale Price	$385,000	$420,000	$435,000	$500,000	$602,000	$642,500	$500,000
Ave. Sale price	$462,097	$514,954	$557,259	$624,223	$765,300	$791,868	$631,386
Ave. Size (sq. ft.)	1,494	1,495	1,552	1,626	1,561	1,548	1,556
Ave. Sale Price per sq.ft.	$311	$345	$365	$384	$493	$521	$408
Maximum Sale Price	$2,337,500	$2,450,000	$5,300,000	$5,200,000	$5,550,000	$5,300,000	$5,550,000
Minimum Sale Price	$71,000	$100,500	$46,000	$3,500	$50,000	$75,000	$3,500

Single Family Homes	2017	2018	2019	2020	2021	2022 YTD (a)	All Sales
Number of Sales	333	322	368	585	483	367	2,458
Median Sale Price	$389,000	$425,000	$440,000	$505,000	$613,000	$650,000	$505,000
Ave. Sale price	$462,217	$525,288	$563,064	$632,835	$783,050	$809,834	$641,131
Ave. Size (sq. ft.)	1,505	1,512	1,577	1,659	1,585	1,579	1,580
Ave. Sale Price per sq.ft.	$310	$349	$362	$381	$496	$522	$408
Maximum Sale Price	$2,200,000	$2,450,000	$5,300,000	$5,200,000	$5,550,000	$5,300,000	$5,550,000
Minimum Sale Price	$71,000	$100,500	$46,000	$3,500	$75,000	$75,000	$3,500

Condominiums	2017	2018	2019	2020	2021	2022 YTD (a)	All Sales
Number of Sales	15	19	21	40	30	27	152
Median Sale Price	$295,000	$265,000	$346,500	$354,250	$417,500	$480,000	$363,750
Ave. Sale price	$459,433	$339,816	$455,524	$498,275	$479,533	$547,667	$473,803
Ave. Size (sq. ft.)	1,236	1,203	1,106	1,144	1,171	1,118	1,156
Ave. Sale Price per sq.ft.	$328	$289	$421	$417	$445	$505	$414
Maximum Sale Price	$2,337,500	$799,000	$1,250,000	$2,700,000	$1,180,000	$1,349,000	$2,700,000
Minimum Sale Price	$180,000	$168,000	$97,500	$165,000	$50,000	$232,500	$50,000

Note:
(a) As of December 15, 2022.

Sources: ListSource; BAE, 2022.

City of South Lake Tahoe — VHR Housing Stock

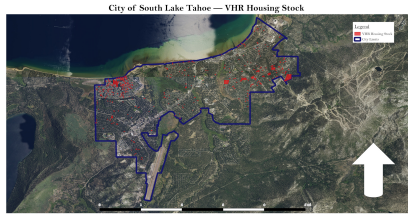

Within the City of South Lake Tahoe's municipal boundary limits, there are nearly 400 residences with five or more bedrooms. Depicted in this map are just the 300 "VHR-maximum" style residences with five or more bedrooms, with 44 of these having six or more bedrooms. The City is currently spending over $900,000 per year on the wasteful Supportive Village debacle which destroyed, subsidized, and privatized public conservancy land. The price per bedroom for these residences is $1,000 per bedroom, including on low-income housing. The City should acquire these mansions and direct tenants there into a workforce housing cooperative. Our primary purpose of "Measure T" was to fund VHR residences for local residents.

ASSESSOR'S PROPERTY #(OWNER)	OWNER NAME	CA DRE	OWNER ADDRESS	CITY	STATE	ZIP	BEDROOMS	SALES	Value/Bedroom
023-320-050	1222 VERDILLO TR		1222 VERDILLO TR	LAS VEGAS	NV	89117	5	$1,115,000	$223,000
023-320-050	1222 VERDILLO TR		1222 VERDILLO TR	LAS VEGAS	NV	89117	5	$1,115,000	$223,000
023-561-060	2387 BEACH DR		2387 BEACH DR	CARSON	NV	89706	5	$1,800,000	$357,143
029-312-021	2 HILTOP DR LTD		50 NW 183RD A 1 UNIT	MIAMI	FL	33169	5	$1,125,000	$225,000

SUGAR PINE VILLAGE WILL DESTROY 11 ACRES OF CONSERVED LANDS

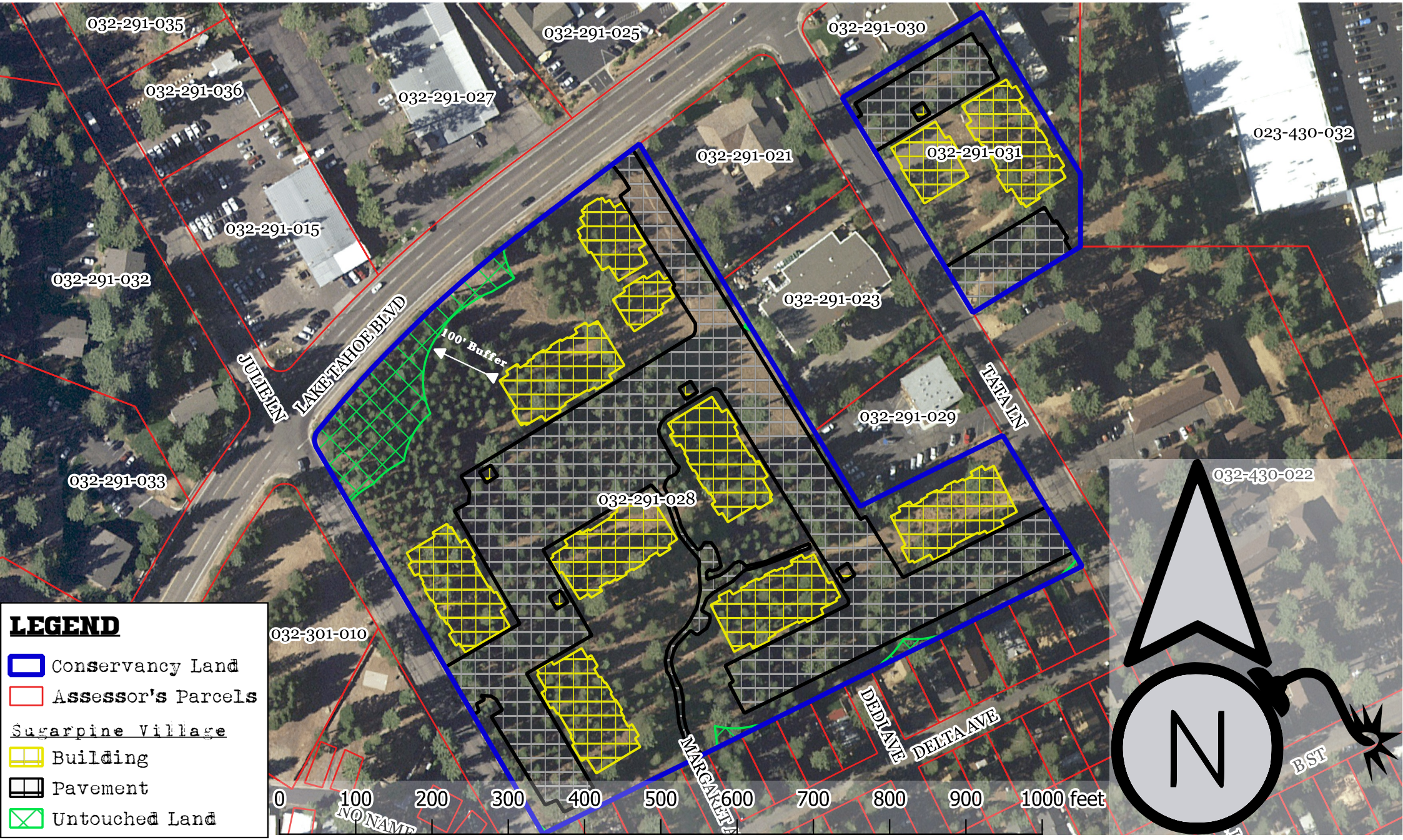

The California Tahoe Conservancy was established in 1985 to lead efforts to restore and enhance the extraordinary natural and recreational resources of the Lake Tahoe Basin. Parcels 28 and 31 were purchased just a few years later in the spring of 1989 towards this goal. In the decades since, development interests have hijacked the Conservancy, with plans to destroy and pave over a healthy stand of forest habitat releasing thousands of tons of climate-warming CO2 from this "carbon sink." The construction footprint will be 6.5 acres of the combined 11.6 acre lot. A statutory (PRC § 4291) 100' buffer from structures for "defensible space" will result in the clearcutting of 95% of the conserved lands with only 0.56 acres of habitat remaining.

Assessor Parcel Number 03229128100

1989-0015341 • B: 03107 P: 641 • GRANT DEED

Recording Date	Grantor (2)	Grantee
03/28/1989 12:00 AM	**PESKIN HENRIETTA ETAL** **PESKIN LEON D ETAL**	**CAL ST RESOURCES AGCY**

Office of the Assessor

Historical Property Information

Parcel Number: 032-291-28-100

Property Address: 1860 LAKE TAHOE BLVD

Assessor's information is for assessment and tax purposes only and should not be relied upon for status of development or building purposes.

Property Description:

Primary Use**: **30, VACANT COMMERCIAL LAND**
Subdivision Tract Number: **275**
Subdivision Tract Name: **TAHOE VALLEY CENTER UNIT NO 3**
APN Status: **11, Inactive - Non-Taxable**
Reference: **POR L 5**
Tax Rate Area: **002-002**
School District:
Last Appraisal Effective Date: **2/1/1975**
Last Appraisal Reason:
MPR Card: **032-291-28**

The **USE is only reviewed at the time of the last taxable event, and may not be a legal use

Associated Maps for: **032-291-28-100**

Most Recent Plat:	Assessor's Plat 032-29
Historical Plat:	Historical Plat 032-29
Subdivision Maps:	Tahoe Vly Cntr #3: C-109
	Tahoe Vly Cntr #3: C-109A

2020 - 2021 Taxable Property Values for: **032-291-28-100**

Property	Value
Land Total	$0
Improvement Total	$0
Personal property Total	$0
Total Roll	$0
(Exemptions Total)	$0
Net Roll	$0

Event List for: **032-291-28-100**

Roll	Event Date	Bill Status	Event Status	Seq #	Event Type	Stmt. Status	ID	Tax Bill #	Value
2018	1/1/2018	Inactive	Annual Roll	1	Roll	No Bill			$0
2017	1/1/2017	Inactive	Annual Roll	1	Roll	No Bill			$0
2016	1/1/2016	Inactive	Annual Roll	1	Roll	No Bill			$0
2015	1/1/2015	Inactive	Annual Roll	1	Roll	No Bill			$0
2014	1/1/2014	Inactive	Annual Roll	1	Roll	No Bill			$0
2013	1/1/2013	Inactive	Annual Roll	1	Roll	No Bill			$0
2012	1/1/2012	Inactive	Annual Roll	1	Roll	No Bill			$0
2011	1/1/2011	Inactive	Annual Roll	1	Roll	No Bill			$0
2010	1/1/2010	Inactive	Annual Roll	1	Roll	No Bill			$0
2009	1/1/2009	Inactive	Annual Roll	1	Roll	No Bill			$0
2008	1/1/2008	Inactive	Annual Roll	1	Roll	No Bill			$0
2007	1/1/2007	Inactive	Annual Roll	1	Roll	No Bill			$0
2006	1/1/2006	Inactive	Annual Roll	1	Roll	No Bill			$0
2005	1/1/2005	Inactive	Annual Roll	1	Roll	No Bill			$0
2004	1/1/2004	Inactive	Annual Roll	1	Roll	No Bill			$0
2003	1/1/2003	Inactive	Annual Roll	1	Roll	No Bill			$0
2002	1/1/2002	Inactive	Annual Roll	1	Roll	No Bill			$0
2001	1/1/2001	Inactive	Annual Roll	1	Roll	No Bill			$0
2000	1/1/2000	Inactive	Annual Roll	1	Roll	No Bill			$0
1999	1/1/1999	Inactive	Annual Roll	1	Roll	No Bill			$0
1998	1/1/1998	Inactive	Annual Roll	1	Roll	No Bill			$0
1997	1/1/1997	Inactive	Annual Roll	1	Roll	No Bill			$0
1996	3/1/1996	Inactive	Annual Roll	1	Roll	No Bill			$0
1995	3/1/1995	Inactive	Annual Roll	1	Roll	No Bill			$0

1994	3/1/1994	Inactive	Annual Roll	1	Roll	No Bill			$0
1993	3/1/1993	Inactive	Annual Roll	1	Roll	No Bill			$0
1992	3/1/1992	Inactive	Annual Roll	1	Roll	No Bill			$0
1991	3/1/1991	Inactive	Annual Roll	1	Roll	No Bill			$0
1990	3/1/1990	Inactive	Annual Roll	1	Roll	No Bill			$0
1989	3/1/1989	Inactive	Annual Roll	1	Roll	No Bill			$0
1988	3/1/1988	Active	Annual Roll	1	Roll	Pending			$30,165

Property Characteristics for: **032-291-28-100**

Property Characteristic	Description
Book Category Number	2032
Current Record Flag	Yes

Parcel Split Background for: **032-291-28-100**

This Parcel Has No Split Background Records.

Related Accounts for: **032-291-28-100**

This Parcel Has No Related Accounts.

Owner Change History for: **032-291-28-100**

Recorded Document: 1989-3107641
Record Change Date: 3/28/1989
Effective Owner Change Date: 3/28/1989
Preliminary Change of Ownership: **1989-3107641**

Recorded Document:
Recorder's Book and Page: 0909-188
Record Change Date: 11/21/1968
Effective Owner Change Date: 11/21/1968
Preliminary Change of Ownership: **1-0909188**

Assessor Parcel Number 03229131100

1989-0018637 • B: 03117 P: 37 • GRANT DEED

Recording Date	Grantor (10)	Grantee
04/13/1989 12:00 AM	**WEIR PAULINE ETAL** **MORELAND CAROL C ETAL** **MORELAND W D ETAL** **WEIR DONALD E ETAL** **WEIR PATRICIA ETAL**	**CAL ST RESOURCES AGCY**

Office of the Assessor

Historical Property Information

Parcel Number: 032-291-31-100

Property Address: 1029 TATA LN

Assessor's information is for assessment and tax purposes only and should not be relied upon for status of development or building purposes.

Property Description:

Primary Use**: **82, PARKING LOT**
Subdivision Tract Number: **275**
Subdivision Tract Name: **TAHOE VALLEY CENTER UNIT NO 3**
APN Status: **11, Inactive - Non-Taxable**
Reference: **PM 2/52/2**
Tax Rate Area: **002-002**
School District:
Last Appraisal Effective Date: **2/1/1979**
Last Appraisal Reason:
MPR Card: **032-291-31**

The **USE is only reviewed at the time of the last taxable event, and may not be a legal use

Associated Maps for: **032-291-31-100**

Most Recent Plat:	Assessor's Plat 032-29
Historical Plat:	Historical Plat 032-29
Subdivision Maps:	Tahoe Vly Cntr #3: C-109
	Tahoe Vly Cntr #3: C-109A

2020 - 2021 Taxable Property Values for: **032-291-31-100**

Property	Value
Land Total	$0
Improvement Total	$0
Personal property Total	$0
Total Roll	$0
(Exemptions Total)	$0
Net Roll	$0

Event List for: **032-291-31-100**

Roll	Event Date	Bill Status	Event Status	Seq #	Event Type	Stmt. Status	ID	Tax Bill #	Value
2018	1/1/2018	Inactive	Annual Roll	1	Roll	No Bill			$0
2017	1/1/2017	Inactive	Annual Roll	1	Roll	No Bill			$0
2016	1/1/2016	Inactive	Annual Roll	1	Roll	No Bill			$0
2015	1/1/2015	Inactive	Annual Roll	1	Roll	No Bill			$0
2014	1/1/2014	Inactive	Annual Roll	1	Roll	No Bill			$0
2013	1/1/2013	Inactive	Annual Roll	1	Roll	No Bill			$0
2012	1/1/2012	Inactive	Annual Roll	1	Roll	No Bill			$0
2011	1/1/2011	Inactive	Annual Roll	1	Roll	No Bill			$0
2010	1/1/2010	Inactive	Annual Roll	1	Roll	No Bill			$0
2009	1/1/2009	Inactive	Annual Roll	1	Roll	No Bill			$0
2008	1/1/2008	Inactive	Annual Roll	1	Roll	No Bill			$0
2007	1/1/2007	Inactive	Annual Roll	1	Roll	No Bill			$0
2006	1/1/2006	Inactive	Annual Roll	1	Roll	No Bill			$0
2005	1/1/2005	Inactive	Annual Roll	1	Roll	No Bill			$0
2004	1/1/2004	Inactive	Annual Roll	1	Roll	No Bill			$0
2003	1/1/2003	Inactive	Annual Roll	1	Roll	No Bill			$0
2002	1/1/2002	Inactive	Annual Roll	1	Roll	No Bill			$0
2001	1/1/2001	Inactive	Annual Roll	1	Roll	No Bill			$0
2000	1/1/2000	Inactive	Annual Roll	1	Roll	No Bill			$0
1999	1/1/1999	Inactive	Annual Roll	1	Roll	No Bill			$0
1998	1/1/1998	Inactive	Annual Roll	1	Roll	No Bill			$0
1997	1/1/1997	Inactive	Annual Roll	1	Roll	No Bill			$0
1996	3/1/1996	Inactive	Annual Roll	1	Roll	No Bill			$0
1995	3/1/1995	Inactive	Annual Roll	1	Roll	No Bill			$0

1994	3/1/1994	Inactive	Annual Roll	1	Roll	No Bill			$0
1993	3/1/1993	Inactive	Annual Roll	1	Roll	No Bill			$0
1992	3/1/1992	Inactive	Annual Roll	1	Roll	No Bill			$0
1991	3/1/1991	Inactive	Annual Roll	1	Roll	No Bill			$0
1990	3/1/1990	Inactive	Annual Roll	1	Roll	No Bill			$0
1989	3/1/1989	Inactive	Annual Roll	1	Roll	No Bill			$0
1988	3/1/1988	Active	Annual Roll	1	Roll	Pending			$118,307

Property Characteristics for: **032-291-31-100**

Property Characteristic	Description
Acreage	1.600 ac
Book Category Number	2032
Current Record Flag	Yes

Parcel Split Background for: **032-291-31-100**

This Parcel Has No Split Background Records.

Related Accounts for: **032-291-31-100**

Account Number	Property Type	Status
9-002-013-0010	Possessory	Active, Non-Billable

Owner Change History for: **032-291-31-100**

Recorded Document: 1989-3117037
Record Change Date: 4/13/1989
Effective Owner Change Date: 4/13/1989
Preliminary Change of Ownership: **1989-3117037**

Recorded Document:
Recorder's Book and Page: 2404-278
Record Change Date: 2/27/1985
Effective Owner Change Date: 2/27/1985
Preliminary Change of Ownership: **1-2404278**

Recorded Document:
Recorder's Book and Page: 1676-339
Record Change Date: 9/21/1978
Effective Owner Change Date: 9/21/1978
Preliminary Change of Ownership: **1-1676339**

Recorded Document:
Recorder's Book and Page: 1638-195
Record Change Date: 6/8/1978
Effective Owner Change Date: 6/8/1978
Preliminary Change of Ownership: **1-1638195**

Recorded Document:
Recorder's Book and Page: 1480-388
Record Change Date: 3/30/1977
Effective Owner Change Date: 3/30/1977
Preliminary Change of Ownership: **1-1480388**

Environmental Pollution 310 (2022) 119888

Contents lists available at ScienceDirect

Environmental Pollution

journal homepage: www.elsevier.com/locate/envpol

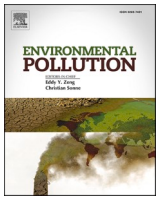

Up in smoke: California's greenhouse gas reductions could be wiped out by 2020 wildfires☆

Michael Jerrett [a,*], Amir S. Jina [b], Miriam E. Marlier [a]

[a] Department of Environmental Health Sciences, Fielding School of Public Health, University of California, Los Angeles, 650 Charles E. Young Dr. S., 56-070 CHS Box 951772, Los Angeles, CA, 90095, USA
[b] Harris School of Public Policy, University of Chicago, 1307 East 60th Street, Chicago, IL, 60637, USA

ARTICLE INFO

Keywords:
Climate change
Wildfires
Greenhouse gas emissions
Economic impacts

ABSTRACT

In this short communication, we estimate that California's wildfire carbon dioxide equivalent (CO_2e) emissions from 2020 are approximately two times higher than California's total greenhouse gas (GHG) emission reductions since 2003. Without considering future vegetation regrowth, CO_2e emissions from the 2020 wildfires could be the second most important source in the state above either industry or electrical power generation. Regrowth may partly of fully occur over a long period, but due to exigencies of the climate crisis most of the regrowth will not occur quickly enough to avert greater than 1.5 degrees of warming. Global monetized damages caused by CO_2e from in 2020 wildfire emissions amount to some $7.1 billion USD. Our analysis suggests that significant societal benefits could accrue from larger investments in improved forest management and stricter controls on new development in fire-prone areas at the wildland-urban interface.

1. Introduction

Recent evidence suggests that climate change contributes to increased wildfire activity in the western United States (Abatzoglou and Williams, 2016). California's summer wildfire burned area increased eightfold from 1972 to 2018 (Williams et al., 2019), and statewide climate change projections predict an amplification of wildfire risk due to higher temperatures and drier conditions (Westerling, 2018). Climate change exacerbates fire risks already stoked by increasing development near the wildland-urban interface (WUI) that have made humans the main ignition source in California (Keeley and Syphard, 2018), as well as decades of fire suppression and underinvestment in preventive measures such as mechanical clearing or prescribed burns (Keeley and Syphard, 2021; Kolden, 2019; Radeloff et al., 2018). Wildfires, in turn, release GHG emissions that can contribute to climate change.

California experienced its most disastrous wildfire year on record in 2020. CalFire, the state agency responsible for leading California's wildfire prevention and suppression, reports that 1.7 million hectares burned in 2020 (CalFire, 2022). Many of the worst fire years in California's history have occurred in the past 20 years, with eighteen of the top 20 most destructive fires in terms of loss of life and property since 2000 and five in 2020 alone (CalFire, 2021). The 2020 fires have been followed by another extreme fire season with 1.0 million hectares burned in 2021.

In addition to the immediate loss of life and property, hospital admissions and premature deaths have likely happened because of the smoke exposure (Cascio, 2018; Fann et al., 2018; Reid et al., 2016; Wang et al., 2020), which blanketed large parts of the state with tens of millions of people with unhealthy air quality that persisted for months in some locations. Recent estimates put the economic costs of direct health costs at $32 billion for 2018 (Wang et al., 2020). Future climate projections suggest that wildfires will become an increasingly important source of air pollution in the western U.S. (Ford et al., 2018; Liu et al., 2016).

When forests burn and are not balanced by vegetation regrowth, they shift from a natural sink to a source of carbon (van der Werf et al., 2017). This can represent a positive climate feedback loop in which increased GHG emissions contribute to climate change and further increase wildfire risk. Although wildfires are a natural feature of many ecosystems in California, the increase in severe and frequent wildfire events has raised the possibility of transformed post-fire ecosystems as new plant communities regrow following fire events that alter carbon

☆ This paper has been recommended for acceptance by Pavlos Kassomenos.

* Corresponding author.
E-mail addresses: mjerrett@ucla.edu (M. Jerrett), mmarlier@ucla.edu (M.E. Marlier).

https://doi.org/10.1016/j.envpol.2022.119888
Received 10 April 2022; Received in revised form 1 July 2022; Accepted 31 July 2022
Available online 5 August 2022
0269-7491/© 2022 The Authors. Published by Elsevier Ltd. This is an open access article under the CC BY license (http://creativecommons.org/licenses/by/4.0/).

sequestration potential (Bowman et al., 2020). Regrowth relies on several factors including species burned, drought, and active replanting (Kibler, 2019). Even if long-term regrowth occurs, however, the carbon emissions occurring in the next 15–20 years will make it difficult to reach emission reduction targets needed to avert the 1.5 degree C increases in mean global temperature advocated by the Intergovernmental Panel on Climate Change (IPCC) (IPCC, 2018). Recent studies on the Australian wildfires have suggested that the magnitude of the fires in combination with the broadleaf species being burned likely places fires somewhere in between carbon neutrality and complete emissions (van der Velde et al., 2021).

In this short communication, we quantify the likely carbon emissions that occurred in 2020 from wildfire activity in California. We then situate these emissions in the context of other leading GHG emissions sectors in California. We conclude with policy recommendations for reporting of routine wildfire emissions and for increased investment in preventive measures.

1.1. Data and methods

Given substantial uncertainties among fire emissions inventories (Liu et al., 2020), we obtained multiple sources of fire emissions data for 2003–2020. First, we accessed satellite-based fire CO_2 emissions from the Global Fire Emissions Database version 4 with small fires (GFED4s) (1997-present; considered preliminary since 2017) and Global Fire Assimilation System version 1.2 (GFAS) using FIRECAM (Liu et al., 2020). These inventories represent "bottom-up" and "top-down" approaches to fire emissions estimation, respectively, and have shown the best correspondence with aerosol observations in North America (Carter et al., 2020). Although GFED and GFAS do not distinguish between wildfires and other landscape fires such as agricultural or prescribed burns, we expect this contribution to be minor in California. We also obtained wildfire-specific emissions estimates from the California Air Resources Board (CARB) (2000–2020), which combines individual fire perimeters with a wildland fire emissions model (CARB, 2020). The average across inventories is 127 mmt CO_2e for 2020 (ranging from 101 to 171 mmt CO_2e) and 18 mmt CO_2e for 2003–2019 (ranging from 15 to 22 mmt CO_2e).

We next compared wildfire emissions to sectoral GHG emissions for 2003–2020 to maintain consistency with availability for all three wildfire emissions inventories (CARB, 2021). In 2019, the CARB reported 418 mmt CO_2e emissions for all sources with the top 3 being transportation (166 mmt CO_2e), electrical power generation (59 mmt CO_2e), and industry (88 mmt CO_2e). For 2020, we assume constant emissions from the year 2019, as this was the last year where the CARB estimated sector-specific contributions to CO_2e, although this may be an underestimate due to potential emissions reductions during the COVID-19 pandemic (Liu et al., 2021).

Finally, to assess the socioeconomics benefits of reducing these CO_2 emissions, without considering the co-benefits of air pollution reductions, we apply the social cost of carbon (SC–CO_2). The SC-CO_2 is an estimate of the marginal damage caused by the emissions of an extra ton of CO_2 today in net present value. This value, adopted by the Biden administration in February 2021, is $51 per ton with a 3% discount rate in 2020 USD (Interagency Working Group, 2016). We also apply a value of the SC-CO_2 where damages are restricted only to the United States. While this lower value of $7.1 per ton in 2020 (Governmental Accountability Office, 2020) does not capture the global nature of emissions, it does allow us to attribute the local component of global damages caused by the fires.

2. Results

We first compared sectoral emissions to wildfire emissions, which indicate an approximate release of 127 mmtCO_2e in 2020, nearly seven times the 2003–2019 mean. From 2003 to 2019, California's GHG emissions declined by 65 mmt CO_2e (−13%), largely driven by reductions from the electric power generation sector. The 2020 fire season alone is two times higher than California's total GHG emissions reductions and would comprise 49 percent of California's 2030 total greenhouse emissions target of 260 mmtCO_2e (Fig. 1) (CARB, 2017).

Global monetized damages caused only by CO_2 from California's fire emissions in 2020 is approximately $7.09 billion in net present value when applying SC-CO_2 from the Biden Administration with a constant 3% discount rate. This value is reduced to approximately $986.9 million in damage for the U.S. when considering only domestic damages. If we consider what this implies for California only, we calculate the median damages to California as a percent of U.S. damages in 2080–2099 implied by Hsiang et al. (2017). This gives values of 8.5%, 12.1%, 9.4% for Representative Concentration Pathways (RCPs) 2.6, 4.5, and 8.5 respectively. Scaling the previous U.S.-only value to the average of these percentages, this would imply that the carbon emissions-only damages for California would be approximately $98.7 million in net present value.

3. Conclusions

In this short communication, we analyzed the likely CO_2e emissions from wildfires in California during 2020. Averaging three fire emissions estimates, we find that approximately 127 mmt CO_2e were emitted in 2020. We emphasize that our wildfire emissions estimates do not consider subsequent vegetation regrowth following fires so this is considered an upper bound for net wildfire GHG contributions to the atmosphere. This regrowth, however, could take decades or longer depending on the type of ecosystem that burned.

If we compare fire GHG emissions to total GHG emissions of 418 mmt CO_2e total in 2019, this amounts to a 30% increase in total emissions by all sectors. This makes the GHG emissions from wildfires the second most important source in the state, after transportation (166 mmtCO_2e), but above either industry or electrical power generation (88 and 59 mmt CO_2e, respectively). Viewed from the perspective of what this means for wildfire emission reductions from all other sectors combined, if we compare to reductions from 2003 to 2019 from 483 to 418 mmt CO_2e, the likely amount of increase from the fires is close to double all the emission reductions achieved in the state from 2003 to 2019.

The economic damages are informative for two key reasons. First, they represent a currently unquantified aspect of damages due to fires that are incurred globally, in the U.S., and in California itself. These damages should be counted in addition to fire control costs, damages from air pollution, and direct loss of life and property. Second, they provide a benchmark against which to compare the costs of prevention measures, based purely on climate change mitigation, and not including co-benefits of reduced pollution, lower property risk and loss, and other damages associated with fire risk. The Federal government and California recently signed a memorandum of understanding to increase to 1 million acres per year forest treatment to prevent wildfires in the State (State of California, 2020); in 2021, California invested $1.5 billion in wildfire resilience programs, including prescribed burning (California Wildfire & Forest Resilience Task Force, 2022). If future treatments are moderately effective and reduce wildfire risk and subsequent CO_2e emissions by 20%, this would reduce 20% of the total $7.09 billion in externality costs that we have calculated (i.e., $1.42 billion in benefits). Including the carbon mitigation benefits further justifies the wildfire prevention costs.

Our analysis suggests several notable bit findings. First, wildfires in California have become a major and growing source of GHG emissions. Over the long to very long term, regrowth could alleviate some of the emissions, but this is unlikely to occur on the time scale necessary to meet near and medium-term emission targets needed to avert passing the 1.5 degree C threshold. Second, the magnitude of the emissions makes wildfires the second most important source of emissions in 2020 behind transportation emissions, and one that appears likely to grow

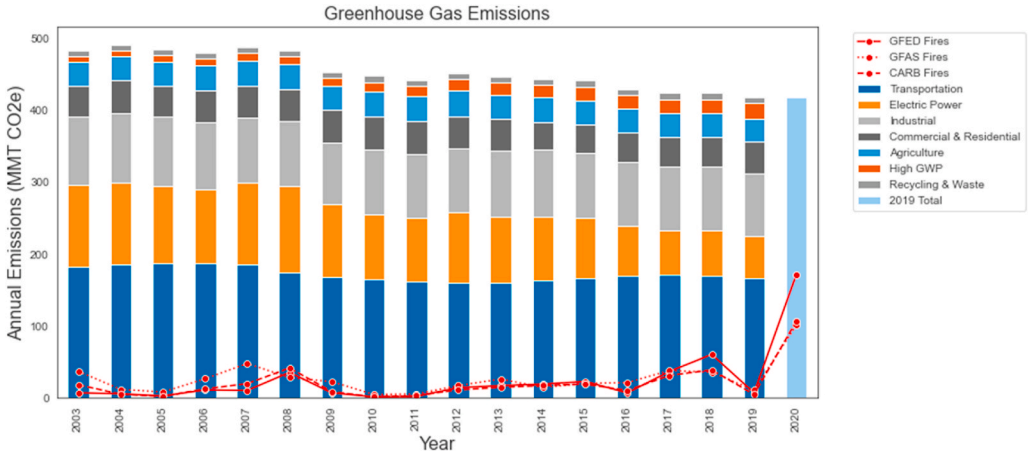

Fig. 1. Annual emissions from individual sectors and wildfire emissions. CARB, GFAS1.2, and GFED4s wildfire emissions shown as red lines (not considering vegetation regrowth). **Note:** Since data is not yet available, 2020 non-fire emissions are assumed to be equal to CARB 2019 estimates. (For interpretation of the references to colour in this figure legend, the reader is referred to the Web version of this article.)

with future climate change. Average wildfire emissions from the past five years (~46 mmt CO_2e from 2016 to 2020) ranks above the most recent individual contributions from the Commercial & Residential, Agriculture, Recycling & Waste, and High Global Warming Potential sectors. The latter includes fluorine-containing gases that destroy stratospheric ozone; sources include electricity transmission and distribution and semiconductor manufacturing. Third, wildfire emissions in 2020 essentially negate 18 years of reductions in GHG emissions from other sectors by a factor of two. Fourth, the additional global damages due only to the contribution of these emissions to climate change can be valued at $7.09 billion.

The findings imply several research directions and policy actions. The externalities caused by fire emissions incurs damages globally and in California, and the economic value should be considered alongside other direct costs of fires (Feo et al., 2020), including prevention and suppression. Wildfire emissions are not routinely reported with other key emission sources such as transportation, industry, and power generation. While wildfire emissions tend to be more variable than other sectors, it is still important to track these emissions to ensure near and medium-term emission reduction targets are met. A likely consequence is that wildfire emissions have not received nearly the same level of societal investment or attention as emissions from other sectors. Although wildfires are to some extent natural occurrences, human activity contributes to making wildfires "unnatural disasters" through anthropogenic climate change and development at the WUI in fire prone areas. Moreover, forest management policies focused on fire suppression rather than on preventive measures such as mechanical clearing and prescribed burning activities also likely increases the risk of large, destructive wildfires. If fires are no longer in balance with ecosystem regrowth, we risk different vegetation communities regrowing with less potential for carbon sequestration. A need also exists to develop accessible quantitative tools for policymakers and the public to understand how wildfire risk can be reduced through better management, how much loss of life and property can be avoided, and how much it will cost to achieve these goals. This will allow for more accurate assessment of investments in improved forest management or prevention of development in fire prone areas at the wildland-urban interface.

Author statement

M. Jerrett: Conceptualization, Methodology, Writing – original draft, Reviewing & Editing. A. Jina: Methodology, Writing-Reviewing & Editing. M. Marlier: Conceptualization, Methodology, Writing – original draft, Reviewing & Editing.

Declaration of competing interest

The authors declare that they have no known competing financial interests or personal relationships that could have appeared to influence the work reported in this paper. Funding for Dr. Jerrett was supplied by the UCLA Center for Healthy Climate Solutions.

Data availability

Data will be made available on request.

References

Abatzoglou, J.T., Williams, A.P., 2016. Impact of anthropogenic climate change on wildfire across western US forests. Proc. Natl. Acad. Sci. USA 113, 11770–11775. https://doi.org/10.1073/pnas.1607171113.

Bowman, D.M.J.S., Kolden, C.A., Abatzoglou, J.T., Johnston, F.H., Werf, G.R. van der, Flannigan, M., 2020. Vegetation fires in the anthropocene. Nat. Rev. Earth Environ. 1–16. https://doi.org/10.1038/s43017-020-0085-3.

CalFire, 2021. Top 20 most destructive California wildfire. URL, 8.13.21. https://www.fire.ca.gov/media/11417/top20_destruction.pdf.

CalFire, 2022. Stats and events. URL, 6.9.22. https://www.fire.ca.gov/stats-events/.

California Air Resources Board (CARB), 2017. California's 2017 Climate Change Scoping Plan, pp. 1–132.

California Air Resources Board (CARB), 2020. California Wildfire Burn Acreage and Preliminary Emissions Estimates.

California Air Resources Board (CARB), 2021. California Greenhouse Gas Emission Inventory, 2021 Edition. Data available at: https://ww3.arb.ca.gov/cc/inventory/data/data.htm.

California Wildfire & Forest Resilience Task Force, 2022. California's Strategic Plan for Expanding the Use of Beneficial Fire. https://fmtf.fire.ca.gov/.

Carter, T.S., Heald, C.L., Jimenez, J.L., Campuzano-Jost, P., Kondo, Y., Moteki, N., Schwarz, J.P., Wiedinmyer, C., Darmenov, A.S., Silva, A.M. da, Kaiser, J.W., 2020. How emissions uncertainty influences the distribution and radiative impacts of smoke from fires in North America. Atmos. Chem. Phys. 20, 2073–2097. https://doi.org/10.5194/acp-20-2073-2020.

Cascio, W.E., 2018. Wildland fire smoke and human health. Sci. Total Environ. 624, 586–595. https://doi.org/10.1016/j.scitotenv.2017.12.086.

Fann, N., Alman, B., Broome, R.A., Morgan, G.G., Johnston, F.H., Pouliot, G., Rappold, A. G., 2018. The health impacts and economic value of wildland fire episodes in the U. S.: 2008–2012. Sci. Total Environ. 610– 611, 802–809. https://doi.org/10.1016/j.scitotenv.2017.08.024.

Feo, T.J., Evans, S., Mace, A.J., Brady, S.E., Lindsey, B., 2020. The Costs of Wildfire in California: an Independent Review of Scientific and Technical Information. California Council on Science and Technology. California Council on Science and Technology, pp. 1–248.

Ford, B., Martin, M.V., Zelasky, S.E., Fischer, E.V., Anenberg, S.C., Heald, C.L., Pierce, J. R., 2018. Future fire impacts on smoke concentrations, visibility, and health in the contiguous United States. GeoHealth 2, 229–247. https://doi.org/10.1029/2018gh000144.

Government Accountability Office, 2020. Social Cost of Carbon: Identifying a Federal Entity to Address the National Academies' Recommendations Could Strengthen Regulatory Analysis. https://www.gao.gov/assets/gao-20-254.pdf.

Hsiang, S., Kopp, R., Jina, A., Rising, J., Delgado, M., Mohan, S., Rasmussen, D.J., Muir-Wood, R., Wilson, P., Oppenheimer, M., Larsen, K., Houser, T., 2017. Estimating

economic damage from climate change in the United States. Science 356, 1362–1369.
Interagency Working Group, 2016. Technical Support Document:-Technical Update of the Social Cost of Carbon for Regulatory Impact Analysis-Under Executive Order 12866. https://www.whitehouse.gov/wp-content/uploads/2021/02/Technical SupportDocument_SocialCostofCarbonMethaneNitrousOxide.pdf.
IPCC, 2018. Global Warming of 1.5°C. An IPCC Special Report on the impacts of global warming of 1.5°C above pre-industrial levels and related global greenhouse gas emission pathways. In: The Context of Strengthening the Global Response to the Threat of Climate Change, Sustainable Development, and Efforts to Eradicate Poverty. Cambridge University Press, Cambridge, UK and New York, NY, USA.
Keeley, J.E., Syphard, A.D., 2018. Historical patterns of wildfire ignition sources in California ecosystems. Int. J. Wildland Fire 27, 781. https://doi.org/10.1071/wf18026.
Keeley, J.E., Syphard, A.D., 2021. Large California wildfires: 2020 fires in historical context. Fire Ecol 17, 22. https://doi.org/10.1186/s42408-021-00110-7.
Kibler, C.L., 2019. Multi-temporal Remote Sensing of Vegetation Regrowth after a Large Wildfire. Master of Arts Thesis. Department of Geography, University of California, Santa Barbara.
Kolden, C.A., 2019. We're not doing enough prescribed fire in the western United States to mitigate wildfire risk. Fire 2, 30. https://doi.org/10.3390/fire2020030.
Liu, J.C., Mickley, L.J., Sulprizio, M.P., Dominici, F., Yue, X., Ebisu, K., Anderson, G.B., Khan, R.F.A., Bravo, M.A., Bell, M.L., 2016. Particulate air pollution from wildfires in the Western US under climate change. Clim. Change 138, 655–666. https://doi.org/10.1007/s10584-016-1762-6.
Liu, T., Mickley, L.J., Marlier, M.E., DeFries, R.S., Khan, M.F., Latif, M.T., Karambelas, A., 2020. Diagnosing spatial biases and uncertainties in global fire emissions inventories: Indonesia as regional case study. Remote Sens. Environ. 237, 111557 https://doi.org/10.1016/j.rse.2019.111557.
Liu, J., Lipsitt, J., Jerrett, M., Zhu, Y., 2021. Decreases in near-road NO and NO2 concentrations during the COVID-19 pandemic in California. Environ. Sci. Technol. Lett. 8, 161–167. https://doi.org/10.1021/acs.estlett.0c00815.
Radeloff, V.C., Helmers, D.P., Kramer, H.A., Mockrin, M.H., Alexandre, P.M., Bar-Massada, A., Butsic, V., Hawbaker, T.J., Martinuzzi, S., Syphard, A.D., Stewart, S.I., 2018. Rapid growth of the US wildland-urban interface raises wildfire risk. Proc. Natl. Acad. Sci. USA 115, 3314–3319. https://doi.org/10.1073/pnas.1718850115.
Reid, C.E., Brauer, M., Johnston, F.H., Jerrett, M., Balmes, J.R., Elliott, C.T., 2016. Critical review of health impacts of wildfire smoke exposure. Environ. Health Perspect. 124, 1334–1343. https://doi.org/10.1289/ehp.1409277.
State of California, 2020. USDA Forest Service Pacific Southwest Region. Agreement for Shared Stewardship of California's Forest and Rangelands, pp. 1–9.
van der Velde, I.R., van der Werf, G.R., Houweling, S., Maasakkers, J.D., Borsdorff, T., Landgraf, J., Tol, P., van Kempen, T.A., van Hees, R., Hoogeveen, R., Veefkind, J.P., Aben, I., 2021. Vast CO2 release from Australian fires in 2019–2020 constrained by satellite. Nature 597, 366–369. https://doi.org/10.1038/s41586-021-03712-y.
van der Werf, G.R., Randerson, J.T., Giglio, L., van Leeuwen, T.T., Chen, Y., Rogers, B.M., Mu, M., van Marle, M.J.E., Morton, D.C., Collatz, G.J., Yokelson, R.J., Kasibhatla, P. S., 2017. Global fire emissions estimates during 1997–2016. Earth Syst. Sci. Data 9, 697–720. https://doi.org/10.5194/essd-9-697-2017.
Wang, D., Guan, D., Zhu, S., Kinnon, M.M., Geng, G., Zhang, Q., Zheng, H., Lei, T., Shao, S., Gong, P., Davis, S.J., 2020. Economic footprint of California wildfires in 2018. Nat. Sustain. 1–9 https://doi.org/10.1038/s41893-020-00646-7.
Westerling, A.L., 2018. Wildfire Simulations for California's Fourth Climate Change Assessment: Projecting Changes in Extreme Wildfire Events with a Warming Climate, California's Fourth Climate Change Assessment, California Energy Commission. California's Fourth Climate Change Assessment. California Energy Commission.
Williams, A.P., Abatzoglou, J.T., Gershunov, A., Guzman-Morales, J., Bishop, D.A., Balch, J.K., Lettenmaier, D.P., 2019. Observed impacts of anthropogenic climate change on wildfire in California. Earth's Future 7, 892–910. https://doi.org/10.1029/2019ef001210.

LETTER

doi:10.1038/nature12914

Rate of tree carbon accumulation increases continuously with tree size

N. L. Stephenson[1], A. J. Das[1], R. Condit[2], S. E. Russo[3], P. J. Baker[4], N. G. Beckman[3]†, D. A. Coomes[5], E. R. Lines[6], W. K. Morris[7], N. Rüger[2,8]†, E. Álvarez[9], C. Blundo[10], S. Bunyavejchewin[11], G. Chuyong[12], S. J. Davies[13], Á. Duque[14], C. N. Ewango[15], O. Flores[16], J. F. Franklin[17], H. R. Grau[10], Z. Hao[18], M. E. Harmon[19], S. P. Hubbell[2,20], D. Kenfack[13], Y. Lin[21], J.-R. Makana[15], A. Malizia[10], L. R. Malizia[22], R. J. Pabst[19], N. Pongpattananurak[23], S.-H. Su[24], I-F. Sun[25], S. Tan[26], D. Thomas[27], P. J. van Mantgem[28], X. Wang[18], S. K. Wiser[29] & M. A. Zavala[30]

Forests are major components of the global carbon cycle, providing substantial feedback to atmospheric greenhouse gas concentrations[1]. Our ability to understand and predict changes in the forest carbon cycle—particularly net primary productivity and carbon storage—increasingly relies on models that represent biological processes across several scales of biological organization, from tree leaves to forest stands[2,3]. Yet, despite advances in our understanding of productivity at the scales of leaves and stands, no consensus exists about the nature of productivity at the scale of the individual tree[4–7], in part because we lack a broad empirical assessment of whether rates of absolute tree mass growth (and thus carbon accumulation) decrease, remain constant, or increase as trees increase in size and age. Here we present a global analysis of 403 tropical and temperate tree species, showing that for most species mass growth rate increases continuously with tree size. Thus, large, old trees do not act simply as senescent carbon reservoirs but actively fix large amounts of carbon compared to smaller trees; at the extreme, a single big tree can add the same amount of carbon to the forest within a year as is contained in an entire mid-sized tree. The apparent paradoxes of individual tree growth increasing with tree size despite declining leaf-level[8–10] and stand-level[10] productivity can be explained, respectively, by increases in a tree's total leaf area that outpace declines in productivity per unit of leaf area and, among other factors, age-related reductions in population density. Our results resolve conflicting assumptions about the nature of tree growth, inform efforts to understand and model forest carbon dynamics, and have additional implications for theories of resource allocation[11] and plant senescence[12].

A widely held assumption is that after an initial period of increasing growth, the mass growth rate of individual trees declines with increasing tree size[4,5,13–16]. Although the results of a few single-species studies have been consistent with this assumption[15], the bulk of evidence cited in support of declining growth is not based on measurements of individual tree mass growth. Instead, much of the cited evidence documents either the well-known age-related decline in net primary productivity (hereafter 'productivity') of even-aged forest stands[10] (in which the trees are all of a similar age) or size-related declines in the rate of mass gain per unit leaf area (or unit leaf mass)[8–10], with the implicit assumption that declines at these scales must also apply at the scale of the individual tree. Declining tree growth is also sometimes inferred from life-history theory to be a necessary corollary of increasing resource allocation to reproduction[11,16]. On the other hand, metabolic scaling theory predicts that mass growth rate should increase continuously with tree size[6], and this prediction has also received empirical support from a few site-specific studies[6,7]. Thus, we are confronted with two conflicting generalizations about the fundamental nature of tree growth, but lack a global assessment that would allow us to distinguish clearly between them.

To fill this gap, we conducted a global analysis in which we directly estimated mass growth rates from repeated measurements of 673,046 trees belonging to 403 tropical, subtropical and temperate tree species, spanning every forested continent. Tree growth rate was modelled as a function of log(tree mass) using piecewise regression, where the independent variable was divided into one to four bins. Conjoined line segments were fitted across the bins (Fig. 1).

For all continents, aboveground tree mass growth rates (and, hence, rates of carbon gain) for most species increased continuously with tree mass (size) (Fig. 2). The rate of mass gain increased with tree mass in each model bin for 87% of species, and increased in the bin that included the largest trees for 97% of species; the majority of increases were statistically significant (Table 1, Extended Data Fig. 1 and Supplementary Table 1). Even when we restricted our analysis to species achieving the largest sizes (maximum trunk diameter >100 cm; 33% of species), 94% had increasing mass growth rates in the bin that included the largest trees. We found no clear taxonomic or geographic patterns among the 3% of species with declining growth rates in their largest trees, although the small number of these species (thirteen) hampers inference. Declining species included both angiosperms and gymnosperms in seven of the 76 families in our study; most of the seven families had only one or two declining species and no family was dominated by declining species (Supplementary Table 1).

When we log-transformed mass growth rate in addition to tree mass, the resulting model fits were generally linear, as predicted by metabolic scaling theory[6] (Extended Data Fig. 2). Similar to the results of our main

[1]US Geological Survey, Western Ecological Research Center, Three Rivers, California 93271, USA. [2]Smithsonian Tropical Research Institute, Apartado 0843-03092, Balboa, Republic of Panama. [3]School of Biological Sciences, University of Nebraska, Lincoln, Nebraska 68588, USA. [4]Department of Forest and Ecosystem Science, University of Melbourne, Victoria 3121, Australia. [5]Department of Plant Sciences, University of Cambridge, Cambridge CB2 3EA, UK. [6]Department of Geography, University College London, London WC1E 6BT, UK. [7]School of Botany, University of Melbourne, Victoria 3010, Australia. [8]Spezielle Botanik und Funktionelle Biodiversität, Universität Leipzig, 04103 Leipzig, Germany. [9]Jardín Botánico de Medellín, Calle 73, No. 51D-14, Medellín, Colombia. [10]Instituto de Ecología Regional, Universidad Nacional de Tucumán, 4107 Yerba Buena, Tucumán, Argentina. [11]Research Office, Department of National Parks, Wildlife and Plant Conservation, Bangkok 10900, Thailand. [12]Department of Botany and Plant Physiology, Buea, Southwest Province, Cameroon. [13]Smithsonian Institution Global Earth Observatory—Center for Tropical Forest Science, Smithsonian Institution, PO Box 37012, Washington, DC 20013, USA. [14]Universidad Nacional de Colombia, Departamento de Ciencias Forestales, Medellín, Colombia. [15]Wildlife Conservation Society, Kinshasa/Gombe, Democratic Republic of the Congo. [16]Unité Mixte de Recherche—Peuplements Végétaux et Bioagresseurs en Milieu Tropical, Université de la Réunion/CIRAD, 97410 Saint Pierre, France. [17]School of Environmental and Forest Sciences, University of Washington, Seattle, Washington 98195, USA. [18]State Key Laboratory of Forest and Soil Ecology, Institute of Applied Ecology, Chinese Academy of Sciences, Shenyang 110164, China. [19]Department of Forest Ecosystems and Society, Oregon State University, Corvallis, Oregon 97331, USA. [20]Department of Ecology and Evolutionary Biology, University of California, Los Angeles, California 90095, USA. [21]Department of Life Science, Tunghai University, Taichung City 40704, Taiwan. [22]Facultad de Ciencias Agrarias, Universidad Nacional de Jujuy, 4600 San Salvador de Jujuy, Argentina. [23]Faculty of Forestry, Kasetsart University, ChatuChak Bangkok 10900, Thailand. [24]Taiwan Forestry Research Institute, Taipei 10066, Taiwan. [25]Department of Natural Resources and Environmental Studies, National Dong Hwa University, Hualien 97401, Taiwan. [26]Sarawak Forestry Department, Kuching, Sarawak 93660, Malaysia. [27]Department of Botany and Plant Pathology, Oregon State University, Corvallis, Oregon 97331, USA. [28]US Geological Survey, Western Ecological Research Center, Arcata, California 95521, USA. [29]Landcare Research, PO Box 40, Lincoln 7640, New Zealand. [30]Forest Ecology and Restoration Group, Department of Life Sciences, University of Alcalá, Alcalá de Henares, 28805 Madrid, Spain. †Present addresses: Mathematical Biosciences Institute, Ohio State University, Columbus, Ohio 43210, USA (N.G.B.); German Centre for Integrative Biodiversity Research (iDiv), Halle-Jena-Leipzig, 04103 Leipzig, Germany (N.R.).

©2014 Macmillan Publishers Limited. All rights reserved

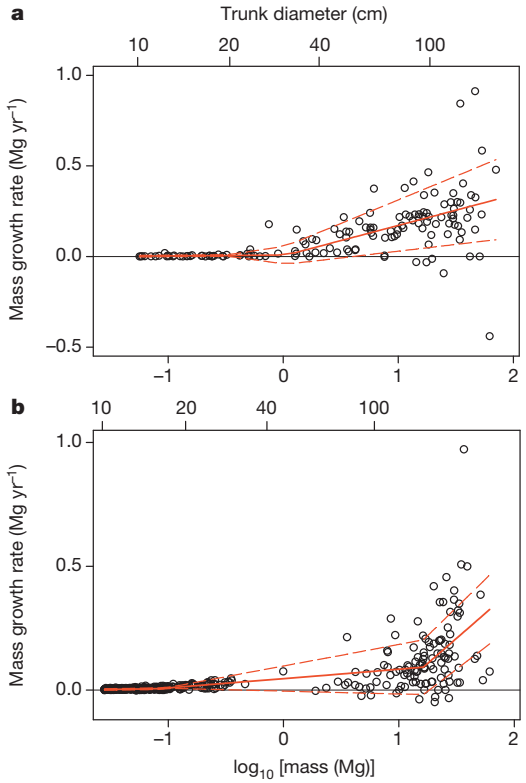

Figure 1 | Example model fits for tree mass growth rates. The species shown are the angiosperm species (*Lecomtedoxa klaineana*, Cameroon, 142 trees) (**a**) and gymnosperm species (*Picea sitchensis*, USA, 409 trees) (**b**) in our data set that had the most massive trees (defined as those with the greatest cumulative aboveground dry mass in their five most massive trees). Each point represents a single tree; the solid red lines represent best fits selected by our model; and the dashed red lines indicate one standard deviation around the predicted values.

analysis using untransformed growth, of the 381 log-transformed species analysed (see Methods), the log-transformed growth rate increased in the bin containing the largest trees for 96% of species.

In absolute terms, trees 100 cm in trunk diameter typically add from 10 kg to 200 kg of aboveground dry mass each year (depending on species), averaging 103 kg per year. This is nearly three times the rate for trees of the same species at 50 cm in diameter, and is the mass equivalent to adding an entirely new tree of 10–20 cm in diameter to the forest each year. Our findings further indicate that the extraordinary growth recently reported in an intensive study of large *Eucalyptus regnans* and *Sequoia sempervirens*[7], which included some of the world's most massive individual trees, is not a phenomenon limited to a few unusual species. Rather, rapid growth in giant trees is the global norm, and can exceed 600 kg per year in the largest individuals (Fig. 3).

Our data set included many natural and unmanaged forests in which the growth of smaller trees was probably reduced by asymmetric competition with larger trees. To explore the effects of competition, we calculated mass growth rates for 41 North American and European species that had published equations for diameter growth rate in the absence of competition. We found that, even in the absence of competition, 85% of the species had mass growth rates that increased continuously with tree size (Extended Data Fig. 3), with growth curves closely resembling those in Fig. 2. Thus, our finding of increasing growth not only has broad generality across species, continents and forest biomes (tropical, subtropical and temperate), it appears to hold regardless of competitive environment.

Importantly, our finding of continuously increasing growth is compatible with the two classes of observations most often cited as evidence of declining, rather than increasing, individual tree growth: with increasing tree size and age, productivity usually declines at the scales of both tree organs (leaves) and tree populations (even-aged forest stands).

First, although growth efficiency (tree mass growth per unit leaf area or leaf mass) often declines with increasing tree size[8–10], empirical observations and metabolic scaling theory both indicate that, on average, total tree leaf mass increases as the square of trunk diameter[17,18]. A typical tree that experiences a tenfold increase in diameter will therefore undergo a roughly 100-fold increase in total leaf mass and a 50–100-fold

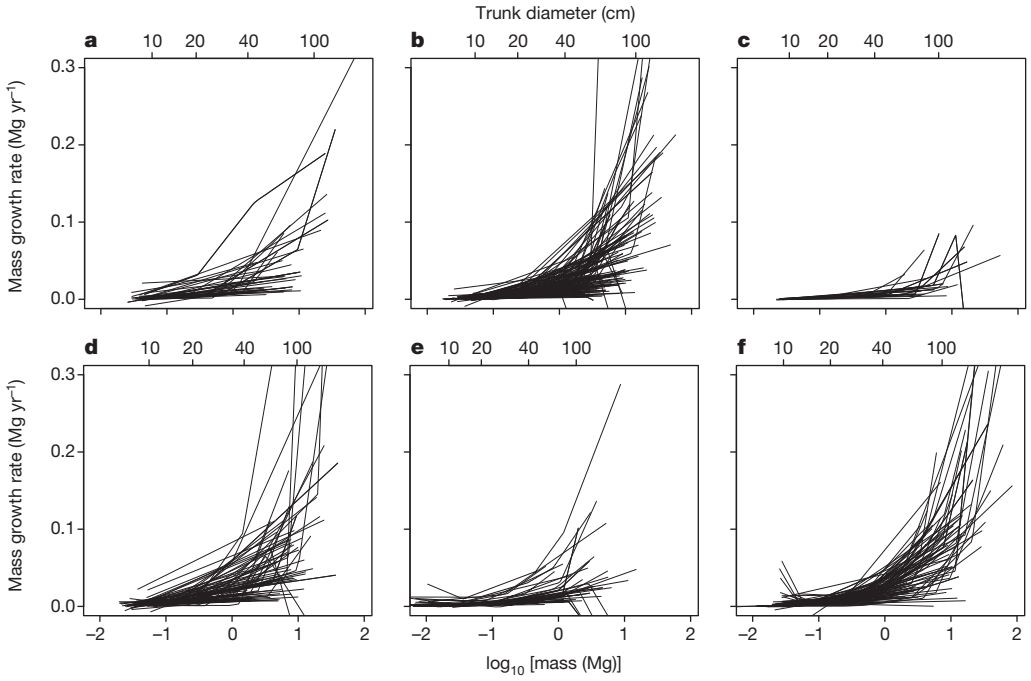

Figure 2 | Aboveground mass growth rates for the 403 tree species, by continent. **a**, Africa (Cameroon, Democratic Republic of the Congo); **b**, Asia (China, Malaysia, Taiwan, Thailand); **c**, Australasia (New Zealand); **d**, Central and South America (Argentina, Colombia, Panama); **e**, Europe (Spain); and **f**, North America (USA). Numbers of trees, numbers of species and percentages with increasing growth are given in Table 1. Trunk diameters are approximate values for reference, based on the average diameters of trees of a given mass.

©2014 Macmillan Publishers Limited. All rights reserved

Table 1 | Sample sizes and tree growth trends by continent

Continent	Number of trees	Number of species	Percentage of species with increasing mass growth rate in the largest trees (percentage significant at $P \leq 0.05$)
Africa	15,366	37	100.0 (86.5)
Asia	43,690	136	96.3 (89.0)
Australasia	45,418	22	95.5 (95.5)
Central and South America	18,530	77	97.4 (92.2)
Europe	439,889	42	90.5 (78.6)
North America	110,153	89	98.9 (94.4)
Total	673,046	403	96.8 (89.8)

The largest trees are those in the last bin fitted by the model. Countries are listed in the legend for Fig. 2.

increase in total leaf area (depending on size-related increases in leaf mass per unit leaf area[19,20]). Parallel changes in growth efficiency can range from a modest increase (such as in stands where small trees are suppressed by large trees)[21] to as much as a tenfold decline[22], with most changes falling in between[8,9,19,22]. At one extreme, the net effect of a low (50-fold) increase in leaf area combined with a large (tenfold) decline in growth efficiency would still yield a fivefold increase in individual tree mass growth rate; the opposite extreme would yield roughly a 100-fold increase. Our calculated 52-fold greater average mass growth rate of trees 100 cm in diameter compared to those 10 cm in diameter falls within this range. Thus, although growth efficiency often declines with increasing tree size, increases in a tree's total leaf area are sufficient to overcome this decline and cause whole-tree carbon accumulation rate to increase.

Second, our findings are similarly compatible with the well-known age-related decline in productivity at the scale of even-aged forest stands. Although a review of mechanisms is beyond the scope of this paper[10,23], several factors (including the interplay of changing growth efficiency and tree dominance hierarchies[24]) can contribute to declining productivity at the stand scale. We highlight the fact that increasing individual tree growth rate does not automatically result in increasing stand productivity because tree mortality can drive orders-of-magnitude reductions in population density[25,26]. That is, even though the large trees in older, even-aged stands may be growing more rapidly, such stands have fewer trees. Tree population dynamics, especially mortality, can thus be a significant contributor to declining productivity at the scale of the forest stand[23].

For a large majority of species, our findings support metabolic scaling theory's qualitative prediction of continuously increasing growth at the scale of individual trees[6], with several implications. For example, life-history theory often assumes that tradeoffs between plant growth and reproduction are substantial[11]. Contrary to some expectations[11,16], our results indicate that for most tree species size-related changes in reproductive allocation are insufficient to drive long-term declines in growth rates[6]. Additionally, declining growth is sometimes considered to be a defining feature of plant senescence[12]. Our findings are thus relevant to understanding the nature and prevalence of senescence in the life history of perennial plants[27].

Finally, our results are relevant to understanding and predicting forest feedbacks to the terrestrial carbon cycle and global climate system[1–3]. These feedbacks will be influenced by the effects of climatic, land-use and other environmental changes on the size-specific growth rates and size structure of tree populations—effects that are already being observed in forests[28,29]. The rapid growth of large trees indicates that, relative to their numbers, they could play a disproportionately important role in these feedbacks[30]. For example, in our western USA old-growth forest plots, trees >100 cm in diameter comprised 6% of trees, yet contributed 33% of the annual forest mass growth. Mechanistic models of the forest carbon cycle will depend on accurate representation of productivity across several scales of biological organization, including calibration and validation against continuously increasing carbon accumulation rates at the scale of individual trees.

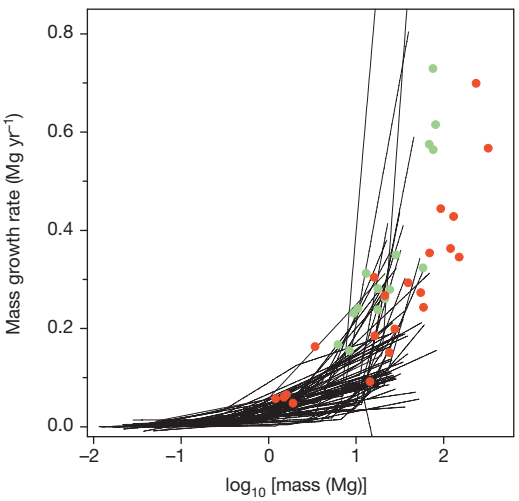

Figure 3 | Aboveground mass growth rates of species in our data set compared with *E. regnans* and *S. sempervirens*. For clarity, only the 58 species in our data set having at least one tree exceeding 20 Mg are shown (lines). Data for *E. regnans* (green dots, 15 trees) and *S. sempervirens* (red dots, 21 trees) are from an intensive study that included some of the most massive individual trees on Earth[7]. Both axes are expanded relative to those of Fig. 2.

METHODS SUMMARY

We estimated aboveground dry mass growth rates from consecutive diameter measurements of tree trunks—typically measured every five to ten years—from long-term monitoring plots. Analyses were restricted to trees with trunk diameter ≥10 cm, and to species having ≥40 trees in total and ≥15 trees with trunk diameter ≥30 cm. Maximum trunk diameters ranged from 38 cm to 270 cm among species, averaging 92 cm. We converted each diameter measurement (plus an accompanying height measurement for 16% of species) to aboveground dry mass, M, using published allometric equations. We estimated tree growth rate as $G = \Delta M/\Delta t$ and modelled G as a function of $\log(M)$ for each species using piecewise regression. The independent variable $\log(M)$ was divided into bins and a separate line segment was fitted to G versus $\log(M)$ in each bin so that the line segments met at the bin divisions. Bin divisions were not assigned a priori, but were fitted by the model separately for each species. We fitted models with 1, 2, 3 and 4 bins, and selected the model receiving the most support by Akaike's Information Criterion for each species. Our approach thus makes no assumptions about the shape of the relationship between G and $\log(M)$, and can accommodate increasing, decreasing or hump-shaped relationships. Parameters were fitted with a Gibbs sampler based on Metropolis updates, producing credible intervals for model parameters and growth rates at any diameter; uninformative priors were used for all parameters. We tested extensively for bias, and found no evidence that our results were influenced by model fits failing to detect a final growth decline in the largest trees, possible biases introduced by the 47% of species for which we combined data from several plots, or possible biases introduced by allometric equations (Extended Data Figs 4 and 5).

Online Content Any additional Methods, Extended Data display items and Source Data are available in the online version of the paper; references unique to these sections appear only in the online paper.

Received 5 August; accepted 27 November 2013.
Published online 15 January 2014.

1. Pan, Y. *et al.* A large and persistent carbon sink in the world's forests. *Science* **333,** 988–993 (2011).

©2014 Macmillan Publishers Limited. All rights reserved

2. Medvigy, D., Wofsy, S. C., Munger, J. W., Hollinger, D. Y. & Moorcroft, P. R. Mechanistic scaling of ecosystem function and dynamics in space and time: Ecosystem Demography model version 2. *J. Geophys. Res.* **114,** G01002 (2009).
3. Caspersen, J. P., Vanderwel, M. C., Cole, W. G. & Purves, D. W. How stand productivity results from size- and competition-dependent growth and mortality. *PLoS ONE* **6,** e28660 (2011).
4. Kutsch, W. L. *et al.* in *Old-Growth Forests: Function, Fate and Value* (eds Wirth, C., Gleixner, G. & Heimann, M.) 57–79 (Springer, 2009).
5. Meinzer, F. C., Lachenbruch, B. & Dawson, T. E. (eds) *Size- and Age-Related Changes in Tree Structure and Function* (Springer, 2011).
6. Enquist, B. J., West, G. B., Charnov, E. L. & Brown, J. H. Allometric scaling of production and life-history variation in vascular plants. *Nature* **401,** 907–911 (1999).
7. Sillett, S. C. *et al.* Increasing wood production through old age in tall trees. *For. Ecol. Manage.* **259,** 976–994 (2010).
8. Mencuccini, M. *et al.* Size-mediated ageing reduces vigour in trees. *Ecol. Lett.* **8,** 1183–1190 (2005).
9. Drake, J. E., Raetz, L. M., Davis, S. C. & DeLucia, E. H. Hydraulic limitation not declining nitrogen availability causes the age-related photosynthetic decline in loblolly pine (*Pinus taeda* L.). *Plant Cell Environ.* **33,** 1756–1766 (2010).
10. Ryan, M. G., Binkley, D. & Fownes, J. H. Age-related decline in forest productivity: pattern and process. *Adv. Ecol. Res.* **27,** 213–262 (1997).
11. Thomas, S. C. in *Size- and Age-Related Changes in Tree Structure and Function* (eds Meinzer, F. C., Lachenbruch, B. & Dawson, T. E.) 33–64 (Springer, 2011).
12. Thomas, H. Senescence, ageing and death of the whole plant. *New Phytol.* **197,** 696–711 (2013).
13. Carey, E. V., Sala, A., Keane, R. & Callaway, R. M. Are old forests underestimated as global carbon sinks? *Glob. Change Biol.* **7,** 339–344 (2001).
14. Phillips, N. G., Buckley, T. N. & Tissue, D. T. Capacity of old trees to respond to environmental change. *J. Integr. Plant Biol.* **50,** 1355–1364 (2008).
15. Piper, F. I. & Fajardo, A. No evidence of carbon limitation with tree age and height in *Nothofagus pumilio* under Mediterranean and temperate climate conditions. *Ann. Bot.* **108,** 907–917 (2011).
16. Weiner, J. & Thomas, S. C. The nature of tree growth and the ''age-related decline in forest productivity''. *Oikos* **94,** 374–376 (2001).
17. Jenkins, J. C., Chojnacky, D. C., Heath, L. S. & Birdsey, R. A. *Comprehensive Database of Diameter-based Biomass Regressions for North American Tree Species* General Technical Report NE-319, http://www.nrs.fs.fed.us/pubs/6725 (USDA Forest Service, Northeastern Research Station, 2004).
18. Niklas, K. J. & Enquist, B. J. Canonical rules for plant organ biomass partitioning and annual allocation. *Am. J. Bot.* **89,** 812–819 (2002).
19. Thomas, S. C. Photosynthetic capacity peaks at intermediate size in temperate deciduous trees. *Tree Physiol.* **30,** 555–573 (2010).
20. Steppe, K., Niinemets, Ü. & Teskey, R. O. in *Size- and Age-Related Changes in Tree Structure and Function* (eds Meinzer, F. C., Lachenbruch, B. & Dawson, T. E.) 235–253 (Springer, 2011).
21. Gilmore, D. W. & Seymour, R. S. Alternative measures of stem growth efficiency applied to *Abies balsamea* from four canopy positions in central Maine, USA. *For. Ecol. Manage.* **84,** 209–218 (1996).
22. Kaufmann, M. R. & Ryan, M. G. Physiographic, stand, and environmental effects on individual tree growth and growth efficiency in subalpine forests. *Tree Physiol.* **2,** 47–59 (1986).
23. Coomes, D. A., Holdaway, R. J., Kobe, R. K., Lines, E. R. & Allen, R. B. A general integrative framework for modelling woody biomass production and carbon sequestration rates in forests. *J. Ecol.* **100,** 42–64 (2012).
24. Binkley, D. A hypothesis about the interaction of tree dominance and stand production through stand development. *For. Ecol. Manage.* **190,** 265–271 (2004).
25. Pretzsch, H. & Biber, P. A re-evaluation of Reineke's rule and stand density index. *For. Sci.* **51,** 304–320 (2005).
26. Kashian, D. M., Turner, M. G., Romme, W. H. & Lorimer, C. G. Variability and convergence in stand structural development on a fire-dominated subalpine landscape. *Ecology* **86,** 643–654 (2005).
27. Munné-Bosch, S. Do perennials really senesce? *Trends Plant Sci.* **13,** 216–220 (2008).
28. Jump, A. S., Hunt, J. M. & Peñuelas, J. Rapid climate change-related growth decline at the southern range edge of *Fagus sylvatica. Glob. Change Biol.* **12,** 2163–2174 (2006).
29. Lindenmayer, D. B., Laurance, W. F. & Franklin, J. F. Global decline in large old trees. *Science* **338,** 1305–1306 (2012).
30. Enquist, B. J., West, G. B. & Brown, J. H. Extensions and evaluations of a general quantitative theory of forest structure and dynamics. *Proc. Natl Acad. Sci. USA* **106,** 7046–7051 (2009).

Supplementary Information is available in the online version of the paper.

Acknowledgements We thank the hundreds of people who have established and maintained the forest plots and their associated databases; M. G. Ryan for comments on the manuscript; C. D. Canham and T. Hart for supplying data; C. D. Canham for discussions and feedback; J. S. Baron for hosting our workshops; and Spain's Ministerio de Agricultura, Alimentación y Medio Ambiente (MAGRAMA) for granting access to the Spanish Forest Inventory Data. Our analyses were supported by the United States Geological Survey (USGS) John Wesley Powell Center for Analysis and Synthesis, the USGS Ecosystems and Climate and Land Use Change mission areas, the Smithsonian Institution Global Earth Observatory—Center for Tropical Forest Science (CTFS), and a University of Nebraska-Lincoln Program of Excellence in Population Biology Postdoctoral Fellowship (to N.G.B.). In addition, X.W. was supported by National Natural Science Foundation of China (31370444) and State Key Laboratory of Forest and Soil Ecology (LFSE2013-11). Data collection was funded by a broad range of organizations including the USGS, the CTFS, the US National Science Foundation, the Andrews LTER (NSF-LTER DEB-0823380), the US National Park Service, the US Forest Service (USFS), the USFS Forest Inventory and Analysis Program, the John D. and Catherine T. MacArthur Foundation, the Andrew W. Mellon Foundation, MAGRAMA, the Council of Agriculture of Taiwan, the National Science Council of Taiwan, the National Natural Science Foundation of China, the Knowledge Innovation Program of the Chinese Academy of Sciences, Landcare Research and the National Vegetation Survey Database (NVS) of New Zealand, the French Fund for the Global Environment and Fundación ProYungas. This paper is a contribution from the Western Mountain Initiative, a USGS global change research project. Any use of trade names is for descriptive purposes only and does not imply endorsement by the USA government.

Author Contributions N.L.S. and A.J.D. conceived the study with feedback from R.C. and D.A.C., N.L.S., A.J.D., R.C. and S.E.R. wrote the manuscript. R.C. devised the main analytical approach and wrote the computer code. N.L.S., A.J.D., R.C., S.E.R., P.J.B., N.G.B., D.A.C., E.R.L., W.K.M. and N.R. performed analyses. N.L.S., A.J.D., R.C., S.E.R., P.J.B., D.A.C., E.R.L., W.K.M., E.Á., C.B., S.B., G.C., S.J.D., Á.D., C.N.E., O.F., J.F.F., H.R.G., Z.H., M.E.H., S.P.H., D.K., Y.L., J.-R.M., A.M., L.R.M., R.J.P., N.P., S.-H.S., I-F.S., S.T., D.T., P.J.v.M., X.W., S.K.W. and M.A.Z. supplied data and sources of allometric equations appropriate to their data.

Author Information Fitted model parameters for each species have been deposited in USGS's ScienceBase at http://dx.doi.org/10.5066/F7JS9NFM. Reprints and permissions information is available at www.nature.com/reprints. The authors declare no competing financial interests. Readers are welcome to comment on the online version of the paper. Correspondence and requests for materials should be addressed to N.L.S. (nstephenson@usgs.gov).

©2014 Macmillan Publishers Limited. All rights reserved

METHODS

Data. We required that forest monitoring plots provided unbiased samples of all living trees within the plot boundaries, and that the trees had undergone two trunk diameter measurements separated by at least one year. Some plots sampled minimally disturbed old (all-aged) forest, whereas others, particularly those associated with national inventories, sampled forest stands regardless of past management history. Plots are described in the references cited in Supplementary Table 1.

Our raw data were consecutive measurements of trunk diameter, D, with most measurements taken 5 to 10 years apart (range, 1–29 years). D was measured at a standard height on the trunk (usually 1.3–1.4 m above ground level), consistent across measurements for a tree. Allometric equations for 16% of species required, in addition to consecutive measurements of D, consecutive measurements of tree height.

We excluded trees exhibiting extreme diameter growth, defined as trunks where D increased by $\geq 40\ \mathrm{mm\ yr^{-1}}$ or that shrank by $\geq 12s$, where s is the standard deviation of the D measurement error, $s = 0.9036 + 0.006214D$ (refs 31, 32); outliers of these magnitudes were almost certainly due to error. By being so liberal in allowing negative growth anomalies, we erred on the side of reducing our ability to detect increases in tree mass growth rate. Using other exclusion values yielded similar results, as did a second approach to handling error in which we reanalysed a subset of our models using a Bayesian method that estimates growth rates after accounting for error, based on independent plot-specific data quantifying measurement error[33].

To standardize minimum D among data sets, we analysed only trees with $D \geq 10$ cm at the first census. To ensure adequate samples of trees spanning a broad range of sizes, we restricted analyses to species having both ≥ 40 trees in total and also ≥ 15 trees with $D \geq 30$ cm at the first census. This left us with 673,046 trees belonging to 403 tropical and temperate species in 76 families, spanning twelve countries and all forested continents (Supplementary Table 1). Maximum trunk diameters ranged from 38 cm to 270 cm among species, and averaged 92 cm.

Estimating tree mass. To estimate each tree's aboveground dry mass, M, we used published allometric equations relating M to D (or for 16% of species, relating M to D and tree height). Some equations were species-specific and others were specific to higher taxonomic levels or forest types, described in the references in Supplementary Table 1. The single tropical moist forest equation of ref. 34 was applied to most tropical species, whereas most temperate species had unique species-specific equations. Most allometric equations are broadly similar, relating $\log(M)$ to $\log(D)$ linearly, or nearly linearly—a familiar relationship in allometric scaling of both animals and plants[35]. Equations can show a variety of differences in detail, however, with some adding $\log(D)$ squared and cubed terms. All equations make use of the wood density of individual species, but when wood density was not available for a given species we used mean wood density for a genus or family[36].

Using a single, average allometry for most tropical species, and mean wood density for a genus or family for several species, limits the accuracy of our estimates of M. However, because we treat each species separately, it makes no difference whether our absolute M estimates are more accurate in some species than in others, only that they are consistent within a species and therefore accurately reveal whether mass growth rates increase or decrease with tree size.

For two regions—Spain and the western USA—allometric equations estimated mass only for a tree's main stem rather than all aboveground parts, including branches and leaves. But because leaf and stem masses are positively correlated and their growth rates are expected to scale isometrically both within and among species[18,37,38], results from these two regions should not alter our qualitative conclusions. Confirming this, the percentage of species with increasing stem mass growth rate in the last bin for Spain and the western USA (93.4% of 61 species) was similar to that from the remainder of regions (97.4% of 342 species) ($P = 0.12$, Fisher's exact test).

Modelling mass growth rate. We sought a modelling approach that made no assumptions about the shape of the relationship between aboveground dry mass growth rate, G, and aboveground dry mass, M, and that could accommodate monotonically increasing, monotonically decreasing, or hump-shaped relationships. We therefore chose to model G as a function of $\log(M)$ using piecewise linear regression. The range of the x axis, $X = \log(M)$, is divided into a series of bins, and within each bin G is fitted as a function of X by linear regression. The position of the bins is adaptive: it is fitted along with the regression terms. Regression lines are required to meet at the boundary between bins. For a single model-fitting run the number of bins, B, is fixed. For example, if $B = 2$, there are four parameters to be fitted for a single species: the location of the boundary between bins, X_1; the slope of the regression in the first bin, S_1; the slope in the second bin, S_2; and an intercept term. Those four parameters completely define the model. In general, there are $2B$ parameters for B bins.

Growth rates, while approximately normally distributed, were heteroskedastic, with the variance increasing with mass (Fig. 1), so an additional model was needed for the standard deviation of G, σ_G, as a function of $\log(M)$. The increase of σ_G with $\log(M)$ was clearly not linear, so we used a three-parameter model:

$$\sigma_G = k \qquad (\text{for } \log(M) < d)$$

$$\sigma_G = a + b\log(M) \qquad (\text{for } \log(M) \geq d)$$

where the intercept a is determined by the values of k, d and b. Thus σ_G was constant for smaller values of $\log(M)$ (below the cutoff d), then increased linearly for larger $\log(M)$ (Fig. 1). The parameters k, d and b were estimated along with the parameters of the growth model.

Parameters of both the growth and standard deviation models were estimated in a Bayesian framework using the likelihood of observing growth rates given model predictions and the estimated standard deviation of the Gaussian error function. A Markov chain Monte Carlo chain of parameter estimates was created using a Gibbs sampler with a Metropolis update[39,40] written in the programming language R (ref. 41) (a tutorial and the computer code are available through http://ctfs.arnarb.harvard.edu/Public/CTFSRPackage/files/tutorials/growthfitAnalysis). The sampler works by updating each of the parameters in sequence, holding other parameters fixed while the relevant likelihood function is used to locate the target parameter's next value. The step size used in the updates was adjusted adaptively through the runs, allowing more rapid convergence[40]. The final Markov chain Monte Carlo chain describes the posterior distribution for each model parameter, the error, and was then used to estimate the posterior distribution of growth rates as estimated from the model. Priors on model parameters were uniform over an unlimited range, whereas the parameters describing the standard deviation were restricted to >0. Bin boundaries, X_i, were constrained as follows: (1) boundaries could only fall within the range of X, (2) each bin contained at least five trees, and (3) no bin spanned less than 10% of the range of X. The last two restrictions prevented the bins from collapsing to very narrow ranges of X in which the fitted slope might take absurd extremes.

We chose piecewise regression over other alternatives for modelling G as a function of M for two main reasons. First, the linear regression slopes within each bin provide precise statistical tests of whether G increases or decreases with X, based on credible intervals of the slope parameters. Second, with adaptive bin positions, the function is completely flexible in allowing changes in slope at any point in the X range, with no influence of any one bin on the others. In contrast, in parametric models where a single function defines the relationship across all X, the shape of the curve at low X can (and indeed must) influence the shape at high X, hindering statistical inference about changes in tree growth at large size.

We used $\log(M)$ as our predictor because within a species M has a highly non-Gaussian distribution, with many small trees and only a few very large trees, including some large outliers. In contrast, we did not log-transform our dependent variable G so that we could retain values of $G \leq 0$ that are often recorded in very slowly growing trees, for which diameter change over a short measurement interval can be on a par with diameter measurement error.

For each species, models with 1, 2, 3 and 4 bins were fitted. Of these four models, the model receiving the greatest weight of evidence by Akaike Information Criterion (AIC) was selected. AIC is defined as the log-likelihood of the best-fitting model, penalized by twice the number of parameters. Given that adding one more bin to a model meant two more parameters, the model with an extra bin had to improve the log-likelihood by 4 to be considered a better model[42].

Assessing model fits. To determine whether our approach might have failed to reveal a final growth decline within the few largest trees of the various species, we calculated mass growth rate residuals for the single most massive individual tree of each species. For 52% of the 403 species, growth of the most massive tree was underestimated by our model fits (for example, Fig. 1a); for 48% it was overestimated (for example, Fig. 1b). These proportions were indistinguishable from 50% ($P = 0.55$, binomial test), as would be expected for unbiased model fits. Furthermore, the mean residual (observed minus predicted) mass growth rate of these most massive trees, $+0.006\ \mathrm{Mg\ yr^{-1}}$, was statistically indistinguishable from zero ($P = 0.29$, two-tailed t-test). We conclude that our model fits accurately represent growth trends up through, and including, the most massive trees.

Effects of combined data. To achieve sample sizes adequate for analysis, for some species we combined data from several different forest plots, potentially introducing a source of bias: if the largest trees of a species disproportionately occur on productive sites, the increase in mass growth rate with tree size could be exaggerated. This might occur because trees on less-productive sites—presumably the sites having the slowest-growing trees within any given size class—could be underrepresented in the largest size classes. We assessed this possibility in two ways.

First, our conclusions remained unchanged when we compared results for the 53% of species that came uniquely from single large plots with those of the 47% of species whose data were combined across several plots. Proportions of species with increasing mass growth rates in the last bin were indistinguishable between the two groups (97.6% and 95.8%, respectively; $P = 0.40$, Fisher's exact test). Additionally,

©2014 Macmillan Publishers Limited. All rights reserved

the shapes and magnitudes of the growth curves for Africa and Asia, where data for each species came uniquely from single large plots, were similar to those of Australasia, Europe and North America, where data for each species were combined across several plots (Table 1, Fig. 2 and Extended Data Fig. 2). (Data from Central and South America were from both single and combined plots, depending on species.)

Second, for a subset of combined-data species we compared two sets of model fits: (1) using all available plots (that is, the analyses we present in the main text), and (2) using only plots that contained massive trees—those in the top 5% of mass for a species. To maximize our ability to detect differences, we limited these analyses to species with large numbers of trees found in a large number of plots, dispersed widely across a broad geographic region. We therefore analysed the twelve Spanish species that each had more than 10,000 individual trees (Supplementary Table 1), found in 34,580 plots distributed across Spain. Massive trees occurred in 6,588 (19%) of the 34,580 plots. We found no substantial differences between the two analyses. When all 34,580 plots were analysed, ten of the twelve species showed increasing growth in the last bin, and seven showed increasing growth across all bins; when only the 6,588 plots containing the most massive trees were analysed, the corresponding numbers were eleven and nine. Model fits for the two groups were nearly indistinguishable in shape and magnitude across the range of tree masses. We thus found no evidence that the potential for growth differences among plots influenced our conclusions.

Effects of possible allometric biases. For some species, the maximum trunk diameter D in our data sets exceeded the maximum used to calibrate the species' allometric equation. In such cases our estimates of M extrapolate beyond the fitted allometry and could therefore be subject to bias. For 336 of our 403 species we were able to determine D of the largest tree that had been used in calibrating the associated allometric equations. Of those 336 species, 74% (dominated by tropical species) had no trees in our data set with D exceeding that used in calibrating the allometric equations, with the remaining 26% (dominated by temperate species) having at least one tree with D exceeding that used in calibration. The percentage of species with increasing G in the last bin for the first group (98.0%) was indistinguishable from that of the second group (96.6%) ($P = 0.44$, Fisher's exact test). Thus, our finding of increasing G with tree size is not affected by the minority of species that have at least one tree exceeding the maximum value of D used to calibrate their associated allometric equations.

A bias that could inflate the rate at which G increases with tree size could arise if allometric equations systematically underestimate M for small trees or overestimate M for large trees[43]. For a subset of our study species we obtained the raw data—consisting of measured values of D and M for individual trees—needed to calibrate allometric equations, allowing us to determine whether the particular form of those species' allometric equations was prone to bias, and if so, the potential consequences of that bias.

To assess the potential for allometric bias for the majority (58%) of species in our data set—those that used the empirical moist tropical forest equation of ref. 34—we reanalysed the data provided by ref. 34. The data were from 1,504 harvested trees representing 60 families and 184 genera, with D ranging from 5 cm to 156 cm; the associated allometric equation relates $\log(M)$ to a third-order polynomial of $\log(D)$. Because the regression of M on D was fitted on a log–log scale, this and subsequent equations include a correction of $\exp[(\mathrm{RSE})^2/2]$ for the error in back-transformation, where RSE is the residual standard error from the statistical model[44]. Residuals of M for the equation revealed no evident biases (Extended Data Fig. 4a), suggesting that we should expect little (if any) systematic size-related biases in our estimates of G for the 58% of our species that used this equation.

Our simplest form of allometric equation—applied to 22% of our species—was $\log(M) = a + b\log(D)$, where a and b are taxon-specific constants. For nine of our species that used equations of this form (all from the temperate western USA: *Abies amabilis, A. concolor, A. procera, Pinus lambertiana, Pinus ponderosa, Picea sitchensis, Pseudotsuga menziesii, Tsuga heterophylla* and *T. mertensiana*) we had values of both D and M for a total of 1,358 individual trees, allowing us to fit species-specific allometric equations of the form $\log(M) = a + b\log(D)$ and then assess them for bias. Residual plots showed a tendency to overestimate M for the largest trees (Extended Data Fig. 4b), with the possible consequence of inflating estimates of G for the largest relative to the smallest trees of these species.

To determine whether this bias was likely to alter our qualitative conclusion that G increases with tree size, we created a new set of allometric relations between D and M —one for each of the nine species—using the same piecewise linear regression approach we used to model G as a function of M. However, because our goal was to eliminate bias rather than seek the most parsimonious model, we fixed the number of bins at four, with the locations of boundaries between the bins being fitted by the model. Our new allometry using piecewise regressions led to predictions of M with no apparent bias relative to D (Extended Data Fig. 4c). This new, unbiased allometry gave the same qualitative results as our original, simple allometry regarding the relationship between G and M: for all nine species, G increased in the bin containing the largest trees, regardless of the allometry used (Extended Data Fig. 5). We conclude that any bias associated with the minority of our species that used the simple allometric equation form was unlikely to affect our broad conclusion that G increases with tree size in a majority of tree species.

As a final assessment, we compared our results to those of a recent study of *E. regnans* and *S. sempervirens*, in which M and G had been calculated from intensive measurements of aboveground portions of trees without the use of standard allometric equations[7]. Specifically, in two consecutive years 36 trees of different sizes and ages were climbed, trunk diameters were systematically measured at several heights, branch diameters and lengths were measured (with subsets of foliage and branches destructively sampled to determine mass relationships), wood densities were determined and ring widths from increment cores were used to supplement measured diameter growth increments. The authors used these measurements to calculate M for each of the trees in each of the two consecutive years, and G as the difference in M between the two years[7]. *E. regnans* and *S. sempervirens* are the world's tallest angiosperm and gymnosperm species, respectively, so the data set was dominated by exceptionally large trees; most had $M \geq 20$ Mg, and M of some individuals exceeded that of the most massive trees in our own data set (which lacked *E. regnans* and *S. sempervirens*). We therefore compared *E. regnans* and *S. sempervirens* to the 58 species in our data set that had at least one individual with $M \geq 20$ Mg. Sample sizes for *E. regnans* and *S. sempervirens*—15 and 21 trees, respectively—fell below our required ≥40 trees for fitting piecewise linear regressions, so we simply plotted data points for individual *E. regnans* and *S. sempervirens* along with the piecewise regressions that we had already fitted for our 58 comparison species (Fig. 3).

As reported by ref. 7, G increased with M for both *E. regnans* and *S. sempervirens*, up to and including some of the most massive individual trees on the Earth (Fig. 3). Within the zone of overlapping M between the two data sets, G values for individual *E. regnans* and *S. sempervirens* trees fell almost entirely within the ranges of the piecewise regressions we had fitted for our 58 comparison species. We take these observations as a further indication that our results, produced using standard allometric equations, accurately reflect broad relationships between M and G.

Fitting log–log models. To model $\log(G)$ as a function of $\log(M)$, we used the binning approach that we used in our primary analysis of mass growth rate (described earlier). However, in log-transforming growth we dropped trees with $G \leq 0$. Because negative growth rates become more extreme with increasing tree size, dropping them could introduce a bias towards increasing growth rates. Log-transformation additionally resulted in skewed growth rate residuals. Dropping trees with $G \leq 0$ caused several species to fall below our threshold sample size, reducing the total number of species analysed to 381 (Extended Data Fig. 2).

Growth in the absence of competition. We obtained published equations for 41 North American and European species, in 46 species-site combinations, relating species-specific tree diameter growth rates to trunk diameter D and to neighbourhood competition[45–49]. Setting neighbourhood competition to zero gave us equations describing estimated annual D growth as a function of D in the absence of competition. Starting at $D_0 = 10$ cm, we sequentially (1) calculated annual D growth for a tree of size D_t, (2) added this amount to D_t to determine D_{t+1}, (3) used an appropriate taxon-specific allometric equation to calculate the associated tree masses M_t and M_{t+1}, and (iv) calculated tree mass growth rate G_t of a tree of mass M_t in the absence of competition as $M_{t+1} - M_t$. For each of the five species that had separate growth analyses available from two different sites, we required that mass growth rate increased continuously with tree size at both sites for the species to be considered to have a continuously increasing mass growth rate. North American and European allometries were taken from refs 17 and 50, respectively, with preference given to allometric equations based on power functions of tree diameter, large numbers of sampled trees, and trees spanning a broad range of diameters. For the 47% of European species for which ref. 50 had no equations meeting our criteria, we used the best-matched (by species or genus) equations from ref. 17.

31. Condit, R. *et al.* Tropical forest dynamics across a rainfall gradient and the impact of an El Niño dry season. *J. Trop. Ecol.* **20,** 51–72 (2004).
32. Condit, R. *et al.* The importance of demographic niches to tree diversity. *Science* **313,** 98–101 (2006).
33. Rüger, N., Berger, U., Hubbell, S. P., Vieilledent, G. & Condit, R. Growth strategies of tropical tree species: disentangling light and size effects. *PLoS ONE* **6,** e25330 (2011).
34. Chave, J. *et al.* Tree allometry and improved estimation of carbon stocks and balance in tropical forests. *Oecologia* **145,** 87–99 (2005).
35. Sibly, R. M., Brown, J. H. & Kodric-Brown, A. (eds) *Metabolic Ecology: A Scaling Approach* (John Wiley & Sons, 2012).
36. Zanne, A. E. *et al.* Data from: Towards a worldwide wood economics spectrum. In *Dryad Digital Data Repository*, http://dx.doi.org/10.5061/dryad.234 (2009).
37. Enquist, B. J. & Niklas, K. J. Global allocation rules for patterns of biomass partitioning in seed plants. *Science* **295,** 1517–1520 (2002).

©2014 Macmillan Publishers Limited. All rights reserved

38. Niklas, K. J. Plant allometry: is there a grand unifying theory? *Biol. Rev.* **79,** 871–889 (2004).
39. Metropolis, N., Rosenbluth, A. W., Rosenbluth, M. N., Teller, A. H. & Teller, E. Equation of state calculations by fast computing machines. *J. Chem. Phys.* **21,** 1087–1092 (1953).
40. Rüger, N., Huth, A., Hubbell, S. P. & Condit, R. Determinants of mortality across a tropical lowland rainforest community. *Oikos* **120,** 1047–1056 (2011).
41. R Development Core Team. *R: A Language and Environment for Statistical Computing* (R Foundation for Statistical Computing, 2009).
42. Hilborn, R. & Mangel, M. *The Ecological Detective: Confronting Models with Data* (Princeton Univ. Press, 1997).
43. Chambers, J. Q., Dos Santos, J., Ribeiro, R. J. & Higuchi, N. Tree damage, allometric relationships, and above-ground net primary production in central Amazon forest. *For. Ecol. Manage.* **152,** 73–84 (2001).
44. Baskerville, G. L. Use of logarithmic regression in the estimation of plant biomass. *Can. J. For. Res.* **2,** 49–53 (1972).
45. Canham, C. D. *et al.* Neighborhood analyses of canopy tree competition along environmental gradients in New England forests. *Ecol. Appl.* **16,** 540–554 (2006).
46. Coates, K. D., Canham, C. D. & LePage, P. T. Above- versus below-ground competitive effects and responses of a guild of temperate tree species. *J. Ecol.* **97,** 118–130 (2009).
47. Pretzsch, H. & Biber, P. Size-symmetric versus size-asymmetric competition and growth partitioning among trees in forest stands along an ecological gradient in central Europe. *Can. J. For. Res.* **40,** 370–384 (2010).
48. Gómez-Aparicio, L., García-Valdés, R., Ruíz-Benito, P. & Zavala, M. A. Disentangling the relative importance of climate, size and competition on tree growth in Iberian forests: implications for forest management under global change. *Glob. Change Biol.* **17,** 2400–2414 (2011).
49. Das, A. The effect of size and competition on tree growth rate in old-growth coniferous forests. *Can. J. For. Res.* **42,** 1983–1995 (2012).
50. Zianis, D., Muukkonen, P., Makipaa, R. & Mencuccini, M. Biomass and stem volume equations for tree species in Europe. *Silva Fennica Monogr.* **4,** 1–63 (2005).

©2014 **Macmillan Publishers Limited. All rights reserved**

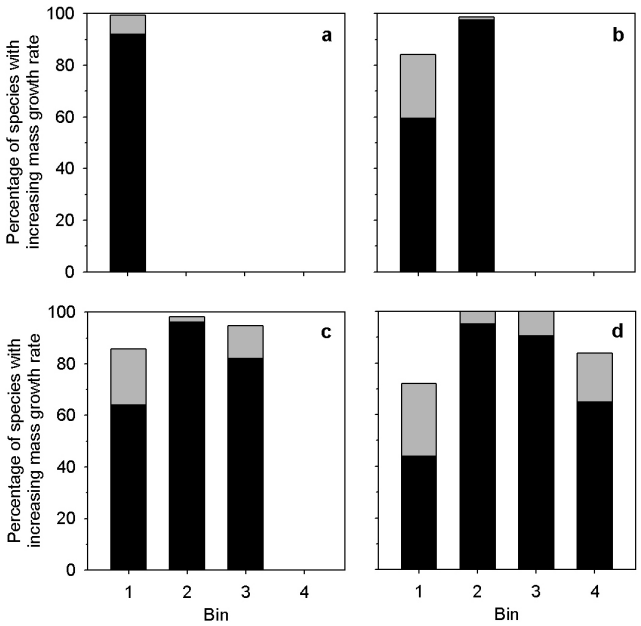

Extended Data Figure 1 | Summary of model fits for tree mass growth rates. Bars show the percentage of species with mass growth rates that increase with tree mass for each bin; black shading indicates percentage significant at $P \leq 0.05$. Tree masses increase with bin number. **a**, Species fitted with one bin (165 species); **b**, Species fitted with two bins (139 species); **c**, Species fitted with three bins (56 species); and **d**, Species fitted with four bins (43 species).

©2014 Macmillan Publishers Limited. All rights reserved

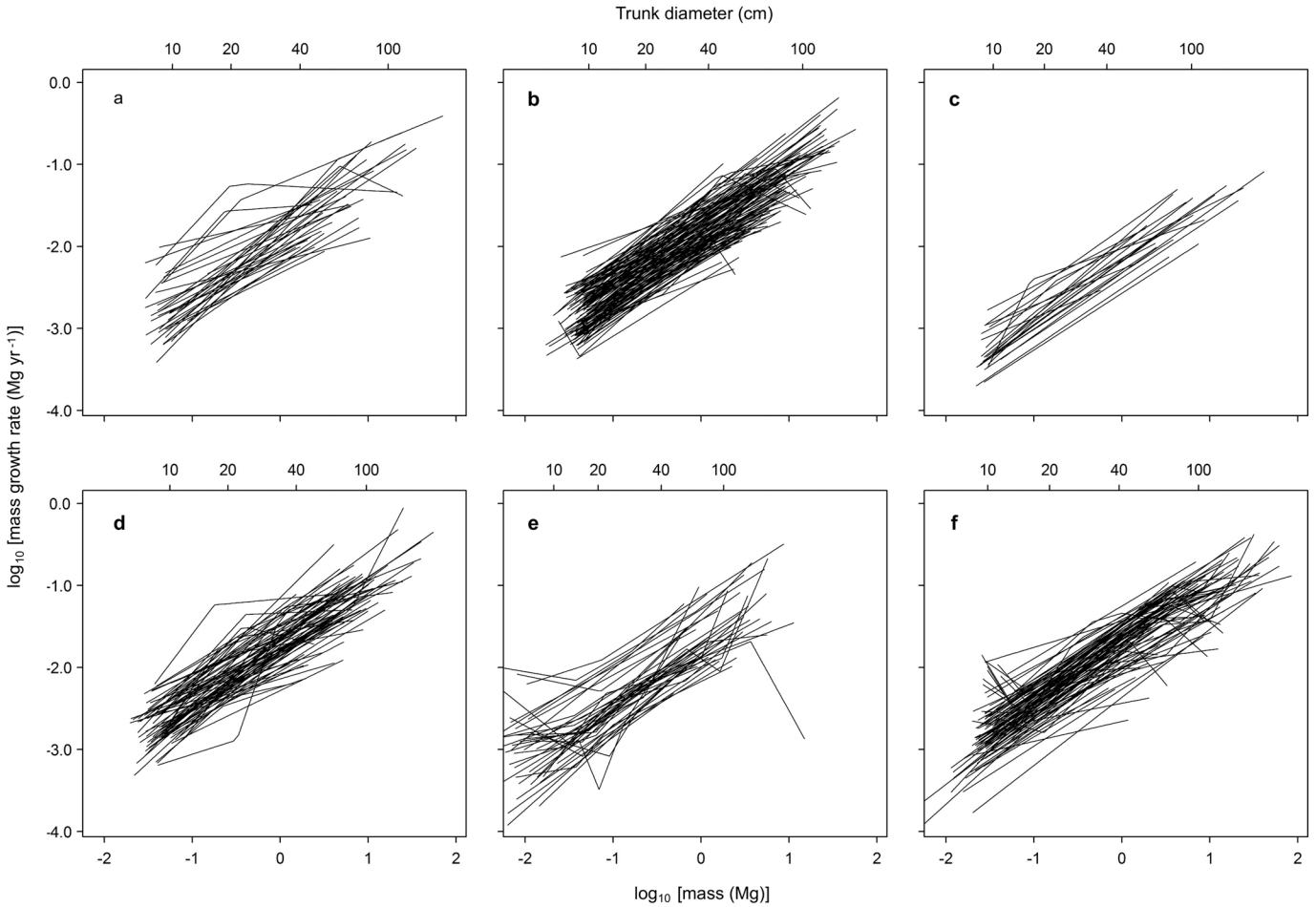

Extended Data Figure 2 | Log–log model fits of mass growth rates for 381 tree species, by continent. Trees with growth rates ≤ 0 were dropped from the analysis, reducing the number of species meeting our threshold sample size for analysis. **a**, Africa (33 species); **b**, Asia (123 species); **c**, Australasia (22 species); **d**, Central and South America (73 species); **e**, Europe (41 species); and **f**, North America (89 species). Trunk diameters are approximate values for reference, based on the average diameters of trees of a given mass.

©2014 Macmillan Publishers Limited. All rights reserved

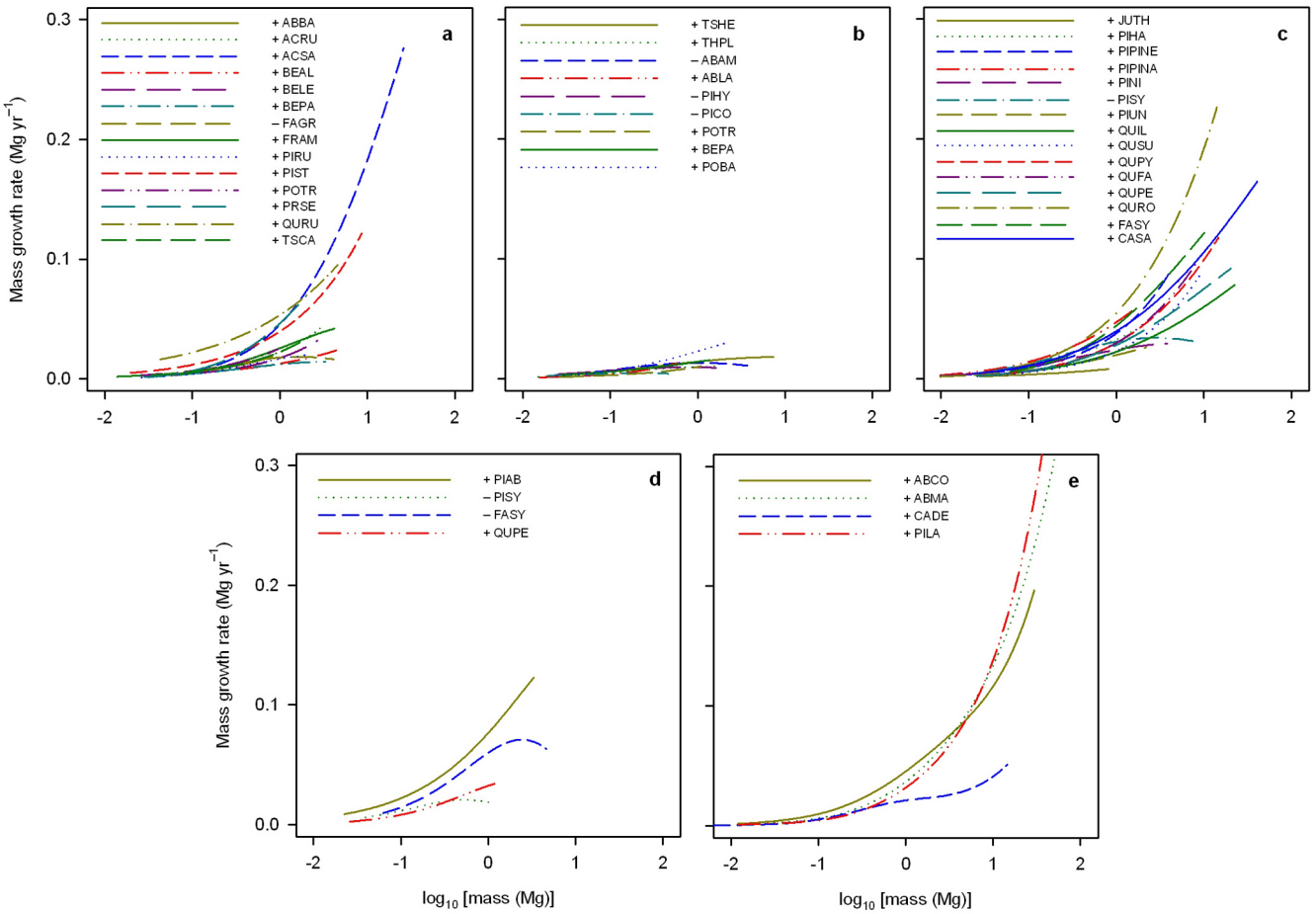

Extended Data Figure 3 | Aboveground mass growth rates for 41 tree species in the absence of competition. The '+' or '−' symbol preceding each species code indicates, respectively, species with mass growth rates that increased continuously with tree size or species with mass growth rates that declined in the largest trees. Sources of the diameter growth equations used to calculate mass growth were: **a**, ref. 45; **b**, ref. 46; **c**, ref. 48; **d**, ref. 47; and **e**, ref. 49. ABAM, *Abies amabilis*; ABBA, *Abies balsamea*; ABCO, *Abies concolor*; ABLA, *Abies lasiocarpa*; ABMA, *Abies magnifica*; ACRU, *Acer rubrum*; ACSA, *Acer saccharum*; BEAL, *Betula alleghaniensis*; BELE, *Betula lenta*; BEPA, *Betula papyrifera*; CADE, *Calocedrus decurrens*; CASA, *Castanea sativa*; FAGR, *Fagus grandifolia*; FASY, *Fagus sylvatica*; FRAM, *Fraxinus americana*; JUTH, *Juniperus thurifera*; PIAB, *Picea abies*; PICO, *Pinus contorta*; PIHA, *Pinus halepensis*; PIHY, *Picea* hybrid (a complex of *Picea glauca*, *P. sitchensis* and *P. engelmannii*); PILA, *Pinus lambertiana*; PINI, *Pinus nigra*; PIPINA, *Pinus pinaster*; PIPINE, *Pinus pinea*; PIRU, *Picea rubens*; PIST, *Pinus strobus*; PISY, *Pinus sylvestris*; PIUN, *Pinus uncinata*; POBA, *Populus balsamifera* ssp. *trichocarpa*; POTR, *Populus tremuloides*; PRSE, *Prunus serotina*; QUFA, *Quercus faginea*; QUIL, *Quercus ilex*; QUPE, *Quercus petraea*; QUPY, *Quercus pyrenaica*; QURO, *Quercus robar*; QURU, *Quercus rubra*; QUSU, *Quercus suber*; THPL, *Thuja plicata*; TSCA, *Tsuga canadensis*; and TSHE, *Tsuga heterophylla*.

©2014 Macmillan Publishers Limited. All rights reserved

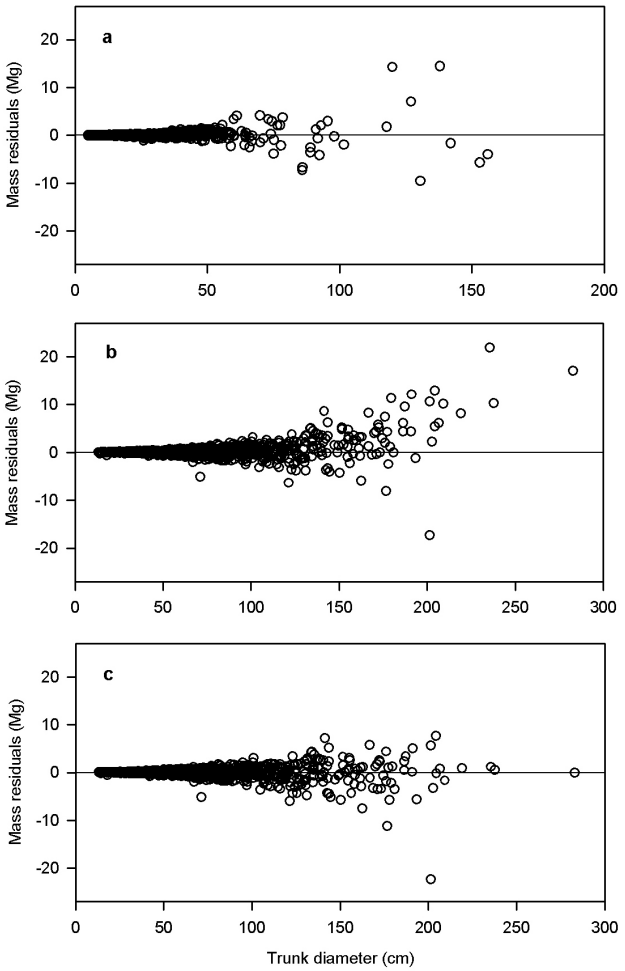

Extended Data Figure 4 | Residuals of predicted minus observed tree mass. **a**, The allometric equation for moist tropical forests[34]—used for the majority of tree species—shows no evident systematic bias in predicted aboveground dry mass, *M*, relative to trunk diameter ($n = 1{,}504$ trees). **b**, In contrast, our simplest form of allometric equation—used for 22% of our species and here applied to nine temperate species—shows an apparent bias towards overestimating *M* for large trees ($n = 1{,}358$ trees). **c**, New allometries that we created for the nine temperate species removed the apparent bias in predicted *M*.

©2014 Macmillan Publishers Limited. All rights reserved

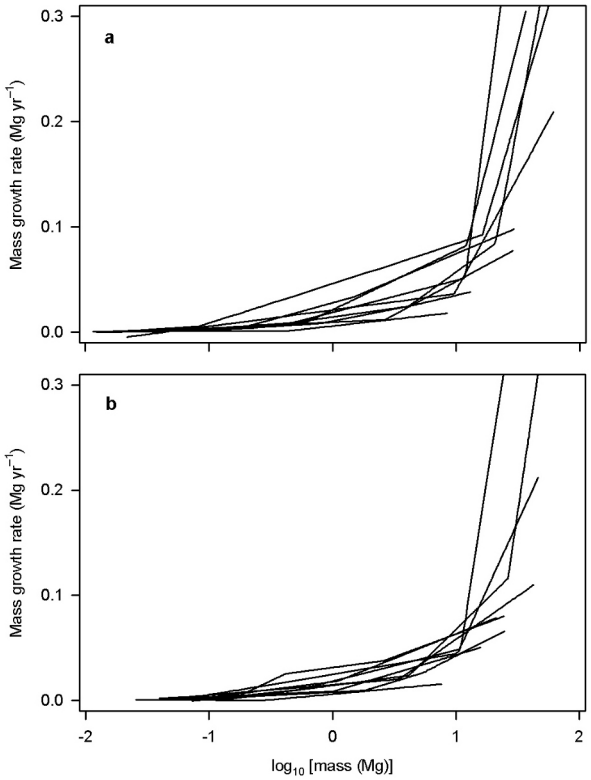

Extended Data Figure 5 | Estimated mass growth rates of the nine temperate species of Extended Data Fig. 4. Growth was estimated using the simplest form of allometric model [$\log(M) = a + b\log(D)$] (**a**) and our allometric models fitted with piecewise linear regression (**b**). Regardless of the allometric model form, all nine species show increasing G in the largest trees.

©2014 Macmillan Publishers Limited. All rights reserved

RESEARCH ARTICLE SUMMARY

CLIMATE CHANGE

Exceeding 1.5°C global warming could trigger multiple climate tipping points

David I. Armstrong McKay*, Arie Staal, Jesse F. Abrams, Ricarda Winkelmann, Boris Sakschewski, Sina Loriani, Ingo Fetzer, Sarah E. Cornell, Johan Rockström, Timothy M. Lenton*

INTRODUCTION: Climate tipping points (CTPs) are a source of growing scientific, policy, and public concern. They occur when change in large parts of the climate system—known as tipping elements—become self-perpetuating beyond a warming threshold. Triggering CTPs leads to significant, policy-relevant impacts, including substantial sea level rise from collapsing ice sheets, dieback of biodiverse biomes such as the Amazon rainforest or warm-water corals, and carbon release from thawing permafrost. Nine policy-relevant tipping elements and their CTPs were originally identified by Lenton *et al.* (2008). We carry out the first comprehensive reassessment of all suggested tipping elements, their CTPs, and the timescales and impacts of tipping. We also highlight steps to further improve understanding of CTPs, including an expert elicitation, a model intercomparison project, and early warning systems leveraging deep learning and remotely sensed data.

RATIONALE: Since the original identification of tipping elements there have been substantial advances in scientific understanding from paleoclimate, observational, and model-based studies. Additional tipping elements have been proposed (e.g., parts of the East Antarctic ice sheet) and the status of others (e.g., Arctic summer sea ice) has been questioned. Observations have revealed that parts of the West Antarctic ice sheet may have already passed a tipping point. Potential early warning signals of the Greenland ice sheet, Atlantic Meridional Overturning Circulation, and Amazon rainforest destabilization have been detected. Multiple abrupt shifts have been found in climate models. Recent work has suggested that up to 15 tipping elements are now active (Lenton *et al.*, 2019). Hence it is timely to synthesize this new knowledge to provide a revised shortlist of potential tipping elements and their CTP thresholds.

RESULTS: We identify nine global "core" tipping elements which contribute substantially to Earth system functioning and seven regional "impact" tipping elements which contribute substantially to human welfare or have great value as unique features of the Earth system (see figure). Their estimated CTP thresholds have significant implications for climate policy: Current global warming of ~1.1°C above pre-industrial already lies within the lower end of five CTP uncertainty ranges. Six CTPs become likely (with a further four possible) within the Paris Agreement range of 1.5 to <2°C warming, including collapse of the Greenland and West Antarctic ice sheets, die-off of low-latitude coral reefs, and widespread abrupt permafrost thaw. An additional CTP becomes likely and another three possible at the ~2.6°C of warming expected under current policies.

CONCLUSION: Our assessment provides strong scientific evidence for urgent action to mitigate climate change. We show that even the Paris Agreement goal of limiting warming to well below 2°C and preferably 1.5°C is not safe as 1.5°C and above risks crossing multiple tipping points. Crossing these CTPs can generate positive feedbacks that increase the likelihood of crossing other CTPs. Currently the world is heading toward ~2 to 3°C of global warming; at best, if all net-zero pledges and nationally determined contributions are implemented it could reach just below 2°C. This would lower tipping point risks somewhat but would still be dangerous as it could trigger multiple climate tipping points. ■

The list of author affiliations is available in the full article online.
*Corresponding author. Email: d.mckay@exeter.ac.uk (D.I.A.M.); t.m.lenton@exeter.ac.uk (T.M.L.)
Cite this article as D. I. Armstrong McKay *et al.*, *Science* **377**, eabn7950 (2022). DOI: 10.1126/science.abn7950

READ THE FULL ARTICLE AT
https://doi.org/10.1126/science.abn7950

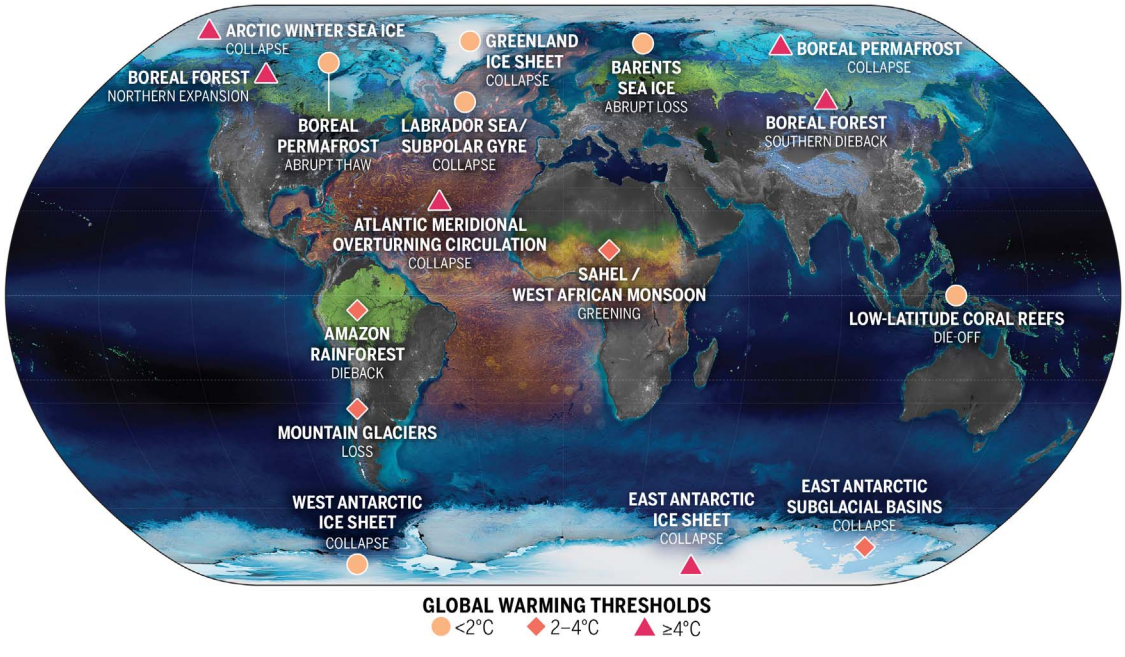

The location of climate tipping elements in the cryosphere (blue), biosphere (green), and ocean/atmosphere (orange), and global warming levels at which their tipping points will likely be triggered. Pins are colored according to our central global warming threshold estimate being below 2°C, i.e., within the Paris Agreement range (light orange, circles); between 2 and 4°C, i.e., accessible with current policies (orange, diamonds); and 4°C and above (red, triangles).

Downloaded from https://www.science.org at Cardiff University on September 08, 2022

RESEARCH ARTICLE

CLIMATE CHANGE

Exceeding 1.5°C global warming could trigger multiple climate tipping points

David I. Armstrong McKay[1,2,3,4]*, Arie Staal[1,2,5], Jesse F. Abrams[3], Ricarda Winkelmann[6], Boris Sakschewski[6], Sina Loriani[6], Ingo Fetzer[1,2], Sarah E. Cornell[1,2], Johan Rockström[1,6], Timothy M. Lenton[3]*

Climate tipping points occur when change in a part of the climate system becomes self-perpetuating beyond a warming threshold, leading to substantial Earth system impacts. Synthesizing paleoclimate, observational, and model-based studies, we provide a revised shortlist of global "core" tipping elements and regional "impact" tipping elements and their temperature thresholds. Current global warming of ~1.1°C above preindustrial temperatures already lies within the lower end of some tipping point uncertainty ranges. Several tipping points may be triggered in the Paris Agreement range of 1.5 to <2°C global warming, with many more likely at the 2 to 3°C of warming expected on current policy trajectories. This strengthens the evidence base for urgent action to mitigate climate change and to develop improved tipping point risk assessment, early warning capability, and adaptation strategies.

Climate tipping points (CTPs) have emerged as a growing research topic and source of public concern (*1*–*3*). Tipping points are defined as "a critical threshold at which a tiny perturbation can qualitatively alter the state or development of a system" (*1*). Several large-scale Earth system components, termed tipping elements, were identified with evidence for tipping points that could be triggered by human activities this century. The initial shortlist constituted Arctic summer sea ice, the Greenland ice sheet (GrIS), the West Antarctic ice sheet (WAIS), Atlantic Meridional Overturning Circulation (now AMOC, previously THC), the El Niño Southern Oscillation, the Indian Summer monsoon, the Sahara/Sahel and West African Monsoon, the Amazon rainforest (AMAZ), and boreal forest. A literature review (*1*) and corresponding expert elicitation (*4*) provided early estimates of the temperature thresholds and potential interactions of these tipping elements. Subsequent work showed how recognition of CTPs considerably affects risk analysis and supports measures to minimize global warming to the Paris target of 1.5°C (*5*, *6*).

Since these early estimates (*1*), there have been considerable advances in our knowledge of CTPs including observations of nonlinear changes in the climate system, statistical early warning methods, paleoclimate evidence, upgraded Earth system models (ESMs), and improved offline models of particular elements (e.g., ice sheets and vegetation). Notably, observations and models suggest that parts of the WAIS may be approaching (*7*, *8*) or have even passed a tipping point (*9*, *10*). Early warning indicators have revealed potential destabilization of the GrIS, AMOC, and AMAZ (*11*–*13*). However, many ESMs still lack processes important for resolving potential tipping behavior—e.g., bias toward AMOC stability (*14*)—or underestimating current tropical carbon sink declines (*15*). Potential causal interactions among tipping elements (*4*) are such that overall tipping of one element increases the likelihood of tipping others (*16*), possibly risking a "tipping cascade" of impacts that may further amplify global warming (*2*, *3*). In the worst case scenario, interactions might produce a global CTP (*3*).

The list of tipping elements has evolved over time (*1*–*3*, *5*) (table S1). Different studies have proposed potential additions including southwest North America, the Yedoma permafrost region, the North Atlantic subpolar gyre (*17*), low-latitude coral reefs, the East Antarctic Ice Sheet (EAIS), Arctic winter sea ice (AWSI), Alpine glaciers (*5*), the northern polar jet stream (*3*), the Congo rainforest (*18*), and the Wilkes and Aurora subglacial basins in East Antarctica (*2*). A range of abrupt shifts have been identified in CMIP5 models (*19*), some of which are not in elements on the original shortlist such as boreal tundra or Antarctic sea ice. Conversely, arguments have been made that Arctic summer sea ice (*20*, *21*), El Niño–Southern Oscillation (ENSO) (*22*, *23*), and monsoons (*24*) should not be classified as CTPs. Numerous temperature threshold estimates have been made since (*1*) with some being revised markedly downward—notably WAIS (*2*, *25*). The recent the Intergovernmental Panel on Climate Change (IPCC) AR6 WG1 report identifies up to 15 candidates [table 4.10 in (*23*)] but was not explicit about their temperature thresholds (*23*).

Here we reassess the climate tipping elements based on the substantial literature published since (*1*), focusing on those triggerable by global warming. We clarify the definition of tipping elements and points and propose a new categorization separating global "core" and regional "impact" tipping elements. We then provide an updated list and assessment of the global mean surface temperature (GMST) range at which each candidate CTP could occur as well as their timescales and climate impacts. Finally we combine this information to assess the likelihood of triggering CTPs at successive global warming levels.

Defining tipping points and tipping elements

Given multiple inconsistent definitions of a CTP in the literature, we anchor on the technical definition provided by (*1*): A tipping point is a threshold in a (forcing) "control parameter" at which a small additional perturbation (within natural variability of ~0.2°C) causes a qualitative change [significantly larger than the standard deviation of natural variability in (*1*)] in the future state of a system [see (*1*) and SM for the full definition]. Here, our specific definition is as follows: Tipping points occur when change in part of the climate system becomes (i) self-perpetuating beyond (ii) a warming threshold as a result of asymmetry in the relevant feedbacks, leading to (iii) substantial and widespread Earth system impacts. We now explain key aspects of this definition in more detail.

Self-perpetuating change

Self-perpetuation mechanisms are critical to the existence of a tipping point in a system, beyond which they propel qualitative change such that even if forcing of the system ceases the qualitative change usually continues to unfold regardless (*20*). IPCC AR6 sometimes uses tipping point to refer to a class of abrupt change in which the subsequent rate of change is independent of the forcing [1.4.4.3 of (*26*)], although this is not part of AR6's core CTP definition [4.7.2 of (*23*)]. Self-perpetuation is usually due to positive feedback within a system attaining sufficient strength to overcome stabilizing negative feedbacks and (temporarily) reach a "runaway" condition (in which an initial change propagating around a feedback loop gives rise to an additional change that is at least as large as the initial change and so on). Most positive feedbacks never attain this condition and instead simply amplify the original driver in a constrained way. Notably, Arctic summer sea ice loss involves the positive ice-albedo feedback, but unlike year-round sea ice loss, that feedback alone is not strong enough to produce a clear threshold

[1]Stockholm Resilience Centre, Stockholm University, Stockholm, Sweden. [2]Bolin Centre for Climate Research, Stockholm University, Stockholm, Sweden. [3]Global Systems Institute, University of Exeter, Exeter, UK. [4]Georesilience Analytics, Leatherhead, UK. [5]Copernicus Institute of Sustainable Development, Utrecht University, Utrecht, Netherlands. [6]Potsdam Institute for Climate Impact Research, Potsdam, Germany.
*Corresponding author. Email: d.mckay@exeter.ac.uk (D.I.A.M.); t.m.lenton@exeter.ac.uk (T.M.L.)

Downloaded from https://www.science.org at Cardiff University on September 08, 2022

beyond which loss would continue even if global warming stopped (*20*, *21*). Consequently, we describe such feedbacks as "threshold-free".

(Ir)reversibility

Tipping points usually lead to irreversible qualitative change but reversible tipping points are possible as a special case (*1*). Many tipping points result from crossing bifurcation points or attraction basin boundaries in bistable systems, with the resulting hysteresis making tipping effectively irreversible on human timescales. However, self-perpetuating change can also occur across noncatastrophic thresholds in unistable systems (*27*) (supplementary text S1). Other definitions of CTPs are more restrictive and require irreversibility, for example: "a system reorganizes… and does not return to the initial state even if the drivers of the change are abated" [6.1.1 of (*22*)]. The IPCC AR6 does not require irreversibility as this is difficult to prove for long timescales given model limitations: "A tipping point is a critical threshold beyond which a system reorganizes, often abruptly and/or irreversibly" [4.7.2 of (*23*)]. AR6 uses abruptness and irreversibility as proxies for tipping dynamics but does not specify criteria for system reorganization and sometimes does not clearly differentiate which abrupt and/or irreversible changes are considered tipping points (e.g., irreversible ocean temperature change is listed alongside potential tipping points in table 4.10 of (*23*) and box 12.1 in table 1 of (*28*) but has no clear critical threshold).

Timescale and abruptness

We allow for CTPs (e.g., in ice sheets) in which the resulting qualitative change is slower than the anthropogenic forcing causing it—i.e., not abrupt in the sense defined as faster than the cause (*29*). We only require that the transition to a new state occurs at a rate determined by the climate (sub)system itself (*29*). The resulting committed (often irreversible) qualitative changes can unfold over centuries to millennia [here we relax the ethical time horizon of (*1*) from ~1 thousand years (ky) to ~10 ky], but crucially they can increase short-term impacts (e.g., rate of sea level rise). Other authors require a tipping point to produce abrupt change (*30*) thereby excluding events such as ice sheet collapse. The IPCC defines abrupt change as "substantially faster than the rate of change in recent history" in AR6 [1.4.4.3 of (*26*)], which could allow for slower changes than anthropogenic forcing. However, AR6 also gave a more restrictive timescale-based definition for abrupt climate change as taking place over a few decades or less (i.e., as fast as anthropogenic forcing) and persisting for at least a few decades [4.7.2 of (*23*)]. More than a dozen abrupt changes have been found in CMIP5 model output (*19*) (table S2) but such changes could simply be the result of an abrupt change in forcing without involving CTPs. Below we assess which abrupt changes indicate potential tipping elements and which do not involve self-perpetuating feedback.

Spatial scale

Tipping elements are defined as components of the Earth system that are at least subcontinental in scale (of the order of 1000 km, i.e., ~1 M km_2) and could pass a tipping point as a result of actions this century (*1*). If self-perpetuating change (and a corresponding tipping point) occurs at a subcontinental scale then this qualifies as a global core tipping element. However, there are many examples of runaway feedback and associated tipping points at smaller spatial scales. Where a change in forcing (e.g., temperature) is fairly uniform across a large spatial scale, such that a smaller-scale tipping point is crossed near-synchronously in many locations that span a subcontinental scale (e.g., coral bleaching across the Great Barrier Reef or committed loss of Himalayan glaciers), then these are considered potential regional impact tipping elements. However, where systems exhibit localized tipping points (1 m to 1 km) at different forcing levels such that change does not self-perpetuate beyond a clear shared threshold (e.g., methane hydrates), these are classed as threshold-free feedbacks because the accumulated global consequences of multiple localized tipping events remain roughly proportional to the forcing.

Impacts

Climate tipping elements in (*1*) either (i) contribute significantly to the overall mode of operation of the Earth system (such that tipping them modifies the overall state of the whole system), (ii) contribute significantly to human welfare (such that tipping them affects >~100 million people), or (iii) have great value in themselves as a unique feature of the Earth system [expanded from the biosphere used in (*1*)]. Global core tipping elements must meet criterion (i) whereas regional impact tipping elements must meet criterion (ii) or (iii) but not (i). Regarding (i), crossing a tipping point need not involve feedback to global atmospheric composition or temperature—self-perpetuating feedback can exist entirely within a tipping element (*1*)—but there is usually causal coupling to other tipping elements such as through heat, salt, water, carbon, or momentum fluxes (*4*). Often there is feedback to global warming and where this exceeds ±0.1°C (i.e., natural variability and the triggering perturbation) we consider this to meet criterion (i). Thus, near-synchronous, large-scale crossing of smaller-scale tipping points can qualify as a global core tipping element if it changes warming by >0.1°C.

The climate tipping elements

Based on current observations, paleorecords, and model runs subsequent to (*1*), we draw up a longlist of proposed climate tipping elements. Together with expert judgment for each proposed element, we summarize the evidence and confidence levels for self-perpetuation, temperature thresholds, hysteresis or irreversibility, transition timescales, and global or regional impacts on climate (Materials and Methods, table S3, and supplementary text S2). Based on this evidence and the definitions in the preceding section, we shortlist global core and regional impact climate tipping elements (Table 1 and Fig. 1). Other candidate tipping elements that we consider uncertain, unlikely, or that have threshold-free feedbacks are discussed in the supplementary text along with differences with past assessments (table S4).

Cryosphere

Arctic sea ice (AWSI/BARI)

An abrupt collapse in AWSI (*31*) is observed in some CMIP5 models beyond ~4.5°C (*19*, *32*), which arises either from asymmetry in ice formation and loss timescales creating a threshold response or from local positive feedback cycles. Hence we class AWSI as a global core tipping element (medium confidence), with a best estimate threshold of ~6.3°C (4.5 to 8.7°C, based on CMIP5) (high confidence), timescales of 20 years (10 to 100 years) (high confidence), and GMST feedback of ~+0.6°C (high confidence) [~+0.25°C when free of summer ice; regional ~+0.6 to 1.2°C (low confidence)]. A subcase is abrupt loss of Barents Sea winter ice (BARI), which occurs at ~1.6°C in two CMIP5 models (*19*), is self-reinforced by an increased inflow of warm Atlantic waters (*33*), and has substantial impacts on atmospheric circulation, European climate, and potentially the AMOC (*34*). We consider BARI a probable regional impact tipping element (medium confidence) with a threshold of 1.6°C (1.5 to 1.7°C) (low confidence), a timescale of ~25 years (low confidence), and regional warming (high confidence). By contrast Arctic summer sea ice (ASSI)—despite declining rapidly since the 1970s and outpacing previous IPCC projections since the 1990s—is responding linearly to cumulative emissions (*35*). This decline is amplified by the ice-albedo feedback and possibly feedbacks to cloud cover but damped by negative heat loss feedbacks (*20*). CMIP6 models better capture historical ASSI decline and project that ice-free Septembers will occur occasionally above 1.5°C GMST, become common beyond 2°C, and remain permanent at ~3°C (*36*). However, the linear modeled and observed responses suggest that ASSI is unlikely to feature a tipping point beyond which loss would self-perpetuate (*21*, *36*). Hence, we recategorize ASSI as a threshold-free feedback.

Greenland ice sheet (GrIS)

The GrIS is shrinking at an accelerated rate as a result of both net surface melt and accelerated

Downloaded from https://www.science.org at Cardiff University on September 08, 2022

Table 1. Table showing our literature-based threshold, timescale, and impact estimates for the tipping elements we categorize as global core or regional impact. Element acronym colors indicate Earth system domain (blue, cryosphere; green, biosphere; orange, ocean-atmosphere), and element name and estimate colors indicate subjective confidence levels (green, high; yellow, medium; red, low). Bolded element names indicate elements featured in previous climate tipping element characterizations.

Category	Proposed climate tipping element (and tipping point)		Threshold (°C)			Timescale (years)			Maximum impact* (°C)	
			Est.	Min	Max	Est.	Min	Max	Global	Region
Global core tipping elements	**GrIS**	**Greenland Ice Sheet (collapse)**	1.5	0.8	3.0	10k	1k	15k	0.13	0.5 to 3.0
	WAIS	**West Antarctic Ice Sheet (collapse)**	1.5	1.0	3.0	2k	500	13k	0.05	1.0
	LABC	Labrador-Irminger Seas / SPG Convection (collapse)	1.8	1.1	3.8	10	5	50	-0.50	-3.0
	EASB	East Antarctic Subglacial Basins (collapse)	3.0	2.0	6.0	2k	500	10k	0.05	?
	AMAZ	**Amazon Rainforest (dieback)**	3.5	2.0	6.0	100	50	200	Partial: 30 GtC / 0.1°C Total: 75 GtC / 0.2°C	0.4 to 2.0
	PFTP	**Boreal Permafrost (collapse)**	4.0	3.0	6.0	50	10	300	125-250 GtC / 175-350 GtCe / 0.2-0.4°C	~
	AMOC	**Atlantic M.O. Circulation (collapse)**	4.0	1.4	8.0	50	15	300	-0.50	-4 to -10
	AWSI	**Arctic Winter Sea Ice (collapse)**	6.3	4.5	8.7	20	10	100	0.60	0.6 to 1.2
	EAIS	**East Antarctic Ice Sheet (collapse)**	7.5	5.0	10.0	?	10k	?	0.60	2.0
	REEF	**Low -latitude Coral Reefs (die-off)**	1.5	1.0	2.0	10	~	~	~	~
Regional impact tipping elements	**PFAT**	**Boreal Permafrost (abrupt thaw)**	1.5	1.0	2.3	200	100	300	Abrupt thaw adds 50% to gradual: 10 GtC/14 GtCe/ .04°C per °C @2100; 25 GtC/35 GtCe/ .11°C per °C @2300	~
	BARI	Barents Sea Ice (abrupt loss)	1.6	1.5	1.7	25	?	?	~	+
	GLCR	**Mountain Glaciers (loss)**	2.0	1.5	3.0	200	50	1k	0.08	+
	SAHL	**Sahel and W. African Monsoon (greening)**	2.8	2.0	3.5	50	10	500	~	+
	BORF	**Boreal Forest (southern dieback)**	4.0	1.4	5.0	100	50	?	+52GtC / net -0.18°C	-0.5 to -2
	TUND	**Boreal Forest (northern expansion)**	4.0	1.5	7.2	100	40	?	-6 GtC / net +0.14°C	0.5-1.0

*Feedback strength in °C per °C for abrupt permafrost thaw is calculated relative to preindustrial and declines with further degrees of warming (by ~21% per °C).

calving (*37*, *38*) and shows early warning signals consistent with approaching a tipping point in west Greenland (*11*). Both ice sheet modeling and paleoclimate data indicate that a GrIS tipping point can occur when the melt-elevation feedback gets strong enough to support self-propelling melt (as an ice sheet surface loses height, it enters warmer air and thus melts faster) (*1*). Different models give a critical threshold of ~1.6°C (0.8 to 3.2°C) (*39*), ~1.5°C (*40*), or 2.7±0.2°C (*41*). Paleoclimate and model evidence shows that ice only reaches full coverage below ~0.3 to 0.5°C [~300 parts per million (ppm) CO_2] (*39*, *42*). Hysteresis allows GrIS to exist above this growth threshold once formed (*39*) but paleorecords indicate that GrIS partially retreats above this threshold (*42*) and likely collapsed during the long MIS-11 interglacial which was considerably warmer (>1.5°C) (*43*). A coupled ice sheet–atmosphere model found no collapse threshold (*44*), leading AR6 to state that there is limited evidence for irreversible GrIS loss below 3°C (*21*). However, some irreversible loss occurs beyond 3.5 m sea level equivalent (equivalent to ~2 to 2.5°C) (*44*), indicating self-perpetuating feedback. GrIS collapse would shift the Earth system to a unipolar icehouse state and affect other tipping elements (particularly the AMOC), hence qualifying as a global core tipping element (high confidence). Our best estimates for GrIS include a threshold of ~1.5°C (0.8 to 3°C) (high confidence), timescales of 10 ky (1 to 15 ky) (medium confidence), and GMST feedback of ~+0.13°C (regional ~+0.5 to 3°C) (low confidence). The timescale of ice sheet meltdown gets shorter the greater the temperature threshold is exceeded (*40*), with a minimum of ~1000 years.

West Antarctic ice sheet (WAIS)

Large parts of the WAIS are grounded below sea level; if the grounding line in these marine ice sheet basins reaches retrograde slopes, this may lead to the onset of marine ice sheet instability (MISI) and crossing of a tipping point (*7*, *8*, *45*). MISI is based on a feedback between the grounding line retreat and ice flux across the grounding line as it reaches thicker ice. This can lead to self-sustaining retreat and is hypothesized to have driven past collapses of the WAIS during previous warmer interglacial periods with high sea levels (*21*, *46*). Some glaciers in the Amundsen Sea Embayment are already close to this threshold and experiencing substantial grounding line retreat (*9*). The grounding line of Thwaites glacier is only ~30 km away from the subglacial ridge and retreating at ~1 km per year (*47*); eventual collapse may already be inevitable (*10*, *45*). Models support irreversible retreat being underway for present levels of ocean warming (*25*, *48*) and suggest that losing Thwaites glacier may destabilize much of WAIS (*7*). Under sustained

Downloaded from https://www.science.org at Cardiff University on September 08, 2022

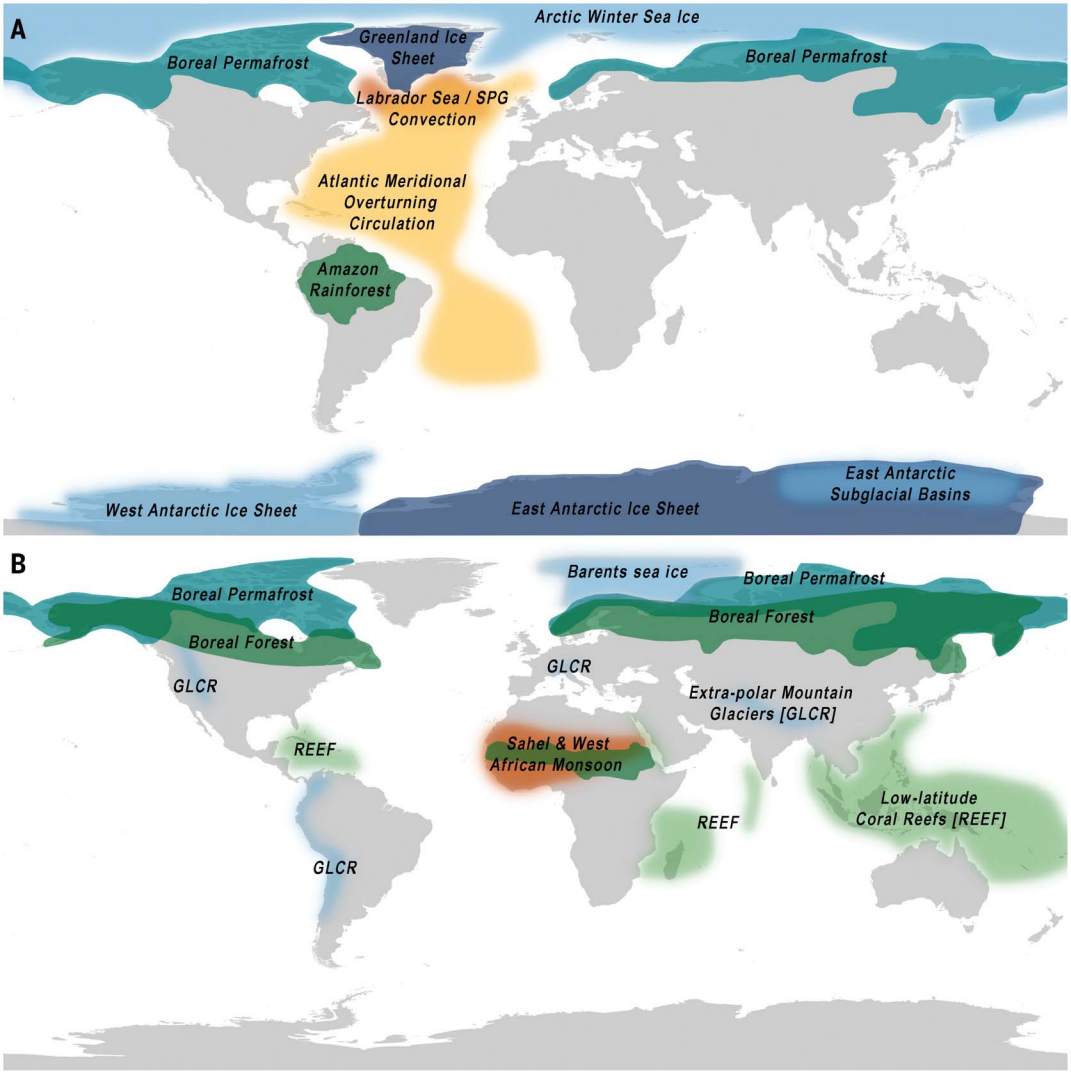

Fig. 1. Maps showing the global core (**A**) and regional impact (**B**) climate tipping elements identified in this study. Blue, green, and orange areas represent cryosphere, biosphere, and ocean-atmosphere elements, respectively.

1°C warming one model shows partial WAIS collapse with mass loss peaking at ~2°C warming (*25*). Hence we retain WAIS as a core global tipping element (high confidence) with a best estimate threshold of ~1.5°C [1 to 3°C, down from 3.5 to 5.5°C in (*1*)] (high confidence), timescales of 2 ky (500 years to 13 ky) (medium confidence), and GMST feedback of ~+0.05°C (regional ~+1°C) (low confidence). Higher threshold exceedance reduces the transition timescale to a minimum of ~500 years (*40*).

East Antarctic subglacial basins (EASB)

Recent data and models have shown that several subglacial basins of the EAIS—particularly the Wilkes, Aurora, and Recovery Basins—are also affected by MISI (*21*, *25*, *49*–*51*). These basins may also be subject to marine ice cliff instability in which the collapse of floating ice shelves creates unstable ice cliffs at the marine edge of the ice sheet which can retreat faster, but the importance of this process is disputed (*49*, *51*). One model indicates that Wilkes collapse may be committed by 3 to 4°C (*25*). Paleoclimate evidence for a higher mid-Pliocene sea level (+5 to 25 m) indicates that parts of the EASB (together with the GrIS and WAIS) were likely absent when the world was ~2.5 to 4°C warmer (*21*, *42*, *52*). By contrast sea levels of +6 to 13 m at 1.1 to 2.1°C in MIS-11 do not require substantial EASB contribution (assuming WAIS and GrIS were lost) (*50*). Hence we class EASB as a core global tipping element (high confidence) with best estimates for a tipping threshold of 3°C (2 to 6°C) (medium confidence), timescales of 2 ky (500 y to 10 ky) (medium confidence), and an uncertain GMST feedback provisionally assumed to be similar to WAIS (i.e., ~+0.05°C) (low confidence).

East Antarctic ice sheet (EAIS)

The land-grounded bulk of the EAIS is the world's largest ice sheet, containing the equivalent of ~50 m of sea level potential (*25*). Paleorecords indicate that growth occurred once atmospheric CO_2 fell below ~650 to 1000 ppm (~6 to 9°C) (*42*). Modeled ice sheets often exhibit alternative ice-covered or ice-free stable states for a range of global boundary conditions (*53*). As a result of this hysteresis the EAIS is expected to remain stable at CO_2 levels well beyond 650 ppm, helping it to survive through the warm mid-Miocene Climatic Optimum ~16 Mya (~2 to 4°C) (*42*). However, long-term stabilization at >1000 ppm CO_2 and ~8 to 10°C warming could cause total disintegration (*25*). Once past this threshold, self-perpetuating feedbacks amplify ice loss (*39*). The loss of EAIS would have global effects and hence is categorized as a global core

Downloaded from https://www.science.org at Cardiff University on September 08, 2022

tipping element (medium confidence). Although unlikely, under high emissions [e.g., Representative Concentration Pathway (RCP) 8.5] and high climate sensitivity it might conceivably be committed to during this century or thereafter. Our best estimates for the EAIS are a tipping threshold of ~7.5°C (5 to 10°C) (medium confidence), timescales of >10 ky (medium confidence), and GMST feedback of ~+0.6°C (regional ~+2°C) (low confidence).

Boreal permafrost (PFTP/PFAT)

Permanently frozen soils and sediments in boreal regions contain ~1035 gigatonnes of carbon (GtC) that can be partly released as CO_2 and methane upon thawing (*54*). Although initially lacking evidence for a synchronous large-scale threshold (*1*), subsequent assessments recognized that part(s) of the permafrost could be considered a tipping element (*3*, *17*). Here we separate permafrost into three components with different dynamics: gradual thaw [PFGT; a threshold-free feedback (high confidence)] (*54*–*56*) (see SM); abrupt thaw [PFAT; a regional impact tipping element (medium confidence)], and collapse [PFTP: a global core tipping element (low confidence)]. Abrupt thaw processes (PFAT) such as slope slumping and thermokarst lake formation (*54*) could increase emissions by 50 to 100% relative to gradual thaw (*57*), involve localized tipping dynamics (e.g., continued thaw subsidence after initiation) and could occur near-synchronously on a subcontinental scale. Our best estimates for PFAT include a tipping threshold of 1.5°C (1 to 2.3°C) (medium confidence), a timescale of 200 years (100 to 300<years) (medium confidence), and an additional ~50% emissions beyond gradual thaw (~10 to 25 GtC per °C) (medium confidence). Finally, abrupt permafrost drying at ~4°C (*58*) and/or sufficiently rapid regional warming (>9°C) corresponding to ~5°C globally (*17*, *59*) could act as a trigger for permafrost collapse (PFTP) driven by internal heat production in carbon-rich permafrost—"the compost bomb" instability (*60*, *61*). The Yedoma deep ice- and carbon-rich permafrost (containing ~115 GtC in Yedoma deposits, ~400 GtC across the Yedoma domain) is particularly vulnerable as fast thaw processes can expose previously isolated deep deposits (*54*, *59*). This and other carbon-rich regions vulnerable to abrupt drying at >4°C (*58*) could have considerable feedback to global temperatures. Our best estimates for PFTP include a threshold of 4°C (3 to 6°C) (low confidence), a timescale of 50 years (10 to 300 years) (medium confidence), and emissions on the order of ~125 to 250 GtC (ΔGMST ~+0.2 to 0.4°C) (low confidence).

Mountain glaciers (GLCR)

Alpine glaciers outside Greenland and Antarctica have individual mass balance thresholds and elevation feedbacks yet large-scale synchronous losses are projected in several key regions at specific global warming levels. In transient simulations, peak water from European glacier melt is expected at ~1°C (*62*) with near-total loss expected to be committed at ~2°C (*20*). Global peak water occurs at ~2°C but committed eventual loss is expected at lower temperatures (*63*). Long model integrations show that global warming of 1.5 to 2°C is sufficient to lead to the eventual loss of most extra-polar glaciers (and possibly even polar glaciers) (*40*, *64*). RCP4.5 (>2°C by 2100) puts most lower-latitude glaciers on a path to significant losses beyond 2100 (*21*). Glaciers in High Mountain Asia last longer than elsewhere but reach peak water at ~2°C with significant social impacts for South Asia (*62*). Given the considerable human impacts of glacier loss (*63*) we categorize mountain glaciers as a regional impact tipping element (medium confidence). Our best estimate includes a threshold of ~2°C (1.5 to 3°C) (medium confidence), a timescale of 200 years (50 years to 1 ky) (medium confidence), and GMST feedback of ~+0.08°C (regionally greater) (low confidence).

Southern Ocean sea ice features abrupt events in some climate models (*19*) but because of uncertain dynamics and low confidence in projections it is classed as an uncertain tipping element (see SM). Marine methane hydrates are classed as a threshold-free feedback and Tibetan plateau snow is classed as uncertain (see SM).

Ocean-Atmosphere (circulation)

North Atlantic subpolar gyre / Labrador-Irminger Sea convection (LABC)

Convection in the Labrador and Irminger Seas in the North Atlantic—part of the subpolar gyre (SPG)—abruptly collapses in some models as a result of warming-induced stratification, a state which is then maintained by self-reinforcing convection feedbacks (*19*, *65*) giving two alternative stable states with or without deep convection. Abrupt future SPG collapse occurs in nine runs across five CMIP5 models at 1.1 to 2.0°C, in one additional model run at 3.8°C (*19*, *65*), and in four CMIP6 models in the 2040s (~1 to 2°C) (*66*). In some models SPG collapse affects AMOC strength but SPG and AMOC have distinct feedback dynamics and patterns of impacts, and SPG collapse can occur much faster than AMOC collapse. The North Atlantic cooling trend (i.e., the "warming hole") is centered over the SPG and in models is often closely linked to SPG weakening (*65*, *66*), although others have associated it with AMOC slowdown (*67*). SPG collapse causes a concentrated North Atlantic regional cooling of ~2 to 3°C, potential global cooling of up to ~0.5°C, a northward-shifted jet stream, weather extremes in Europe, and southward shift of the intertropical convergence zone (ITCZ) (*65*, *66*). Given clear tipping dynamics and global impact we class SPG as a global core tipping element (medium confidence), with a best estimate threshold of ~1.8°C (1.1 to 3.8°C) (high confidence), a timescale of 10 years (5 to 50 years) (high confidence), and GMST feedback of ~0.5°C (regional ~−3°C) (low confidence).

Atlantic meridional overturning circulation (AMOC)

The AMOC is self-sustaining due to salt-advection feedback (northward movement of warm water increases its density as a result of cooling and evaporation supporting the deep convection that drives the circulation). Import of salt at the southern boundary of the Atlantic also supports alternative strong and weak AMOC stable states with multiple abrupt switches between them observed in the past (*68*). Global warming increases Arctic precipitation, freshwater runoff from Greenland, and sea surface temperatures, which together slow down the AMOC by inhibiting deep convection. The AMOC is inferred from some reconstructions to have weakened by ~15% over the past ~50 years (*67*) and early warning signals in indirect AMOC footprints are consistent with the current AMOC "strong" state losing stability (*12*). However, the IPCC gives low confidence on historical AMOC trends (*21*). The Special Report on the Ocean and Cryosphere in a Changing Climate (SROCC) (*22*) assessed AMOC collapse occurring during the 21st century to be very unlikely but physically plausible; however, this was increased to unlikely (medium confidence) in AR6 (*21*). AMOC collapse is triggered in three runs of one CMIP5 model at 1.4 to 1.9°C and in two runs of an additional model at 2.2 to 2.5°C (*19*, *65*) in contrast to gradual declines in other CMIP5 and CMIP6 models (*21*). However, AR6 assessed CMIP models as generally tending toward "unrealistic stability" with respect to observational constraints (*14*, *21*). They also neglect meltwater forcing from rapid GrIS melt (*21*, *69*). Both factors make the AMOC more vulnerable to collapse. AMOC collapse would have global impacts on temperature and precipitation patterns including North Atlantic cooling, Southern Hemisphere warming, southward-shifted ITCZ, monsoon weakening in Africa and Asia, monsoon strengthening in the Southern Hemisphere leading to drying in the Sahel and parts of Amazonia, and reduced natural carbon sinks (*70*–*73*). Hence AMOC is retained as a core global tipping element (medium confidence) with a best estimate threshold of ~4°C [1.4 to 8°C versus 3.5 to 5.5°C in (*1*)] (low confidence), timescales of ~50 years (15 to 300 years) (medium confidence), and a GMST feedback of −0.5°C (low confidence) [regional −4 to −10°C, highly heterogeneous global pattern (medium confidence)].

Downloaded from https://www.science.org at Cardiff University on September 08, 2022

The Indian summer monsoon (and other monsoon systems) have been reclassified as uncertain climate tipping elements because of a lack of evidence for a warming-related threshold behavior. Equatorial stratocumulus cloud breakup and Indian Ocean upwelling are uncertain as a result of limited evidence. Global ocean anoxia is uncertain because the global warming level required for weathering-induced anoxia is unclear. ENSO is reclassified as an unlikely tipping element as it lacks a clear self-perpetuation threshold. Arctic ozone hole expansion is reclassified as unlikely as it is now improbable that it would be triggerable as a result of climate change. The Northern Polar Jet stream is classed unlikely because instability as a result of climate change remains uncertain and no threshold has been proposed. (All of the above elements are discussed in more detail in the supplementary materials.)

Biosphere

Amazon rainforest (AMAZ)

The Amazon forest biome stores ~150 to 200 GtC (*3*, *74*, *75*) and historically has been a important sink for human CO_2 emissions (*15*). However, in intact forests this sink has declined since the 1990s (*15*) and ~17% of the Amazon forest has been lost to deforestation since the 1970s, a rate that has accelerated since 2019 (*75*). A combination of a climate change-induced drying trend, unprecedented droughts, and anthropogenic degradation in the south and east has led to the biome as a whole becoming a net carbon source (*74*). It has also lost resilience across ~76% of its area (*13*). Rainfall is projected to further decline and the dry season is expected to lengthen in southern and eastern areas of the forest in response to further warming, likely worsening this trend (*75*). The Amazon forest recycles around a third of the Amazon basin's rainfall on average (*76*) and up to ~70% in parts of the basin (*77*), particularly during the critical dry season as the forest maintains transpiration fluxes (*76*). This and localized fire feedbacks mean that ~40% of the Amazon forest is estimated to currently be in a bistable state, increasing to ~66% on an RCP8.5 trajectory (*18*, *77*), and rainforest loss could initiate self-reinforcing drying that tips this portion into a degraded or savanna-like state. Widespread Amazon dieback was originally projected at either 3 to 4°C of warming or ~40% deforestation (*78*) but uncertain synergistic interaction might lower the deforestation threshold to only ~20 to 25% (*79*). More recent ESMs tend not to simulate climate-induced Amazon dieback and emergent constraints indicate lower rainforest sensitivity to warming (*80*). However, two CMIP5 models exhibit dieback at 2.5 and 6.2°C (*19*). Additionally, CMIP5 ESMs underestimate observed tree mortality (*15*) and likely overestimate CO_2 fertilization (*81*), potentially making these models undersensitive to dieback. Given the size of the region affected by even partial dieback and its global impacts we categorize the Amazon forest as a global core tipping element (medium confidence). Our best estimates for AMAZ are a threshold of ~3.5°C (2 to 6°C) independent of deforestation (likely lower with deforestation) (low confidence), timescales of 100 years (50 to 200 years) (low confidence), and partial dieback of 40% (i.e., current bistable area) leading to emissions of ~30 GtC along with biogeophysical feedbacks (see SM) to a GMST feedback of ~+0.1° (regional +0.4 to 2°C) (medium confidence).

Boreal forest (BORF/TUND)

The boreal forest (or taiga) encircling the Arctic region features multiple stable states of tree cover as a result of feedbacks including albedo and fire (*82*, *83*). We classify it as a regional impact tipping element with two potential CTPs associated with abrupt dieback at its southern edge (BORF) (medium confidence) and abrupt expansion at its northern edge (tundra greening) (TUND) (medium confidence). Warming is projected to destabilize the southern edge, where factors such as hydrological changes, increased fire frequency, and bark beetle outbreaks can lead to self-reinforcing feedbacks driving regionally synchronized forest dieback (on the order of 100 km) to a grass-dominated steppe or prairie state (*83*). Models project that regime shifts may start in this area at ~1.5°C and become widespread by >3.5°C (*84*, *85*). Dieback may also be rate-dependent (*85*). Our best estimates for BORF is a threshold of ~4°C (1.4 to 5°C) (low confidence), timescales of 100 years (50+ years) (low confidence), and partial (~50%) dieback leading to emissions of ~52 GtC, which—along with countervailing biogeophysical feedbacks such as increased albedo and reduced evapotranspiration—leads to a net GMST feedback of ~−0.18°C (medium confidence) [regional ~−0.5 to 2°C (low confidence)]. Northward expansion of the forest into the current tundra biome may also feature self-perpetuation dynamics (e.g., by causing further local warming through albedo feedback). Models suggest that regime shifts may begin in this northern area at ~1.5°C and become widespread by ~3.5°C (*84*), with abrupt high latitude forest expansion occurring in one CMIP5 model at 7.2°C (*19*). For TUND our best estimates are for a threshold at ~4°C (1.5 to 7.2°C) (low confidence), timescales of 100 years (40+ years) (low confidence), and partial (~50%) uptake of ~6 GtC which along with countervailing biogeophysical feedbacks (decreased albedo, increased evapotranspiration) leads to a net GMST feedback of +0.14°C per °C (regional ~+0.5 to 1°C) (low confidence).

Sahel vegetation and the West African monsoon (SAHL)

Paleoevidence indicates multiple abrupt shifts into and out of African Humid Periods with associated greening of the Sahara in response to gradual changes in orbital forcing (*86*). AMOC weakening and associated warming of the Equatorial East Atlantic also caused past collapses of the West African monsoon (WAM) (*70*, *86*, *87*). Dust aerosol-rainfall positive feedbacks amplify change alongside well-established vegetation-rainfall positive feedbacks but many models still underestimate self-amplifying feedbacks and cannot reproduce the extent of past rainfall and vegetation changes (*86*). By contrast, a model optimized against present observations and mid-Holocene reconstructions recently reproduced abrupt transitions in Saharan vegetation with potential tipping dynamics (*88*). In future projections with GHG forcing, global (CMIP5 and CMIP6) and some regional Coordinated Regional Climate Downscaling Experiment (CORDEX) climate models tend to predict strengthening of the WAM and wetting and northward expansion of the central and eastern Sahel (as well as drying in coastal west Africa) (*23*, *70*, *89*–*91*), which tend to green the Sahel (*86*). Abrupt increases in vegetation in the Eastern Sahel occur in three ESM runs at 2.1 to 3.5°C (*19*). In other global models more gradual WAM strengthening and vegetation shifts are predicted but in some regional climate models the WAM instead collapses (*89*). Clearly the existence of a future tipping threshold for the WAM and Sahel remains uncertain as does its sign but given multiple past abrupt shifts, known weaknesses in current models, and huge regional impacts but modest global climate feedback, we retain the Sahel/WAM as a potential regional impact tipping element (low confidence). We adopt the scenario of abrupt wetting and greening with a threshold of ~2.8°C (2 to 3.5°C) (low confidence), a timescale of 50 years (10 to 500 years) (low confidence), and uncertain Earth system impacts (regional warming) (medium confidence).

Low-latitude coral reefs (REEF)

Tropical and subtropical coral reefs are threatened by anthropogenic pressures including overfishing, direct damage, sedimentation, ocean acidification, and global warming (*92*). When water temperatures exceed a certain threshold coral irreversibly expel their symbiotic algae resulting in coral bleaching, thereby triggering coral death (*93*). Ocean acidification worsens warming-induced degradation. Coral collapse would remove one of the Earth's most biodiverse ecosystems, affecting the wider marine food web, ocean nutrient and carbon cycling, and livelihoods of millions of people worldwide (*92*). Although coral bleaching is a

Downloaded from https://www.science.org at Cardiff University on September 08, 2022

localized process synchronous bleaching can occur at the ~1000 km scale (as seen for the Great Barrier Reef), and further warming is expected to cause widespread bleaching (*93*). Adaptation may be possible with slower warming rates (*92*) but the IPCC has projected 70 to 90% tropical and subtropical coral reef loss at 1.5°C with near total loss by 2°C (*90*). Given regionally synchronized tipping dynamics with significant human but indirect climate impacts, we categorize warm-water coral reefs as a regional impact tipping element (high confidence). Our best estimates are for a threshold of ~1.5°C (1 to 2°C) (high confidence), timescales of ~10 years (medium confidence), and negligible GMST feedback (high confidence). Beyond the biosphere elements listed, the ocean biological pump and land/ocean carbon sink are unlikely to be tipping elements although they may feature nonlinearities (see SM).

Implications for climate policy and preventing dangerous levels of global warming

Figure 2A summarizes our temperature threshold estimates for each tipping element making the shortlists (others are summarized in the supplementary text). Here we define crossing a CTP as "possible" beyond its minimum temperature threshold and "likely" beyond its central estimate.

This revised assessment of CTPs has significant implications for climate policy by determining levels of global warming that prevent tipping to either committed changes in Earth system function or major damage to future societies. A risk minimization approach such as this seeks to avoid minimum estimated thresholds but this no longer appears possible for some tipping elements.

Current warming is ~1.1°C above preindustrial and even with rapid emission cuts warming will reach ~1.5°C by the 2030s (*23*). We cannot rule out that WAIS and GrIS tipping points have already been passed (see above) and several other tipping elements have minimum threshold values within the 1.1 to 1.5°C range. Our best estimate thresholds for GrIS, WAIS, REEF, and abrupt permafrost thaw (PFAT) are ~1.5°C although WAIS and GrIS collapse may still be avoidable if GMST returns below 1.5°C within an uncertain overshoot time (likely decades) (*94*). Setting aside achievability (and recognizing internal climate variability of ~±0.1°C), this suggests that ~1°C is a level of global warming that minimizes the likelihood of crossing CTPs. This is consistent with the <0.5 to 1°C range of Holocene temperature variability whereas past interglacials ≤1.5 to 2°C had up to 10 to 13 m higher sea level (*21*, *95*).

The chance of triggering CTPs is already non-negligible and will grow even with stringent climate mitigation (SSP1-1.9 in Fig. 2, B and C). Nevertheless, achieving the Paris Agreement's aim to pursue efforts to limit warming to 1.5°C would clearly be safer than keeping global warming below 2°C (*90*) (Fig. 2). Going from 1.5 to 2°C increases the likelihood of committing to WAIS and GrIS collapse near complete warm-water coral die-off, and abrupt permafrost thaw; further, the best estimate threshold for LABC collapse is crossed. The likelihood of triggering AMOC collapse, Boreal forest shifts, and extra-polar glacier loss becomes non-negligible at >1.5°C and glacier loss becomes likely by ~2°C. A cluster of abrupt shifts occur in ESMs at 1.5 to 2°C (*19*). Although not tipping elements, ASSI loss could become regular by 2°C, gradual permafrost thaw would likely become widespread beyond 1.5°C, and land carbon sink weakening would become significant by 2°C.

Recent net zero targets if implemented could limit peak warming to ~1.95°C (1.3 to 3°C), but as of November 2021 current policies are estimated to result in ~2.6 °C (1.9 °C to 3.7 °C) by 2100 (*96*). Therefore 2 to 3°C by 2100 is currently likely with matching of pledges with policies key to determining where warming ends up in this range. Going from 2 to 3°C, maximum estimated thresholds for abrupt permafrost thaw, GrIS, WAIS, and extra-polar glaciers are passed, suggesting that tipping them would become very likely. The likelihood of triggering EASB collapse, Amazon dieback, and West African monsoon shift (Sahel greening) becomes non-negligible at ~2°C and increases at ~3°C. Subpolar gyre collapse, boreal forest dieback, and AMOC collapse also become more likely. Although not tipping elements, above 2°C the Arctic would very likely become summer ice–free and land carbon sink-to-source transitions would become widespread.

If the moderate ambition of current policies is not improved and climate sensitivity or carbon cycle feedbacks turn out to be higher than the median assumption then warming of up to ~4°C is possible by 2100, and >4°C cannot be ruled out if future policy ambition declines and/or implementation falters. Going from 3 to 5°C, EASB collapse becomes very likely, Amazon dieback becomes likely >3.5°C, boreal forest shifts likely >4°C, and large-scale permafrost collapse becomes possible at >3°C and likely >4°C. AMOC collapse may become likely >4°C but with high uncertainty (1.4 to 8°C range) and AWSI collapse becomes possible >4.5°C. Warming of >5°C, although very unlikely this century, becomes plausible in the longer-term under higher climate sensitivities with current or reversed policies. This risks EAIS collapse and a commitment of ~55 m of sea level rise if warming stabilizes >5°C for multiple centuries. Other tipping elements, if not already triggered—e.g., Amazon dieback, widespread Permafrost collapse—would very likely be committed and AMOC collapse and AWSI collapse would become increasingly likely. Equatorial stratocumulus cloud breakup occurs in one model beyond ~6°C (*97*) and if plausible would represent a global CTP to a "hothouse" climate state (*3*).

Discussion

Tipping elements and their tipping points were treated independently in this assessment but there are multiple causal interactions between them with risks of triggering cascades among CTPs (*2*, *4*, *16*), some mediated through temperature. The strength and in some cases even the sign of identified interactions is uncertain (*4*). Nevertheless, their combined effect tends to lower CTP temperature thresholds (*6*, *16*). The present assessment would likely amplify this effect, further strengthening the incentive for ambitious mitigation.

Some of the threshold and impact estimates are highly uncertain (e.g., AMOC, BORF/TUND, AMAZ, SAHL, PFTP) as are the transition timescales of many elements. Some proposed elements remain too uncertain to categorize (e.g., EQSC, ANOX, INSM, AABW, Congo rainforest), and others considered unlikely to feature tipping dynamics (e.g., ENSO, JETS) cannot yet be fully ruled out (see SM). Other tipping elements may yet be discovered. It may be possible to safely overshoot CTPs in slower elements such as ice sheets (*94*) but the allowable overshoot times need further research. Spatial pattern formation might allow some biosphere elements to evade direct tipping (*98*) but this needs to be assessed.

To further our understanding of the likelihood of crossing CTPs an updated expert elicitation [building on (*4*)] is overdue. A horizon-scanning exercise and systematic scanning of CMIP6 model output [following (*19*)] and a tipping point model intercomparison project could help identify more candidate tipping elements and refine assessment of their likelihood. Further model improvements and model-data intercomparison are essential. Early warning methods are starting to reveal whether tipping elements are destabilizing for parts of GrIS (*11*), AMOC (*12*), and the Amazon (*13*), and can reveal proximity to a CTP (*11*). These could be augmented with deep learning techniques (*99*). Systematic application to observational and remotely sensed data together with targeted new observing systems could begin to provide a CTP early warning system (*100*).

Conclusion

The UNFCCC stipulates that all countries commit to avoid dangerous climate change, translated through the Paris climate agreement into keeping GMST well below 2°C and aiming for 1.5°C. Our assessment of climate tipping elements and their tipping points suggests that danger may be approached

Downloaded from https://www.science.org at Cardiff University on September 08, 2022

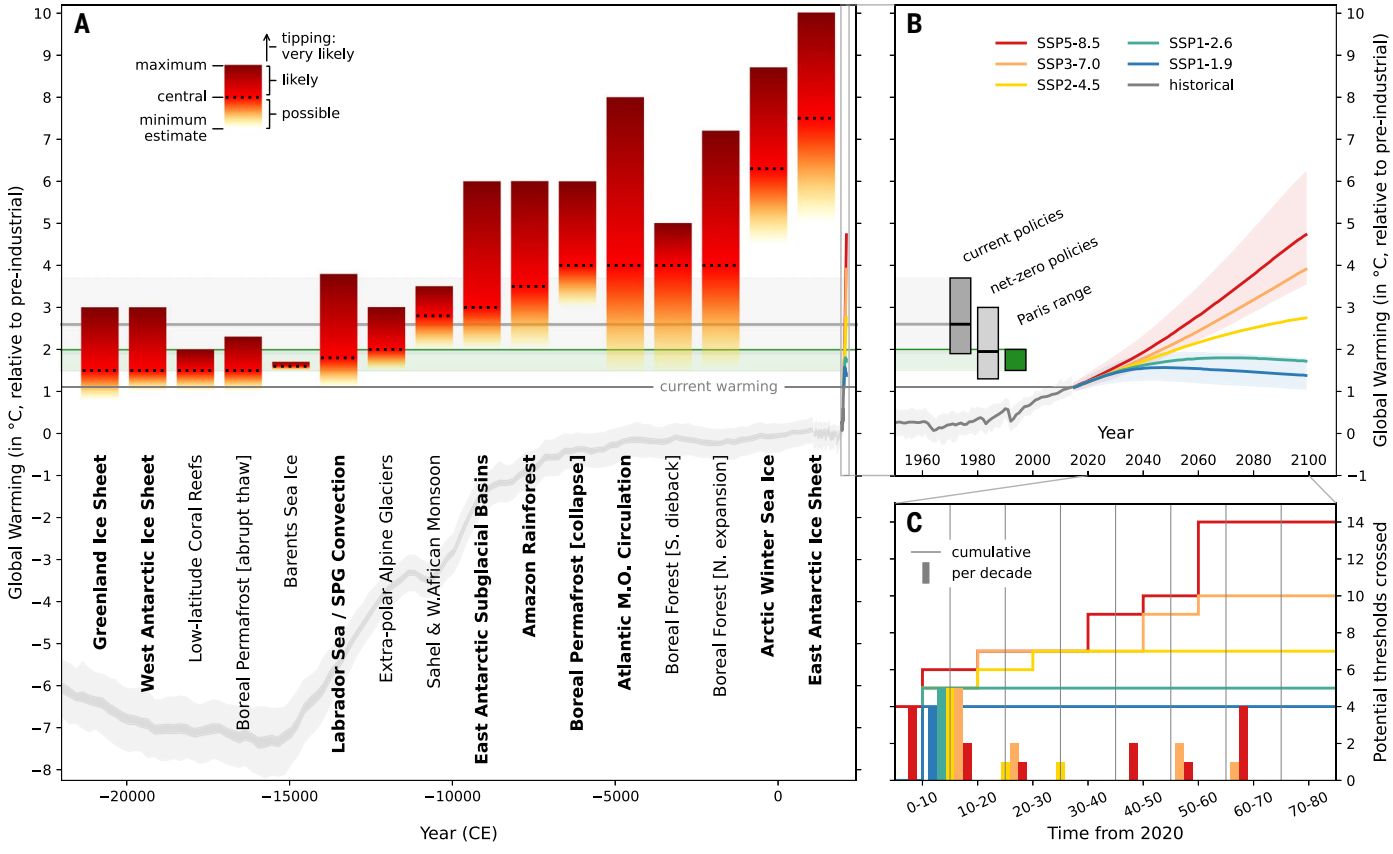

Fig. 2. Our global warming threshold estimates for global core and regional impact climate tipping elements. Tipping elements (**A**) relative to IPCC SSP projections and likely future scenarios given current policies and targets (**B**) and how many thresholds may be crossed per Shared Socioeconomic Pathways (SSP) projection (**C**). Bars in (A) show the minimum (base, yellow), central (line, red), and maximum (top, dark red) threshold estimates for each element (bold font, global core; regular font, regional impact), with a paleorecord of GMST over the past ~25 ky (*95*) and projections of future climate change (green, SSP1-1.9; yellow, SSP1-2.6; orange, SSP2-4.5; red, SSP3-7.0; purple, SSP5-8.5) from IPCC AR6 (*23*) shown for context. Future projections are shown in more detail in (B) along with estimated 21st century warming trajectories for current and net-zero policies (gray bars, extending into (A); horizontal lines show central estimates, bar height the uncertainty ranges) as of November 2021 (*96*) versus the Paris Agreement range of 1.5 to <2°C (green bar). The number of thresholds potentially passed in the coming decades depending on SSP trajectory in (C) is shown per decade (bars) and cumulatively (lines).

even earlier. The Earth may have left a safe climate state beyond 1°C global warming. A significant likelihood of passing multiple climate tipping points exists above ~1.5°C, particularly in major ice sheets. Tipping point likelihood increases further in the Paris range of 1.5 to <2°C warming. Current policies leading to ~2 to 3°C warming are unsafe because they would likely trigger multiple climate tipping points. Our updated assessment of climate tipping points provides strong scientific support for the Paris Agreement and associated efforts to limit global warming to 1.5°C.

Materials and Methods

We mined the literature subsequent to (*1*), including studies of paleoclimate change, observed change, early warning signals, future model projections, underlying theory, and existing assessments, to draw up a longlist of possible candidate tipping elements (table S3). For each we extracted information on evidence for self-perpetuation, temperature thresholds, hysteresis/irreversibility, transition timescales, and global/regional impacts on climate, on which we then use subjective expert judgment to determine our best estimates. From this evidence (or lack of it) we drew up shortlists (Table 1) of 'core' global tipping elements and regional 'impact' tipping elements (Fig. 1), for which we summarize the rationale in the main text and supplementary text S2 and S3. Candidates that did not make the shortlists (table S3) are classed as: (a) 'uncertain' tipping elements—due to limited evidence for self-perpetuating feedback and threshold behavior; (b) 'unlikely' tipping elements—possessing only localized tipping or nonfeedback response to climate change; and (c) 'threshold-free feedbacks'—where positive feedbacks exist but are not strong enough to self-perpetuate. Different parts or phenomena of some systems—notably permafrost—are assigned to different categories. We give (very low, low, medium, high, very high) confidence levels based on the IPCC's confidence rating system (as a product of the authors' judgements of both the robustness and the degree of agreement of the assessed literature) (*101*) for the estimates of central, minimum, and maximum temperature thresholds, timescales of transition, and global and local impacts on climate (supplementary text S2). We define crossing a CTP as 'possible' beyond its minimum temperature threshold and 'likely' beyond its best estimate. Differences with past lists of tipping elements are described in table S4.

REFERENCES AND NOTES

1. T. M. Lenton *et al.*, Tipping elements in the Earth's climate system. *Proc. Natl. Acad. Sci. U.S.A.* **105**, 1786–1793 (2008). doi: 10.1073/pnas.0705414105; pmid: 18258748
2. T. M. Lenton *et al.*, Climate tipping points - too risky to bet against. *Nature* **575**, 592–595 (2019). doi: 10.1038/d41586-019-03595-0; pmid: 31776487
3. W. Steffen *et al.*, Trajectories of the Earth System in the Anthropocene. *Proc. Natl. Acad. Sci. U.S.A.* **115**, 8252–8259 (2018). doi: 10.1073/pnas.1810141115; pmid: 30082409
4. E. Kriegler, J. W. Hall, H. Held, R. Dawson, H. J. Schellnhuber, Imprecise probability assessment of tipping points in the climate system. *Proc. Natl. Acad. Sci. U.S.A.* **106**, 5041–5046 (2009). doi: 10.1073/pnas.0809117106; pmid: 19289827

Downloaded from https://www.science.org at Cardiff University on September 08, 2022

5. H. J. Schellnhuber, S. Rahmstorf, R. Winkelmann, Why the right climate target was agreed in Paris. *Nat. Clim. Chang.* **6**, 649–653 (2016). doi: 10.1038/nclimate3013
6. Y. Cai, T. M. Lenton, T. S. Lontzek, Risk of multiple interacting tipping points should encourage rapid CO2 emission reduction. *Nat. Clim. Chang.* **6**, 520–525 (2016). doi: 10.1038/nclimate2964
7. J. Feldmann, A. Levermann, Collapse of the West Antarctic Ice Sheet after local destabilization of the Amundsen Basin. *Proc. Natl. Acad. Sci. U.S.A.* **112**, 14191–14196 (2015). doi: 10.1073/pnas.1512482112; pmid: 26578762
8. M. S. Waibel, C. L. Hulbe, C. S. Jackson, D. F. Martin, Rate of Mass Loss Across the Instability Threshold for Thwaites Glacier Determines Rate of Mass Loss for Entire Basin. *Geophys. Res. Lett.* **45**, 809–816 (2018). doi: 10.1002/2017GL076470
9. E. Rignot, J. Mouginot, M. Morlighem, H. Seroussi, B. Scheuchl, Widespread, rapid grounding line retreat of Pine Island, Thwaites, Smith, and Kohler glaciers, West Antarctica, from 1992 to 2011. *Geophys. Res. Lett.* **41**, 3502–3509 (2014). doi: 10.1002/2014GL060140
10. I. Joughin, B. E. Smith, B. Medley, Marine Ice Sheet Collapse Potentially Under Way for the Thwaites Glacier Basin, West Antarctica. *Science* **344**, 735–738 (2014). doi: 10.1002/2014GL060140
11. N. Boers, M. Rypdal, Critical slowing down suggests that the western Greenland Ice Sheet is close to a tipping point. *Proc. Natl. Acad. Sci. U.S.A.* **118**, e2024192118 (2021). doi: 10.1073/pnas.2024192118; pmid: 34001613
12. N. Boers, Observation-based early-warning signals for a collapse of the Atlantic Meridional Overturning Circulation. *Nat. Clim. Chang.* **11**, 680–688 (2021). doi: 10.1038/s41558-021-01097-4
13. C. A. Boulton, T. M. Lenton, N. Boers, Pronounced loss of Amazon rainforest resilience since the early 2000s. *Nat. Clim. Chang.* **12**, 271–278 (2022). doi: 10.1038/s41558-022-01287-8
14. W. Liu, S.-P. Xie, Z. Liu, J. Zhu, Overlooked possibility of a collapsed Atlantic Meridional Overturning Circulation in warming climate. *Sci. Adv.* **3**, e1601666 (2017). doi: 10.1126/sciadv.1601666; pmid: 28070560
15. W. Hubau *et al*., Asynchronous carbon sink saturation in African and Amazonian tropical forests. *Nature* **579**, 80–87 (2020). doi: 10.1038/s41586-020-2035-0; pmid: 32132693
16. N. Wunderling, J. F. Donges, J. Kurths, R. Winkelmann, Interacting tipping elements increase risk of climate domino effects under global warming. *Earth Syst. Dyn.* **12**, 601–619 (2021). doi: 10.5194/esd-12-601-2021
17. T. M. Lenton, Arctic climate tipping points. *Ambio* **41**, 10–22 (2012). doi: 10.1007/s13280-011-0221-x; pmid: 22270703
18. A. Staal *et al*., Hysteresis of tropical forests in the 21st century. *Nat. Commun.* **11**, 4978 (2020). doi: 10.1038/s41467-020-18728-7; pmid: 33020475
19. S. Drijfhout *et al*., Catalogue of abrupt shifts in Intergovernmental Panel on Climate Change climate models. *Proc. Natl. Acad. Sci. U.S.A.* **112**, E5777–E5786 (2015). doi: 10.1073/pnas.1511451112; pmid: 26460042
20. A. Levermann *et al*., Potential climatic transitions with profound impact on Europe. *Clim. Change* **110**, 845–878 (2012). doi: 10.1007/s10584-011-0126-5
21. B. Fox-Kemper *et al*., "Climate Change 2021: The Physical Science Basis. Contribution of Working Group I to the Sixth Assessment Report of the Intergovernmental Panel on Climate Change" V. Masson-Delmotte *et al*, Eds. (Cambridge Univ. Press, 2021).
22. M. Collins *et al*., "IPCC Special Report on the Ocean and Cryosphere in a Changing Climate" H.-O. Pörtner *et al*., Eds. (2019); pp. 589–655.
23. J. Y. Lee *et al*., "Climate Change 2021: The Physical Science Basis. Contribution of Working Group I to the Sixth Assessment Report of the Intergovernmental Panel on Climate Change" V. Masson-Delmotte *et al*., Eds. (Cambridge Univ. Press, 2021).
24. W. R. Boos, T. Storelvmo, Near-linear response of mean monsoon strength to a broad range of radiative forcings. *Proc. Natl. Acad. Sci. U.S.A.* **113**, 1510–1515 (2016). doi: 10.1073/pnas.1517143113; pmid: 26811462
25. J. Garbe, T. Albrecht, A. Levermann, J. F. Donges, R. Winkelmann, The hysteresis of the Antarctic Ice Sheet. *Nature* **585**, 538–544 (2020). doi: 10.1038/s41586-020-2727-5; pmid: 32968257
26. D. Chen *et al*., "Climate Change 2021: The Physical Science Basis. Contribution of Working Group I to the Sixth Assessment Report of the Intergovernmental Panel on Climate Change" V. Masson-Delmotte *et al*., Eds. (Cambridge Univ. Press, 2021).
27. M. Scheffer *et al*., Early-warning signals for critical transitions. *Nature* **461**, 53–59 (2009). doi: 10.1038/nature08227; pmid: 19727193
28. R. Ranasinghe *et al*., "Climate Change 2021: The Physical Science Basis. Contribution of Working Group I to the Sixth Assessment Report of the Intergovernmental Panel on Climate Change" V. Masson-Delmotte *et al*., Eds. (Cambridge Univ. Press, 2021), p. 73.
29. National Research Council, *Abrupt Climate Change: Inevitable Surprises* (The National Academies Press, 2002); https://www.nap.edu/catalog/10136.
30. R. E. Kopp, R. L. Shwom, G. Wagner, J. Yuan, Tipping elements and climate–economic shocks: Pathways toward integrated assessment. *Earths Future* **4**, 346–372 (2016). doi: 10.1002/2016EF000362
31. C. Hankel, E. Tziperman, The Role of Atmospheric Feedbacks in Abrupt Winter Arctic Sea Ice Loss in Future Warming Scenarios. *J. Clim.* **34**, 4435–4447 (2021). doi: 10.1175/JCLI-D-20-0558.1
32. P. J. Hezel, T. Fichefet, F. Massonnet, Modeled Arctic sea ice evolution through 2300 in CMIP5 extended RCPs. *Cryosphere* **8**, 1195–1204 (2014). doi: 10.5194/tc-8-1195-2014
33. D. Docquier, R. Fuentes-Franco, T. Koenigk, T. Fichefet, Sea Ice—Ocean Interactions in the Barents Sea Modeled at Different Resolutions. *Front. Earth Sci.* **8**, 1–21 (2020). doi: 10.3389/feart.2020.00172
34. F. Lehner, A. Born, C. C. Raible, T. F. Stocker, Amplified Inception of European Little Ice Age by Sea Ice–Ocean–Atmosphere Feedbacks. *J. Clim.* **26**, 7586–7602 (2013). doi: 10.1175/JCLI-D-12-00690.1
35. I. Allison *et al*., "The Copenhagen Diagnosis" (The Univ. of New South Wales Climate Change Research Centre, 2009); https://www.ccrc.unsw.edu.au/sites/default/files/Copenhagen_Diagnosis_LOW.pdf).
36. D. Notz, S. Community, Arctic Sea Ice in CMIP6. *Geophys. Res. Lett.* **47**, 1–26 (2020). doi: 10.1029/2019GL086749
37. M. D. King *et al*., Dynamic ice loss from the Greenland Ice Sheet driven by sustained glacier retreat. *Commun. Earth Environ.* **1**, 1–7 (2020). doi: 10.1038/s43247-020-0001-2
38. A. Shepherd *et al*., Mass balance of the Greenland Ice Sheet from 1992 to 2018. *Nature* **579**, 233–239 (2020).
39. A. Robinson, R. Calov, A. Ganopolski, Multistability and critical thresholds of the Greenland ice sheet. *Nat. Clim. Chang.* **2**, 429–432 (2012). doi: 10.1038/nclimate1449
40. J. Van Breedam, H. Goelzer, P. Huybrechts, Semi-equilibrated global sea-level change projections for the next 10 000 years. *Earth Syst. Dyn.* **11**, 953–976 (2020). doi: 10.5194/esd-11-953-2020
41. B. Noël, L. van Kampenhout, J. T. M. Lenaerts, W. J. van de Berg, M. R. van den Broeke, A 21st Century Warming Threshold for Sustained Greenland Ice Sheet Mass Loss. *Geophys. Res. Lett.* **48**, 1–9 (2021). doi: 10.1029/2020GL090471
42. G. L. Foster, E. J. Rohling, Relationship between sea level and climate forcing by CO2 on geological timescales. *Proc. Natl. Acad. Sci. U.S.A.* **110**, 1209–1214 (2013). doi: 10.1073/pnas.1216073110; pmid: 23292932
43. A. J. Christ *et al*., A multimillion-year-old record of Greenland vegetation and glacial history preserved in sediment beneath 1.4 km of ice at Camp Century. *Proc. Natl. Acad. Sci. U.S.A.* **118**, e2021442118 (2021). doi: 10.1073/pnas.2021442118; pmid: 33723012
44. J. M. Gregory, S. E. George, R. S. Smith, Large and irreversible future decline of the Greenland ice sheet. *Cryosphere* **14**, 4299–4322 (2020). doi: 10.5194/tc-14-4299-2020
45. R. B. Alley *et al*., Oceanic Forcing of Ice-Sheet Retreat: West Antarctica and More. *Annu. Rev. Earth Planet. Sci.* **43**, 207–231 (2015). doi: 10.1146/annurev-earth-060614-105344
46. C. S. M. Turney *et al*., Early Last Interglacial ocean warming drove substantial ice mass loss from Antarctica. *Proc. Natl. Acad. Sci. U.S.A.* **117**, 3996–4006 (2020). doi: 10.1073/pnas.1902469117; pmid: 32047039
47. H. Yu, E. Rignot, H. Seroussi, M. Morlighem, Impact of iceberg calving on the retreat of Thwaites Glacier, West Antarctica over the next century with different calving laws and ocean thermal forcing. *Geophys. Res. Lett.* **46**, 14539–14547 (2019). doi: 10.1002/2017GL072514
48. R. J. Arthern, C. R. Williams, The sensitivity of West Antarctica to the submarine melting feedback. *Geophys. Res. Lett.* **44**, 2352–2359 (2017). doi: 10.1002/2017GL072514
49. T. L. Edwards *et al*., Revisiting Antarctic ice loss due to marine ice-cliff instability. *Nature* **566**, 58–64 (2019). doi: 10.1038/s41586-019-0901-4; pmid: 30728522
50. P. U. Clark *et al*., Oceanic forcing of penultimate deglacial and last interglacial sea-level rise. *Nature* **577**, 660–664 (2020). doi: 10.1038/s41586-020-1931-7; pmid: 31996820
51. R. M. DeConto *et al*., The Paris Climate Agreement and future sea-level rise from Antarctica. *Nature* **593**, 83–89 (2021). doi: 10.1038/s41586-021-03427-0; pmid: 33953408
52. D. J. Wilson *et al*., Ice loss from the East Antarctic Ice Sheet during late Pleistocene interglacials. *Nature* **561**, 383–386 (2018). doi: 10.1038/s41586-018-0501-8; pmid: 30232420
53. E. Gasson, R. M. DeConto, D. Pollard, R. H. Levy, Dynamic Antarctic ice sheet during the early to mid-Miocene. *Proc. Natl. Acad. Sci. U.S.A.* **113**, 3459–3464 (2016). doi: 10.1073/pnas.1516130113; pmid: 26903645
54. E. A. G. Schuur *et al*., Climate change and the permafrost carbon feedback. *Nature* **520**, 171–179 (2015). doi: 10.1038/nature14338; pmid: 25855454
55. A. Vaks *et al*., Speleothems Reveal 500,000-Year History of Siberian Permafrost. *Science* **340**, 183–186 (2013). doi: 10.1038/nature14338; pmid: 25855454
56. J. G. Canadell *et al*., "Climate Change 2021: The Physical Science Basis. Contribution of Working Group I to the Sixth Assessment Report of the Intergovernmental Panel on Climate Change" V. Masson-Delmotte *et al*., Eds. (Cambridge Univ. Press, 2021).
57. M. R. Turetsky *et al*., Carbon release through abrupt permafrost thaw. *Nat. Geosci.* **13**, 138–143 (2020). doi: 10.1038/s41561-019-0526-0
58. B. Teufel, L. Sushama, Abrupt changes across the Arctic permafrost region endanger northern development. *Nat. Clim. Chang.* **9**, 858–862 (2019). doi: 10.1038/s41558-019-0614-6
59. J. Strauss *et al*., Deep Yedoma permafrost: A synthesis of depositional characteristics and carbon vulnerability. *Earth Sci. Rev.* **172**, 75–86 (2017). doi: 10.1016/j.earscirev.2017.07.007
60. C. M. Luke, P. M. Cox, Soil carbon and climate change: From the Jenkinson effect to the compost-bomb instability. *Eur. J. Soil Sci.* **62**, 5–12 (2011). doi: 10.1111/j.1365-2389.2010.01312.x
61. J. Hollesen, H. Matthiesen, A. B. Møller, B. Elberling, Permafrost thawing in organic Arctic soils accelerated by ground heat production. *Nat. Clim. Chang.* **5**, 574–578 (2015). doi: 10.1038/nclimate2590
62. M. Huss, R. Hock, Global-scale hydrological response to future glacier mass loss. *Nat. Clim. Chang.* **8**, 135–140 (2018). doi: 10.1038/s41558-017-0049-x
63. R. Hock *et al*., "IPCC Special Report on the Ocean and Cryosphere in a Changing Climate" H.-O. Pörtner *et al*., Eds. (Cambridge Univ. Press, 2019), pp. 131–202.
64. P. U. Clark *et al*., Consequences of twenty-first-century policy for multi-millennial climate and sea-level change. *Nat. Clim. Chang.* **6**, 360–369 (2016). doi: 10.1038/nclimate2923
65. G. Sgubin, D. Swingedouw, S. Drijfhout, Y. Mary, A. Bennabi, Abrupt cooling over the North Atlantic in modern climate models. *Nat. Commun.* **8**, 14375 (2017). doi: 10.1038/ncomms14375; pmid: 28198383
66. D. Swingedouw *et al*., On the risk of abrupt changes in the North Atlantic subpolar gyre in CMIP6 models. *Ann. N. Y. Acad. Sci.* **1504**, 187–201 (2021). doi: 10.1111/nyas.14659; pmid: 34212391
67. L. Caesar, S. Rahmstorf, A. Robinson, G. Feulner, V. Saba, Observed fingerprint of a weakening Atlantic Ocean overturning circulation. *Nature* **556**, 191–196 (2018). doi: 10.1038/s41586-018-0006-5; pmid: 29643485
68. J. Lynch-Stieglitz, The Atlantic Meridional Overturning Circulation and Abrupt Climate Change. *Annu. Rev. Mar. Sci.* **9**, 83–104 (2017). doi: 10.1146/annurev-marine-010816-060415; pmid: 27814029
69. J. Lohmann, P. D. Ditlevsen, Risk of tipping the overturning circulation due to increasing rates of ice melt. *Proc. Natl. Acad. Sci. U.S.A.* **118**, e2017989118 (2021). doi: 10.1073/pnas.2017989118; pmid: 33619095
70. H. Douville *et al*., "Climate Change 2021: The Physical Science Basis. Contribution of Working Group I to the Sixth Assessment Report of the Intergovernmental Panel on Climate Change" V. Masson-Delmotte *et al*., Eds. (Cambridge Univ. Press, 2021), p. 73.
71. L. C. Jackson *et al*., Global and European climate impacts of a slowdown of the AMOC in a high resolution GCM. *Clim. Dyn.* **45**, 3299–3316 (2015). doi: 10.1007/s00382-015-2540-2

Downloaded from https://www.science.org at Cardiff University on September 08, 2022

72. S. Drijfhout, Competition between global warming and an abrupt collapse of the AMOC in Earth's energy imbalance. *Sci. Rep.* **5**, 14877 (2015). doi: 10.1038/srep14877; pmid: 26437599
73. A. Bozbiyik, M. Steinacher, F. Joos, T. F. Stocker, L. Menviel, Fingerprints of changes in the terrestrial carbon cycle in response to large reorganizations in ocean circulation. *Clim. Past* **7**, 319–338 (2011). doi: 10.5194/cp-7-319-2011
74. L. V. Gatti *et al*., Amazonia as a carbon source linked to deforestation and climate change. *Nature* **595**, 388–393 (2021). doi: 10.1038/s41586-021-03629-6; pmid: 34262208
75. Science Panel for the Amazon (SPA), "Executive Summary of the Amazon Assessment Report 2021" C. Nobre *et al*., Eds. (United Nations Sustainable Development Solutions Network, 2021); https://www.theamazonwewant.org/wp-content/uploads/2021/09/SPA-Executive-Summary-11Mb.pdf.
76. A. Staal *et al*., Forest-rainfall cascades buffer against drought across the Amazon. *Nat. Clim. Chang.* **8**, 539–543 (2018). doi: 10.1038/s41558-018-0177-y
77. D. C. Zemp *et al*., Self-amplified Amazon forest loss due to vegetation-atmosphere feedbacks. *Nat. Commun.* **8**, 14681 (2017). doi: 10.1038/ncomms14681; pmid: 28287104
78. C. A. Nobre *et al*., Land-use and climate change risks in the Amazon and the need of a novel sustainable development paradigm. *Proc. Natl. Acad. Sci. U.S.A.* **113**, 10759–10768 (2016). doi: 10.1073/pnas.1605516113; pmid: 27638214
79. T. E. Lovejoy, C. Nobre, Amazon Tipping Point. *Sci. Adv.* **4**, eaat2340 (2018). doi: 10.1126/sciadv.aat2340; pmid: 29492460
80. P. M. Cox *et al*., Sensitivity of tropical carbon to climate change constrained by carbon dioxide variability. *Nature* **494**, 341–344 (2013). doi: 10.1038/nature11882; pmid: 23389447
81. C. Terrer *et al*., Nitrogen and phosphorus constrain the CO2 fertilization of global plant biomass. *Nat. Clim. Chang.* **9**, 684–689 (2019). doi: 10.1038/s41558-019-0545-2
82. B. Abis, V. Brovkin, Environmental conditions for alternative tree-cover states in high latitudes. *Biogeosciences* **14**, 511–527 (2017). doi: 10.5194/bg-14-511-2017
83. M. Scheffer, M. Hirota, M. Holmgren, E. H. Van Nes, F. S. Chapin3rd, Thresholds for boreal biome transitions. *Proc. Natl. Acad. Sci. U.S.A.* **109**, 21384–21389 (2012). doi: 10.1073/pnas.1219844110; pmid: 23236159
84. D. Gerten *et al*., Asynchronous exposure to global warming: Freshwater resources and terrestrial ecosystems. *Environ. Res. Lett.* **8**, 034032 (2013). doi: 10.1088/1748-9326/8/3/034032
85. C. D. Koven, Boreal carbon loss due to poleward shift in low-carbon ecosystems. *Nat. Geosci.* **6**, 452–456 (2013). doi: 10.1038/ngeo1801
86. F. S. R. Pausata *et al*., The Greening of the Sahara: Past Changes and Future Implications. *One Earth* **2**, 235–250 (2020). doi: 10.1016/j.oneear.2020.03.002
87. M. W. Schmidt, P. Chang, A. O. Parker, L. Ji, F. He, Deglacial Tropical Atlantic subsurface warming links ocean circulation variability to the West African Monsoon. *Sci. Rep.* **7**, 15390 (2017). doi: 10.1038/s41598-017-15637-6; pmid: 29133905
88. P. O. Hopcroft, P. J. Valdes, Paleoclimate-conditioning reveals a North Africa land-atmosphere tipping point. *Proc. Natl. Acad. Sci. U.S.A.* **118**, e2108783118 (2021). doi: 10.1073/pnas.2108783118; pmid: 34725155
89. A. Dosio *et al*., Projected future daily characteristics of African precipitation based on global (CMIP5, CMIP6) and regional (CORDEX, CORDEX-CORE) climate models. *Clim. Dyn.* **57**, 3135–3158 (2021). doi: 10.1007/s00382-021-05859-w
90. O. Hoegh-Guldberg *et al*., "Impacts of 1.5°C Global Warming on Natural and Human Systems. In: Global Warming of 1.5°C. An IPCC Special Report on the impacts of global warming of 1.5°C above pre-industrial levels and related global greenhouse gas emission pathways, in the context of strengthening the global response to the threat of climate change, sustainable development, and efforts to eradicate poverty." V. Masson-Delmotte *et al*., Eds. (2018), pp. 175–311.
91. A. Erfanian, G. Wang, M. Yu, R. Anyah, Multimodel ensemble simulations of present and future climates over West Africa: Impacts of vegetation dynamics. *J. Adv. Model. Earth Syst.* **8**, 1411–1431 (2016). doi: 10.1002/2016MS000660
92. T. P. Hughes *et al*., Coral reefs in the Anthropocene. *Nature* **546**, 82–90 (2017). doi: 10.1038/nature22901; pmid: 28569801
93. K. Frieler *et al*., Limiting global warming to 2 °C is unlikely to save most coral reefs. *Nat. Clim. Chang.* **3**, 165–170 (2013). doi: 10.1038/nclimate1674
94. P. D. L. Ritchie, J. J. Clarke, P. M. Cox, C. Huntingford, Overshooting tipping point thresholds in a changing climate. *Nature* **592**, 517–523 (2021). doi: 10.1038/s41586-021-03263-2; pmid: 33883733
95. M. B. Osman *et al*., Globally resolved surface temperatures since the Last Glacial Maximum. *Nature* **599**, 239–244 (2021). doi: 10.1038/s41586-021-03984-4; pmid: 34759364
96. M. Meinshausen *et al*., Realization of Paris Agreement pledges may limit warming just below 2 °C. *Nature* **604**, 304–309 (2022). doi: 10.1038/s41586-022-04553-z; pmid: 35418633
97. T. Schneider, C. M. Kaul, K. G. Pressel, Possible climate transitions from breakup of stratocumulus decks under greenhouse warming. *Nat. Geosci.* **12**, 163–167 (2019). doi: 10.1038/s41561-019-0310-1
98. M. Rietkerk, R. Bastiaansen, S. Banerjee, J. Van De Koppel, Evasion of tipping in complex systems through spatial pattern formation. **374**, abj0359 (2021). doi: 10.1038/s41561-019-0310-1
99. T. M. Bury *et al*., Deep learning for early warning signals of tipping points. *Proc. Natl. Acad. Sci. U.S.A.* **118**, e2106140118 (2021). doi: 10.1073/pnas.2106140118; pmid: 34544867
100. T. M. Lenton, Early warning of climate tipping points. *Nat. Clim. Chang.* **1**, 201–209 (2011). doi: 10.1038/nclimate1143

ACKNOWLEDGMENTS

Funding: This work was initiated and supported by the European Research Council Advanced Investigator project "Earth Resilience in the Anthropocene" ERC-2016-ADG-743080 (to D.I.A.M., A.S., S.C., I.F., and J.R.). This work is part of the Earth Commission which is hosted by Future Earth and is the science component of the Global Commons Alliance. The Global Commons Alliance is a sponsored project of Rockefeller Philanthropy Advisors, with support from Oak Foundation, MAVA, Porticus, Gordon and Betty Moore Foundation, Herlin Foundation, and the Global Environment Facility. (to D.I.A.M., J.F.A., R.W., B.S., S.L., and J.R.). This work was also supported by the Leverhulme Trust RPG-2018-046 (to T.M.L. and D.I.A.M.) and the Turing Fellowship (to T.M.L.). **Author contributions:** Conceptualization: D.I.A.M., A.S., I.F., S.E.C., and T.M.L. Methodology: D.I.A.M. and T.M.L. Investigation: D.I.A.M. Validation: A.S., J.F.A., R.W., B.S., I.F., and T.M.L. Visualization: J.F.A., B.S., and S.L. Funding acquisition: J.R. Data curation: D.I.A.M. Writing – original draft: D.I.A.M. and T.M.L. Writing – review and editing: D.I.A.M., A.S., J.F.A., R.W., B.S., S.L., I.F., S.E.C., J.R., and T.M.L. **Competing interests:** The authors declare no competing financial interests. **Data and materials availability:** All data are available in the manuscript or the supplementary materials. **License information:** Copyright © 2022 the authors, some rights reserved; exclusive licensee American Association for the Advancement of Science. No claim to original US government works. https://www.sciencemag.org/about/science-licenses-journal-article-reuse

SUPPLEMENTARY MATERIALS

science.org/doi/10.1126/science.abn7950
Materials and Methods
Supplementary Text
Tables S1 to S4
References (*101*–*312*)
Data S1

Submitted 21 December 2021; accepted 27 July 2022
10.1126/science.abn7950

Downloaded from https://www.science.org at Cardiff University on September 08, 2022

Science

Exceeding 1.5°C global warming could trigger multiple climate tipping points

David I. Armstrong McKayArie StaalJesse F. AbramsRicarda WinkelmannBoris SakschewskiSina LorianiIngo FetzerSarah E. CornellJohan RockströmTimothy M. Lenton

Science, 377 (6611), eabn7950. • DOI: 10.1126/science.abn7950

Getting tipsy

Climate tipping points are conditions beyond which changes in a part of the climate system become self-perpetuating. These changes may lead to abrupt, irreversible, and dangerous impacts with serious implications for humanity. Armstrong McKay *et al*. present an updated assessment of the most important climate tipping elements and their potential tipping points, including their temperature thresholds, time scales, and impacts. Their analysis indicates that even global warming of 1°C, a threshold that we already have passed, puts us at risk by triggering some tipping points. This finding provides a compelling reason to limit additional warming as much as possible. —HJS

View the article online
https://www.science.org/doi/10.1126/science.abn7950
Permissions
https://www.science.org/help/reprints-and-permissions

Downloaded from https://www.science.org at Cardiff University on September 08, 2022

Use of this article is subject to the Terms of service

Science (ISSN) is published by the American Association for the Advancement of Science. 1200 New York Avenue NW, Washington, DC 20005. The title *Science* is a registered trademark of AAAS.
Copyright © 2022 The Authors, some rights reserved; exclusive licensee American Association for the Advancement of Science. No claim to original U.S. Government Works

Tipping elements in the Earth's climate system

Timothy M. Lenton*†, Hermann Held‡, Elmar Kriegler‡§, Jim W. Hall¶, Wolfgang Lucht‡, Stefan Rahmstorf‡, and Hans Joachim Schellnhuber†‡‖**

School of Environmental Sciences, University of East Anglia, and Tyndall Centre for Climate Change Research, Norwich NR4 7TJ, United Kingdom; ‡Potsdam Institute for Climate Impact Research, P.O. Box 60 12 03, 14412 Potsdam, Germany; §Department of Engineering and Public Policy, Carnegie Mellon University, Pittsburgh, PA 15213-3890; ¶School of Civil Engineering and Geosciences, Newcastle University, and Tyndall Centre for Climate Change Research, Newcastle NE1 7RU, United Kingdom; and ‖Environmental Change Institute, Oxford University, and Tyndall Centre for Climate Change Research, Oxford OX1 3QY, United Kingdom

**This contribution is part of the special series of Inaugural Articles by members of the National Academy of Sciences elected on May 3, 2005.

Edited by William C. Clark, Harvard University, Cambridge, MA, and approved November 21, 2007 (received for review June 8, 2007)

The term "tipping point" commonly refers to a critical threshold at which a tiny perturbation can qualitatively alter the state or development of a system. Here we introduce the term "tipping element" to describe large-scale components of the Earth system that may pass a tipping point. We critically evaluate potential policy-relevant tipping elements in the climate system under anthropogenic forcing, drawing on the pertinent literature and a recent international workshop to compile a short list, and we assess where their tipping points lie. An expert elicitation is used to help rank their sensitivity to global warming and the uncertainty about the underlying physical mechanisms. Then we explain how, in principle, early warning systems could be established to detect the proximity of some tipping points.

Earth system | tipping points | climate change | large-scale impacts | climate policy

Human activities may have the potential to push components of the Earth system past critical states into qualitatively different modes of operation, implying large-scale impacts on human and ecological systems. Examples that have received recent attention include the potential collapse of the Atlantic thermohaline circulation (THC) (1), dieback of the Amazon rainforest (2), and decay of the Greenland ice sheet (3). Such phenomena have been described as "tipping points" following the popular notion that, at a particular moment in time, a small change can have large, long-term consequences for a system, i.e., "little things can make a big difference" (4).

In discussions of global change, the term tipping point has been used to describe a variety of phenomena, including the appearance of a positive feedback, reversible phase transitions, phase transitions with hysteresis effects, and bifurcations where the transition is smooth but the future path of the system depends on the noise at a critical point. We offer a formal definition, introducing the term "tipping element" to describe subsystems of the Earth system that are at least subcontinental in scale and can be switched—under certain circumstances—into a qualitatively different state by small perturbations. The tipping point is the corresponding critical point—in forcing and a feature of the system—at which the future state of the system is qualitatively altered.

Many of the systems we consider do not yet have convincingly established tipping points. Nevertheless, increasing political demand to define and justify binding temperature targets, as well as wider societal interest in nonlinear climate changes, makes it timely to review potential tipping elements in the climate system under anthropogenic forcing (5) (Fig. 1). To this end, we organized a workshop entitled "Tipping Points in the Earth System" at the British Embassy, Berlin, which brought together 36 leading experts, and we conducted an expert elicitation that involved 52 members of the international scientific community. Here we combine a critical review of the literature with the results of the workshop to compile a short list of potential policy-relevant future tipping elements in the climate system. Results from the expert elicitation are used to rank a subset of these tipping elements in terms of their sensitivity to global warming and the associated uncertainty. Then we consider the prospects for early warning of an approaching tipping point.

Defining a Tipping Element and Its Tipping Point

Previous reviews (6–10) have defined "abrupt climate change" as occurring "when the climate system is forced to cross some threshold, triggering a transition to a new state at a rate determined by the climate system itself and faster than the cause" (8), which is a case of bifurcation (i.e., one that focuses on equilibrium properties, implying some degree of irreversibility). We have formulated a much broader definition of a tipping element, because (*i*) we wish to include nonclimatic variables; (*ii*) there may be cases where the transition is slower than the anthropogenic forcing causing it; (*iii*) there may be no abruptness, but a slight change in control may have a qualitative impact in the future; and (*iv*) for several important phase changes, state-of-the-art models differ as to whether the transition is reversible or irreversible (in principle).

We consider "components" (Σ) of the Earth system that are associated with a specific region (or collection of regions) of the globe and are at least subcontinental in scale (length scale of order $\approx$1,000 km). A full formal definition of a tipping element is given in supporting information (SI) *Appendix 1*. For the cases considered herein, a system Σ is a tipping element if the following condition is met:

1. The parameters controlling the system can be transparently combined into a single control ρ, and there exists a critical control value ρ_{crit} from which any significant variation by $\delta\rho > 0$ leads to a qualitative change ($\hat{F}$) in a crucial system feature F, after some observation time $T > 0$, measured with respect to a reference feature at the critical value, i.e.,

$$|F(\rho \geq \rho_{\mathrm{crit}} + \delta\rho|T) - F(\rho_{\mathrm{crit}}|T)| \geq \hat{F} > 0. \qquad [1]$$

This inequality applies to forcing trajectories for which a slight deviation above a critical value that continues for some time inevitably induces a qualitative change. This change may oc-

Author contributions: T.M.L., H.H., E.K., J.W.H., and H.J.S. designed research; T.M.L., H.H., E.K., J.W.H., W.L., S.R., and H.J.S. performed research; T.M.L., H.H., E.K., and J.W.H. analyzed data; and T.M.L., H.H., E.K., and H.J.S. wrote the paper.

The authors declare no conflict of interest.

This article is a PNAS Direct Submission.

Freely available online through the PNAS open access option.

†To whom correspondence may be addressed. E-mail: t.lenton@uea.ac.uk or john@pik-potsdam.de.

This article contains supporting information online at www.pnas.org/cgi/content/full/0705414105/DC1.

© 2008 by The National Academy of Sciences of the USA

Downloaded from https://www.pnas.org by 151.80.148.159 on February 21, 2023 from IP address 151.80.148.159.

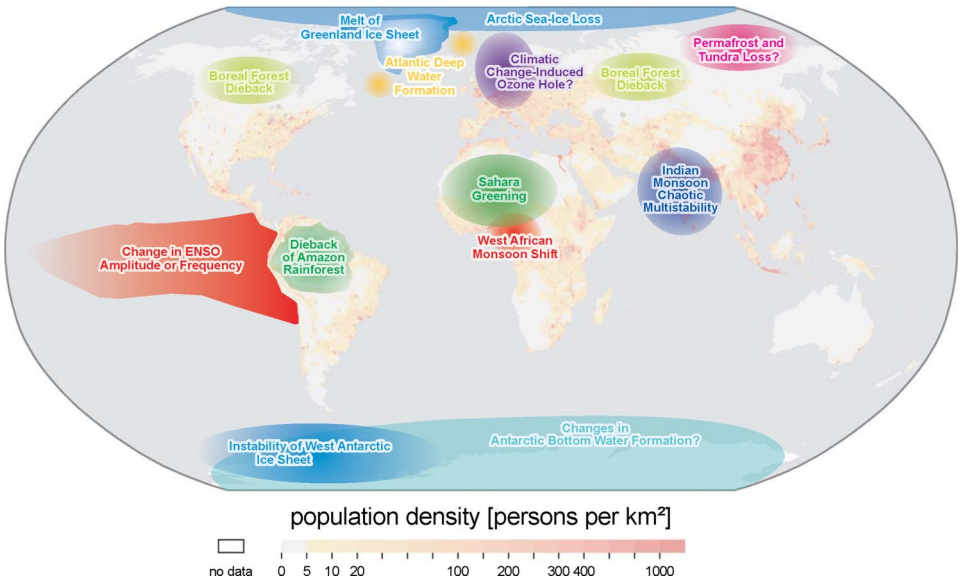

Fig. 1. Map of potential policy-relevant tipping elements in the climate system, updated from ref. 5 and overlain on global population density. Subsystems indicated could exhibit threshold-type behavior in response to anthropogenic climate forcing, where a small perturbation at a critical point qualitatively alters the future fate of the system. They could be triggered this century and would undergo a qualitative change within this millennium. We exclude from the map systems in which any threshold appears inaccessible this century (e.g., East Antarctic Ice Sheet) or the qualitative change would appear beyond this millennium (e.g., marine methane hydrates). Question marks indicate systems whose status as tipping elements is particularly uncertain.

cur immediately after the cause or much later. The definition encompasses equilibrium properties with threshold behavior as well as critical rates of forcing. In its equilibrium application, it includes all orders of phase transition and the most common bifurcations found in nature: saddle-node and Hopf bifurcations. The definition could in principle be applied at any time, e.g., in Earth's history. The feature of the system and the parameter(s) that influence it need not be climate variables. Critical conditions may be reached autonomously (without human interference), and natural variability could trigger a qualitative change.

Here we restrict ourselves to tipping elements that may be accessed by human activities and are potentially relevant to current policy. We define the subset of policy-relevant tipping elements by adding to condition 1 the following conditions:

2. Human activities are interfering with the system Σ such that decisions taken within a "political time horizon" ($T_P > 0$) can determine whether the critical value for the control ρ_{crit} is reached. This occurs at a critical time (t_{crit}) that is usually within T_P but may be later because of a commitment to further change made during T_P.
3. The time to observe a qualitative change plus the time to trigger it lie within an "ethical time horizon" (T_E); $t_{crit} + T \leq T_E$. T_E recognizes that events too far away in the future may not have the power of influencing today's decisions.
4. A significant number of people care about the fate of the component Σ, because it contributes significantly to the overall mode of operation of the Earth system (such that tipping it modifies the qualitative state of the whole system), it contributes significantly to human welfare (such that tipping it impacts on many people), or it has great value in itself as a unique feature of the biosphere. A qualitative change should correspondingly be defined in terms of impacts.

Conditions 2–4 give our definition of a policy-relevant tipping element an ethical dimension, which is inevitable because a focus on policy requires the inclusion of normative judgements. These enter in the choices of the political time horizon (T_P), the ethical time horizon (T_E), and the qualitative change that fulfills condition 4. We suggest a maximum $T_P \sim 100$ years based on the human life span and our (limited) ability to consider the world we are leaving for our grandchildren, noting also the Intergovernmental Panel on Climate Change (IPCC) focus on this timescale. We suggest $T_E \sim 1{,}000$ years based on the lifetime of civilizations, noting that this is longer than the timescale of nation states and current political entities. Thus, we focus on the consequences of decisions enacted within this century that trigger a qualitative change within this millennium, and we exclude tipping elements whose fate is decided after 2100.

In the limit $\delta\rho \to 0$, condition 1 would only include vanishing equilibria and first-order phase transitions. Instead we consider that a "small" perturbation $\delta\rho$ should not exceed the magnitude of natural variability in ρ. Considering global temperature, climate variability on interannual to millennial timescales is 0.1–0.2°C. Alternatively, a popular target is to limit anthropogenic global mean temperature increase to 2°C, and we take a "small" perturbation to be 10% of this. Either way, $\delta\rho \sim 0.2$°C seems reasonable.

One useful way of classifying tipping elements is in terms of the time, T, over which a qualitative change is observed: (*i*) rapid, abrupt, or spasmodic tipping occurs if the observation time is very small compared with T_P (but $T \neq 0$); (*ii*) gradual or episodic tipping occurs if the observation time is intermediate (e.g., of order T_P); and (*iii*) slow or asymptotic tipping occurs if the observation time is very long (in particular, $T \to T_E$).

Several key questions arise. What are the potential policy-relevant tipping elements of the Earth system? And for each: What is the mechanism of tipping? What is the key feature F of interest? What are the parameter(s) projecting onto the control ρ, and their value(s) near ρ_{crit}? How long is the transition time T? What are the associated uncertainties?

Policy-Relevant Tipping Elements in the Climate System

Earth's history provides evidence of nonlinear switches in state or modes of variability of components of the climate system (6–10). Such past transitions may highlight potential tipping elements under anthropogenic forcing, but the boundary conditions under which they occurred were different from today, and anthropogenic forcing is generally more rapid and often different in pattern (11). Therefore, locating potential future tipping points requires some use of predictive models, in combination with paleodata and/or historical data.

Here we focus on policy-relevant potential future tipping elements in the climate system. We considered a long list of candidates (Fig. 1, Table 1), and from literature review and the aforementioned workshop, we identified a short list of candidates that meet conditions 1–4 (top nine rows in Table 1). To meet condition 1, there needed to be some theoretical basis (>1 model study) for expecting a system to exhibit a critical threshold

Downloaded from https://www.pnas.org by 151.80.148.159 on February 21, 2023 from IP address 151.80.148.159.

Table 1. Policy-relevant potential future tipping elements in the climate system and (below the empty line) candidates that we considered but failed to make the short list*

Tipping element	Feature of system, F (direction of change)	Control parameter(s), ρ	Critical value(s),† ρ_{crit}	Global warming†‡	Transition timescale,† T	Key impacts
Arctic summer sea-ice	Areal extent (−)	Local ΔT_{air}, ocean heat transport	Unidentified§	+0.5–2°C	≈10 yr (rapid)	Amplified warming, ecosystem change
Greenland ice sheet (GIS)	Ice volume (−)	Local ΔT_{air}	+≈3°C	+1–2°C	>300 yr (slow)	Sea level +2–7 m
West Antarctic ice sheet (WAIS)	Ice volume (−)	Local ΔT_{air}, or less ΔT_{ocean}	+≈5–8°C	+3–5°C	>300 yr (slow)	Sea level +5 m
Atlantic thermohaline circulation (THC)	Overturning (−)	Freshwater input to N Atlantic	+0.1–0.5 Sv	+3–5°C	≈100 yr (gradual)	Regional cooling, sea level, ITCZ shift
El Niño–Southern Oscillation (ENSO)	Amplitude (+)	Thermocline depth, sharpness in EEP	Unidentified§	+3–6°C	≈100 yr (gradual)	Drought in SE Asia and elsewhere
Indian summer monsoon (ISM)	Rainfall (−)	Planetary albedo over India	0.5	N/A	≈1 yr (rapid)	Drought, decreased carrying capacity
Sahara/Sahel and West African monsoon (WAM)	Vegetation fraction (+)	Precipitation	100 mm/yr	+3–5°C	≈10 yr (rapid)	Increased carrying capacity
Amazon rainforest	Tree fraction (−)	Precipitation, dry season length	1,100 mm/yr	+3–4°C	≈50 yr (gradual)	Biodiversity loss, decreased rainfall
Boreal forest	Tree fraction (−)	Local ΔT_{air}	+≈7°C	+3–5°C	≈50 yr (gradual)	Biome switch
Antarctic Bottom Water (AABW)*	Formation (−)	Precipitation–Evaporation	+100 mm/yr	Unclear¶	≈100 yr (gradual)	Ocean circulation, carbon storage
Tundra*	Tree fraction (+)	Growing degree days above zero	Missing‖	—	≈100 yr (gradual)	Amplified warming, biome switch
Permafrost*	Volume (−)	$\Delta T_{permafrost}$	Missing‖	—	<100 yr (gradual)	CH_4 and CO_2 release
Marine methane hydrates*	Hydrate volume (−)	$\Delta T_{sediment}$	Unidentified§	Unclear¶	10^3 to 10^5 yr ($>T_E$)	Amplified global warming
Ocean anoxia*	Ocean anoxia (+)	Phosphorus input to ocean	+≈20%	Unclear¶	≈10^4 yr ($>T_E$)	Marine mass extinction
Arctic ozone*	Column depth (−)	Polar stratospheric cloud formation	195 K	Unclear¶	<1 yr (rapid)	Increased UV at surface

N, North; ITCZ, Inter-tropical Convergence Zone; EEP, East Equatorial Pacific; SE, Southeast.
*See *SI Appendix 2* for more details about the tipping elements that failed to make the short list.
†Numbers given are preliminary and derive from assessments by the experts at the workshop, aggregation of their opinions at the workshop, and review of the literature.
‡Global mean temperature change above present (1980–1999) that corresponds to critical value of control, where this can be meaningfully related to global temperature.
§Meaning theory, model results, or paleo-data suggest the existence of a critical threshold but a numerical value is lacking in the literature.
¶Meaning either a corresponding global warming range is not established or global warming is not the only or the dominant forcing.
‖Meaning no subcontinental scale critical threshold could be identified, even though a local geographical threshold may exist.

(ρ_{crit}) at a subcontinental scale, and/or past evidence of threshold behavior. Where the proposed ρ_{crit} could be meaningfully related to temperature, condition 2 was evaluated based on an "accessible neighborhood" of global temperatures from the IPCC (12) of 1.1–6.4°C above 1980–1999 that could be committed to over the next $T_P \sim 100$ years, and on recognition that transient warming is generally greater toward the poles and greater on land than in the ocean. Condition 3 was evaluated on the basis of model projections, known shortcomings of the models, and paleodata. Our collective judgement was used to evaluate condition 4.

Our short list differs from that of the IPCC (ref. 12, chapter 10, especially p. 775 ff, p. 818 ff) because our definition and criteria differ from, and are more explicit than, the IPCC notion of abrupt climate change. The evidence base we use is also slightly different because it encompasses some more recent studies. The authors of this paper and the workshop participants are a smaller group of scientists than the IPCC members, the groups are only partially overlapping, and our analysis was undertaken largely in parallel. We seek to add value to the IPCC overview by injecting a more precise definition and undertaking a complementary, in-depth evaluation.

We now discuss the entries that made our short list and seek to explain significant discrepancies from the IPCC where they arise. Those candidates that did not make the short list (and why) are discussed in *SI Appendix 2*.

Arctic Sea-Ice. As sea-ice melts, it exposes a much darker ocean surface, which absorbs more radiation–amplifying the warming. Energy-balance models suggest that this ice-albedo positive feedback can give rise to multiple stable states of sea-ice (and land snow) cover, including finite ice cap and ice-free states, with ice caps smaller than a certain size being unstable (13). This small ice-cap instability is also found in some atmospheric general circulation models (AGCMs), but it can be largely eliminated by noise due to natural variability (14). The instability is not expected to be relevant to Southern Ocean sea-ice because the Antarctic continent covers the region over which it would be expected to arise (15). Different stable states for the flow rate through the narrow outlets that drain parts of the Arctic basin have also been found in a recent model (16). For both summer and winter Arctic sea-ice, the area coverage is declining at present (with summer sea-ice declining more markedly; ref. 17), and the ice has thinned significantly over a large area. Positive ice-albedo feedback dominates external forcing in causing the thinning and shrinkage since 1988, indicating strong nonlinearity and leading some to suggest that this system may already have passed a tipping point (18), although others disagree (19). In IPCC projections with ocean-atmosphere general circulation

Downloaded from https://www.pnas.org by 151.80.148.159 on February 21, 2023 from IP address 151.80.148.159.

models (OAGCMs) (12), half of the models become ice-free in September during this century (19), at a polar temperature of −9°C (9°C above present) (20). The transition has nonlinear steps in many of the models, but a common critical threshold has yet to be identified (19). Thinning of the winter sea-ice increases the efficiency of formation of open water in summer, and abrupt retreat occurs when ocean heat transport to the Arctic increases rapidly (19). Only two IPCC models (12) exhibit a complete loss of annual sea-ice cover under extreme forcing (20). One shows a nonlinear transition to a new stable state in <10 years when polar temperature rises above −5°C (13°C above present), whereas the other shows a more linear transition. We conclude that a critical threshold for summer Arctic sea-ice loss may exist, whereas a further threshold for year-round ice loss is more uncertain and less accessible this century. Given that the IPCC models significantly underestimate the observed rate of Arctic sea-ice decline (17), a summer ice-loss threshold, if not already passed, may be very close and a transition could occur well within this century.

Greenland Ice Sheet (GIS). Ice-sheet models typically exhibit multiple stable states and nonlinear transitions between them (21). In some simulations with the GIS removed, summer melting prevents its reestablishment (22), indicating bistability, although others disagree (23). Regardless of whether there is bistability, in deglaciation, warming at the periphery lowers ice altitude, increasing surface temperature and causing a positive feedback that is expected to exhibit a critical threshold beyond which there is ongoing net mass loss and the GIS shrinks radically or eventually disappears. During the last interglacial (the Eemian), there was a 4- to 6-m higher sea level that must have come from Greenland and/or Antarctica. Increased Arctic summer insolation caused an estimated <3.5°C summertime warming of Greenland, and shrinkage of the GIS contributed an estimated 1.9–3.0 m to sea level, although a widespread ice cap remained (24). Broadly consistent with this, future projections suggest a GIS threshold for negative surface mass balance resides at ≥≈3°C local warming (above preindustrial) (3, 25). Uncertainties are such that IPCC (12) put the threshold at ≈1.9–4.6°C global warming (above preindustrial), which is clearly accessible this century. We give a closer and narrower range (above present) because amplification of warming over Greenland may be greater (26) than assumed (12, 25) because of more rapid sea-ice decline than modeled (17). Also, recent observations show the surface mass balance is declining (12) and contributing to net mass loss from the GIS (27, 28) that is accelerating (28, 29). Finally, existing ice-sheet models are unable to explain the speed of recent changes. These changes include melting and thinning of the coastal margins (30) and surging of outlet glaciers (29, 31), which may be contributed to by the intrusion of warming ocean waters (32). This is partly compensated by some mass gain in the interior (33). There is a lack of knowledge of natural GIS variability, and Greenland temperature changes have differed from the global trend (26), so interpretation of recent observations remains uncertain. If a threshold is passed, the IPCC (12) gives a >1,000-year timescale for GIS collapse. However, given the acknowledged (12) lack of processes that could accelerate collapse in current models, and their inability to simulate the rapid disappearance of continental ice at the end of the last ice age, a lower limit of 300 years is conceivable (34).

West Antarctic Ice Sheet (WAIS). Most of the WAIS is grounded below sea level and has the potential to collapse if grounding-line retreat triggers a strong positive feedback whereby ocean water undercuts the ice sheet and triggers further separation from the bedrock (35–37). The WAIS has retreated at least once during the Pleistocene (38), but the full extent of retreat is not known, nor is whether it occurred in the Eemian or the long, warm interglacial MIS-11 ≈400 ka. Approximately 1–4 m of the Eemian sea-level rise may have come from Antarctica, but some could have been from parts of the East Antarctic Ice Sheet grounded below sea level (and currently thinning at a rapid rate). WAIS collapse may be preceded by the disintegration of ice shelves and the acceleration of ice streams. Ice shelf collapse could be triggered by the intrusion of warming ocean water beneath them or by surface melting. It requires ≈5°C of local warming for surface atmospheric temperatures to exceed the melting point in summer on the major (Ross and Fischner-Ronne) ice shelves (12, 37). The threshold for ocean warming is estimated to be lower (37). The WAIS itself requires ≈8°C of local warming of the surface atmosphere at 75–80°S to reach the melting point in summer (37). Although the IPCC (12) declines to give a threshold, we estimate a range that is clearly accessible this century. Concern is raised by recent inferences from gravity measurements that the WAIS is losing mass (39), and observations that glaciers draining into the Amundsen Sea are losing 60% more ice than they are gaining and hence contributing to sea-level rise (40). They drain a region containing ≈1.3 m of a total ≈5 m of global sea-level rise contained in the WAIS. Although the timescale is highly uncertain, a qualitative WAIS change could occur within this millennium, with collapse within 300 years being a worst-case scenario. Rapid sea-level rise (>1 m per century) is more likely to come from the WAIS than from the GIS.

Atlantic Thermohaline Circulation (THC). A shutoff in North Atlantic Deep Water formation and the associated Atlantic THC can occur if sufficient freshwater (and/or heat) enters the North Atlantic to halt density-driven North Atlantic Deep Water formation (41). Such THC reorganizations play an important part in rapid climate changes recorded in Greenland during the last glacial cycle (42, 43). Hysteresis of the THC has been found in all models that have been systematically tested thus far (44), from conceptual "box" representations of the ocean (45) to OAGCMs (46). The most complex models have yet to be systematically tested because of excessive computational cost. Under sufficient North Atlantic freshwater forcing, all models exhibit a collapse of convection. In some experiments, this collapse is reversible (47) (after the forcing is removed, convection resumes), whereas in others, it is irreversible (48)—indicating bistability. In either case, a tipping point has been passed according to condition 1. The proximity of the present climate to this tipping point varies considerably between models, corresponding to an additional North Atlantic freshwater input of 0.1–0.5 Sv (44). The sensitivity of North Atlantic freshwater input to anthropogenic forcing is also poorly known, but regional precipitation is predicted to increase (12) and the GIS could contribute significantly (e.g., GIS melt over 1,000 years is equivalent to 0.1 Sv). The North Atlantic is observed to be freshening (49), and estimates of recent increases in freshwater input yield 0.014 Sv from melting sea ice (18), 0.007 Sv from Greenland (29), and 0.005 Sv from Eurasian rivers (50), totaling 0.026 Sv, without considering precipitation over the oceans or Canadian river runoff. The IPCC (12) argues that an abrupt transition of the THC is "very unlikely" (probability <10%) to occur before 2100 and that any transition is likely to take a century or more. Our definition encompasses gradual transitions that appear continuous across the tipping point; hence, some of the IPCC runs (ref. 12, p. 773 ff) may yet meet our criteria (but would need to be run for longer to see if they reach a qualitatively different state). Furthermore, the IPCC does not include freshwater runoff from GIS melt. Subsequent OAGCM simulations clearly pass a THC tipping point this century and undergo a qualitative change before the next millennium (48). Both the timescale and the magnitude of forcing are important (51), because a more rapid forcing to a given level can more readily overwhelm the negative feedback

Downloaded from https://www.pnas.org by 151.80.148.159 on February 21, 2023 from IP address 151.80.148.159.

that redistributes salt in a manner that maintains whatever is the current circulation state.

El Niño–Southern Oscillation (ENSO). Gradual anthropogenic forcing is expected, on theoretical grounds, to interact with natural modes of climate variability by altering the relative amount of time that the climate system spends in different states (52). ENSO is the most significant ocean-atmosphere mode, and its variability is controlled by (at least) three factors: zonal mean thermocline depth, thermocline sharpness in the EEP, and the strength of the annual cycle and hence the meridional temperature gradient across the equator (53, 54). Increased ocean heat uptake could cause a permanent deepening of the thermocline in the EEP and a consequent shift from present day ENSO variability to greater amplitude and/or more frequent El Niños (55). However, a contradictory theory postulates sustained La Niña conditions due to stronger warming of the West Equatorial Pacific than the East, causing enhanced easterly winds and reinforcing the up-welling of cold water in the EEP (56). The mid-Holocene had a reduction in ENSO amplitude related to a stronger zonal temperature gradient (57, 58). The globally ≈3°C warmer early Pliocene is characterized by some as having persistent El Niño conditions (59), whereas others disagree (60). Under future forcing, the first OAGCM studies showed a shift from the current ENSO variability to more persistent or frequent El Niño-like conditions. Now that numerous OAGCMs have been intercompared, there is no consistent trend in their transient response and only a small collective probability of a shift toward more persistent or frequent El Niño conditions (61, 62). However, in response to a warmer stabilized climate, the most realistic models simulate increased El Niño amplitude (with no clear change in frequency) (54). This would have large-scale impacts, and even if the transition is smooth and gradual, a tipping point may exist by condition 1. Given also that past climate changes have been accompanied by changes in ENSO, we differ from IPCC (12) and consider there to be a significant probability of a future increase in ENSO amplitude. The required warming can be accessed this century (54) with the transition happening within a millennium, but the existence and location of any threshold is particularly uncertain.

Indian Summer Monsoon (ISM). The land-to-ocean pressure gradient, which drives the monsoon circulation is reinforced by the moisture the monsoon itself carries from the adjacent Indian Ocean (moisture-advection feedback) (63). Consequently, any perturbation that tends to weaken the driving pressure gradient has the potential to destabilize the monsoon circulation. Greenhouse warming that is stronger over land and in the Northern Hemisphere tends to strengthen the monsoon, but increases in planetary albedo over the continent due to aerosol forcing and/or land-use change tend to weaken it. The ISM exhibited rapid changes in variability during the last ice age (64) and the Holocene (65), with an increased strength during recent centuries consistent with Northern Hemisphere warming (66). Recent time series display strongly nonlinear characteristics, from the intraseasonal via the interannual and the decadal to the centennial timescale (67), with the interannual variations lag correlated with the phases of ENSO, although this may be increasingly masked by anthropogenic forcing (68). A simple model (63) predicts collapse of the ISM if regional planetary albedo exceeds ≈0.5, whereas increasing CO_2 stabilizes the monsoon. IPCC projections do not show obvious threshold behavior this century (12), but they do agree that sulfate aerosols would dampen the strength of ISM precipitation, whereas increased greenhouse gases increase the interannual variability of daily precipitation (69). We differ from IPCC (12) on the basis of past apparent threshold behavior of the ISM and because brown haze and land-use-change forcing are poorly captured in the models. Furthermore, conceptual work on the potentially chaotic nature of the ISM (70) has been developed (V. Petoukhov, K. Zickfeld, and H.J.S., unpublished work) to suggest that under some plausible decadal-scale scenarios of land use and greenhouse gas and aerosol forcing, switches occur between two highly nonlinear metastable regimes of the chaotic oscillations corresponding to the "active" and "weak" monsoon phases, on the intraseasonal and interannual timescales. Sporadic bifurcation transitions may also happen from regimes of chaotic oscillations to regimes with highly deterministic oscillations, or to regimes with very weak oscillations.

Sahara/Sahel and West African Monsoon (WAM). Past greening of the Sahara occurred in the mid-Holocene (71–73) and may have happened rapidly in the earlier Bölling-Allerod warming. Collapse of vegetation in the Sahara ≈5,000 years ago occurred more rapidly than orbital forcing (71, 72). The system has been modeled and conceptualized in terms of bistable states that are maintained by vegetation–climate feedback (71, 74). However, it is intimately tied to the WAM circulation, which in turn is affected by sea surface temperatures (SSTs), particularly antisymmetric patterns between the Hemispheres. Greenhouse gas forcing is expected to increase the interhemispheric SST gradient and thereby increase Sahel rainfall; hence, the recent Sahel drought has been attributed to increased aerosol loading cooling the Northern Hemisphere (75). Future 21st century projections differ (75, 76); in two AOGCMs, the WAM collapses, but in one this leads to further drying of the Sahel, whereas in the other it causes wetting due to increased inflow from the West. The latter response is more mechanistically reasonable, but it requires a ≈3°C warming of SSTs in the Gulf of Guinea (76). A third AOGCM with the most realistic present-day WAM predicts no large trend in mean rainfall but a doubling of the number of anomalously dry years by the end of the century (76). If the WAM is disrupted such that there is increased inflow from the West (76), the resulting moisture will wet the Sahel and support greening of the Sahara, as is seen in mid-Holocene simulations (73). Indeed, in an intermediate complexity model, increasing atmospheric CO_2 has been predicted to cause future expansion of grasslands into up to 45% of the Sahara, at a rate of up to 10% of Saharan area per decade (11). In the Sahel, shrub vegetation may also increase due to increased water use efficiency (stomatal closure) under higher atmospheric CO_2 (77). Such greening of the Sahara/Sahel is a rare example of a beneficial potential tipping element.

Amazon Rainforest. A large fraction of precipitation in the Amazon basin is recycled, and, therefore, simulations of Amazon deforestation typically generate ≈20–30% reductions in precipitation (78), lengthening of the dry season, and increases in summer temperatures (79) that would make it difficult for the forest to reestablish, and suggest the system may exhibit bistability. Dieback of the Amazon rainforest has been predicted (2, 80) to occur under ≈3–4°C global warming because of a more persistent El Niño state that leads to drying over much of the Amazon basin (81). Different vegetation models driven with similar climate projections also show Amazon dieback (82), but other global climate models (83) project smaller reductions (or increases) of precipitation and, therefore, do not produce dieback (84). A regional climate model (85) predicts Amazon dieback due to widespread reductions in precipitation and lengthening of the dry season. Changes in fire frequency probably contribute to bistability and will be amplified by forest fragmentation due to human activity. Indeed land-use change alone could potentially bring forest cover to a critical threshold. Thus, the fate of the Amazon may be determined by a complex interplay between direct land-use change and the response of regional precipitation and ENSO to global forcing.

Downloaded from https://www.pnas.org by 151.80.148.159 on February 21, 2023 from IP address 151.80.148.159.

Boreal Forest. The boreal system exhibits a complex interplay between tree physiology, permafrost, and fire. Under climate change, increased water stress, increased peak summer heat stress causing increased mortality, vulnerability to disease and subsequent fire, as well as decreased reproduction rates could lead to large-scale dieback of the boreal forests (77, 86), with transitions to open woodlands or grasslands. In interior boreal regions, temperate tree species will remain excluded from succession due to frost damage in still very cold winters. Continental steppe grasslands will expand at the expense of boreal forest where soil moisture along the arid timberline ecotone declines further (87), amplified through concurrent increases in the frequency of fires. Newly unfrozen soils that regionally drain well, and reductions in the amount of snow, also support drying, more fire and hence less biomass. In contrast, increased thaw depth and increased water-use efficiency under elevated CO_2 will tend to increase available soil moisture, decreasing fire frequency and increasing woody biomass. Studies suggest a threshold for boreal forest dieback of ≈3°C global warming (77, 86), but limitations in existing models and physiological understanding make this highly uncertain.

Others. We remind the reader that we considered other candidate tipping elements, which are not listed here because they did not meet conditions 2–4 for policy relevance. Some are listed in Table 1 and discussed in *SI Appendix 2*.

Ranking the Threat

Given our identification of policy-relevant tipping elements in the climate system, how do we decide which pose the greatest threat to society and, therefore, need the greatest attention? The first step is to asses the sensitivity of each tipping element to global warming and the associated uncertainties, including the confidence of the community in the argument for tipping element status. Our workshop and systematic review of the literature addressed this. In addition, formal elicitations of expert beliefs have frequently been used to bring current understanding of model studies, empirical evidence, and theoretical considerations to bear on policy-relevant variables (88). From a natural science perspective, a general criticism is that expert beliefs carry subjective biases and, moreover, do not add to the body of scientific knowledge unless verified by data or theory. Nonetheless, expert elicitations, based on rigorous protocols from statistics (89–91) and risk analysis (91, 92), have proved to be a very valuable source of information in public policymaking (93). It is increasingly recognized that they can also play a valuable role for informing climate policy decisions (94). In the field of climate change, formal expert elicitations have been conducted, e.g., on climate sensitivity (95), forest ecosystems (96), the WAIS (97), radiative forcing of aerosols (98), and the THC (99).

On the basis of previous experience (99), we used the aforementioned workshop to initiate an elicitation of expert opinions on, among other things, six potential tipping elements listed in Table 1: reorganization of the Atlantic THC, melt of the GIS, disintegration of the WAIS, Amazon rainforest dieback, dieback of boreal forests, and shift of the ENSO regime to an El Niño-like mean state. The elicitation was based on a computer-based interactive questionnaire that was completed individually by participating experts. Following a pilot phase at the workshop, the questionnaire was distributed to 193 international scientists in October and November 2005; 52 experts returned a completed questionnaire (among them 16 workshop participants and 22 contributors to the IPCC Fourth Assessment Report). Although participation inevitably involved a self-selection process, we assembled a heterogeneous group covering a wide range of expertise (see *SI Appendix 3*). The full results will be presented separately (E.K., J.W.H., H.H., R. Dawson, and H.J.S., unpublished work). Here we report a subset that reflect the range of scientific perspectives to supplement our own assessment of the tipping elements.

In the questionnaire, experts were asked for a pairwise comparison of tipping elements in terms of (*i*) their sensitivity to global mean temperature increase and (*ii*) the uncertainty about the underlying physical mechanisms. The exact questions posed to participants and the breakdown of their responses are described in *SI Appendix 3*. We have identified partial rankings of tipping elements from the collection of expert responses. Because the number of experts commenting on individual pairs of tipping elements varied widely, those rankings could not be established with equal credibility. We highlight the difference in expert consensus by using the symbols ≫ and > for strong and weak consensus upon the ordering, respectively, and by providing the number x that agreed with the direction of the ordering compared with the number y of experts who commented on the pair [given as $x(y)$]. For sensitivity to global mean warming, we find

$$\text{GIS} \;\overset{8(10)\ \text{to WAIS}}{\underset{7(7)\ \text{to THC}}{\gg}}\; \text{WAIS} \;\overset{2(3)}{>}\; \begin{matrix}\text{Amazon rainforest} \\ \\ \text{THC}\end{matrix} \;\overset{}{>}\; \text{THC},$$
$$\text{Amazon rainforest} \;\overset{}{>}\; \text{THC},$$

where the more sensitive tipping element is to the left. Owing to the close link between ENSO and the Amazon rainforest, both were judged of similar sensitivity to warming, but experts were divided as to whether ENSO would be more sensitive than the THC. Boreal forests were only compared with the Amazon rainforest, and three out of five experts judged the former to be more sensitive to global mean warming. Concerning the uncertainty about the physical mechanisms that may give rise to tipping points, we find

$$\begin{matrix}\text{WAIS} \\ \\ \text{Amazon rainforest} \\ \\ \text{ENSO}\end{matrix} \;\overset{\begin{matrix}3(4)\ \text{to THC} \\ \gg \\ 6(9)\ \text{to GIS}\end{matrix}}{\overset{\begin{matrix}2(2)\ \text{to THC} \\ > \\ 1(1)\ \text{to GIS}\end{matrix}}{\overset{\begin{matrix}3{+}2(6)\ \text{to THC} \\ \geq \\ 2(2)\ \text{to GIS}\end{matrix}}{}}}\; \text{THC} \;\overset{6(8)}{\gg}\; \text{GIS},$$

where the more uncertain tipping element is to the left. We display a greater or equal uncertainty about the ENSO compared with the THC, because three and two out of six experts believed the ENSO to be more and similarly uncertain, respectively. In addition, five out of six experts judged the uncertainty about the response of boreal forests to be larger than for the Amazon rainforest.

Taking into account our own analysis of the literature (summarized in the previous section and Table 1) and the expert elicitation (summarized above), the potential tipping elements in the climate system may be grouped into three clusters: (*i*) high sensitivity with smallest uncertainty: GIS and Arctic sea-ice; (*ii*) intermediate sensitivity with largest uncertainty: WAIS, Boreal forest, Amazon rainforest, ENSO, and WAM; (*iii*) low sensitivity with intermediate uncertainty: THC. ISM is not included in the clustering because its forcing differs, but it clearly has large uncertainty. We conclude that the greatest (and clearest) threat

Downloaded from https://www.pnas.org by 151.80.148.159 on February 21, 2023 from IP address 151.80.148.159.

is to the Arctic with summer sea-ice loss likely to occur long before (and potentially contribute to) GIS melt. Tipping elements in the tropics, the boreal zone, and West Antarctica are surrounded by large uncertainty and, given their potential sensitivity, constitute candidates for surprising society. The archetypal example of a tipping element, the THC appears to be a less immediate threat, but the long-term fate of the THC under significant warming remains a source of concern (99).

The Prospects for Early Warning

Establishing early warning systems for various tipping elements would clearly be desirable, but can ρ_{crit} be anticipated before we reach it? In principle, an incipient bifurcation in a dynamical system could be anticipated (100), by looking at the spectral properties of time series data (101), in particular, extracting the longest system-immanent timescale (τ) from the response of the system to natural variability (102). Systems theory reveals (Fig. 2*A*) (*i*) that those tipping points that represent a bifurcation are universally characterized by $\tau \to \infty$ at the threshold, and (*ii*) that in principle τ could be reconstructed through methods of time series analysis. Hence a "degenerate fingerprinting" method has been developed for anticipating a threshold in a spatially extended system and applied to the detection of a threshold in the Atlantic THC, by using time series output from a model of intermediate complexity (102) (Fig. 2*B*).

These studies reveal that if a system is forced slowly (keeping it in quasi-equilibrium), proximity to a threshold may be inferred in a model-independent way. However, if the system is forced faster (as is probably the case for the THC today), a dynamical model will also be needed. Even if there is no bifurcation, determining τ is still worthwhile because it determines the system's linear response characteristics to external forcing, and transitions that are not strictly bifurcations are expected to resemble bifurcation-type behavior to a certain degree. For strongly resource-limited ecosystems that show self-organized patchiness, their observable macrostructure may also provide an indication of their proximity to state changes (103).

If a forewarning system for approaching thresholds is to become workable, then real-time observation systems need to be improved (e.g., building on the Atlantic THC monitoring at 26.5°N). For slow transition systems, notably ocean and ice sheets, observation records also need to be extended further back in time (e.g., for the Atlantic beyond the ≈150-year SST record). Analysis of extended time series data could then be used to improve models (104), e.g., an effort to determine the Atlantic's τ and assimilate it into ocean models could reduce the vast intra- and intermodel (44) spread regarding the proximity to a tipping point (102).

Conclusion

Society may be lulled into a false sense of security by smooth projections of global change. Our synthesis of present knowledge suggests that a variety of tipping elements could reach their critical point within this century under anthropogenic climate change. The greatest threats are tipping the Arctic sea-ice and the Greenland ice sheet, and at least five other elements could surprise us by exhibiting a nearby tipping point. This knowledge should influence climate policy, but a full assessment of policy relevance would require that, for each potential tipping element, we answer the following questions: Mitigation: Can we stay clear of ρ_{crit}? Adaptation: Can $\hat{F}$ be tolerated?

The IPCC provides a thorough overview of mitigation (105) and adaptation (106) work upon which such a policy assessment of tipping elements could be built. Given the scale of potential impacts from tipping elements, we anticipate that they will shift the balance toward stronger mitigation and demand adaptation concepts beyond incremental approaches (107, 108). Policy analysis and implementation will be extremely challenging given the nonconvexities in the human-environment system (109) that will be enhanced by tipping elements, as well as the need to handle intergenerational justice and interpersonal equity over long periods and under conditions of uncertainty (110). A rigorous study of potential tipping elements in human socioeconomic systems would also be welcome, especially to address whether and how a rapid societal transition toward sustainability could be triggered, given that some models suggest there exists a tipping point for the transition to a low-carbon-energy system (111).

It seems wise to assume that we have not yet identified all potential policy-relevant tipping elements. Hence, a systematic search for further tipping elements should be undertaken, drawing on both paleodata and multimodel ensemble studies. Given the large uncertainty that remains about tipping ele-

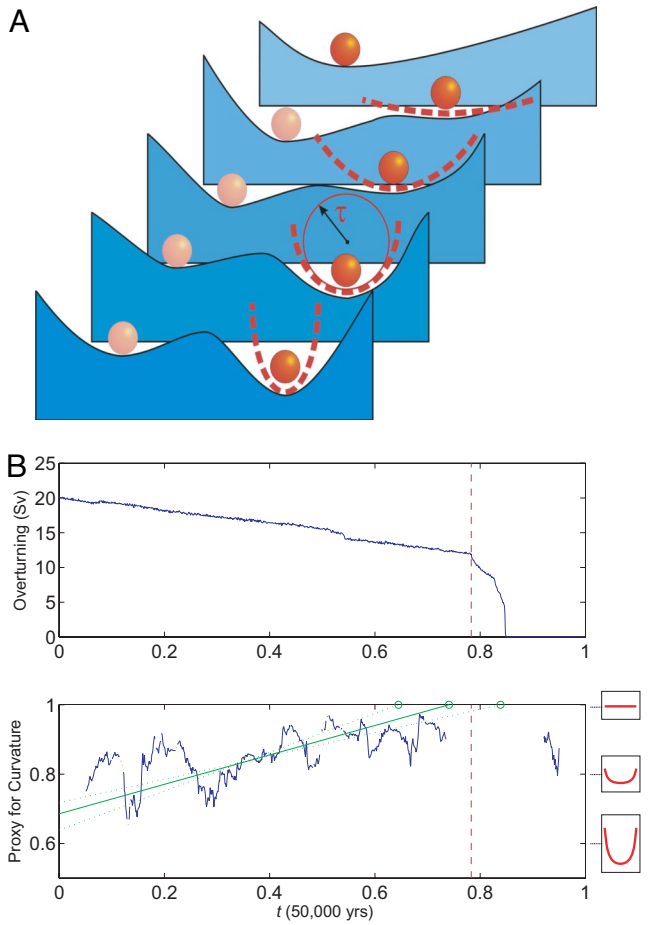

Fig. 2. Method for estimating the proximity to a tipping point. (*A*) Schematic approach: The potential wells represent stable attractors, and the ball, the state of the system. Under gradual anthropogenic forcing (progressing from dark to light blue potential), the right potential well becomes shallower and finally vanishes (threshold), causing the ball to abruptly roll to the left. The curvature of the well is inversely proportional to the system's response time τ to small perturbations. "Degenerate fingerprinting" (102) extracts τ from the system's noisy, multivariate time series and forecasts the vanishing of local curvature. (*B*) Degenerate fingerprinting "in action": Shown is an example for the Atlantic meridional overturning circulation. (*Upper*) Overturning strength under a 4-fold linear increase of atmospheric CO_2 over 50,000 years in the CLIMBER-2 model with weak, stochastic freshwater forcing. Eventually, the circulation collapses without early warning. (*Lower*) Overturning replaced by a proxy of the shape of the potential (as in *A*). Although the signal is noisier in *Lower* than it is in *Upper*, it allows forecasting of the location of the threshold (data taken from ref. 102). The solid green line is a linear fit, and the dashed green lines are 95% error bars.

Downloaded from https://www.pnas.org by 151.80.148.159 on February 21, 2023 from IP address 151.80.148.159.

ments, there is an urgent need to improve our understanding of the underlying physical mechanisms determining their behavior, so that policy makers are able "to avoid the unmanageable, and to manage the unavoidable" (112).

ACKNOWLEDGMENTS. We thank the British Embassy in Berlin for hosting the workshop "Tipping Points in the Earth System" on October 5–6, 2005, and all of the participants of the workshop and the expert elicitation. M. Wodinski prepared Fig. 1. We thank O. Edenhofer, V. Petoukhov, the editor W. C. Clark, and four anonymous referees for their suggestions that improved the paper. T.M.L.'s work is part of the Natural Environment Research Council GENIEfy (NE/C515904), Quaternary QUEST (NE/D001706), and Feedbacks QUEST (NE/F001657) projects. H.H. was supported by the Volkswagen Foundation under Grant II/78470. E.K. is supported by a Marie Curie International Fellowship (MOIF-CT-2005–008758) within the 6th European Community Framework Program, with research infrastructure partly provided by the Climate Decision Making Center (National Science Foundation Grant SES-0345798). W.L.'s work is a contribution to the Leibniz Association's project on the Biosphere, Society and Global Change. H.J.S. is a Senior James Martin Fellow at Oxford University.

1. Rahmstorf S, Ganopolski A (1999) *Clim Change* 43:353–367.
2. Cox PM, Betts RA, Jones CD, Spall SA, Totterdell IJ (2000) *Nature* 408:184–187.
3. Huybrechts P, De Wolde J (1999) *J Clim* 12:2169–2188.
4. Gladwell M (2000) *The Tipping Point*: *How Little Things Can Make a Big Difference* (Little Brown, New York).
5. Schellnhuber H-J, Held H (2002) in *Managing the Earth: The Eleventh Linacre Lectures*, eds Briden J, Downing T (Oxford Univ Press, Oxford), pp 5–34.
6. Rahmstorf S (2001) in *Encyclopedia of Ocean Sciences*, eds Steele J, Thorpe S, Turekian K (Academic, London), pp 1–6.
7. Lockwood JG (2001) *Int J Climatol* 21:1153–1179.
8. National Research Council (2002) *Abrupt Climate Change: Inevitable Surprises* (Natl Acad Press, Washington, DC).
9. Alley RB, Marotzke J, Nordhaus WD, Overpeck JT, Peteet DM, Pielke RA, Pierrehumbert RT, Rhines PB, Stocker TF, Talley LD, Wallace JM (2003) *Science* 299:2005–2010.
10. Rial JA, Pielke RA, Beniston M, Claussen M, Canadel J, Cox P, Held H, De Noblet-Ducoudre N, Prinn R, Reynolds JF, Salas JD (2004) *Clim Change* 65:11–38.
11. Claussen M, Brovkin V, Ganopolski A, Kubatzki C, Petoukhov V (2003) *Clim Change* 57:99–118.
12. IPCC (2007) *Climate Change 2007: The Physical Science Basis. Contribution of Working Group I to the Fourth Assessment Report of the Intergovernmental Panel on Climate Change*, eds Solomon S, Qin D, Manning M, Chen Z, Marquis M, Averyt KB, Tignor M, Miller HL (Cambridge Univ Press, Cambridge, UK).
13. North GR (1984) *J Atmos Sci* 41:3390–3395.
14. Lee W-H, North GR (1995) *Clim Dyn* 11:242–246.
15. Morales Maqueda MA, Willmott AJ, Bamber JL, Darby MS (1998) *Clim Dyn* 14:329–352.
16. Hibler WD, Hutchings JK, Ip CF (2006) *Ann Glaciol* 44:339–344.
17. Stroeve J, Holland MM, Meier W, Scambos T, Serreze M (2007) *Geophys Res Lett* 34:L09501.
18. Lindsay RW, Zhang J (2005) *J Clim* 18:4879–4894.
19. Holland MM (2006) *Geophys Res Lett* 33:L23503.
20. Winton M (2006) *Geophys Res Lett* 33:L23504.
21. Saltzman B (2002) *Dynamical Paleoclimatology* (Academic, London).
22. Toniazzo T, Gregory JM, Huybrechts P (2004) *J Clim* 17:21–33.
23. Lunt DJ, De Noblet-Ducoudre N, Charbit S (2004) *Clim Dyn* 23:679–694.
24. Otto-Bliesner BL, Marshall SJ, Overpeck JT, Miller GH, Hu A, CAPE Last Interglacial Project Members (2006) *Science* 311:1751–1753.
25. Gregory JM, Huybrechts P (2006) *Philos Trans R Soc A* 364:1709–1731.
26. Chylek P, Lohmann U (2005) *Geophys Res Lett* 32:L14705.
27. Mitrovica JX, Tamislea ME, Davis JL, Milne GA (2001) *Nature* 409:1026–1029.
28. Velicogna I, Wahr J (2006) *Nature* 443:329–331.
29. Rignot E, Kanagaratnam P (2006) *Science* 311:986–990.
30. Krabill W, Abdalati W, Frederick E, Manizade S, Martin C, Sonntag J, Swift R, Thomas R, Wright W, Yungel J (2000) *Science* 289:428–430.
31. Joughin I, Abdalati W, Fahnestock M (2004) *Nature* 432:608–610.
32. Bindschadler R (2006) *Science* 311:1720–1721.
33. Johannessen OM, Khvorostovsky K, Miles MW, Bobylev LP (2005) *Science* 310:1013–1016.
34. Hansen JE (2005) *Clim Change* 68:269–279.
35. Mercer JH (1978) *Nature* 271:321–325.
36. Oppenheimer M (1998) *Nature* 393:325–332.
37. Oppenheimer M, Alley RB (2004) *Clim Change* 64:1–10.
38. Scherer RP, Aldahan A, Tulaczyk S, Possnert G, Engelhardt H, Kamb B (1998) *Science* 281:82–85.
39. Velicogna I, Wahr J (2006) *Science* 311:1754–1756.
40. Thomas R, Rignot E, Casassa G, Kanagaratnam P, Acuña C, Akins T, Brecher H, Frederick E, Gogineni P, Krabill W, *et al.* (2004) *Science* 306:255–258.
41. Stocker TF, Wright DG (1991) *Nature* 351:729–732.
42. Rahmstorf S (2002) *Nature* 419:207–214.
43. Ganopolski A, Rahmstorf S (2001) *Nature* 409:153–158.
44. Rahmstorf S, Crucifix M, Ganopolski A, Goosse H, Kamenkovich I, Knutti R, Lohmann G, Marsh R, Mysak LA, Wang Z, Weaver AJ (2005) *Geophys Res Lett* 32:L23605.
45. Stommel H (1961) *Tellus* 13:224–230.
46. Lenton TM, Marsh R, Price AR, Lunt DJ, Aksenov Y, Annan JD, Cooper-Chadwick T, Cox SJ, Edwards NR, Goswami S, *et al.* (2007) *Clim Dyn* 29:591–613.
47. Vellinga M, Wood RA (2002) *Clim Change* 54:251–267.
48. Mikolajewicz U, Gröger M, Maier-Reimer E, Schurgers G, Vizcaíno M, Winguth AME (2007) *Clim Dyn* 28:599–633.
49. Curry R, Dickson B, Yashayaev I (2003) *Nature* 426:826–829.
50. Peterson BJ, Holmes RM, McClelland JW, Vörösmarty CJ, Lammers RB, Shiklomanov AI, Shiklomanov IA, Rahmstorf S (2002) *Science* 298:2171–2173.
51. Stocker TF, Schmittner A (1997) *Nature* 388:862–865.
52. Palmer TN (1999) *J Clim* 12:575–591.
53. Philander SG, Federov A (2003) *Annu Rev Earth Planet Sci* 31:579–594.
54. Guilyardi E (2006) *Clim Dyn* 26:329–348.
55. Timmermann A, Oberhuber J, Bacher A, Esch M, Latif M, Roeckner E (1999) *Nature* 398:694–697.
56. Cane MA, Clement AC, Kaplan A, Kushnir Y, Pozdnyakov D, Seager R, Zebiak SE, Murtugudde R (1997) *Science* 275:957–960.
57. Brown J, Collins M, Tudhope A (2006) *Adv Geosci* 6:29–33.
58. Koutavas A, deMenocal PB, Olive GC, Lynch-Stieglitz J (2006) *Geology* 34:993–996.
59. Wara MW, Ravelo AC, Delaney ML (2005) *Science* 309:758–761.
60. Rickaby REM, Halloran P (2005) *Science* 307:1948–1952.
61. Collins M, Groups TCM (2005) *Clim Dyn* 24:89–104.
62. van Oldenborgh GJ, Philip SY, Collins M (2005) *Ocean Sci* 1:81–95.
63. Zickfeld K, Knopf B, Petoukhov V, Schellnhuber HJ (2005) *Geophys Res Lett* 32:L15707.
64. Burns SJ, Fleitmann D, Matter A, Kramers J, Al-Subbary AA (2003) *Science* 301:1365–1367.
65. Gupta AK, Anderson DM, Overpeck JT (2003) *Nature* 431:354–357.
66. Anderson DM, Overpeck JT, Gupta AK (2002) *Science* 297:596–599.
67. Webster PJ, Magaña VO, Palmer TN, Shukla J, Tomas RA, Yanai M, Yasunari T (1998) *J Geophys Res* 103:14451–14510.
68. Meehl GA, Arblaster JM (2003) *Clim Dyn* 21:659–675.
69. Lal M, Cubasch U, Voss R, Waszkewitz J (1995) *Curr Sci India* 69:752–763.
70. Mittal AK, Dwivedi S, Pandey AC (2003) *Indian J Radio Space Phys* 32:209–216.
71. Claussen M, Kubatzki C, Brovkin V, Ganopolski A, Hoelzmann P, Pachur H-J (1999) *Geophys Res Lett* 26:2037–2040.
72. de Menocal P, Oritz J, Guilderson T, Adkins J, Sarnthein M, Baker L, Yarusinsky M (2000) *Quat Sci Rev* 19:347–361.
73. Patricola CM, Cook KH (2007) *J Clim* 20:694–716.
74. Brovkin V, Claussen M, Petoukhov V, Ganopolski A (1998) *J Geophys Res* 103:31613–31624.
75. Held IM, Delworth TL, Lu J, Findell KL, Knutson TR (2005) *Proc Natl Acad Sci USA* 102:17891–17896.
76. Cook KH, Vizy EK (2006) *J Clim* 19:3681–3703.
77. Lucht W, Schaphoff S, Erbrecht T, Heyder U, Cramer W (2006) *Carbon Balance Manage* 1:6.
78. Zeng N, Dickinson RE, Zeng X (1996) *J Clim* 9:859–883.
79. Kleidon A, Heimann M (2000) *Clim Dyn* 16:183–199.
80. Cox PM, Betts RA, Collins M, Harris PP, Huntingford C, Jones CD (2004) *Theor Appl Climatol* 78:137–156.
81. Betts RA, Cox PN, Collins M, Harris PP, Huntingford C, Jones CD (2004) *Theor Appl Climatol* 78:157–175.
82. White A, Cannell MGR, Friend AD (1999) *Global Environ Change* 9:S21–S30.
83. Li W, Fu R, Dickinson RE (2006) *J Geophys Res* 111:D02111.
84. Schaphoff S, Lucht W, Gerten D, Sitch S, Cramer W, Prentice IC (2006) *Clim Change* 74:97–122.
85. Cook KH, Vizy EK (2008) *J Clim*, in press.
86. Joos F, Prentice IC, Sitch S, Meyer R, Hooss G, Plattner G-K, Gerber S, Hasselmann K (2001) *Global Biogeochem Cycles* 15:891–907.
87. Hogg EH, Schwarz AG (1997) *J Biogeogr* 24:527–534.
88. Morgan MG, Henrion M (1990) *Uncertainty: A Guide to Dealing with Uncertainty in Quantitative Risk and Policy Analysis* (Cambridge Univ Press, New York).
89. Kadane JB, Wolfson LJ (1998) *J R Stat Soc Ser D* 47:3–17.
90. O'Hagan A (1998) *J R Stat Soc Ser D* 47:21–35.
91. Cooke RM (1991) *Experts in Uncertainty* (Oxford Univ Press, Oxford).
92. Apostolakis G (1990) *Science* 250:1359–1364.
93. National Research Council (2002) *Estimating the Public Health Benefits of Proposed Air Pollution Regulations* (Natl Acad Press, Washington, DC).
94. Oppenheimer M, O'Neill BC, Webster M, Agrawala S (2007) *Science* 317:1505–1506.
95. Morgan MG, Keith DW (1995) *Environ Sci Technol* 29:468–476.
96. Morgan MG, Pitelka LF, Shevliakova E (2001) *Clim Change* 49:279–307.
97. Vaughan DG, Spouge JR (2002) *Clim Change* 53:65–91.
98. Morgan MG, Adams PJ, Keith DW (2006) *Clim Change* 75:195–214.
99. Zickfeld K, Levermann A, Morgan MG, Kuhlbrodt T, Rahmstorf S, Keith DW (2007) *Clim Change* 82:235–265.
100. Wiesenfeld K (1985) *Phys Rev A* 32:1744–1751.
101. Kleinen T, Held H, Petschel-Held G (2003) *Ocean Dyn* 53:53–63.
102. Held H, Kleinen T (2004) *Geophys Res Lett* 31:L23207.
103. Rietkerk M, Dekker SC, de Ruiter PC, van de Koppel J (2004) *Science* 305:1926–1929.
104. Schmittner A, Latif M, Schneider B (2005) *Geophys Res Lett* 32:L23710.
105. IPCC (2007) *Climate Change 2007: Mitigation of Climate Change. Contribution of Working Group III to the Fourth Assessment Report of the Intergovernmental Panel on Climate Change*, eds Metz B, Davidson OR, Bosch PR, Dave R, Meyer LA (Cambridge Univ Press, Cambridge, UK).
106. IPCC (2007) *Climate Change 2007: Impacts, Adaptation and Vulnerability. Contribution of Working Group II to the Fourth Assessment Report of the Intergovernmental Panel on Climate Change*, eds Parry ML, Canziani OF, Palutikof JP, van der Linden PJ, Hanson CE (Cambridge Univ Press, Cambridge, UK).
107. Janssen MA, Ostrom E (2006) *Global Environ Change* 16:237–239.
108. Eakin H, Luers AL (2006) *Annu Rev Environ Resour* 31:365–394.
109. Dasgupta P, Mäler K-G (2003) *Environ Resour Econ* 26:499–525.
110. Dasgupta P (2008) *Rev Environ Econ Policy*, in press.
111. Edenhofer O, Lessman K, Kemfert C, Grubb M, Köhler J (2006) *Energy J: Special Issue on Endogenous Technological Change and the Economics of Atmospheric Stabilisation* Special Issue 1:57–108.
112. Scientific Expert Group on Climate Change (2007) *Confronting Climate Change: Avoiding the Unmanageable and Managing the Unavoidable*, Report prepared for the United Nations Commission on Sustainable Development, eds Bierbaum RM, Holdren JP, MacCracken MC, Moss RH, Raven PH (Sigma Xi, Research Triangle Park, NC, and United Nations Foundation, Washington, DC).

Downloaded from https://www.pnas.org by 151.80.148.159 on February 21, 2023 from IP address 151.80.148.159.

CALIFORNIA
TAHOE
CONSERVANCY

May 19, 2022

John Hitchcock
Planning Manager
Development Services Department
1053 Tata Lane
South Lake Tahoe, CA 96150

Re: Proposed Tourist Core Area Plan/Specific Plan Amendment Initial Study/Mitigated Negative Declaration and Initial Environmental Checklist/Finding of No Significant Impact

BOARD MEMBERS

NATURAL RESOURCES AGENCY
Wade Crowfoot, Secretary

DEPARTMENT OF FINANCE
Keely Bosler, Director
Gayle Miller, Designee

SENATE PUBLIC MEMBER
Jay Hansen

ASSEMBLY PUBLIC MEMBER
Adam Acosta

CITY OF SOUTH LAKE TAHOE
Tamara Wallace

EL DORADO COUNTY
Sue Novasel, Chair

PLACER COUNTY
Cindy Gustafson, Vice Chair

U.S. FOREST SERVICE (ex-officio)
Erick Walker

VACANT
Executive Director

JANE FREEMAN
Deputy Director

Dear Mr. Hitchcock,

On behalf of the California Tahoe Conservancy (Conservancy), we appreciate the opportunity to provide comments on the City of South Lake Tahoe's (City) proposed Tourist Core Area Plan/Specific Plan Amendment (amendment) Initial Study/Mitigated Negative Declaration and Initial Environmental Checklist/Finding of No Significant Effect (IS/MND). Our agency jointly manages Van Sickle Bi-State Park (Park) with Nevada Division of State Parks (NDSP). The Conservancy believes the Park will be negatively impacted by the rezoning of El Dorado County Assessment Number (AN) 029-240-011 from recreation to tourist center mixed use and the associated 10-unit housing project (housing project) analyzed in the IS/MND. In addition, we are concerned that possible actions associated with the housing project on the adjacent private parcel (AN 029-441-003) (private parcel) that is at the entrance to the Park could impact the Park and visitor experience.

The Conservancy provided comments during the scoping period concerning impacts to the historic character and natural aesthetic of the Park entrance; increased vehicle traffic and pedestrian safety; and management issues related to new user trails, personal storage, parking, and trash resulting from the proposed amendment and housing project. The Conservancy appreciates the IS/MND modifications made by the City in response to our comments including removal of the private parcel from the amendment and inclusion of the six-foot tall rod iron fence as mitigation. However, we believe the amendment and associated housing project still have potential negative impacts to the Park.

We are writing to describe these potential issues and request the City modify the IS/MND and housing project to address our concerns. Our primary concern is that the City inadequately analyzes potential environmental impacts to the Park in the IS/MND, and does not sufficiently

mitigate the environmental impacts caused by the proposed amendment and housing project.

1. In section 5.4.3 Aesthetics, the City fails to consider the potential environmental impacts of the amendment and housing project to the Park. The housing project as proposed is visible from the Park and will degrade the welcoming historic character and natural aesthetic of the Park. The Conservancy and NDSP specifically designed the Park to promote pedestrian access and highlight the forested and natural appeal of the area. The housing project will remove mature trees and replace them with newly constructed buildings and parking lots. The resulting change may diminish the Park's aesthetic appeal and reduce visitors' experience.

2. In section 5.4.6 Biological Resources, the City does not adequately consider impacts to riparian habitat. The removal of the previous development required restoration of the stream environment zone (SEZ) on this site. The SEZ connects to a portion of the Park. A fully restored and functioning SEZ could provide treatment of run-off that improves lake clarity and vegetative screening for the housing project. However, the restoration in 2009 did not result in a fully functioning SEZ and additional restoration and monitoring efforts are needed.

Given the potential environmental impacts highlighted above, the Conservancy believes the City should apply appropriate measures to avoid or mitigate the impacts. The Conservancy requests onsite mitigation measures for the housing project for each of the resource areas. The mitigation measures should include installing vegetative screening around buildings and parking lots and enhancing SEZ restoration and vegetation.

In addition, the Conservancy is concerned the developer could utilize the recreation zoning of the private parcel for future development that impacts the viewshed, biological resources, and SEZ bordering the Park. The Conservancy requests the City takes steps to limit future development on the private parcel as a mitigation measure of the amendment. The Conservancy foresees a combination of four mitigation measures to accomplish this:

1. Rezone the private parcel from recreation to open space;
2. Deed restrict the private parcel from any future development;
3. Relinquish the reservation to "the Lane Access Easement", recorded on September 16th, 2009 and found in the official records of El Dorado County as document number 20090047163; and,
4. Acquire the entire private parcel or the portion containing Park improvements for appraised market value.

The private parcel contains SEZ and undeveloped land serving as a partial viewshed buffer of the housing project from the east side of the project at the entrance to the Park. The Conservancy believes mitigation measures, including open space zoning, deed restrictions, relinquishment of reservation, or acquisition of the parcel will ensure the

existing screening of the housing project remains and potential future uses will not impact existing SEZ and biological resources bordering the Park.

Additionally, the relinquishment of the reservation described in number three above ensures public safety and vehicle traffic concerns raised in the scoping period are mitigated. The easement reservation allows the developer to use the Park entrance to access development on the private parcel, which would cross a pedestrian access trail. This creates a conflict and safety concerns for pedestrians. In addition, vehicular access to the Park is closed from sunset to sunrise during the summer and from November 1 to May 1 during the winter. The Conservancy manages the entrance by opening and closing the gate at the designated times. Private access through the Park entrance will make it more difficult for the Conservancy to effectively do so.

The above listed mitigation measures are not exhaustive and the Conservancy requests to be involved in negotiating what final mitigation measures will be included and implemented. The Conservancy requests all mitigation measures be specific and enforceable in this IS/MND.

In summary, we appreciate the opportunity to comment on the IS/MND. We believe that the proposed amendment and housing project have the potential to negatively impact the Park as detailed above. We look forward to further discussing with the City how these issues will be addressed in the IS/MND and considered in the planning and implementation of the proposed amendment and housing project. Please follow-up with Mr. Nick Meyer, nick.meyer@tahoe.ca.gov or (530) 543-6073, with any questions or concerns.

Sincerely,

Jane Freeman

Jane Freeman
Deputy Director

Cc: Janice Keillor, Deputy Administrator, Nevada Division of State Parks
Allen Wooldridge, Tahoe Region Manager, Nevada Division of State Parks
Brett Hartley, Van Sickle Ranger, Nevada Division of State Parks

KEEP TAHOE BLUE
League to Save Lake Tahoe

advocate | engage | create

May 19, 2022

City of South Lake Tahoe
John Hitchcock, Planning Manager
1052 Tata Lane
South Lake Tahoe, CA 96150
Phone: (530) 542-7472
Email: jhitchcock@cityofslt.us

Tahoe Regional Planning Agency
Jennifer Self, Principal Planner
P.O. Box 5310
Stateline, NV 89449
Phone: (775) 589-5221
Email: jself@trpa.gov

Re: Initial Study/Mitigated Negative Declaration (IS/MND) for the proposed Tourist Core Area Plan (TCAP) amendments

Dear Mr. Hitchcock and Ms. Self,

As a member of the 2012 Regional Plan Update (RPU) Bi-State Working Group, the League to Save Lake Tahoe (League) appreciates the opportunity to continue to work with the Tahoe Regional Planning Agency (TRPA) and the City of South Lake Tahoe (City) to implement the RPU. Effective implementation of Area Plans is critical to this ongoing effort. The League thanks the City for the opportunity to comment on the Initial Study/Mitigated Negative Declaration (IS/MND) for the proposed Tourist Core Area Plan (TCAP) amendments.

The League commented during the Scoping period and appreciates the "corner lot" (3828 Montreal Road) being taken out of consideration for development in response.

Overview

The League does not support the current proposed TCAP amendments because they are inconsistent with City and TRPA plans and intent. The Colony Inn parcel was intended to be permanently retired and the stream environment zone (SEZ) restored. The SEZ restoration attempt failed. Rezoning the last recreation/conservation land in the TCAP area does not align with the goals and policies of the City's General Plan or TRPA's Regional Plan, which the IS/MND is tiered off of. Because the environmental document only includes one mitigation measure, we are recommending two additional mitigation measures:

1. Restore the SEZ to a functional level and monitor and manage it to ensure it remains functional for the life of the project.
2. Permanently protect the "corner lot" (APN 029-441-003) as Recreation or Open Space through a permanent deed restriction running with the land.

We expect these two mitigation measures to be included for the TCAP amendments and proposed project in order to be approved.

SEZ Impacts and Site Suitability for Development

On March 18, 2008, the City passed a Resolution to permanently retire the Colony Inn site from future development as a condition of transferring the associated tourist accommodation units (TAUs) out of the City limits: "WHEREAS, the Colony Inn located partially Within an area identified for SEZ restoration, Once the Colony Inn is demolished, existing development will be transferred out of the SEZ and the site will be restored and permanently retired, thereby furthering the goals of the Stateline/Ski Run Community Plan and attainment of TRPA's thresholds." [1]

[1] March 18, 2008 City of South Lake Tahoe Staff Report and Resolution.
http://slt.granicus.com/MetaViewer.php?view_id=4&clip_id=181&meta_id=15886

The City included a Policy in the TCAP that aligns with its Resolution and approval of TAU transfers from the Colony Inn site: "Onsite land coverage reduction will occur primarily through environmental redevelopment by providing development incentives in centers that promote the relocation and transfer of land coverage. The City will endeavor, where feasible, to reduce and avoid creating new coverage in order to benefit the objectives of the TCAP and other areas of South Tahoe."[2] This language was discussed at the November 2013 TRPA Governing Board meeting, including whether or not to specifically include the Colony Inn site as a target restoration site. In the end, though a specific site was not targeted for restoration and the Colony Inn site was intended for restoration and permanent retirement as stipulated above.

The City needs to decide whether this amendment meets the intent of the General Plan and TCAP including the goals and policies contained within it. The City's Attorney will also need to determine whether or not a new Resolution is required to allow this Area Plan amendment.

Between 2009 and 2013 the Colony Inn was demolished and the SEZ should have been restored, but the restoration failed. According to TRPA's 2020 SEZ Baseline Report, the Colony Inn site (Colony Inn Meadows) restoration failed.[3] The SEZ only ranked a "C," indicating an unhealthy SEZ due to a ditch running through the entire project, dewatering the meadow and leading to loss of vegetation vigor. With the proposed amendments, the coverage limit would increase from 30 percent to 70 percent, with coverage transfer on applicable lands with capability 4-7. Additional development around the SEZ where headcuts and ditches are present, significantly and irreversibly impact the SEZ which expressly violates the 2008 City Resolution and the intent of SEZ restoration. Regardless of the success of the SEZ restoration efforts, the site was to be permanently retired, in line with the City's 2008 Resolution and enforced by TRPA's approval of the Boulder Bay Community Enhancement Program Project EIS in 2009.[4]

In September, October, and November of 2013, the TRPA Regional Plan Implementation Committee (RPIC) and Governing Board had lengthy discussions internally and with the City and the public. One of the results of the discussion was the City reinforcing that it "wanted to identify [Colony Inn] as a priority site for getting the stream environment zone restoration completed."[5] Other outcomes relevant to these proposed amendments are enshrined in the TCAP itself:

- "The Colony Inn which was located in SEZ lands by the intersection of Montreal Road and Heavenly Village Way was demolished and 64,800 square feet of land coverage was removed and banked, and the site stabilized. The existing tourist accommodation units removed from the site are proposed for transfer to the Boulder Bay Project in North Stateline. A condition of the Boulder Bay permit requires that the property be restored to a functioning SEZ prior to the units being transferred." Page 3-4.
- "The Tourist Core Area Plan responds to the needed SEZ improvements: Restore the disturbed SEZ on the Colony Inn parcel located along Montreal Road." Page 7-5.

[2] October 15, 2013 TCAP. Policy NCR-4.1, page 7-3. https://www.cityofslt.us/DocumentCenter/View/3508/Final-Tourist-Core-Area-Plan?bidId=

[3] December 2020 Lake Tahoe Basin SEZ Baseline Condition Assessment. Report: https://gis.trpa.org/TahoeSEZViewer/SEZ%20baseline%20condition%20assessment_v8.pdf; StoryMap: https://www.google.com/url?q=https://storymaps.arcgis.com/stories/815a21db82944f7f95ce94d76c73a19b&sa=D&source=docs&ust=1652741001866899&usg=AOvVaw2791Wlh0aSr9wKajKr5gZW

[4] November 4, 2009 Boulder Bay CEP Project EIS. https://www.trpa.gov/wp-content/uploads/documents/archive/4_01_Land_Use.pdf

[5] October 24, 2013 Meeting Minutes from TRPA RPIC meeting. Page 19. https://www.trpa.gov/wp-content/uploads/documents/archive/January-29-2014-Governing-Board-Packet.pdf

In July of 2013, the League submitted comments on the TCAP in its early stages of development, including a clarifying question about the Colony Inn site. The November 2013 TRPA Governing Board meeting included responses to comments and #8 directly addresses the Colony Inn site.[6] While the Boulder Bay project has been long-delayed and is currently changing with new ownership of that site, TRPA's transfer rules may still apply and the intent to permanently retire the site is clear.

TRPA Counsel will need to provide an analysis of the SEZ Restoration Credits and requirement to permanently retire and "stabilize" the site based on TRPA Code and TCAP approvals in 2013, and the final intent captured in TCAP.

Recreation/Open Space

The IS/MND for the proposed amendments tiers off of the City's 2011 General Plan and TRPA's 2012 RPU, and references the TCAP.

In the City's General Plan, the parcels that are the subject of the amendments are identified as "Conservation."[7] The General Plan's Conservation designation "provides for the permanent preservation of natural resources, habitat protection, watershed management, public and quasi-public uses, areas that contain public health and safety hazards such as floodways, and areas containing environmentally-sensitive features."[8] The parcels being considered for the amendment are the only General Plan Conservation parcels in the TCAP area, and some of the only infill/smaller lot Conservation parcels in the entire General Plan. This was done deliberately and likely linked to the discussions when Colony Inn was demolished.

In the TCAP, the parcels in question are zoned as recreation. While this questionably aligns with the intent in the General Plan, Recreation districts in the TCAP are "intended to allow a variety of recreation uses such as dispersed recreation and parks. Permissible uses include day use areas and group facilities."[9] The dispersed recreation use most closely aligns with the intent of the Conservation designation in the General Plan. When the TCAP was developed, the Conservation designation arguably should have translated to the Open Space designation which "is intended to preserve land in its present use that would: 1) conserve and enhance natural or scenic resources; 2) protect streams environment zones, sensitive lands, water quality or water supply; 3) promote soil and habitat conservation; 4) enhance recreation opportunities; and/or 5) preserve visual quality along highways, roads, and street corridors or scenic vistas. The land is predominantly open, undeveloped, or in a lightly developed and is suitable for any of the following: natural areas, wildlife and native plant habitat; erosion control facilities, stream environment zones, stream corridors; passive parks; and/or trails for non-motorized activities."[10] This Open Space designation also aligns with TCAP policies NCR-2.3 and R-2.3,[11] which would be very difficult or impossible to implement or achieve if the proposed amendments are approved.

---

[6] November 20, 2013 Response to Comments on the TCAP. Response #8, Page 4. https://www.trpa.gov/wp-content/uploads/documents/archive/6_FINAL_Attachment-E_Responses-to-Comments.pdf

[7] October 15, 2013 TCAP. Figure 2-2.

[8] May 17, 2011 City of South Lake Tahoe General Plan. Land Use Element, page LU-3. https://www.cityofslt.us/DocumentCenter/View/5639/SLTGPU_PD_2-LandUse_Final_2011-05-17?bidId=

[9] October 15, 2013 TCAP. Page 5-6.

[10] *Ibid.*

[11] TCAP Policy NCR-2.3: Encourage the use and access to designated open space for passive recreation uses when they conform to resource restrictions

TCAP Policy R-2.3: Encourage landscaped, small passive parks in and around the Tourist Core

TRPA's Regional Plan (RPU) was updated in 2012, between the adoption of the City's General Plan and the TCAP. The IS/MND, in section 1.8, selected a few TRPA- specific and -referenced goals and policies that this project *may* support but the ones it may conflict with are not included which does not allow a fair assessment of the pros and cons of the proposed project. These include, but are not limited to ROS-2.9, ROS-2.10, ROS-2.11, Land Use Element Goal 1 Policies 2 and 3, Soils Goal 1 Policy 7, Open Space Goal 1, and Stream Environment Standard SC-2.

To comply with the City's and TRPA's land use designations and goals and policies related to open space and recreation, the "corner parcel" at 3828 Montreal Road (APN 029-441-003) needs to be permanently retired as Recreation or Open Space through a deed restriction on the parcel. This would include the access easement associated with the Colony Inn to the Van Sickle access road.

Summary and Recommendations

For this IS/MND to tier off of the City's General Plan and TRPA's Regional Plan, the amendments analyzed must be consistent with those plans. The proposed amendments are not consistent with the land use designations or the majority of the relevant goals and policies in the documents being tiered off of, which sets a dangerous precedent. In addition to the inconsistency, the impacts to recreation, public services, biological resources, land use/planning, population/housing, and overall cumulative impacts have been underestimated, ignored, or not mitigated to less than significant. We recommend three mitigation measures that could put the amendments into conformance with the General Plan and Regional Plan:

1. To mitigate for recreation and public service impacts: enhance the existing mitigation which is Putting up a fence to block access directly to Van Sickle, the future Greenway path, and existing SEZ. Based on the map provided as Figure 2-2 on page 16 of the IS/MND, the fencing needs to go around the entire property and could include tying into the substation fencing. It would be easy to leave the property and get around the fencing as depicted from buildings 7, 8, and 10, pretty easy from building 9, and not difficult from all buildings.
2. To mitigate impacts to biological resources and land/use planning (SEZs): create a new mitigation measure, enforced through a permit condition or deed restriction, requiring the SEZ on the parcel(s) to be restored to a functional state and monitored and maintained for the life of the project.
3. To mitigate for conflicts with land use/planning, impacts on population/housing, and cumulative impacts[12]: create a new mitigation measure, enforced through a permanent deed restriction running with the land, permanently designating the "corner parcel" (3828 Montreal Road, APN 029-441-003) as Recreation or Open Space under the relevant TCAP definition.

Finally, mitigation monitoring reporting requirements and schedule need to be developed before approving the amendments,[13] taking into account the updated and new mitigation measures we recommend.

[12] Pursuant to § 15370 of the CEQA Guidelines, mitigation includes: (a) Avoiding the impact altogether by not taking a certain action or parts of an action. (b) Minimizing impacts by limiting the degree or magnitude of the action and its implementation. (c) Rectifying the impact by repairing, rehabilitating, or restoring the impacted environment. (d) Reducing or eliminating the impact over time by preservation and maintenance operations during the life of the action. (e) Compensating for the impact by replacing or providing substitute resources or environments.

[13] CEQA § 21081.6.: Upon approving a project for which a MND is adopted, the Lead Agency must also adopt a mitigation monitoring or reporting program.

Based on City and TRPA Counsel determination, and any new mitigation measures proposed, the League will consider accepting development of Colony Inn site and the "back parcel" as long as the SEZ is restored and permanently monitored; and the "corner lot" is permanently retired with a deed restriction.

Thank you for the opportunity to provide these comments. Please do not hesitate to contact us to discuss our recommendations and we hope to see an updated IS/MND with additional mitigation measures in order to comply with CEQA and TRPA environmental review, goals, and policies.

Sincerely,

Darcie Goodman Collins, PhD
CEO League to Save Lake Tahoe

PNAS Nexus, 2023, 2, 1–9
https://doi.org/10.1093/pnasnexus/pgad004
Advance access publication 28 February 2023
Research Report

Low-elevation conifers in California's Sierra Nevada are out of equilibrium with climate

Avery P. Hill [a,*], Connor J. Nolan [b], Kyle S. Hemes [b], Trevor W. Cambron [c] and Christopher B. Field [a,b,c]

[a]Department of Biology, Stanford University, Stanford, CA, USA
[b]Woods Institute for the Environment, Stanford University, Stanford, CA, USA
[c]Department of Earth System Science, Stanford University, Stanford, CA, USA
*To whom correspondence should be addressed: Email: aph82@stanford.edu
Edited By: Adelia Bovell-Benjamin

Abstract

Since the 1930s, California's Sierra Nevada has warmed by an average of 1.2°C. Warming directly primes forests for easier wildfire ignition, but the change in climate also affects vegetation species composition. Different types of vegetation support unique fire regimes with distinct probabilities of catastrophic wildfire, and anticipating vegetation transitions is an important but undervalued component of long-term wildfire management and adaptation. Vegetation transitions are more likely where the climate has become unsuitable but the species composition remains static. This vegetation climate mismatch (VCM) can result in vegetation conversions, particularly after a disturbance like wildfire. Here we produce estimates of VCM within conifer-dominated forests in the Sierra Nevada. Observations from the 1930s Wieslander Survey provide a foundation for characterizing the historical relationship between Sierra Nevada vegetation and climate before the onset of recent, rapid climate change. Based on comparing the historical climatic niche to the modern distribution of conifers and climate, ~19.5% of modern Sierra Nevada coniferous forests are experiencing VCM, 95% of which is below an elevation of 2356 m. We found that these VCM estimates carry empirical consequences: likelihood of type-conversion increased by 9.2% for every 10% decrease in habitat suitability. Maps of Sierra Nevada VCM can help guide long-term land management decisions by distinguishing areas likely to transition from those expected to remain stable in the near future. This can help direct limited resources to their most effective uses—whether it be protecting land or managing vegetation transitions—in the effort to maintain biodiversity, ecosystem services, and public health in the Sierra Nevada.

Keywords: ecology, habitat suitability modeling, vegetation transitions, vegetation climate mismatch, climate change, California

Significance Statement

Warming climatic conditions over the last century have led to observable shifts in the spatial organization of dominant tree species in California's Sierra Nevada. Little is known, however, about the extent to which these shifts have tracked the magnitude of climate change. This study maps Vegetation Climate Mismatch in the Sierra Nevada—areas where climate change has left trees in climatic conditions where they have not historically occurred. Different vegetation types support different wildfire regimes, ecosystems, and ecosystem services. Our maps will be useful for anticipating vegetation transitions and informing long-term wildfire and ecosystem management across the Sierra Nevada mountains of California.

Introduction

Warmer and drier conditions prime forests for ignition (1), but climate change also directly affects the species composition of future vegetation. Climate-driven vegetation conversion is an understudied phenomenon in general and a potentially significant determinant of catastrophic wildfire risk that could require changes in management strategies (2–4).

Broadly, climate change has caused vegetation to shift poleward and up-slope (5–7). In long-lived ecosystems like forests, climate change is occurring faster than the ability of many plants to shift their distributions or adapt, resulting in vegetation disequilibrium (8) or vegetation climate mismatch (VCM). Forests experiencing VCM are at risk of converting to alternative species assemblages, particularly after stand-replacing disturbances such as severe wildfire (4). In some cases, VCM can even make forests more susceptible to wildfires (9).

VCM is likely to be found in California's transition zone between low-elevation conifer-dominated forest and angiosperm-dominated vegetation (including mixed chaparral, oak woodland, and mixed broadleaf forest) (Fig. 1; elevation ~1000–1400 m)—where the foothills of the Sierra Nevada end and the mountains of the western flank begin. These forests lie on the warm end of mixed conifer distributions, where canopy dominants include ponderosa pine, sugar pine, and Douglas-fir (10), and understories

Competing Interest: The authors declare that they have no competing interests.
Received: July 16, 2022. **Revised:** December 19, 2022. **Accepted:** January 4, 2023
© The Author(s) 2023. Published by Oxford University Press on behalf of National Academy of Sciences. This is an Open Access article distributed under the terms of the Creative Commons Attribution License (https://creativecommons.org/licenses/by/4.0/), which permits unrestricted reuse, distribution, and reproduction in any medium, provided the original work is properly cited.

Downloaded from https://academic.oup.com/pnasnexus/article/2/2/pgad004/7059010 by guest on 23 March 2023

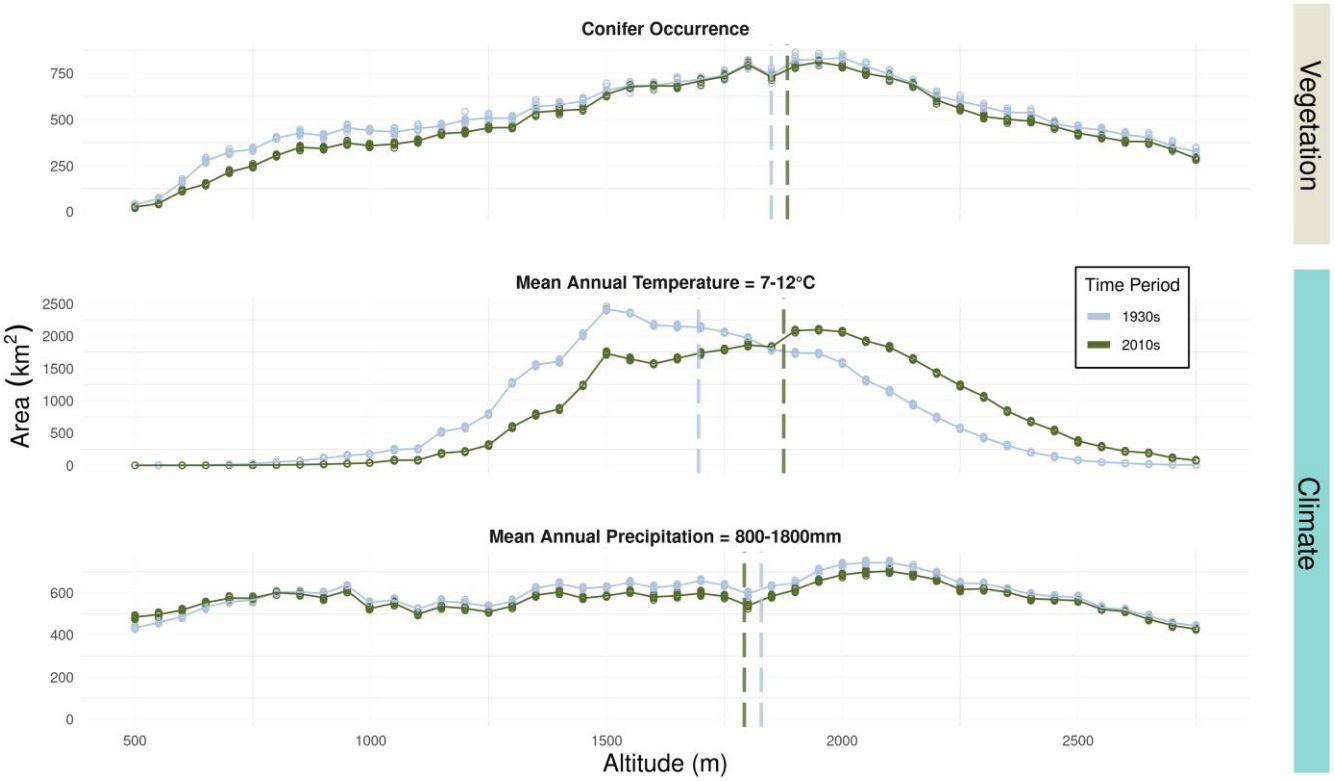

Fig. 1. Observed elevation shifts in temperature, precipitation, and conifers across the study area between 80 years. The elevation distribution of modern conifers (top panel, dark green; mean = 1,884 m, SD = 640 m) was 34 m higher (95% CI = [25 m, 43 m]) than the 1930s conifers (top panel, light blue). This average shift in elevation was far less (by 145 m; 95% CI = [135 m, 156 m]) than the up-slope shift in the nominal 7–12°C Mean Annual Temperature envelope of Sierra Nevada low-elevation conifers (182 m; 95% CI = [179 m, 187 m]) (10). Note that the Mean Temperature envelope of Sierra Nevada low-elevation conifers would be shifted approximately 1°C cooler, if calculated based on the vegetation distribution in the Wieslander survey. Mean Annual Precipitation (bottom panel) decreased between the two time periods at most elevations—more-so at higher elevations—and the average elevation of the MAP envelope of Sierra low-elevation conifers decreased by 37 m (95% CI = [27 m, 49 m]). Circles represent samples with measurement error randomly introduced, and solid lines represent the averages across 10 samples. Vertical dashed lines show the total mean for the time period.

are typically composed of mixed chaparral's characteristic scrub oak, chaparral oak, and manzanita.

Boundaries between conifer-dominated forest and nonconifer vegetation at the western slope of the Sierra Nevada that were established under a previous climate regime may now be out of equilibrium with the current climate, especially if established trees continue to persist, even as climate conditions become unsuitable for seedlings and saplings of the same species. In these settings, stand-replacing fire—which pushes forests back to seedling stages—can trigger a rapid transition from one vegetation type to another (4, 11, 12). These transitions can potentially lead to the local loss of species, ecosystem services, and irrecoverable carbon stocks, depending on the vegetation that replaces these forests—and can also impact future risk of catastrophic wildfire.

Recent human population growth and large wildfires in these lower-elevation conifer forests punctuate the need to assess ecological stability, particularly as it relates to wildfire risk.

Results and discussion

Conceptually, present-day VCM in Sierra Nevada coniferous forests exists if the geographic shift of tree species does not keep pace with climate change. This mismatch between vegetation and climate will make regeneration after disturbance more difficult. The Wieslander survey from the 1930s provides an anachronistically high resolution (minimum mapping unit of 16 ha) and expansive (176,900 km^2) assessment of historical California vegetation (13, 14). Comparing the historical vegetation distribution to modern EVeg maps (15, 16), the mean elevation of conifers has shifted up-slope by 34 m on average (95% CI = [25 m, 43 m]). Over the same time period, the characteristic temperature range for conifers (10) has shifted up-slope by 182 m (95% CI = [179 m, 187 m]), based on historical and contemporary temperature and precipitation at 30 arc-second resolution (17) used to calculate 19 bioclimatic variables for 1915–1955 and 2000–2020. The magnitude of this temperature shift is approximately three to five times greater than the shift of the conifers ($Altitude_{MAT} - Altitude_{conifer}$ = 145 m; 95% CI = [135 m, 156 m]), suggesting the presence of VCM (Fig. 1). In calculating the altitude shifts of both conifer occurrences and temperature variables, 10 pseudo-replicate sets were made by randomly introducing known measurement error (see methods) and bootstrapped 1000 times.

To provide a more accurate and geographically explicit assessment of VCM, we quantified the climatic drivers of conifer distribution (i.e. the climatic niche) within the Sierra Nevada, using the 1930s vegetation data and 800 m resolution climate data (1915–1955) to train a habitat suitability model (HSM) for Sierran conifer forests. The advantage of using these older data is that they come from an era when the vegetation and climate were closer to equilibrium, before the vast majority of human-caused warming (18). Using the *sdm* (v 1.0-89) (19) and *dismo* (v 1.3-3) (20) packages in R (v 4.1.1) (21), we trained a Generalized Additive Model (GAM) on 56,844 conifer presence and 26,504 conifer absence points and 7 bioclimatic variables, using 5-fold

Downloaded from https://academic.oup.com/pnasnexus/article/2/2/pgad004/7059010 by guest on 23 March 2023

spatial-blocking cross-validation for model evaluation ($AUC_{test} = 0.94 \pm 0.039$, $COR = 0.78 \pm 0.079$, $AUC_{train} - AUC_{test} = 0.027 \pm 0.042$). Mean Temperature of the Wettest Quarter (MTWQ) and Mean Annual Precipitation (MAP) were the strongest determinants of conifer distribution in the 1930s, with 52% (SD = 20.9%) and 42% (SD = 13.9%) relative variable importance, respectively (Fig. 2b).

We used this model to predict regions of suitable conifer habitat across time periods from 1960 to 2100. CMIP6 data from scenarios SSP1-2.6 (an ambitious mitigation future) and SSP5-8.5 (a continued high emissions future) were used to predict future changes in habitat suitability. Habitat suitability (*HS*) was divided into three categories: suitable ($HS \geq 0.52$), unsuitable ($0.52 > HS \geq$

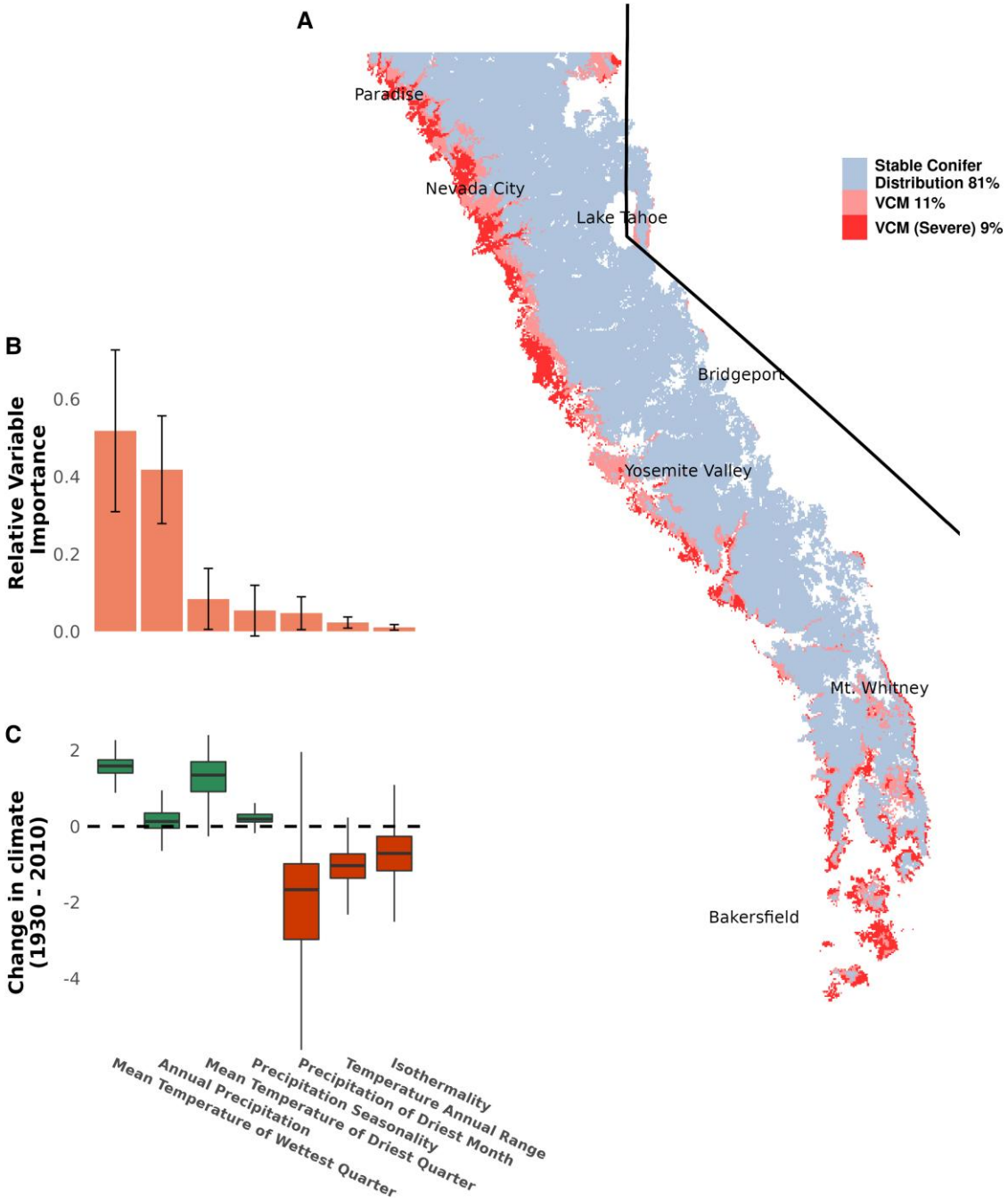

Fig. 2. Estimated conifer VCM in the Sierra Nevada (2015–2020). (a) The conifer HSM projected to contemporary climate and overlayed on the modern conifer distribution (EVeg) reveals that up to 19.5% of modern conifer forest is in VCM, primarily along the low-elevation western slope of the Sierras. The total area of conifers shown is 40,495 km^2, of which ~32,500 km^2 are in equilibrium with the modern climate. (b) Mean Temperature of Wettest Quarter and Mean Annual Precipitation were the most important predictors in the HSM ($mean_{MTWQ} = 0.518$, $SE_{MTWQ} = 0.209$ and $mean_{MAP} = 0.418$, $SE_{MAP} = 0.139$). Standard error bars are included in the barplot. (c) Boxplots show the difference between modern (2015–2020) and historical (1915–1955) climate within the conifer VCM regions. Change in climate is calculated as the number of standard deviations the modern climate differs from the historical period. Though the differences were statistically significant for each climate variable ($p < 8.45 \times 10^{-12}$, independent *t*-test), Precipitation of Driest Month showed the greatest decrease (mean = −2.41, SD = 2.84) and MTWQ the greatest increase (mean = 1.59, SD = 0.329) between the historical and modern climate. Mean Annual Precipitation changed the least within the VCM area (mean = 0.165, SD = 0.395). Boxplots include the median line, a box denoting the interquartile range, and whiskers showing values ±1.5 × the interquartile range.

Downloaded from https://academic.oup.com/pnasnexus/article/2/2/pgad004/7059010 by guest on 23 March 2023

0.18), and severely unsuitable (0.18 > *HS*). These were determined based on habitat suitability thresholds above which 95% and 99% of the historical (Wieslander) conifers occurred (i.e. where sensitivity = 95% and 99%). In other words, less than 5% of historical conifer occurrences were in environmental conditions with *HS* < 0.52, which we characterize as "unsuitable" habitat. When compared with contemporary (2010s) EVeg maps of conifer distributions, these habitat suitability estimates reveal large, contiguous patches of conifer VCM in the Sierra Nevada—particularly along the low-elevation western slopes—that account for 19.5% of modern conifer forests (~7,500 km^2) (Fig. 2a). From 1960 to 2020, the area of conifer VCM has increased consistently (Fig. S1). When projected across the remainder of the 21st century, even the lowest emissions pathway (SSP1-2.6) leads to VCM doubling by the end of the century, if conifer range edges stay static (Fig. 3).

Based on the model, this increase in VCM is primarily attributable to an increase in Mean Temperature of the Warmest Quarter (MTWQ) across the study area between the 1930s and present day (Fig. 2c). The variable response curves (Fig. S2) demonstrate the sensitivity of conifer habitat suitability to high values of MTWQ: above a MTWQ of 0.5°C, habitat suitability drops by approximately 0.1 for every 1°C of warming. This sensitivity of low-elevation conifers to higher temperatures presumably reflects a suite of physiological features that make them less competitive against angiosperms under warm conditions. A number of nonclimatic environmental features, like edaphic characteristics and disturbance regimes, can also be important drivers of conifer range limits, but there is no evidence for consistent patterns of these along the conifer/angiosperm boundaries in the Sierra Nevada (10).

Areas that transitioned from conifer-dominated in the 1930s to angiosperm-dominated in the 2010s generally have lower contemporary conifer habitat suitability than areas that maintained conifer dominance over that time period. Logistic regression indicates that the odds of conifer forests persisting decreased by 9.2% (95% CI = [0.092, 0.093]) for every 0.1 decrease in predicted habitat suitability (Fig. 4b). The areas of the Sierras where conifer-dominated vegetation transitioned to angiosperm-dominated vegetation occur primarily along the lower-elevation western slopes (Fig. 4a). This finding affirms the empirical implications of the low habitat suitability predicted by our model—these areas are at greater risk of eventually converting to nonconifer dominated vegetation. While it is difficult to tease apart the relative contribution of different possible drivers of vegetation transitions observed in this area, it is likely that decreased climatic suitability has compounded the impacts of other activities like logging or fire suppression.

These results are consistent with recent literature documenting observed and expected vegetation change in the Sierra Nevada and climate-induced vegetation transitions more broadly. A number of studies document observed or expected geographic shifts in low-elevation conifer-dominated forests, due at least in part to warming temperatures. Examples come from the Alps (22), Rocky Mountains (11), the state of California (23), and the Sierra Nevada (24). In the Sierra Nevada, studies using the

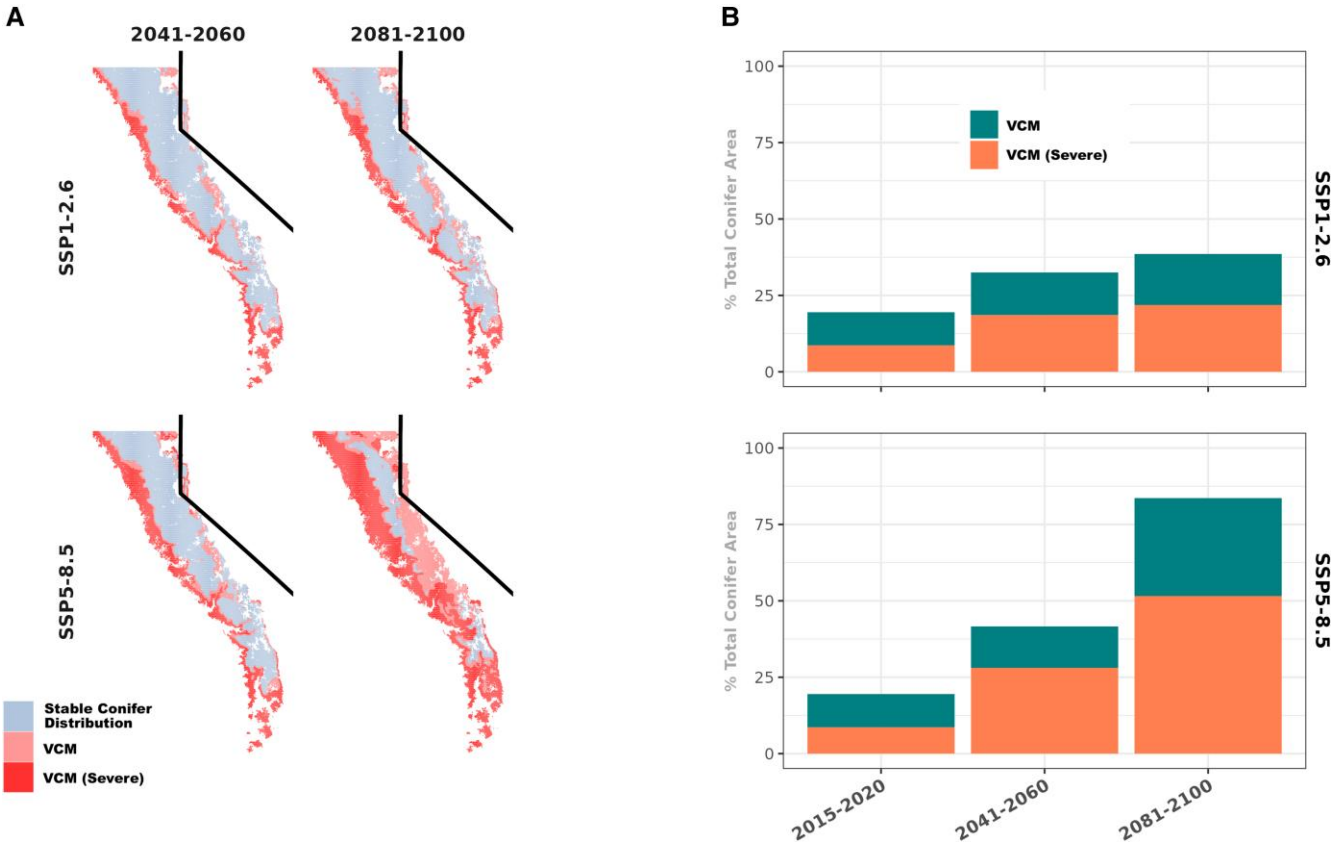

Fig. 3. Future projections of VCM for two emissions pathways. Projection of the conifer HSM to mid-century and late-century climates suggest a dramatic increase in VCM by the end of the century if the contemporary conifer range edges do not move. The expected growth in severe VCM area (SSP1-2.6: 2.53 km^2/yr; SSP5-8.5: 5.98 km^2/yr) outpaced the more moderate VCM growth (SSP1-2.6: 1.54 km^2/yr; SSP5-8.5: 2.95 km^2/yr) under both emissions scenarios. Following the trend in projections of historical VCM (Fig. S1), VCM is expected to increase most along the western slope of the Sierra Nevada.

Downloaded from https://academic.oup.com/pnasnexus/article/2/2/pgad004/7059010 by guest on 23 March 2023

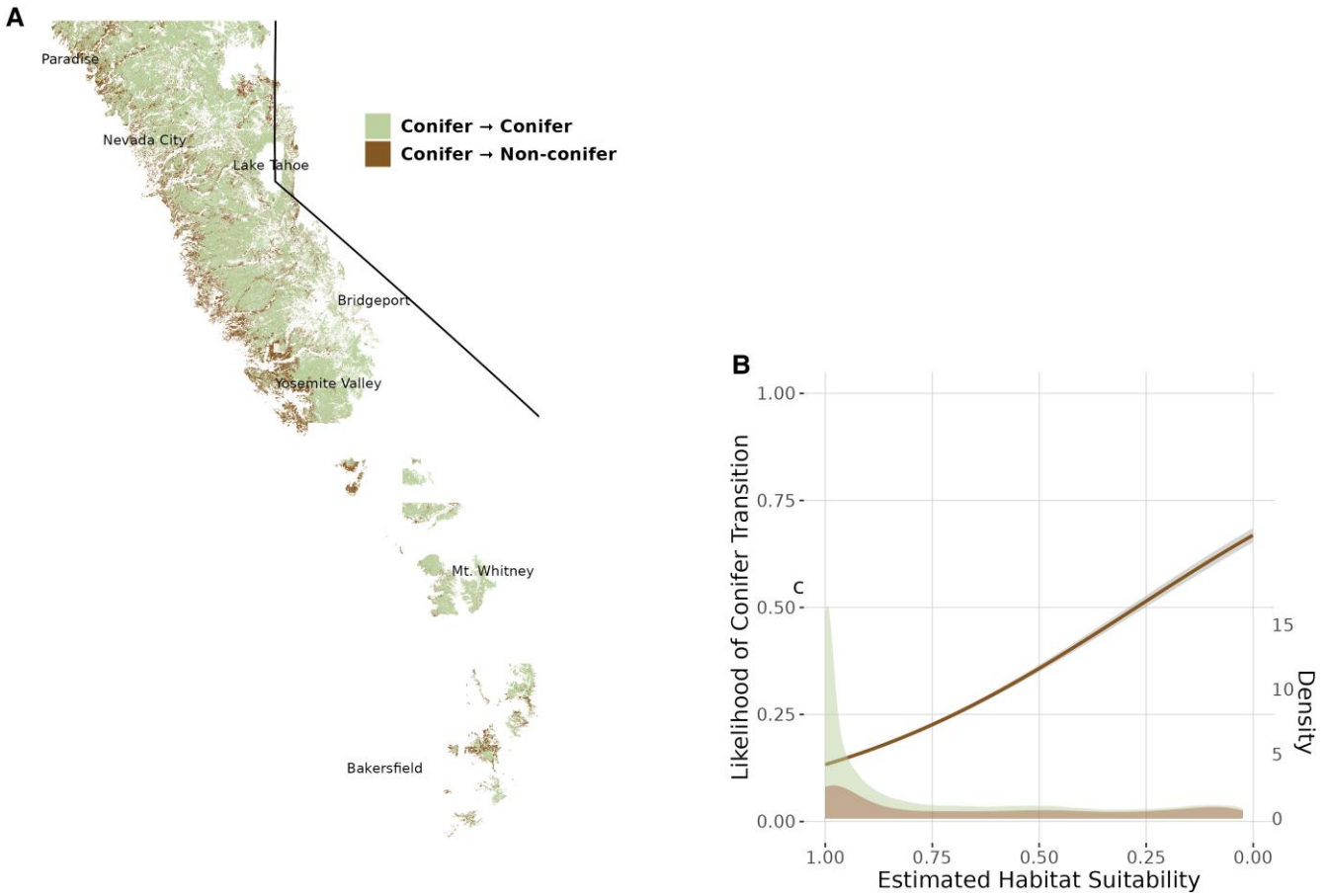

Fig. 4. Habitat suitability of observed vegetation transitions between 1930s and 2010s. Areas that transitioned from conifer-dominated to angiosperm-dominated vegetation from 1930s to present tended to have lower modern conifer habitat suitability ($p < 2 \times 10^{-16}$). (a) All areas in the Sierra Nevada with complete vegetation data from the 1930s (Wieslander) and 2010s (EVeg) area shown. Most transitions from conifer-dominant vegetation are along the low-elevation edges of the historic conifer distribution. (b) The fitted logistic regression line indicates that the odds of conifer forests persisting decreased by 9.2% (95% CI = [0.092, 0.093]) for every 0.1 decrease in predicted habitat suitability. Probability density estimates for the areas of either transition or persistence are included.

Wieslander survey show that an increase in oak or hardwood vegetation is concomitant with a reduction in pine species prevalence (in western El Dorado county in particular, ponderosa pine decreased in area by 570 km^2, and montane hardwood increased by 498 km^2) (25, 26). Fire suppression has played a notable role in shaping the distribution and demography of these Sierra Nevada forests as well, and has worked in concert with warming temperatures to favor hardwood species like *Quercus spp.* while reducing the dominance of less shade-tolerant species like *Pinus spp.* (27). Conifer regeneration failure is likely a major driver of these observed and expected patterns, and researchers such as Shive et al. have found that a combination of climatic shifts and disturbance characteristics (e.g. burn severity) significantly affect the likelihood of conifer regeneration (28).

Is it possible that this analysis based on vegetation maps from the 1930s and the 2010s artificially inflates the area of VCM? Effects of logging prior to the 1930s and differences in mapping criteria warrant evaluation. The contrast between the projected and actual distribution of Sierran conifer forest depends on the robustness of the assumption that 1930s vegetation was in equilibrium with the climate. It is clear that there was little warming before the 1930s and that most of the anthropogenic climate change expected to cause VCM has been within the last few decades (29). Is it also possible that, even in the 1930s, vegetation was out of equilibrium with climate as a result of logging limiting conifers at the warm, dry end of their distribution? Logging was widespread throughout the Sierras in the late 19th and early 20th centuries. By 1945, ~55% of nonsubalpine Sierra Nevada forests were second or third growth forest (30). We do not find evidence that logging consistently led to permanent vegetation conversions, and logged Sierran forests often regrow with the pre-logging dominants. Ponderosa pine forests, for example, can return to dominance within 50 years of being clear-cut (31); Sierran mixed conifer, as few as 12 (32). We think it more unlikely that logging and other anthropogenic impacts would have specifically impacted the low-elevation edge of conifer distributions across the entirety of the Sierras in a way that would meaningfully truncate the estimated climatic niche. In the Manual of Field Instructions (33), Wieslander et al. write: "Except for the following, do not attempt to map smaller units than 40 acres of any type. (1) Remnant woodland and timber types in chaparral areas, or timber types in woodland would always be mapped if 10 acres or more" (pp. 39–40). The use of the word "remnant" implies that the surveyors were sensitive to vegetation transitions and made an effort to classify conifer types even after disturbance, which further mitigates the possibility that anthropogenic vegetation conversions prior to 1930 affected conifer range edges.

Even so, we cannot eliminate the possibility that pre-1930s logging or anthropogenic disturbance led to vegetation conversions and some overestimation of modern VCM. We explored the

Downloaded from https://academic.oup.com/pnasnexus/article/2/2/pgad004/7059010 by guest on 23 March 2023

sensitivity of our results to the possibility that 1930s conifers were missing from the lower-elevation range edge as a result of human activity and, therefore, shifted toward the cool end of their climatic niche (opposite the pattern that has emerged since the 1930s). To do this, we trained HSMs on Wieslander data manipulated such that the highest elevation nonconifer samples were randomly converted to conifer samples. Our results followed the expectation that the area of modern VCM decreases with an assumed expansion of lower-elevation historical conifer distribution (Fig. S6). However, even under the extreme scenario in which the Wieslander survey did not detect conifer vegetation over 2,700 km^2 of the lowest elevation regions that may once have contained conifers, total VCM is still >10% of all modern conifer forests within the study area.

Vegetation mapping criteria were generally similar for the maps from the 1930s and the 2010s, but there are subtle differences in vegetation classification and minimum mapping unit (MMU) size (25). Under the CALVEG classification system, an area is classified as the taller of a set of possible vegetation types if the taller type (e.g. coniferous) occupies >10% of the mapping unit. In contrast, Wieslander VTM has a threshold of 20%. Because the EVeg maps lean towards classifying areas with only a few conifers as conifer-dominant vegetation, the modern maps might exaggerate conifer area at low elevations, contributing to an overestimate of VCM. Likewise, the difference in MMU between the two maps may contribute to an overestimate of modern conifer VCM. The MMU of EVeg (≤1 ha) is smaller than that of the Wieslander data (16 ha total; 4 ha for "timber types" (33)), so EVeg data are more likely to register smaller stands of conifers, which may be more common along the lower-elevation edge of conifer distributions. To compensate for this, our vegetation aggregation method for both the 1930s and 2010s maps is intentionally sensitive to conifer occurrences, registering conifer presence if ≥5% of an 800 m (64 ha) grid cell contains conifer vegetation.

Our first-of-a-kind maps of areas experiencing VCM represent a new consideration when planning for forest management. These VCM forests are at risk of failing to regenerate after a disturbance. The exact mechanisms and sequences of events that lead to vegetation change will vary across the landscape and should be a target of future studies. But overall, VCM requires a move away from simply resisting fire and vegetation change to a more active management approach that directs the changes in a way that is beneficial to ecosystems and the nearby communities (34, 3).

Incorporating VCM into forest management plans will require experimentation and a delicate balancing of constituencies and their interests. There will likely be tradeoffs to be negotiated and difficult decisions to be made. For example, the public is often reticent to engage in large scale thinning or prescribed burns due to economic and esthetic reasons. But these very interventions may be important for forest health and fire safety. These and other interventions that move away from traditional resilience and towards a more "adaptive" or "transformative" resilience are likely to be necessary (35).

Understanding a region's habitat suitability also influences management choice after a disturbance event. Most notably, in a VCM area, efforts to reforest after a fire or other disturbance with the same vegetation type as before are unlikely to be successful. Post-disturbance restoration needs to take into account the species mix and density that can currently be supported, but also the kinds of vegetation that future conditions are likely to support. This requires managers grappling with uncertainty in climate projections as they plan the future of the lands they manage; accessible tools that can synthesize climate projections with species distribution modeling can facilitate this planning process.

Maps of vegetation-climate mismatch can also inform conservation priorities. Habitats that are in equilibrium today and projected to remain in climate equilibrium should be prioritized for protection. In contrast, habitats that are out of equilibrium today or that are projected to go out of equilibrium could be treated to reduce the risk of catastrophic fires. Alternatively, transitions to new vegetation types could be facilitated in forests experiencing VCM. Schemes that incentivize ecosystem management for climate mitigation, like California's forest offset program (36), will need to integrate nonstationary future climate and vegetation risks and opportunities (37).

Conclusion

We have identified, quantified, and mapped vegetation climate mismatch in the Sierra Nevada: a new risk factor relevant to long-term management of catastrophic wildfire. Up to 19.5% of conifer forests are in areas that no longer have suitable climate for conifer regeneration. Thus, when there is a disturbance, such as a large fire, the conifer forest will be unlikely to reestablish. Conifer forests experiencing VCM may also be out-competed by vegetation types like mixed broad-leaf forests and chaparral that are better suited to the new climate and often grow more quickly than conifers, especially at the seedling stage.

Impending vegetation shifts across such a significant portion of California require a change in management strategy and a more long-term framing of catastrophic fire-risk in California.

Tools to prioritize treatment and protection are desperately needed given that more than 20% of California's forestland would benefit from fuel treatments; myriad barriers, including funding, stand in the way (38). Our maps of conifer forest VCM provide new guidance on what types of management are likely to be successful and where. Investments made in better prioritizing conservation, fuel management, and fire mitigation in high-risk forestlands can have compounding returns—economically, ecologically, and in the form of human health and well-being.

Materials and methods

Vegetation data

The US Forest Service's Wieslander Survey (1928–1940) provides the oldest spatially explicit, landscape-scale vegetation data in California. The surveyors mapped dominant vegetation (at a minimum mapping unit of 16 ha) through a combination of plot surveys and remote observation from peaks and vistas (13). We accessed the digitized and georeferenced shapefiles of these maps through Berkeley's Vegetation Type Mapping Project Collection (vtm.berkeley.edu), which cover an area of more than 175,000 km^2 across California (14). While digitizing the maps, Kelly et al. translated the vegetation classification system used by Wieslander to the more contemporary and widely used California Wildlife Habitat Relationships models (CWHR) (39). The geographic error of the basemaps ranges between 127 and 462 m (mean = 232 m) (40).

The Wieslander survey also collected plot data, with ostensibly higher spatial and taxonomic resolution. We used the Wieslander vegetation maps, rather than the plot data, for 4 reasons. (1) The vegetation data provide a much larger sample size than the plot data when up-scaled to 800 m resolution (Fig. S5). Besides the plot data clearly being more sparse, there are also large tracts of land that are mapped in VTM for which there are no plots

Downloaded from https://academic.oup.com/pnasnexus/article/2/2/pgad004/7059010 by guest on 23 March 2023

available (e.g. Lake Tahoe Basin). (2) The more contiguous vegetation data allowed us to estimate the percent cover of different vegetation types and more effectively reconcile the difference in resolution between the occurrence and climate data used to train the habitat suitability model (further details below). (3) The Wieslander vegetation maps appear to be the Wieslander survey's primary data product, and the plots are more of an exercise in surveyor training/ground-truthing (33). From the Wieslander Manual of Field Instructions: "The plots serve as a check on the mapper's field judgment and assist him in an understanding of types. They are used immediately in the field for this purpose" (p. 74). (4) The digitized Wieslander plot data do not include CWHR vegetation data, only species lists, and the primary goal of this study is to find patterns at the scale of vegetation.

We sourced recent vegetation data from the US Forest Service's EVeg (Existing Vegetation) maps for the North Sierra and South Sierra regions (15, 16). These vector maps were produced from source data including NAIP and WorldView-2 using the CALVEG (Classification and Assessment with Landsat of Visible Ecological Groupings) classification system, and have a horizontal positioning accuracy of ~50 m. The North Sierra data were produced from satellite images from 2000 to 2014, while the South Sierra source data ranged from 1995 to 2016. The CALVEG vegetation classes "crosswalk easily" to CWHR classes, which are provided in the EVeg map product (41).

We cropped all vegetation data to the general extent of the Sierra Nevada mountains, which we derived from the Northwestern Forested Mountains ecoregion (42) east of the Central Valley and south of 40°. We added a 45 arc-minute (~70 km) buffer to the southern, western, and eastern extents to include vegetation data from surrounding lower-elevation areas, where available.

Climate data

We sourced contemporary and historical monthly precipitation, maximum temperature, and minimum temperature data from Oregon State University's PRISM (Parameter-elevation Regressions on Independent Slopes Model) Climate Group at 30 arc-second resolution (17). PRISM data are widely used and produced from the interpolation of observations from a multitude of US meteorological stations using a regression model which weights grid cells by their physiographic similarity to the station. Mean absolute error is 1°C for temperature variables and 10% for precipitation variables in the western US (43).

We used the biovars() function from the *dismo* v. 1.3-3 R package to convert the monthly precipitation and temperature variables to 19 bioclimatic variables—including physiologically relevant variables such as mean diurnal temperature range and precipitation of the driest quarter—and produced averages for the following time periods: 1915–1955, 1960–1980, 1980–2000, 2000–2010, 2010–2020, 2015–2020.

The climate data for future scenarios came from the Coupled Model Intercomparison Project Phase 6 (CMIP6). We chose the Shared Socioeconomic Pathways (SSPs) SSP1-2.6 and SSP5-8.5 for the 2041–2060 and 2081–2100 time periods from the CanESM5 (Canadian Centre for Climate Modelling and Analysis, Canada) global circulation model. We chose CANESM5 because its projections for future climate in California are near the middle of results from CMIP6 (44). We downloaded a set of 19 bioclimatic variables at 2.5 arc-minute resolution from the Worldclim dataset (http://www.worldclim.org, accessed on April 27th, 2021) (45). SSP1-2.6 and SSP5-8.5 represent the lowest and highest potential emission scenarios for the next century, and are derived from estimates of future energy and land-use trajectories (46).

Conifer habitat suitability model

We started building the Sierra Nevada conifer habitat suitability model by identifying all CWHR habitat types that were conifer-dominated within the study area. These included Sierran Mixed Conifer, Subalpine Conifer, Douglas Fir, Eastside Pine, Jeffrey Pine, Closed-Cone Pine-Cypress, Lodgepole Pine, Pinyon-Juniper, Ponderosa Pine, Red fir, and White fir. The Montane Hardwood-Conifer type is defined as at least 33% conifer-dominated and 33% hardwood-dominated vegetation (39), which we classified as 50% conifer presence and 50% conifer absence. All other explicitly nonanthropogenic CWHR types were considered conifer absences within the context of the model. To mediate the large difference in resolution between our occurrence and climate data we effectively up-scaled the binary occurrence data. We calculated the percent-cover of conifer presence and absence polygons within the 30 arc-second grid cells of the climate data. If 5% of the grid cell contained conifers, we considered it a presence. If the grid cell contained less than 5% conifer cover and nonconifer vegetation exceeded 5% then it was classified as an absence. Our threshold was chosen to reduce omission error so that the resulting habitat suitability model would capture the breadth of the climatic niche of conifers in the Sierra Nevada.

To reduce collinearity among the 19 bioclimatic predictors within the extent of our study area, we calculated the Variance Inflation Factor (VIF) for the set using the R package *usdm* (47) and incrementally excluded collinear variables until VIF < 10, as recommended. The 7 remaining variables were Mean Temperature of Wettest Quarter, Mean Annual Precipitation, Mean Temperature of Driest Quarter, Precipitation Seasonality, Precipitation of Driest Month, Temperature Annual Range, and Isothermality. Reducing collinearity among predictors helps to increase model efficiency and mitigate uncertainty (48). When transferring models across space or time, differences in predictor collinearity between training data and projecting data can lead to poor performance. We quantified collinearity shift by comparing the correlation matrices of historical predictors to those of the present and future (49). Among the 7 climate variables vetted for collinearity, the greatest absolute shift in r was 0.183 for Isothermality and Mean Annual Precipitation and the average absolute shift in r was 0.005 (Fig. S3).

All of our habitat suitability modeling was completed using the *sdm* (v 1.0-89) (19) and *dismo* (v 1.3-3) (20) packages in R (v 4.1.1) (21). We used five different presence-absence modeling algorithms available from the *sdm* package: Random Forest, Multivariate Adaptive Regression Spline, Generalized Linear Model, Boosted Regression Tree, and BIOCLIM with default settings. We trained each model on historical occurrence and predictor data and used 5-fold cross validation with spatial blocking (block size = 70 km, *blockCV* (v 2.1.4) package (50)) to partition the occurrence data into testing and training sets in order to evaluate model performance. k-fold cross validation works by splitting source data into k groups (or "folds") and iteratively withholding each group as a "test" set while models train on the other k – 1 groups. The metrics of model performance are averaged across all (k) iterations. We used both AUC (the area under the receiver characteristic operating curve) and COR (point-biserial correlation coefficient) as model evaluation metrics. Because model extrapolation was a key feature of this work, we quantified the extent of over-fitting in the models by subtracting the training

Downloaded from https://academic.oup.com/pnasnexus/article/2/2/pgad004/7059010 by guest on 23 March 2023

AUC from the test AUC (51). We selected the GAM model because GAM can perform better than other popular SDM methods when extrapolated to novel environments (52). Test statistics (Fig. S4A) and variable importance (Fig. S4B) across the different methods show that each method produced models with high AUC and COR and the most important predictors were MAP and MTWQ. The relative weighting of MAP and MTWQ was the greatest difference between the models, with GAM, MARS, and GLM weighting MTWQ relatively higher than the decision tree-based methods.

We calculated a series of thresholds for the historical conifer HSM to delineate the probability of presence into three categories: suitable habitat, unsuitable habitat, and severely unsuitable habitat. We defined these thresholds using model sensitivity (i.e. the proportion of true conifer occurrences that are classified as suitable conifer habitat at a given threshold of habitat suitability) where unsuitable habitat was defined as habitat suitability values under which 5% of all Wieslander conifer occurrences occurred (i.e. sensitivity = 0.95). Similarly, severely unsuitable habitat was defined by the habitat suitability threshold which excluded 1% of Wieslander occurrences (i.e. sensitivity = 0.99).

The HSM was used to predict conifer habitat suitability at seven different time slices throughout the 20th and 21st centuries, sourcing PRISM climate variables for present-day and historical time periods and CMIP6 for future projections. At every time slice, we intersected our HSM predictions with observed conifer occurrences from EVeg, to produce maps of conifer forests that grow in suitable, unsuitable, or severely unsuitable climates. We downscaled the future projections to 30 arc-seconds via bilinear interpolation to match the resolution of the other time periods and simplify the comparison of relative area. Estimations of VCM are approximate for time periods outside of the present-day because EVeg conifer maps only reflect the modern distribution.

Acknowledgments

Thank you to Christopher Anderson for meaningful feedback in the early stages of the project.

Supplementary material

Supplementary material is available at *PNAS Nexus* online.

Funding

This project was supported by the Gordon and Betty Moore Foundation.

Author contributions

Conceptualization: A.P.H., C.J.N., K.S.H., T.W.C, and C.B.F. Data Analysis: A.P.H., C.J.N., K.S.H., and T.W.C. Writing—original Draft: A.P.H., C.J.N. Writing—review and editing: A.P.H., C.J.N., K.S.H., and C.B.F.

Data availability

Wieslander survey data are available thanks to the efforts of the VTM Digitization Project (vtm.berkeley.edu). Contemporary vegetation data are available from US Forest Service (www.fs.usda.gov). Historical and contemporary climate data at 800 m resolution are available from the PRISM Climate Group (prism.oregonstate.edu). Future climate data are available from CMIP6 (esgf-node.llnl.gov/projects/cmip6/). Data and code for our analysis are available at github.com/avephill/sierra-nevada-VCM.

References

1 Park Williams A, *et al.* 2019. Observed impacts of anthropogenic climate change on wildfire in California. *Earths Future*. 7(8): 892–910.
2 Nolan C, *et al.* 2018. Past and future global transformation of terrestrial ecosystems under climate change. *Science*. 361(6405): 920–923.
3 Jackson ST. 2021. Transformational ecology and climate change. *Science*. 373(6559):1085–1086.
4 Coop JD, *et al.* 2020. Wildfire-Driven Forest Conversion in Western North American Landscapes. *BioScience*. 70(8):659–673.
5 Gonzalez P, Neilson RP, Lenihan JM, Drapek RJ. 2010. Global patterns in the vulnerability of ecosystems to vegetation shifts due to climate change. *Glob Ecol Biogeogr*. 19(6):755–768.
6 Kelly AE, Goulden ML. 2008. Rapid shifts in plant distribution with recent climate change. *Proc Natl Acad Sci USA*. 105(33): 11823–11826.
7 Parmesan C, Yohe G. 2003. A globally coherent fingerprint of climate change impacts across natural systems. *Nature*. 421(6918): 37–42.
8 Svenning JC, Sandel B. 2013. Disequilibrium vegetation dynamics under future climate change. *Am J Bot*. 100(7):1266–1286.
9 van Mantgem PJ, *et al.* 2013. Climatic stress increases forest fire severity across the western United States. *Ecol Lett*. 16(9): 1151–1156.
10 North M, Collins B, Safford H, Stephenson NL. 2016. Montane forests. In: Mooney HA, Zavaleta E, editors. Ecosystems of California. University of California Press. p. 553–577.
11 Kemp KB, Higuera PE, Morgan P, Abatzoglou JT. 2019. Climate will increasingly determine post-fire tree regeneration success in low-elevation forests, Northern Rockies, USA. *Ecosphere*. 10(1):e02568.
12 Davis KT, *et al.* 2019. Wildfires and climate change push low-elevation forests across a critical climate threshold for tree regeneration. *Proc Natl Acad Sci USA*. 116(13):6193–6198.
13 Wieslander AE. 1935. First steps of the forest survey in California. p. 8.
14 Kelly M, Allen-Diaz B, Kobzina N. 2005. Digitization of a historic dataset: the Wieslander California vegetation type mapping project. *Madroño*. 52(3):191–201.
15 US Forest Service. 2018. EVeg Mid Region 5 South Sierra.
16 US Forest Service. 2019. EVeg Mid Region 5 North Sierra.
17 PRISM Climate Group. 2019. Prism climate data, 2013, 2015.
18 Boden T, Andres R, Marland G. 2017. Global, regional, and national fossil-fuel CO2 emissions (1751–2014) (V. 2017).
19 Naimi B, Araújo MB. 2016. SDM: a reproducible and extensible R platform for species distribution modelling. *Ecography*. 39(4): 368–375.
20 Hijmans RJ, Phillips S, Leathwick J, Elith J. 2021. Package 'dismo'.
21 R Core Team. 2021. R: a language and environment for statistical computing. R Foundation for Statistical Computing, Vienna, Austria.
22 Albrich K, Rammer W, Seidl R. 2020. Climate change causes critical transitions and irreversible alterations of mountain forests. *Glob Chang Biol*. 26(7):4013–4027.
23 Coffield SR, Hemes KS, Koven CD, Goulden ML, Randerson JT. 2021. Climate-driven limits to future carbon storage in California's Wildland ecosystems. *AGU Adv*. 2(3):e2021AV000384.

Downloaded from https://academic.oup.com/pnasnexus/article/2/2/pgad004/7059010 by guest on 23 March 2023

24 Fettig CJ, Mortenson LA, Bulaon BM, Foulk PB. 2019. Tree mortality following drought in the central and southern Sierra Nevada, California, US. *For Ecol Manage*. 432:164–178.
25 Thorne JH, Morgan BJ, Kennedy JA. 2008. Vegetation change over sixty years in the central Sierra Nevada, California, USA. *Madrono*. 55(3):223–237.
26 McIntyre PJ, *et al.* 2015. Twentieth-century shifts in forest structure in California: Denser forests, smaller trees, and increased dominance of oaks. *Proc Natl Acad Sci USA*. 112(5):1458–1463.
27 Dolanc CR, Safford HD, Dobrowski SZ, Thorne JH. 2014. Twentieth century shifts in abundance and composition of vegetation types of the Sierra Nevada, CA, US. *Appl Veg Sci*. 17(3): 442–455.
28 Shive KL, *et al.* 2018. From the stand scale to the landscape scale: predicting the spatial patterns of forest regeneration after disturbance. *Ecol Appl*. 28(6):1626–1639.
29 Dettinger MD, *et al.* 2018. Sierra Nevada summary report. California's Fourth Climate Change Assessment. Report SUM-CCCA4-2018-004.
30 Beardsley D. 1999. Old-growth forests in the Sierra Nevada: by type in 1945 and 1993 and ownership in 1993. Vol. 516. US Department of Agriculture, Forest Service, Pacific Northwest Research Station.
31 Allen BH. 1988. Sierran mixed conifer. A guide to wildlife habitat relationships. Scaramento (CA): California Department of Fish and Game. p. 46–47.
32 Fitzhugh EL. 1990. Ponderosa pine. A guide to wildlife habitat relationships. Scaramento (CA): California Department of Fish and Game. p. 46–47.
33 Wieslander AE, Yates HS, Jensen HA, Johannsen PL. 1933. Manual of field instructions for vegetation type map of California. Technical report. USDA Forest Service.
34 Lynch AJ, *et al.* 2021. Managing for radical ecosystem change: applying the resist-accept-direct (rad) framework. *Front Ecol Environ*. 19(8):461–469.
35 McWethy DB, *et al.* 2019. Rethinking resilience to wildfire. *Nat Sustain*. 2(9):797–804.
36 California Air Resources Board. 2014. Compliance offset protocol U.S. forest projects.
37 Anderegg WRL, *et al.* 2020. Climate-driven risks to the climate mitigation potential of forests. *Science*. 368(6497):eaaz7005.
38 Miller RK, Field CB, Mach KJ. 2020. Barriers and enablers for prescribed burns for wildfire management in California. *Nat Sustain*. 3:101–109.
39 California Department of Fish and Wildlife. 2004. California wildlife habitat relationships.
40 Kelly M, Ueda K-i, Allen-Diaz B. 2007. Considerations for ecological reconstruction of historic vegetation: Analysis of the spatial uncertainties in the California Vegetation Type Map dataset. *Plant Ecol*. 194(1):37–49.
41 USDA Forest Service. Calveg system.
42 U.S. EPA. 2010. Level I ecoregions of north America shapefile. ftp://newftp.epa.gov/EPADataCommons/ORD/Ecoregions/cec˙na/na˙cec˙eco˙l1.zip
43 Daly C, *et al.* 2008. Physiographically sensitive mapping of climatological temperature and precipitation across the conterminous United States. *Int J Climatol*. 28(15):2031–2064.
44 Pierce DW, Kalansky JF, Cayan DR. 2018. Climate, drought, and sea level rise scenarios for California's fourth climate change assessment. California Energy Commission and California Natural Resources Agency.
45 Swart NC, *et al.* 2019. CCCma CanESM5 model output prepared for CMIP6 ScenarioMIP. Medium: application/x-netcdf Version Number: 20210201 Type: dataset.
46 Riahi K, *et al.* 2017. The shared socioeconomic pathways and their energy, land use, and greenhouse gas emissions implications: an overview. *Glob Environ Change*. 42:153–168.
47 Naimi B, Hamm NAS, Groen TA, Skidmore AK, Toxopeus AG. 2014. Where is positional uncertainty a problem for species distribution modelling? *Ecography*. 37(2):191–203.
48 De Marco P, Nóbrega CC. 2018. Evaluating collinearity effects on species distribution models: An approach based on virtual species simulation. *PLoS ONE*. 13(9):e0202403.
49 Feng X, Park DS, Liang Y, Pandey R, Papeş M. 2019. Collinearity in ecological niche modeling: confusions and challenges. *Ecol Evol*. 9(18):10365–10376.
50 Valavi R, Elith J, Lahoz-Monfort JJ, Guillera-Arroita G. 2019. blockCV: an R package for generating spatially or environmentally separated folds for k-fold cross-validation of species distribution models. *Methods Ecol Evol*. 10(2):225–232.
51 Radosavljevic A, Anderson RP. 2014. Making better Maxent models of species distributions: complexity, overfitting and evaluation. *J Biogeogr*. 41(4):629–643.
52 Charney ND, *et al.* 2021. A test of species distribution model transferability across environmental and geographic space for 108 western north American tree species. *Front Ecol Evol*. 9: 689295.

Downloaded from https://academic.oup.com/pnasnexus/article/2/2/pgad004/7059010 by guest on 23 March 2023